

City Research Online

City St George's, University of London

Citation: Edwards, M. W. (1973). A study of the role of donor - acceptor interactions in organic reactions. (Unpublished Doctoral thesis, The City University)

This is the accepted version of the paper.

This version of the publication may differ from the final published version. To cite this item please consult the publisher's version.

Permanent repository link: https://openaccess.city.ac.uk/id/eprint/38366/

Copyright and Reuse: Copyright and Moral Rights remain with the author(s) and/or copyright holders. Copies of full items can be used for personal research or study, educational, or not-for-profit purposes without prior permission or charge, unless otherwise indicated, provided that the authors, title and full bibliographic details are credited, a hyperlink and/or URL is given for the original metadata page and the content is not changed in any way. For full details of reuse please refer to City Research Online policy.

City Research Online: http://openaccess.city.ac.uk/ publications@citystgeorges.ac.uk

A STUDY OF THE ROLE OF DONOR-ACCEPTOR INTERACTIONS IN ORGANIC REACTIONS

A thesis submitted for the degree of Doctor of Philosophy in The City University.

by

M. W. Edwards.

THE CITY UNIVERSITY LIBRARY,
ST. JOHN STREET, LONDON, E.C.1.

The City University,

October , 1973.

Index

		Page
Abstract		i
Abbreviations		ii
Chapter 1 - Literature Survey		
1 - 1	Charge-Transfer Complexes	1
1 - 1 - 1	Theoretical Aspects	1
1 - 1 - 2	Spectra of Charge-Transfer Complexes	3
1 - 1 - 3	Determination of Equilibrium Constants and Extinction Coefficients	6
1 - 1 - 4	Interpretation of Experimental Data	9
1 - 2	The Role of Charge-Transfer Complexes in Reactions	13
1 - 2 - 1	Thermal Reactions	13
1 - 2 - 2	Photochemical Reactions	16
1 - 2 - 3	Biochemical Reactions	17
1 - 3	Cycloaddition Reactions	19
1 - 3 - 1	Woodward-Hoffmann Rules and MO Methods	19
1 - 3 - 2	(4n + 2) Cycloadditions	22
1 - 3 - 3	4n Cycloadditions	26
1 - 4 - 1	Bicyclo [2,2,1] hepta-2,5-diene	29
1 - 4 - 2	Hexamethyl bicyclo [2,2,0] hexadiene	31
1 - 4 - 3	Tetracyanoethylene	33
1 - 5	N.M.R. Studies	34
1 - 5 - 1	Nuclear Magnetic Double Resonance	34
1 - 5 - 2	The Karplus Equations and their Application to Elucidation of Structure	34

Page

1 - 5 - 3 N.M.R. Lanthanide Shift Reagents 36

1 - 5 - 4 N.M.R. Applications to Structures of Cycloadducts 37

Chapter 2 - Experimental Methods

2 - 1 General Methods 39

2 - 2 Spectroscopic Methods 40

Chapter 3 - Nuclear Magnetic Resonance Studies of Cycloadducts and Related Compounds

3 - 1 Introduction 43

3 - 2 Preparation of Adducts 43

3 - 3 Spectral Interpretation and Assignment of Conformation 46

3 - 3 - 1 Norbornadiene/TCNE Adduct 46

3 - 3 - 2 Hexamethyl Dewar benzene/TCNE Adduct 49

3 - 3 - 3 Hexa-trans-2,trans-4-diene/Maleic Anhydride Adduct 51

3 - 3 - 4 Hexa-trans-2,trans-4-diene/TCNE Adduct 53

3 - 3 - 5 1-Methoxybuta-trans-1,3-diene/Maleic Anhydride Adduct 55

3 - 3 - 6 1-Methoxybuta-trans-1,3-diene/TCNE Adduct 58

3 - 3 - 7 1,4-Diphenylbuta-trans-1,trans-3-diene /TCNE Adduct 61

3 - 3 - 8 Hexa-trans-2,trans-4-dienol/TCNE Adduct 63

3 - 3 - 9 2-Methylpenta-1,trans-3-diene/TCNE Adduct 65

3 - 3 - 10 2-Vinyl Naphthalene/TCNE Adduct 68

3 - 3 - 11 Cyclohexa-1,3-diene/TCNE Adduct 70

Page

3 - 3 - 12 α -Phellandrene/TCNE Adduct 74

3 - 3 - 13 Anthracene/Maleic Anhydride and Anthracene/TCNE Adducts 75

3 - 3 - 14 Indole/TCNE and 1,2-Dimethyl Indole/TCNE Adducts 77

Chapter 4 - Norbornadiene/TCNE Reaction

4 - 1 Introduction 80

4 - 2 Purification of Reagents 80

4 - 3 Preparation and Analysis of Adduct 81

4 - 3 - 1 Preparation 81

4 - 3 - 2 T.L.C. 81

4 - 3 - 3 UV/Visible Spectra 81

4 - 3 - 4 IR Spectrum 81

4 - 3 - 5 Mass Spectrum 82

4 - 3 - 6 Conclusion 82

4 - 4 Kinetic Studies 82

4 - 4 - 1 Visible Spectroscopy 83

4 - 4 - 1-1 Determination of K and ε for Complex 83

4 - 4 - 1-2 Determination of Rate Constants 90

4 - 4 - 2 UV Spectroscopy 98

4 - 4 - 2-1 Rate Constants in 1,2-Dichloroethane 99

4 - 4 - 2-2 " " in 1,2-Dichloroethane/Carbon Tetrachloride 103

4 - 4 - 2-3 Investigation of Initial Rapid Reaction 104

4 - 5 Discussion 114

Chapter 5 - Hexamethyl Dewar Benzene/TCNE Reaction

5 - 1 Introduction 117

Page

5 - 2 Purification of Reagents 117

5 - 3 Preparation and Analysis of Adduct 117

5 - 3 - 1 Preparation 117

5 - 3 - 2 T.L.C. 119

5 - 3 - 3 UV/Visible Spectra 119

5 - 3 - 4 IR Spectrum 119

5 - 3 - 5 Mass Spectrum 120

5 - 3 - 6 Conclusion 120

5 - 4 Kinetic Studies 121

5 - 4 - 1 Visible Spectroscopy 121

5 - 4 - 2 UV Spectroscopy 122

5 - 5 Discussion 131

Chapter 6 - Hexa-trans-2,trans-4-diene/Maleic Anhydride Reaction

6 - 1 Introduction 133

6 - 2 Purification of Reagents 133

6 - 3 Preparation and Analysis of the Adduct 134

6 - 3 - 1 Preparation 134

6 - 3 - 2 UV/Visible Spectrum 134

6 - 3 - 3 Infrared Spectrum 134

6 - 3 - 4 Mass Spectrum 135

6 - 4 UV/Visible Spectroscopy 136

6 - 4 - 1 Determination of K and ε for the Charge-transfer complex 138

6 - 4 - 2 Calculation of Rate Constants 140

6 - 5 Discussion 145

Chapter 7 - 1-Methoxybuta-trans-1,3-diene/Maleic Anhydride Reaction

7 - 1 Introduction 148

		Page
7 - 2	Purification of Reagents	148
7 - 3	Preparation and Analysis of the Adduct	149
7 - 3 - 1	Preparation	149
7 - 3 - 2	T.L.C.	150
7 - 3 - 3	UV/Visible Spectrum	150
7 - 3 - 4	Infrared Spectrum	150
7 - 3 - 5	Mass Spectrum	150
7 - 4	Visible Spectroscopy	152
7 - 4 - 1	Determination of K and ε for the Charge-transfer complex	152
7 - 4 - 2	Calculation of Rate Constants	156
7 - 5	Discussion	160

Chapter 8 - Anthracene/Maleic Anhydride Reaction

8 - 1	Introduction	162
8 - 2	Purification of Reagents	163
8 - 3	Preparation and Analysis of the Adduct	163
8 - 3 - 1	Preparation	163
8 - 3 - 2	T.L.C.	163
8 - 3 - 3	UV/Visible Spectrum	163
8 - 3 - 4	Infrared Spectrum	164
8 - 3 - 5	Mass Spectrum	164
8 - 3 - 6	Conclusion	165
8 - 4	Visible Spectroscopy	165
8 - 4 - 1	Determination of K and ε values for the Charge-transfer complex	166
8 - 4 - 1 - 1	Using a Large Excess of Maleic Anhydride	166
8 - 4 - 1 - 2	Using Equimolar Concentrations	170
8 - 4 - 2	Calculation of Rate Constants	173

Page

8 - 4 - 2 - 1 Using a Large Excess of Maleic Anhydride 173

8 - 4 - 2 - 2 Using a Large Excess of Anthracene 177

8 - 4 - 2 - 3 Using Equimolar Concentrations 178

8 - 5 Discussion 180

Chapter 9 - Indole/TCNE Reaction

9 - 1 Introduction 184

9 - 2 Purification of Reagents 184

9 - 3 Preparation and Analysis of the Adduct 184

9 - 3 - 1 Preparation 185

9 - 3 - 2 T.L.C. 185

9 - 3 - 3 UV/Visible Spectrum 185

9 - 3 - 4 Infrared Spectrum 185

9 - 3 - 5 Mass Spectrum 186

9 - 3 - 6 Conclusion 186

9 - 4 Preparation and Analysis of an Intermediate 187

9 - 5 Visible Spectroscopy 188

9 - 5 - 1 Determination of K and ε Values for the Charge-transfer Complex 188

9 - 5 - 2 Determination of Rate Constants 193

9 - 6 Ultraviolet Spectroscopy 196

9 - 7 Discussion 200

Acknowledgements 203

References 204

Abstract.

The reactions in solution between tetracyanoethylene and the electron donating compounds,norbornadiene,hexamethyl Dewar benzene and indole and between maleic anhydride and the compounds anthracene,methoxybutadiene and hexadiene have been studied.The equilibrium constants, enthalpies'and entropies of formation and extinction coefficients of the charge-transfer complexes formed in reaction have been determined using the Benesi-Hildebrand method or using.equimolar concentrations of reactants.

The kinetics of reaction have been investigated using visible and ultraviolet spectroscopy having equimolar,excess of donor or,in one case,excess of acceptor concentrations of reactants.For each reaction the kinetic data has been used to examine the overall mechanism of reaction with particular reference to the role that the charge-transfer complex might play as a reaction intermediate;only in the case of the reactions of norbornadiene and hexamethyl Dewar benzene was a charge-transfer complex indicated as a likely reaction intermediate.

The structures of the products of reaction were determined using elemental analysis,mass spectrometry,infrared and nuclear magnetic resonance spectroscopy.

The conformations in solution of these and other closely related adducts were examined using nuclear magnetic resonance spectroscopy with application of the Karplus equation.

Abbreviations

A -	electron acceptor
D -	electron donor
AD^* -	1:1 charge-transfer complex
AD_2^* -	1:2 charge-transfer complex
$AD^\dagger$ -	a second 1:1 charge-transfer complex
AD -	1:1 adduct formed from A and D
[ ] -	molar concentration
$[\ ]_o$ -	molar concentration at zero time
K -	equilibrium constant for formation of AD^*
k_1 -	experimental first-order rate constant
k_2 -	experimental second-order rate constant. $k_{exp} = k_2$
k_c -	corrected second-order rate constant
d -	optical density (absorbance)
d_o -	optical density at zero time
ε -	extinction coefficient
λ -	wavelength (nm)
λ_{max} -	wavelength of maximum absorbance
l -	cell path-length
t -	time
T -	temperature
τ -	10-δ, where δ is chemical shift (ppm)
J -	spin-spin coupling constant (Hz)
ΔH -	enthalpy of complex formation
ΔS -	entropy of complex formation
ΔE -	energy of activation
ΔS^* -	entropy of activation
N.M.R. -	nuclear magnetic resonance
T.L.C. -	thin layer chromatography

G.L.C. - gas liquid chromatography

UV - ultraviolet

IR - infrared

TCNE - tetracyanoethylene

$Eu(fod)_3$ - Europium tri (1,1,1,2,2,3,3-heptafluoro-7,7-dimethyl-4,6-octane dionate)

n_{20}^{D} - refractive index at 20°C.

y - d_o(TCNE total) - d_o(TCNE extrapolated)/d_o(TCNE total)

Chapter 1 - Literature Survey

1 - 1 Charge-Transfer Complexes

When solutions of certain electron donor and acceptor compounds are mixed together, an immediate formation of colour is observed; this phenomenon may also occur in the solid state. The colours are attributed to molecular complexes known as charge-transfer complexes.

1 - 1 - 1 Theoretical Aspects

Early explanations for these coloured molecular complexes included the proposal for certain covalent links between the components[1] and also the formation of electrostatic interactions between the two molecules.[2] It was suggested[3] that the complex molecule was essentially ionic in character and was formed by electron transfer from the donor to the acceptor molecule. A quantum-mechanical resonance between a no-bond structure and bond between donor and acceptor was proposed.[4] A reversible formation of such a complex by reduction of the activation barrier was suggested as a preliminary step in an irreversible chemical reaction.[4]

Mulliken[5,6,7] formulated a quantum-mechanical model based on valence-bond theory, where the wave function of the normal ground-state of a molecular complex, D,A formed from a donor, D, and acceptor, A, is given by:

$$\Psi_N = a\Psi_o + b\Psi_1 \qquad (1 - 1)$$

Ψ_o is a 'no-bond' wave function corresponding to $\Psi(D,A)$ and Ψ_1 is a 'dative' electron-transfer wave function corresponding to $\Psi(D^+,A^-)$. The full wave functions are given by:

$$\Psi_N = a\Psi(D,A) + b\Psi(D^+,A^-) \qquad (1-2)$$
$$\Psi_E = a^*\Psi(D,A) - b^*\Psi(D^+,A^-)$$

Ψ_E is the excited state wave function having different coefficients a^* and b^*. The transition $\Psi_N \rightarrow \Psi_E$ gives rise to absorption bands in the visible spectrum and hence the complexes are coloured. Ψ_N has an almost covalent character and Ψ_E is almost ionic and the absorptions associated with the transition give rise to an intermolecular charge-transfer spectrum. The actual amount of charge-transfer in the ground-state is concluded[8] to be small after investigations with dipole moment measurements. The electronic transfer is from the highest filled orbital of the donor to the lowest unfilled orbital of the acceptor, the transition energy being given by:

$$\Delta E_{ij} = D_i - A_j + \text{constant} \qquad (1-3)$$

where D_i is the energy-level of the donor and A_j the energy-level of the acceptor.

More recently, molecular orbital theory has also been applied to these π-complexes[9,10], which are formed from π-orbitals in the acceptor and donor molecules. Interaction of the filled orbitals of the donor with the empty anti-bonding orbitals of the acceptor, leads to a net stabilization in energy with a simultaneous transfer of negative charge from donor to acceptor.

Donor and acceptor compounds have been classified as increvalent or sacrificial[11], these being n, σ or π types. An increvalent donor is a compound with a lone pair of (n) non-bonding electrons, an increvalent acceptor having a vacant orbital (v) such as in $SnCl_4$. π-donors and π-acceptors are both sacrificial,

with electrons from bonding orbitals involved in charge-transfer.

The rates of formation of charge-transfer complexes in solution are very high. Recent studies[12] have shown that the rate of formation of the complex between tetracyanoethylene and hexamethylbenzene in solution at -80° is only of the order of ten times slower than the diffusion controlled rate.

1 - 1 - 2 Spectra of Charge-Transfer Complexes.

1 - 1 - 2 - 1 Electronic Absorption Spectra.

The formation of a complex from donor and acceptor molecules results in the appearance of a new band or bands in the absorption spectrum at a longer wavelength than the bands of components which are still present. Enthalpies of formation of the complexes are small,[13] and hence orbital changes in forming the complex are not likely to be large, so that all the transitions observed in the free donor and acceptor molecules should appear in the spectrum of the complex.

The presence of more than one charge-transfer band can be explained if there is more than one energy level in the donor involved in charge transfer, or more than one acceptor energy level available. For example, in the interaction of methylbenzene with chloranil or 1,3,5 - trinitrobenzene, two charge-transfer bands occur in the spectra.[14]

Another explanation for the multiplicity of charge-transfer bands is the formation of complexes in which the donor and acceptor molecules are oriented in different ways and have different interactions[15,16,17] as for the case of tetracyanoethylene-naphthalene complexes where two transitions are observed.

Studies on electron affinities of acceptors[18-20] and ionisation potentials of donors[20-24] have been carried out and

attempts at correlations with the energy of the charge-transfer bands have been made.[25] Solvent effects on absorption bands with charged ground states are shown to be important,[8,24] but not for neutral ground states. It has also been shown[10,15,26-28] for donors that the energy of the charge-transfer band shows an approximate linear correlation with Hückel molecular orbital coefficients.

The extinction coefficient of the charge-transfer complex absorption is proportional to the square of the transition dipole moment[11,29] between ground and excited states, and should increase with increase in resonance interaction between donor and acceptor. However, correlations of the extinction coefficient ε with both ionisation potential of the donor[30,31] and enthalpy of formation of the complex[29] have been made and there is no evidence for a general increase in ε with increasing strength of the complex.

The concept of 'contact' charge-transfer complexes[32-35] has been used to explain some of the anomalous results for extinction coefficients. Such complexes are postulated to arise from random collisions between donor and acceptor molecules with apparent $\varepsilon_{\text{contact}} \rightarrow \infty$, and equilibrium constant $K_{\text{contact}} = 0$.

However, the effect of solvation on the donor, acceptor and complex has been considered, showing a change in $K\varepsilon$ and K values with change in solvent.[36] Such effects were proposed to explain the anomalous results without the need to postulate 'contact' interactions.

1 - 1 - 2 - 2 Infrared and Raman Spectra.

The changes in intensity and energy of vibration bands in going from donor and acceptor molecules to the complexes are generally greater in complexes of σ-donors and σ-acceptors than in

π-π complexes.

Evaluations of intensity increases and frequency shifts in components of complexes in terms of vibronic interactions [37] and electrostatic contributions [38] provide no information as to the relative orientation of donor and acceptor in the complex.

1 - 1 - 2 - 3 Nuclear Magnetic Resonance Spectra.

The chemical shift, δ, for a particular nucleus is very sensitive to the chemical environment, where interactions such as solvent magnetic anisotropic effects, Van der Waals forces, electric field and ring currents are important. If a particular nucleus can exist in two different environments then two chemical shifts will be observed unless the nucleus is exchanging very rapidly between the two. For the case of a nucleus exchanging between either a free donor and complexed donor or free acceptor and complexed acceptor the rates of exchange are so rapid that one signal only is usually observed.[13,39] In most of the N.M.R. studies of charge-transfer complexes the signals of specific protons are shifted in going from the free to the complexed form. Δ_o values defined as $\delta_{free} - \delta_{complex}$ for a given proton have been examined[40-42] in relation to the components of the complexes. In most cases the Δ_o values are accounted for in terms of ring current, electric field and solvent effects.[40-44] When fluorine nuclei in acceptors are studied by ^{19}F N.M.R. shift measurements, there appears to be an increase in Δ_o values with decrease in ionisation potential of the donor.[45] Fluorine nuclei shifts are more dependent on electron density than the corresponding proton shifts[46] and the above effect may be evidence for some transfer of charge in the complex.

1 - 1 - 3 Determination of Equilibrium Constants and Extinction Coefficients.

The methods most commonly used to determine equilibria and extinction coefficients of charge-transfer complexes are those based on ultra-violet and visible spectroscopy. The simplest methods assume the rapid formation of a complex in solution in equilibrium with the donor and acceptor molecules. The complex is treated only as the 1:1 species as represented in (1 - 4).

$$A + D \rightleftharpoons AD^{*} \qquad (1 - 4)$$

The equilibrium constant is given by (1 - 5).

$$K = \left[AD^{*}\right] / \left[A\right]\left[D\right] \qquad (1 - 5)$$

$\left[AD^{*}\right]$, $\left[A\right]$ and $\left[D\right]$ are the equilibrium concentrations of complex, acceptor and donor species respectively. In the visible or ultra-violet region of the spectrum the charge-transfer band has a broad symmetrical appearance and from measurements of optical density it is possible to calculate the equilibrium constant and extinction coefficient for complex formation.

According to Beer's Law, the optical density, d, is given by:

$$d = \varepsilon \ell \left[AD^{*}\right] \qquad (1 - 6)$$

ε is the extinction coefficient of the complex and ℓ is the optical path-length (cm.). If $\left[D\right]_o$ and $\left[A\right]_o$ are the total concentrations of donor and acceptor, then rearranging (1 - 5) gives:

$$K = \left[AD^{*}\right] / \left(\left[A\right]_o - \left[AD^{*}\right]\right)\left(\left[D\right]_o - \left[AD^{*}\right]\right) \qquad (1 - 7)$$

substituting (1 - 6) into (1 - 7) gives:

$$K = \left[AD^{*}\right] / \left(\left[A\right]_o - d/\varepsilon\ell\right)\left(\left[D\right]_o - d/\varepsilon\ell\right) \qquad (1 - 8)$$

Rearrangement of (1 - 8) giving:

$$[A]_o/d = 1/K\ell\varepsilon[D]_o + [A]_o/[D]_o\varepsilon\ell + 1/\varepsilon\ell - [AD^*]/[D]_o\varepsilon\ell \qquad (1 - 9)$$

If the concentration of the donor is much greater than that of the acceptor $[D]_o \gg [A]_o$ then (1 - 9) simplifies to:

$$[A]_o/d = 1/K\varepsilon\ell[D]_o + 1/\varepsilon\ell \qquad (1 - 10)$$

This is known as the Benesi-Hildebrand equation[47] and if values of $[A]_o/d$ are plotted against $1/[D]_o$, the equilibrium constant, K, and extinction coefficient, ε, can be calculated from the slope and the intercept. Variations of this method have been proposed, including the Scott Equation:[48]

$$[D]_o[A]_o/d = [D]_o/\varepsilon + 1/K\varepsilon \qquad (1 - 11)$$

Benesi-Hildebrand plots extrapolate to non-ideal concentrated solutions whereas in (1 - 11) the extrapolation is towards dilute solution. Further rearrangement gives the Foster-Hammick-Wardley equation.[49]

$$d/[D]_o = -Kd + K[A]_o\varepsilon \qquad (1 - 12)$$

Where K may be evaluated directly as the slope when plotting $d/[D]_o$ against -d.

Ketelaar[50-54] and others have developed equations for cases where the absorption of the charge-transfer band overlaps absorption due to the components of the complex. The extinction coefficients of the other species are taken into account.

Relationships for equilibria where $[D]_o < [A]_o$ or where $[D]_o = [A]_o$ can be obtained by denoting the total concentration of one component in terms of the other. If $[D]_o = n[A]_o$,

$$[A]_o/d = (n+1)/n\varepsilon + 1/n K\varepsilon[A]_o \qquad (1-13)$$

There have been few reports of determination of termolecular complex equilibrium constants and extinction coefficients. A measurement of K for a 2:1 donor-acceptor complex has been carried out[55] by first measuring the 1:1 complex equilibrium constant (K_1) by using a large excess of acceptor, (i.e. where there is little 2:1 complex present). From this value measurements were made of the termolecular equilibrium constant (K_2) as in (1 - 14).

$$A + D \underset{K_1}{\rightleftharpoons} AD \overset{D}{\underset{K_2}{\rightleftharpoons}} AD_2 \qquad (1-14)$$

Another important technique used in determination of equilibrium constants and extinction coefficients is N.M.R. spectroscopy. The advantages over the optical methods are that line positions are easier to measure than intensities and also there is no complication from overlapping energy bands of donor and acceptor molecules in the same region as the charge-transfer complex band.

It is possible to derive an analogous expression to the Benesi-Hildebrand equation for use with N.M.R. data. Protons are considered to be undergoing rapid exchange between the complexed and uncomplexed state. It can be shown[43] that when $[D] \gg [A]$

$$\delta^A_{obs} - \delta^A_o = (\delta^A_{AD} - \delta^A_o)\ K[D]_o / (1 + K[D]_o) \qquad (1-15)$$

$\delta^A_{obs}, \delta^A_{AD}, \delta^A_o$ are the chemical shifts of given acceptor protons observed in the complexing medium, in the pure complex and in the uncomplexed state respectively. Δ and Δ_o are defined by

$$\Delta = \delta^A_{obs} - \delta^A_o, \qquad \Delta_o = \delta^A_{AD} - \delta^A_o \qquad (1-16)$$

Combining (1 - 15) and (1 - 16) and rearranging:

$$1/\Delta = 1/K\Delta_o [D]_o + 1/\Delta_o \qquad (1 - 17)$$

This is analogous to the Benesi-Hildebrand equation and values of K and Δ_o can be obtained from plots of $1/\Delta$ against $1/[D]_o$. Values of K derived by this method compare favourably with those from optical measurements.[40-43]

In some systems, measurements of K values have been made by examining nuclei in both donor and acceptor molecules.[41,56,57] However, measurement of non-equivalent nuclei in the same compound have yielded values of K which are different. This may be due to the presence of termolecular species.[58]

Other methods used to determine equilibrium constants and extinction coefficients of charge-transfer complexes have included polarography in which measurements of reduction potentials are made,[59-61] calorimetry,[62-64] dielectric constant measurements [65,66] and osmometry.[67]

1 - 1 - 4 Interpretation of Experimental Data.

Most of the association constant determinations of organic charge-transfer complexes have been in systems where one species, usually the donor is in large excess.

Comparison of results from systems of π-donors and π-acceptors obtained by optical and N.M.R. measurements indicates that there have been only a few systems studied using equimolar concentrations i.e. $[A] = [D]$. These latter measurements may have considerable importance, because the excess donor method is open to several errors, such as (1) The effect of solvent, (2) The presence of termolecular and other complexes, (3) The inherent limitations in the method used to derive K values. For example, in the Benesi-Hildebrand equation, which is the most commonly used method for obtaining constants, extrapolation is to infinite non-ideal concentration of

solution and not to ideal infinite dilution. There have been attempts to examine [68-72] critically the validity of the Benesi-Hildebrand and other methods used to obtain a single, non-zero value for K and a finite constant value for ε. For example, Hammond [68] showed that the effect of experimental errors on the Benesi-Hildebrand method was such as to make it inaccurate for measurement of very small association constants.

It has been suggested[70,73] that reliable equilibrium constants are obtained only when the equilibrium concentration of the complex is of the same order as the equilibrium concentration of the more dilute component. For complexes, having an association constant below 0.1, experimental errors could lead to large deviations from the correct value.

Most methods ignore the fact that the solvent interacts with both donor and acceptor molecules. The equilibrium constant for a given system appears to be dependent on the nature of the solvent.[13] If there is competition for the donor and acceptor molecules by the solvent then a generalised equation can be made.

$$K_{corr} = K_{exp} (1 + K_s [s]) \qquad (1 - 18)$$

Here K_{corr} is the true association constant without solvent competition, K_{exp}, the observed constant, K_s, the solvent-donor or solvent-acceptor association constant and $[s]$, the solvent concentration. More recent solvent theory[74] leads to a prediction of the constancy of the factor $K\varepsilon$ when the concentrations of D and A are varied over a wide range.

Deviations from Beer's Law have been used as an explanation for anomalies in K, when the constancy of $K\varepsilon$ has been disputed.[31]

In general the strongest solvent effects will occur with strong n-donors such as dioxane or ether, or aromatic π-donors such

as benzene and toluene.[13] It has been shown that even carbon tetrachloride may behave as an electron acceptor.[75] When solvent effects are not large, association data of neutral donors and acceptors in inert solvents show that K is highest for the least ionising solvents.[13]

Evidence for the occurence of termolecular species such as DA_2 or D_2A in solution was proposed from the change in equilibrium constant K with change in wavelength.[55] The method involved one of the species in large excess, and therefore conditions favoured formation of termolecular complexes. Values of K were calculated at a number of different wavelengths.

It has been shown[76] that for cases where equimolar concentrations are used, there is no wavelength dependence of K. For equimolar concentrations there may be fewer termolecular species present.

A recent application of synthetic data calculated for systems involving the formation of AD, A_2D and AD_2 suggested[77] that the Benesi-Hildebrand method would appear linear even with termolecular species present in solution. In the latter study, the variation of K with wavelength for the tetracyanoethylene-naphthalene system was too large to be explained solely by the presence of isomeric 1:1 complexes or 'contact' absorptions. A recent study by Deranleau[73] disputed the linearity of the Benesi-Hildebrand equation when termolecular species were present in solution. A microscopic model was used to illustrate averaging processes in the assignment of formation constants for higher-order complexes. The slopes and intercepts of various plots usually applied for the evaluation of weak complexes were derived for a system as shown in (1 - 19):

$$\begin{array}{ccc} & \overset{D}{\rightleftharpoons} & \\ AD(1) & & AD_2(1,2) \\ D \;/\!/ & & /\!/ \\ A & \rightleftharpoons & AD\,(2)+D \\ & \underset{D}{\rightleftharpoons} & \end{array} \qquad (1 - 19)$$

The derivation showed that all of the usual plots were slightly curved over wide ranges of the complex concentrations. The theory of 'contact' complexes mentioned earlier has been criticised by Carter [36] on the basis that no place is given for the role of the solvent. If the solvent complexation is examined then there is no need to involve any 'contact' complexes at all.

Orgel and Mulliken[35] suggested the presence of isomeric 1:1 complexes in solution. If the two or more complexes are assumed to have equal K and $\leq$ values, then plots of Log K v 1/T will not be linear if the enthalpies of formation are different for each complex. The presence of the above complexes was disputed where values of K over limited temperature ranges were calculated.[78]

1 - 2 The role of charge-transfer complexes in reactions.

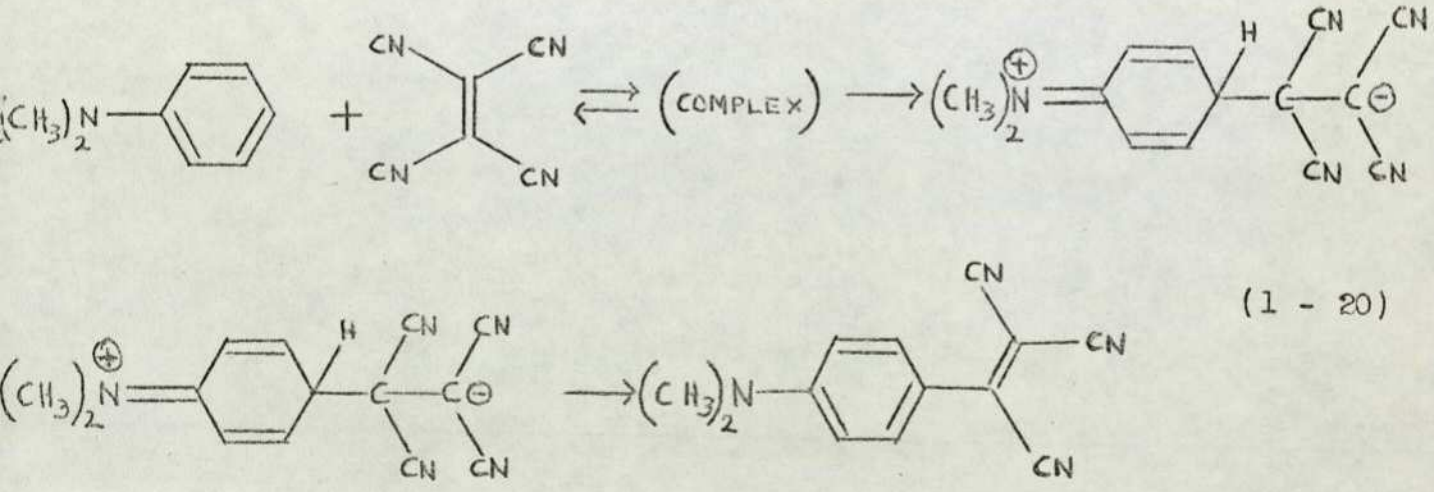
Substitution, cycloaddition and electron-transfer reactions are known where a charge-transfer complex is present.

The fact that the colour attributed to a charge-transfer complex may fade during the course of reaction is not evidence in itself that the complex is directly involved as a reaction intermediate, since it may be formed in a side equilibrium.

Evidence based on kinetic measurements for direct involvement of the charge-transfer complex in reaction has only been found in a few cases.[79-84]

1 - 2 - 1 Thermal Reactions which may proceed through a Charge-Transfer Complex.

The substitution reactions between N-alkylanilines and tetracyanoethylene have been studied in detail,[80,81,83,84,85,90] a colour being formed (λ_{max} 675nm) when the two reactants are mixed together in chloroform. The intensity of the charge-transfer absorption band decreased with time as a colourless intermediate was formed, which slowly changed to the red product, N, N-dimethyl-4-tricyanovinylaniline. The intermediate was proposed[80] to have a zwitterionic structure as in (1 - 20).



(1 - 20)

Rappoport studied the kinetics of formation of the intermediate by observing changes in the charge-transfer complex absorption, and using a large excess of donor.

From graphs of Log d against t it was calculated that the second-order rate constants increased with donor concentration. Various schemes were drawn up to compare the rate constants calculated this way (k_{exp}) with corrected rate constants (k_c) related to total concentrations of acceptor $[A_t]$.

In (1 - 21) the charge-transfer complex was a direct intermediate.

$$D + A \rightleftharpoons AD^* \rightarrow AD \qquad (1 - 21)$$

$$-d\,[A_t]/dt = k_c[AD^*]$$

$$k_{exp} = k_c K / (1 + K[D]_o)$$

In (1 - 22) the charge-transfer complex was formed in a side-equilibrium.

$$D + A \rightleftharpoons AD^*, \quad D + A \longrightarrow AD \qquad (1 - 22)$$

$$-d\,[A]_t/dt = k_c[A]\,[D]_o$$

$$k_{exp} = k_c / (1 + K[D]_o)$$

In (1 - 23) a molecule of donor reacted with the complex to form the adduct plus donor.

$$A + D \rightleftharpoons AD^*, \quad AD^* + D \rightarrow AD + D \qquad (1 - 23)$$

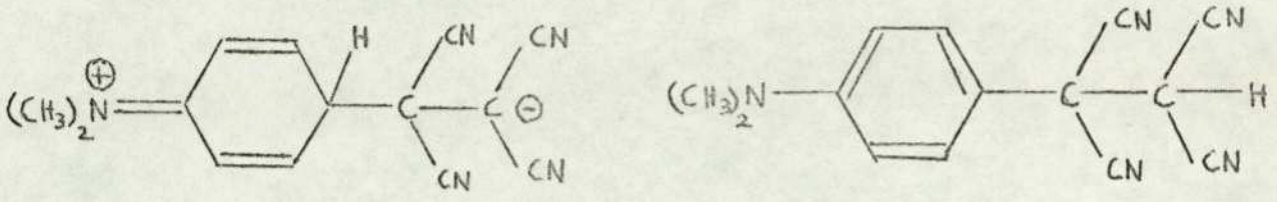
$$-d\,[A]_t/dt = k_c[D]_o\,[AD^*]$$

$$k_{exp} = k_c[D]_o K / (1 + K[D]_o)$$

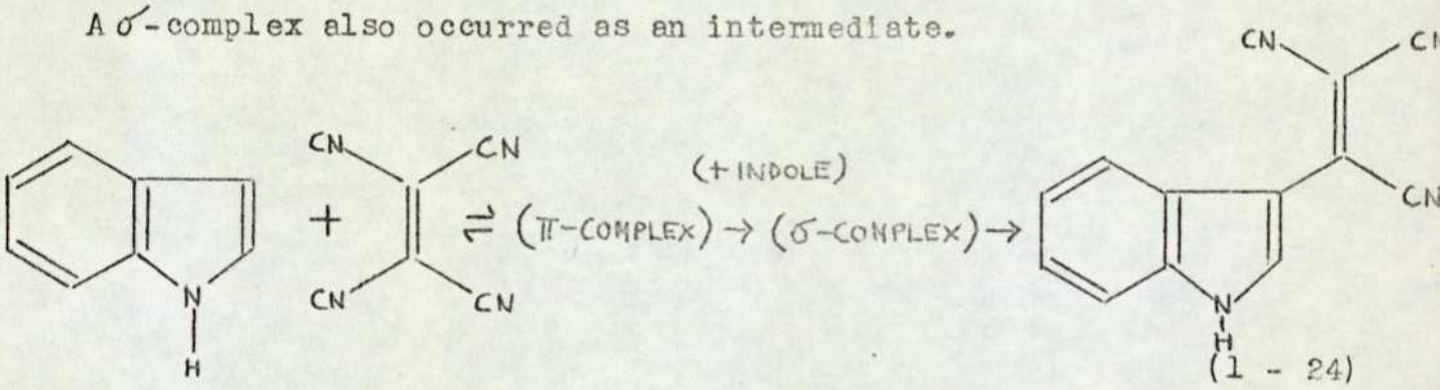
In this latter case the values of k_{exp} should increase with increase in donor concentration, which was the case for the N-N dimethylaniline reaction (1-20). On the basis of this, it was proposed that the donor was involved in the irreversible step from the charge-transfer complex to the intermediate, thus indicating a role for the former in reaction.

Controversy occurred over the actual structure of the intermediate, which was proposed as a zwitterion[80] or a bicyclo - 4,2,0 -octane derivative[86] and could be isolated as a solid.[87]

Recent evidence from infrared and kinetic isotope effects[87-89] indicate that both structures below may be formed reversibly.



Spectroscopic studies indicated the presence of a σ-complex between N-methylaniline and tetracyanoethylene,[84] and a σ-complex in the reaction between TCNE and 2,6-dimethylaniline having a similar structure.[85] In the reaction between indole and tetracyanoethylene a similar mechanism[79,82] was proposed on the basis of kinetic evidence, where K_{exp} increased with donor concentration. A σ-complex also occurred as an intermediate.



(1 - 24)

The decay of the σ-complex to the final product was very slow compared with the rest of reaction; (1 - 24) was a scheme which fitted the results fairly well.

In the cycloaddition reaction between 2,4-hexadienol and tetracyanoethylene[79] a reaction scheme similar to (1 - 23) was proposed on the basis of spectroscopic kinetic evidence.

Kinetic studies[124] on the reaction between maleic anhydride and anthracene in different solvents could not distinguish between (1 - 21) and (1 - 22), as k_{exp} decreased with donor concentration. It was suggested that the complex was an intermediate as it closely resembled the transition state of the reaction. Similar results were obtained in the reactions between 9 - bromo-and 9,10-dibromo-

anthracene with tetracyanoethylene.[91]

A further reaction in which (1 - 22) or (1 - 21) might operate was that between 2,3-dichloro-5,6-dicyano-p-benzoquinone (DDQ) with hexamethylbenzene.[92] More than one adduct was formed after addition had taken place at the termini of the quinone molecules.

The reaction between chloranil and N,N-dimethylaniline, in the absence of solvent, proceeded with the formation of a charge-transfer complex band (λ_{max} 650 nm).[93] This gave several products including crystal violet. On the basis of spectroscopic, electrical conductivity and E.S.R. measurements, the charge-transfer complex was thought to decompose to a radical amine cation and radical quinone anion. Charge-transfer complexes are also thought to be precursors in the formation of radicals in various polymerisation reactions, as for example, the reaction between N-vinylcarbazole and chloranil.[94]

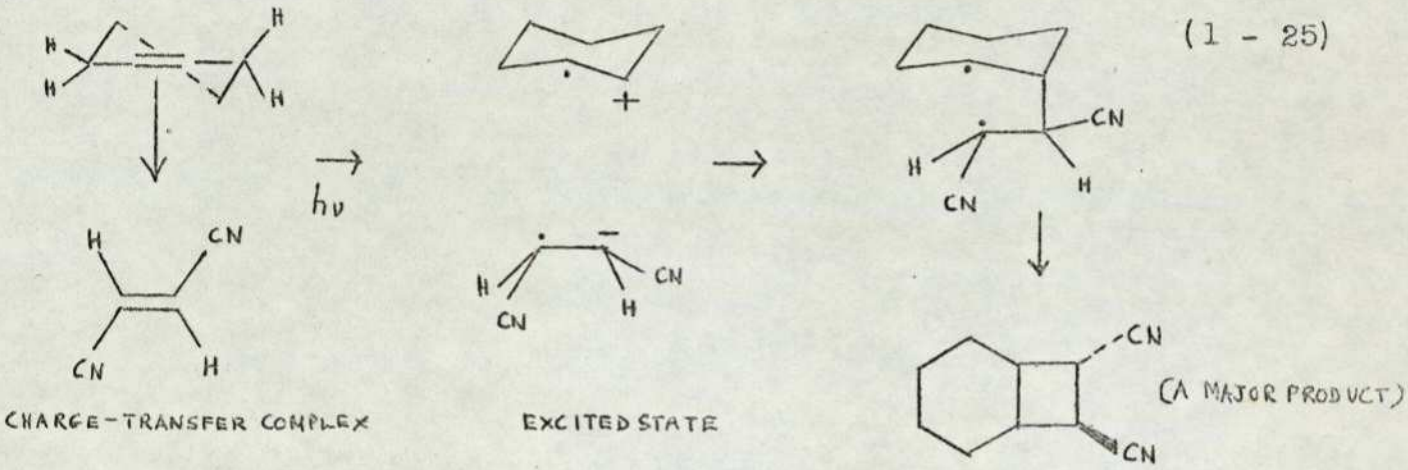
1 - 2 - 2 Photochemical Reactions which may proceed via a Charge-Transfer Complex.

The excited state of a charge-transfer complex as described by MO theory[9,10] has a significant contribution from a dative or ionic structure when an electron has been transferred from donor to acceptor.

If a charge-transfer complex is an intermediate in a photochemical reaction, then excitation of the molecule at the energy region of the charge-transfer band in the visible spectrum should excite the charge-transfer complex to a species which is an effective ionic complex. Thus in the reaction between cyclohexene and olefinic acceptors,[95] including tetracyanoethylene, irradiation of

the solution within the respective charge-transfer energy band gave products which indicate a (2 + 2) addition.

If the reaction is to pass through a charge-transfer complex, the most favourable arrangement is for the double bonds to lie parallel, one vertically above the other. In the case of fumaronitrile[95] the course of reaction may be:-



(1 - 25)

For the reaction between maleicanhydride and benzene to form the 2:1 adduct,[96] irradiation below 280nm results in reaction. Neither excited state benzene nor maleic anhydride absorbs in this region and it is possible that the reaction proceeds thus via the charge-transfer complex.

1 - 2 - 3 Biochemical Reactions which may pass through the Charge-Transfer Complex.

No clear evidence exists for a specific role played by charge-transfer complexes in biological reactions. The transfer of charge from one molecule to another could pass through such a complex and the fact that charge-transfer complexes are usually about 3.2 - 3.4Å apart facilitate interactions between mobile molecules over comparatively long separations. Such reactions as transfer of charge are vitally important in biochemical reactions, such as in photosynthesis and oxidative phosphorylation. Although charge-transfer complexes have been shown to be formed in biological

systems, the highly complicated nature of these systems has hindered the application of methods used to examine the possible role of the complexes in reaction. Spectroscopic measurements of charge-transfer bands are hindered by the likely presence of the component molecules of the complex having overlapping bands in that spectral region. Possible reactions proceeding through such complexes are those between indoles and hydrocarbons, as donors, and flavins, including riboflavin (Vitamin B_2) as acceptors.

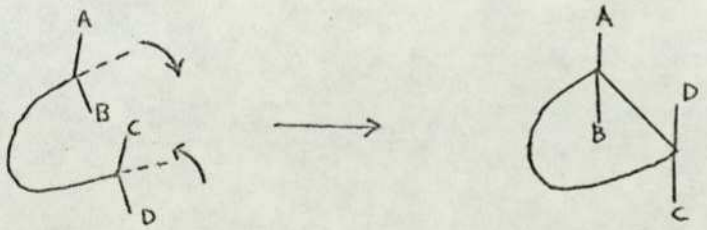
Evidence based on spectroscopy[97-99] suggests that a charge-transfer complex may be a precursor in the formation of flavin semi-quinones. Recently,[100] the formation of charge-transfer complexes as possible intermediates in the reaction between prolines and p-benzoquinone has been reported. In general, although charge-transfer complexes have been observed for a large number of donor-acceptor interactions such as nucleosides-chloranil, indoles-flavins, indoles-chloranil, porphyrins-trinitrobenzene, polycyclic hydrocarbons-proteins etc.[13,101] the possible role of the complexes in biological reactions of this nature is so far unproven.

1 - 3 Cycloaddition Reactions.

Interest in this important class of reaction has been revived in the past few years. This is mainly due to the formulation of the Woodward-Hoffmann rules[102-104] and the current development of techniques such as G.L.C. and N.M.R. spectroscopy, which have opened up the field and have led to the discovery of new reactions of this class. Recently, cycloaddition reactions have been considered as one of several types of reaction known as pericyclic reactions.[105]

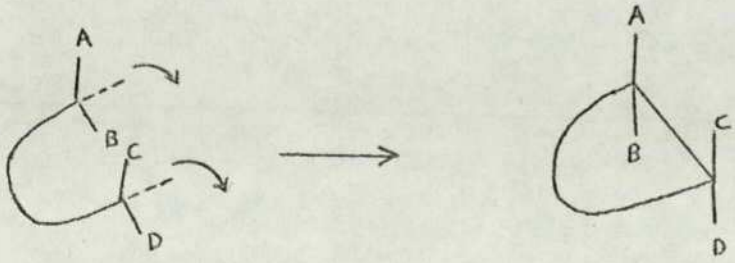
1 - 3 - 1 Woodward-Hoffmann Rules and MO Methods

Initially Woodward and Hoffmann[102-104] applied rules to electrocyclic reactions, which consisted of the formation or cleavage of a single bond between termini of a linear system containing π-electrons. They predicted the geometrical arrangement of the substituents of the products in terms of conrotatory or disrotatory movement of the termini. They based such predictions on the conservation of symmetry of orbitals during reaction or on the symmetry of the highest occupied molecular orbital of the reactant.



DISROTATORY

(1 - 26)



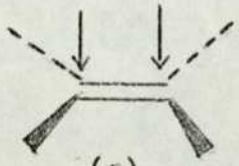
CONROTATORY

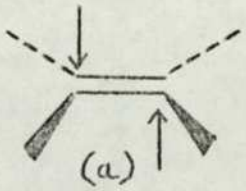
Table 1 - 1 Woodward-Hoffmann rules for cyclisation reactions.

No. of π electrons in system (n is any integer)	Thermally allowed, Photochemically forbidden	Thermally forbidden, Photochemically allowed
4n	Conrotatory	Disrotatory
4n + 2	Disrotatory	Conrotatory

For example, in the transformation of cyclobutene to butadiene there should be a conrotatory movement for a thermally allowed reaction.

Applying the same principle of conservation of orbital symmetry elements during the course of reaction, Woodward and Hoffmann derived rules for cycloaddition reactions[104] where two different π-systems reacted. In this case geometrical differences in the products arose from the two different geometrical types of cycloaddition, namely suprafacial and antarafacial cycloaddition. A suprafacial process is one in which bonds made or broken lie on the same face of the system undergoing reaction, whereas antarafacial processes occur when newly formed or broken bonds lie on opposite faces of the reacting system.



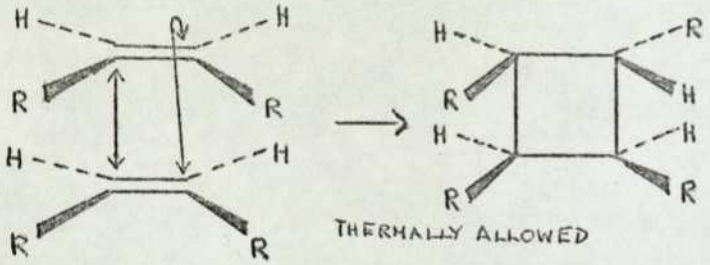


The test for whether suprafacial (s), or antarafacial (a) additions had taken place was to examine the configuration of the substituents in reactants and products.

Table 1 - 2 Woodward-Hoffmann rules for cycloadditions.

No. of π-electrons (p + q)	Thermally allowed Photochemically forbidden	Thermally forbidden Photochemically allowed
4n	$p_s + q_a$	$p_s + q_s$
	$p_a + q_s$	$p_a + q_a$
4n + 2	$p_s + q_s$	$p_s + q_a$
	$p_a + q_a$	$p_a + q_s$

In the possible (2 + 2) addition of substituted ethylenes to give a substituted cyclobutane, the Woodward-Hoffmann rules predict a $(\pi^2_s + \pi^2_a)$ cycloaddition. Whereas configuration is retained at the suprafacial centre, there is inversion at the carbon atom for antarafacial addition.



(1 - 27)

Cycloadditions as well as electrocyclic reactions, were considered by Frontier Orbital (FO) methods[106] which examine only the highest occupied molecular orbital (HOMO) and the lowest vacant molecular orbital (LVMO) of reactants. In the Diels-Alder reaction the symmetries of $(HOMO)_{diene}$ and $(LVMO)_{dienophile}$ were correlated during the course of reaction deriving modes of addition correctly predicted by the Woodward-Hoffmann rules.

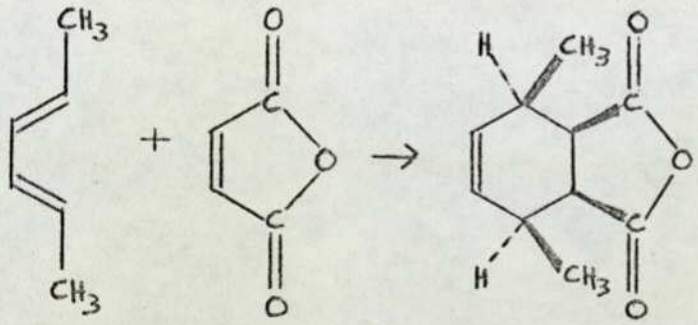
Another theory applied was the Perturbation Molecular Orbital theory (PMO)[105,107-109] in which energies of the molecular orbitals of the possible transition states of cycloadditions were calculated. This method has been used to describe the pathway of pericyclic reactions,[104,105] defined as concerted reactions involving transition

states, where all first-order bond changes occur on a closed curve. The PMO method has been used to examine whether the transition states for reaction are aromatic, non-aromatic or antiaromatic and hence to predict the structure of the products. For example, in the Diels-Alder reaction, for a $\pi 4_s + \pi 2_s$ cycloaddition, an aromatic transition state was predicted, leading to the (4 + 2) cycloadduct.

1 - 3 - 2 (4n + 2) Cycloadditions.

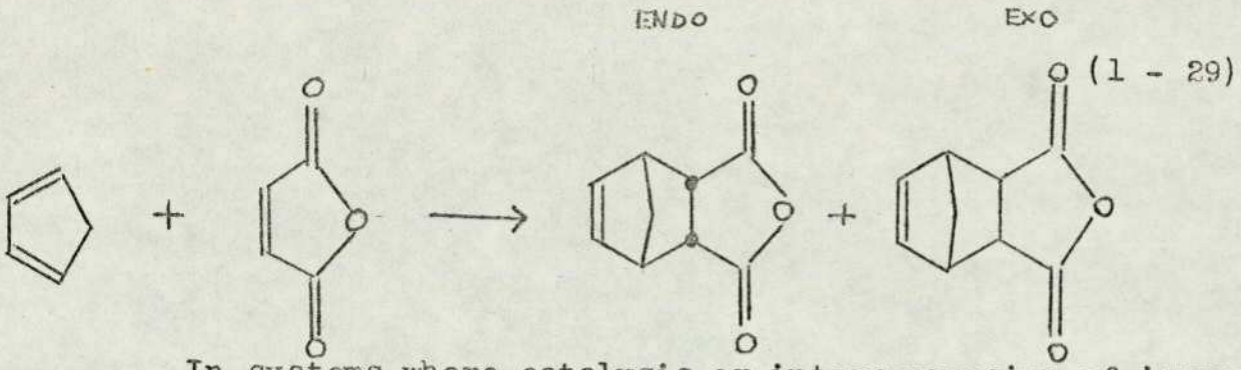
1 - 3 - 2 - 1 Diels-Alder Reactions.

The Diels-Alder reaction involves the 1,4-cycloaddition of an electron-deficient alkene (dienophile) to a conjugated diene.[110-115] The Woodward-Hoffmann rules predict that the reaction should be a thermally allowed suprafacial-suprafacial $\pi 4_s + \pi 2_s$ concerted cycloaddition and in practice this reaction always occurs in a cis-manner with the steric arrangement of substituents in diene and dienophile preserved in the 1:1 adduct. In the addition of trans-2, trans-4-hexadiene to maleic anhydride the all cis product is formed.



(1 - 28)

Another important feature of this reaction is the possible formation of exo or endo products. In practice it has been found that endo is almost exclusively formed,[116] even though it is thermodynamically less stable.



(1 - 29)

In systems where catalysis or interconversion of isomers is easy, the thermodynamically controlled exo isomer may be formed later. The endo effect has been explained[117] in terms of dipole-induced dipole forces between polar groups in dienophile and diene. More recently in an MO treatment,[103,104] symmetry controlled secondary orbital interactions in the transition state, which lowered its energy, were considered effective in producing the kinetically controlled endo product.

Electron donating groups attached to the diene and electron-withdrawing groups attached to the dienophile accelerate the reaction to a limited extent.[110,115] There is only a small positive solvent effect and a large negative entropy of activation ($\Delta S^{\ddagger} \simeq -40$ e.u.) indicating a high degree of ordering in the transition state. These findings point to a concerted mechanism in which the transition state has only a small separation of charge, rather than a two-step reaction involving a zwitterionic or biradical intermediate.[110,115,118,119]

This concerted mechanism, is also indicated by other methods such as PMO, in which a symmetrical aromatic cyclic transition state is more stable than a linear non-aromatic transition state which would occur in a two-step process.[105]

In 1942 Woodward[120] suggested that the charge-transfer complexes formed in solution were possible intermediates in the Diels-Alder reaction and their role has been discussed.[13,79,90,118,121-124] In one case, the reaction between trans 2,4-hexadienol and tetra-

cyanoethylene,[79] kinetic data suggested an involvement of the charge-transfer complex in reaction. From the results it was postulated that the complex reacted with donor to give the adduct (see Scheme 1 - 23).

In the reaction between anthracene and maleic anhydride to give the 9,10-adduct, kinetic studies of the disappearance of the charge-transfer complex during the course of reaction were carried out.[124] Using a large excess of maleic anhydride, it was concluded that the complex was either a direct intermediate or formed in a side-equilibrium (see Scheme 1 - 21 or 1 - 22). The small solvent effects and consistently large negative entropy of activation values obtained for this reaction and others similar[123] indicated a concerted mechanism for reaction between anthracene and dienophiles.

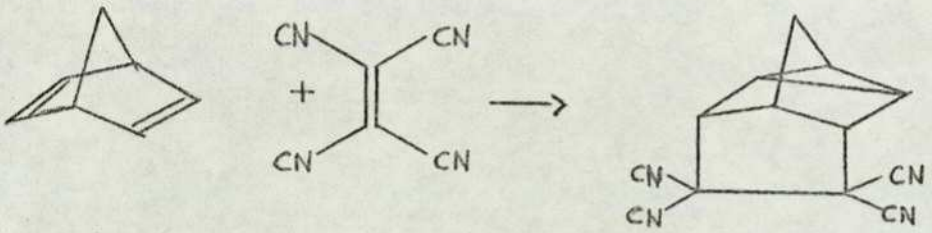
Tetracyanoethylene and 1 - substituted - 1 - (2 - naphthyl) - ethenes react to form Diels-Alder adducts and charge-transfer complexes occur during the course of reaction.[121,122] The kinetics of these reactions have been studied and association constants for the charge-transfer complexes measured. It was suggested that as a plot of log (association constant) versus log (rate constant) for reaction was approximately linear, some involvement of the complexes in reaction occurred.[122] Another study concluded that the charge-transfer complex in the reaction between vinylnaphthalene and tetracyanoethylene might be formed in a side-equilibrium.[121]

Although increase in donor strength of the diene and increase in acceptor strength of the dienophile favour rates of Diels-Alder reactions and charge-transfer complex formation, the role of the latter is still uncertain.

1 - 3 - 2 - 2 (2 + 2 + 2) Cycloadditions.

(2 + 2 + 2) cycloaddition reactions occur between three non-conjugated 2-electron systems, two of which may be in the same molecule as shown by the addition of tetracyanoethylene to norbornadiene to form tetracyanoquadricyclo $\left[2, 2, 1, 0^{2,6}\, 2^{3,5}\right]$ nonane.[125,126] (1 - 30).

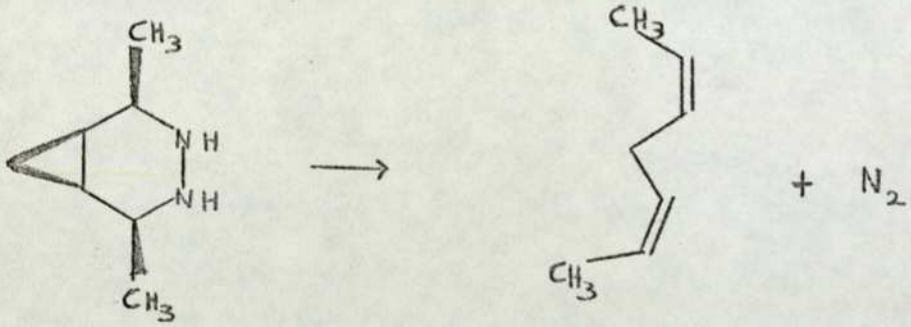
(1 - 30)



The thermally suprafacial ($\pi 2_s + \pi 2_s + \pi 2_s$) cycloaddition occurs as predicted, although there are two other thermally allowed ($\pi 2_s + \pi 2_a + \pi 2_a$) reactions possible.[104]

In the related (2 + 2 + 2) retroaddition from cyclic hydrazo compounds to heptadienes, the syn-cis compound shown in (1 - 31) produced the cis-cis heptadiene almost exclusively.

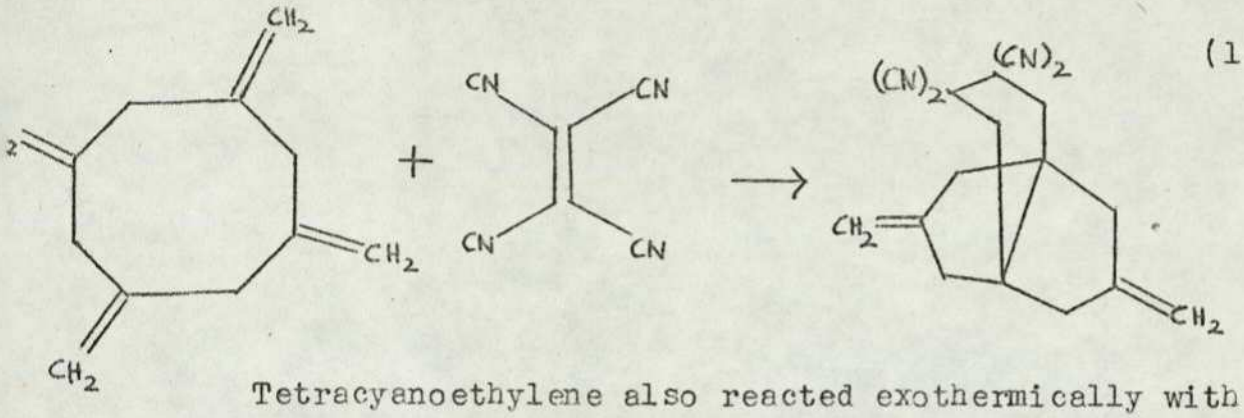
(1 - 31)



It was argued[127] that this stereospecific reaction was evidence for the preference of ($\pi 2_s + \pi 2_s + \pi 2_s$) reaction over the possible ($\pi 2_s + \pi 2_a + \pi 2_a$) reactions, and a concerted rather than two-step process.

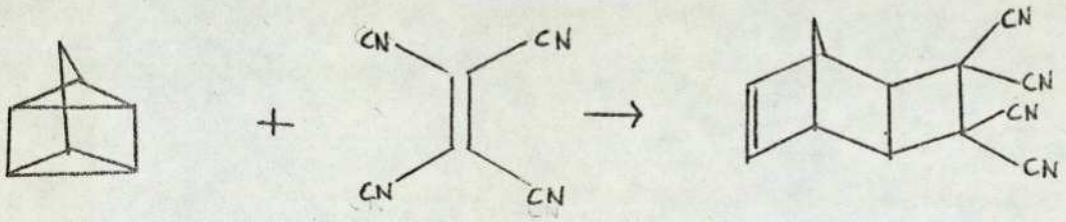
In the 1,7-cycloaddition reaction between tetracyanoethylene and 1, 3, 5, 7-tetramethylene cyclooctane[128] a colour attributable

to a charge-transfer complex was also formed in the solution.



(1 - 32)

Tetracyanoethylene also reacted exothermically with quadricyclane [129] to give the exo product via a ($\pi 2_s + \sigma 2_s + \sigma 2_s$) pathway.



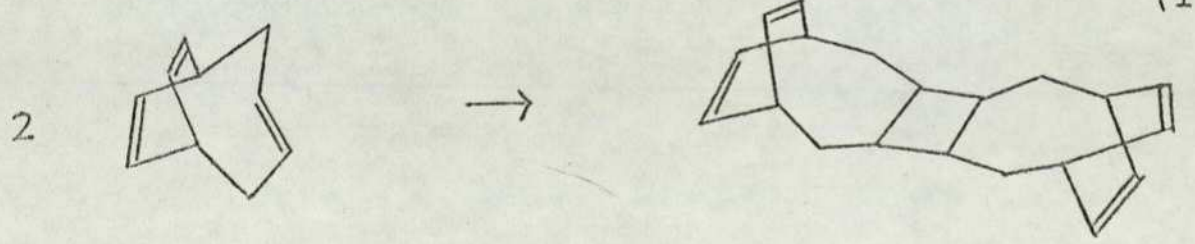
(1 - 33)

There is little evidence, so far, to suggest that charge-transfer complexes take part in this type of reaction.

1 - 3 - 3 4n Cycloadditions.

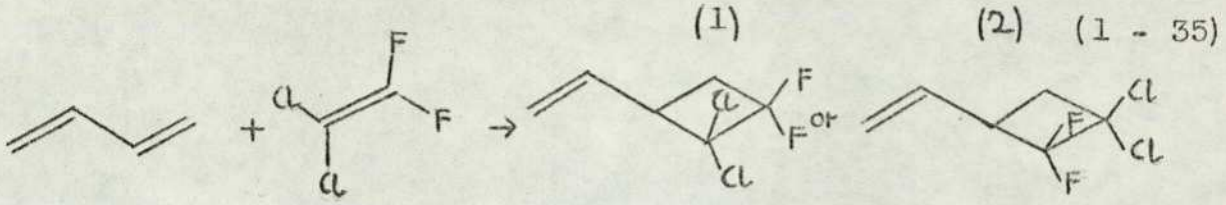
The Woodward-Hoffmann rules predict that for a reaction between two substituted ethylenes, a thermal $\pi 2_s + \pi 2_s$ addition is forbidden but photochemically permitted, whereas a $\pi 2_s + \pi 2_a$ thermal addition is permitted. One of the few examples of such a reaction is the dimerisation of the bicyclodecatriene to its dimer.[130]

(1 - 34)



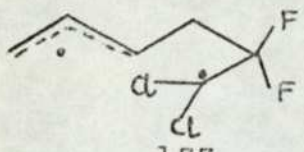
Radical intermediates have been postulated in (2 + 2) cyclo-

additions.[131-136] In the addition of 1,1-dichloro-2,2-difluoroethylene to transoid butadienes, the product (1) was almost exclusively formed.[132]



In a concerted mechanism a mixture of both compounds might be expected. It is known that a radical stabilized by chlorine atoms is more stable than one with fluorine atoms, so the biradical shown was postulated as an intermediate.

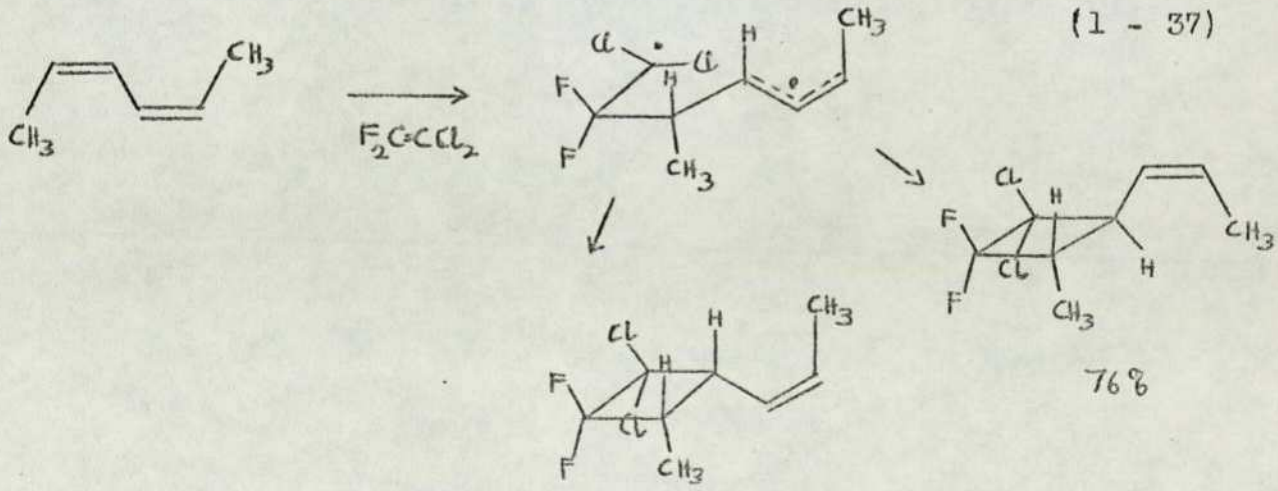
(1 - 36)



The same arguments were applied[133] to the reaction between two acrylonitrile molecules in which only specific products were formed.

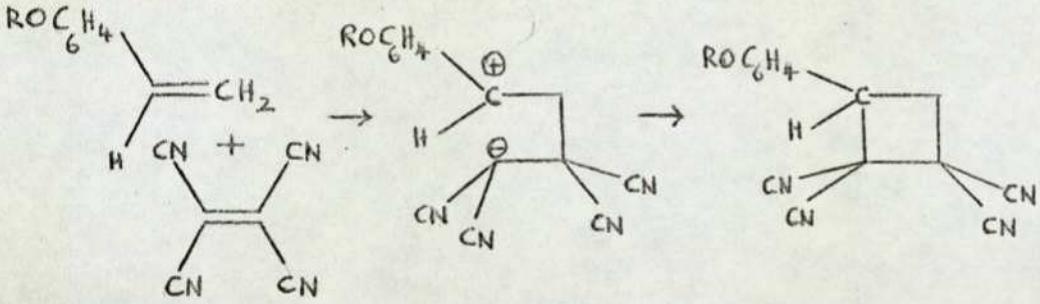
An important factor considered in related reactions was the possible rotation of substituents about a C-C single bond in the intermediate diradical, competing with the ring closure reaction. This would lead to a loss of stereoselectivity, which would never occur in a concerted reaction, as shown[131] by reaction between isomers of hexadiene and dichlorodifluoroethylene.

(1 - 37)



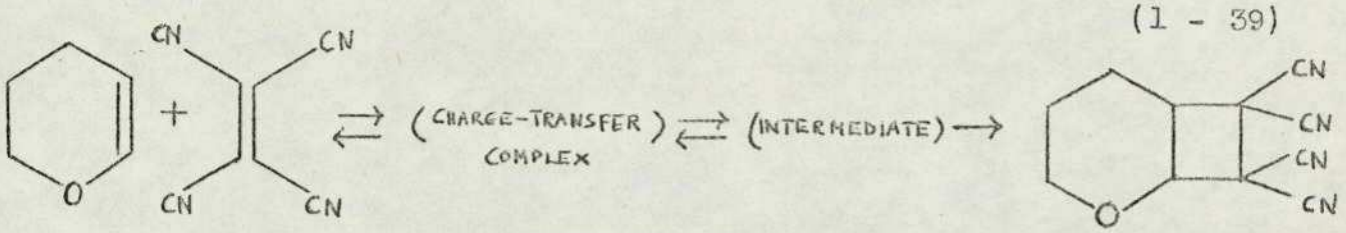
In the formation of four-membered rings from ketenes and substituted olefins, the high negative entropy of activation and slight dependence of rate on solvent polarity[137,138] indicate a concerted reaction as does recent evidence from reactions between dimethylketenes and various olefins,[139] in which a ($\pi 2_s + \pi 2_a$) pathway is postulated.

Tetracyanoethylene reacts with alkenes to give charge-transfer complexes which fade as the reaction proceeds, forming the cyclobutane derivatives.[140] Rate studies of the reaction between tetracyanoethylene and p-alkoxystyrene showed[136] that the rate was very sensitive to solvent polarity. The thermal ($\pi 2_s + \pi 2_s$) cycloaddition is thermally forbidden and the ($\pi 2_s + \pi 2_a$) addition rarely occurs. It was thus suggested that an intermediate zwitterion was formed as shown:



(1 - 38)

A general mechanism has been proposed[8] for the reaction between tetracyanoethylene and vinylethers, involving initial formation of a charge-transfer complex, followed by electron-transfer and subsequent formation of an ionic structure, before forming the product. In the reaction between dihydropyran and tetracyanoethylene,[121] a second equilibrium after formation of the complex was postulated, prior to the reaction giving the cyclobutane product, in order to explain the initial rapid disappearance of the tetracyanoethylene.



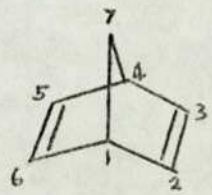
(1 - 39)

A study of the cyclobutane adduct formed from anethole[79] and tetracyanoethylene showed that there was a small decrease in rate with increasing donor concentration, suggesting that the charge-transfer complex was formed in a side-equilibrium as in scheme (1 - 22).

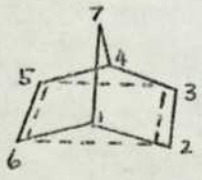
1 - 4 - 1 Bicyclo [2, 2, 1] hepta-2, 5-diene (Norbornadiene).

This is a bicyclic non-conjugated diene, prepared by dechlorination of 5,6-dichloro-2-norbornene.[141] A comparison[142] of the ultraviolet spectra of samples of bicycloheptene (λ_{max} 195nm) and bicycloheptadiene (λ_{max} 205, 214, 220 and 230nm) in ethanol indicates some degree of homoallylic resonance between the two ethylene groups in the latter.

Calculations showed[142,143] that the Kekulé structure for bicycloheptadiene in the ground state was essentially correct, whereas in the excited state, there was interaction between atoms 2, 6 and 3, 5.



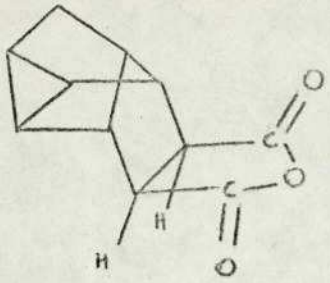
GROUND STATE



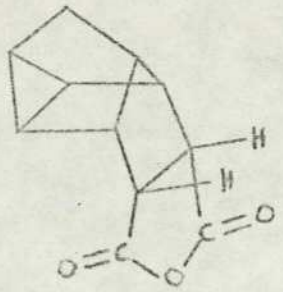
EXCITED STATE

Norbornadiene reacts with dienophiles such as maleic anhydride[144] in which either the endo or exo product could theoretically be formed. It has been shown that, in fact, the endo product is almost exclusively formed,[145] as in the usual Diels-Alder addition.

EXO ADDUCT

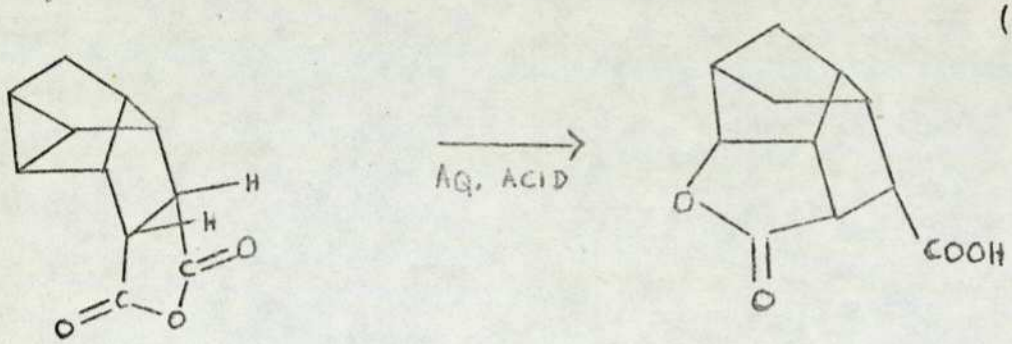


ENDO ADDUCT



The endo adduct formed was shown to form an internal lactone, impossible to obtain with an exo adduct.

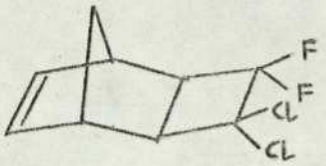
(1 - 40)



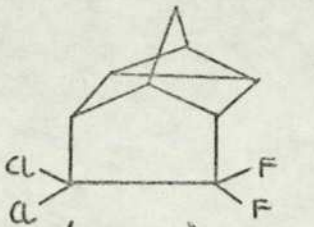
The kinetics of addition of tetracyanoethylene to bicycloheptadiene to give 8,8,9,9-tetracyanoquadricyclo $[2,2,1,0^{2,6}2^{3,5}]$ nonane (section 1 - 3 - 2 - 2) have been studied.[146] Solvent effects and the possibility of dipolar intermediates were examined, but complications arose from the fact that complexing occurred with the mainly aromatic solvents, effectively removing some of the dienophile from the reaction. The general conclusions reached were that although the rate of reaction increased with increase in solvent polarity, this was not sufficient to postulate a dipolar transition state, but only one in which some polarisation had occurred. A large negative entropy of activation (-30 e.u.) was found, consistent with values for most Diels-Alder reactions.

Competition between a (2 + 2) and $(\pi 2_s + \pi 2_s + \pi 2_s)$ cycloaddition apparently occurs in the reaction between bicycloheptadiene and 1,1-dichlorodifluoroethylene.[147] In this case, the (2 + 2)

cycloadduct is formed in greater yield, indicating a possible preference for exo attack on the ring.



(2+2) ADDUCT



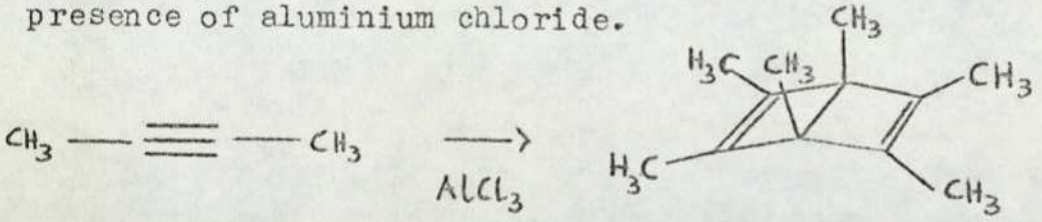
(2+2+2) ADDUCT

Although charge-transfer complexes have been observed in reactions between bicycloheptadiene and dienophiles, their role in reaction has not yet been elucidated.

1 - 4 - 2 Hexamethylbicyclo [2,2,0] hexadiene (hexamethyl Dewar benzene.

The first substituted Dewar benzene was synthesised in 1962[148] by photoisomerisation of tri-t-butyl benzene.

Hexamethyl Dewar benzene was recently satisfactorily synthesised[149] by catalytic trimerisation of 2-butyne in the presence of aluminium chloride.

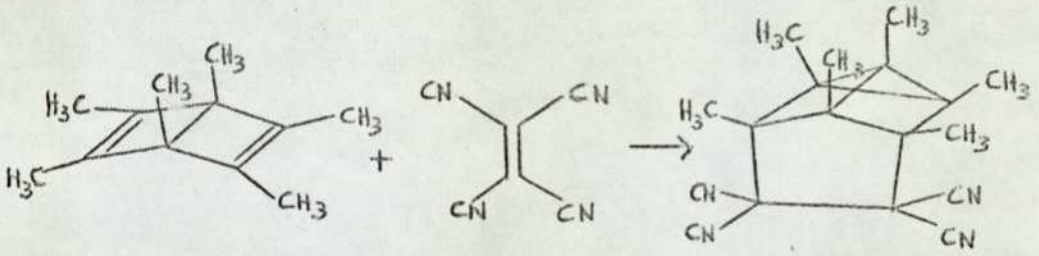


(1 - 41)

This compound can be considered analogous to a substituted bicycloheptadiene. Interesting features of this molecule are the very long bond-length (1.63Å) of the bridging bond, determined[150] by gas-phase electron diffraction, and the fact that the activation energy of the thermal rearrangement of cis-hexamethyl Dewar benzene to hexamethyl benzene is 37 Kcal/mole[151] even though the latter is thermodynamically more stable by 65 Kcal/mole. The disrotatory

cleavage of the central bond is symmetry-forbidden by the Woodward-Hoffmann rules[104] and this may well account for the large activation energy in which the reactant passes by a concerted process to the substituted benzene. The formation of a skewed intermediate was not excluded as a possibility for the reaction. A trans-hexamethyl Dewar benzene would appear to be too unstable to exist as this would pass by a symmetry-allowed process to the substituted benzene.

The double bonds in this molecule appear to be well placed for concerted ($\pi 2_s + \pi 2_s + \pi 2_s$) cycloaddition with dienophiles. Tetracyanoethylene was reported[152] to react with hexamethyl Dewar benzene to give the quadri-cyclooctane adduct, analogous to substituted norbornadienes.

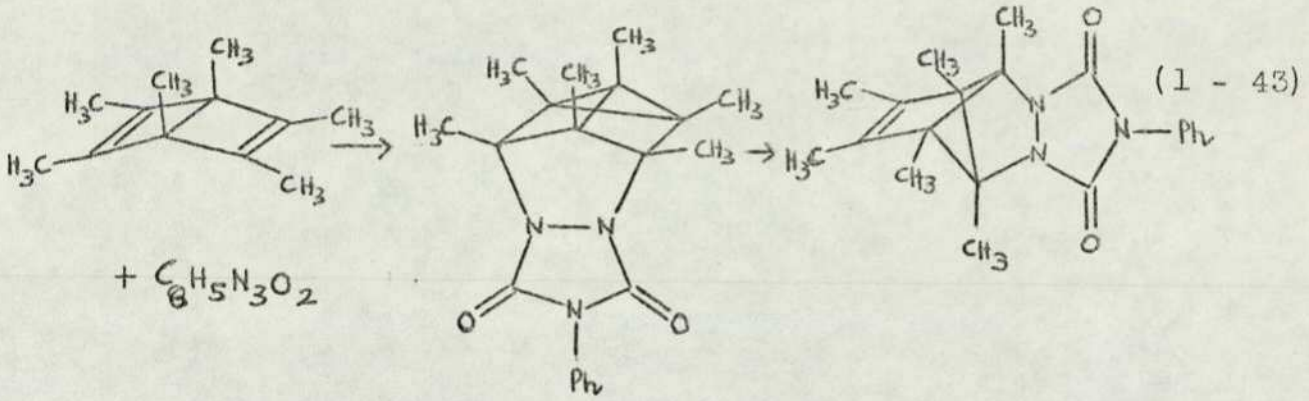


(1 - 42)

However, for reactions with other dienophiles there appear to be divergent directions of attack on the hydrocarbon. For instance, whereas addition of chlorosulphonyl isocyanate to hexamethyl Dewar benzene appears to proceed by preferential endo attack to give a rearranged product,[153] the dipolar species, phenyl azide[154] and ethyl N-sulphonyl carbamate[155], appear to bond initially on the exo face, the latter reaction product rearranging.

A rearranged product is also obtained in the reaction with the strong dienophile, 4-phenyl-1,2,4-triazoline-3,5-diene in polar solvents.[152,156] It was proposed that the ($\pi 2_s + \pi 2_s + \pi 2_s$) adduct, whose structure was assigned on the basis of its N.M.R.

spectrum, was formed as an intermediate, and this then rearranged to the final product.



The reasons for the different directions of attack of electrophiles and dipolar species on hexamethyl Dewar benzene are not yet fully understood.

1 - 4 - 3 Tetracyanoethylene.

Tetracyanoethylene was the first percyanoölefin to be prepared by Cairns and his co-workers in 1957.[157,158] The main method used was the chlorination-dehydrochlorination of malononitrile. Tetracyanoethylene is one of the strongest electron acceptors known and reacts with a wide range of electron donor compounds including dienes,[158-160] aromatic compounds,[123,146] nitrogen compounds[79-85,161] and forms cyclobutane (2 + 2) derivatives with olefins.[162] It rapidly forms coloured charge-transfer complexes with a wide range of compounds.[10,13,163-166] Recently the rate of formation of the complex between tetra cyanoethylene and hexamethyl benzene was determined[12] by a temperature-jump method.

1 - 5 Nuclear Magnetic Resonance Studies.

1 - 5 - 1 Nuclear Magnetic Double Resonance.

Considerable progress has been made recently in the development and application of double and multiple resonance methods since their original discovery in 1954.[167,168] Double resonance leading to spin decoupling can lead to an analysis of complex spectra, especially in overlapping multiplet systems, detection of hidden resonances, accurate determination of coupling constants and a determination of the relative signs of the latter in suitable cases.[169-177] In general, in double resonance experiments, transitions between energy levels of a nuclear spin system in a static magnetic field, H_o, are measured in the presence of two oscillating magnetic fields H_1 and H_2. H_1 is used to observe the resonance of one type of nucleus and H_2 for the perturbation of a second type of nucleus. In proton spin decoupling, used in this study, irradiation of one nucleus leads to a change in the observed signal of the other nucleus as the spin-spin coupling between the two is removed. This technique has been used in many instances for homonuclear and heteronuclear systems, but the cases of special interest for this survey are those in which cyclo-adducts of Diels-Alder reactions have been examined to determine their structure and stereochemistry. (see Section 1 - 5 - 4)

1 - 5 - 2 The Karplus Equations and their Application to Elucidation of Structure.

Using a valence-bond method in 1959, Karplus[178] predicted an approximate relationship between the dihedral angle ϕ and vicinal coupling constant $J_{H-C-C-H}$, in ethanic and ethylenic molecules. This usually takes the form:

$$J = J_o \cos^2\phi - 0.3 \quad [0^\circ \leq \phi \leq 90^\circ] \qquad (1 - 44)$$
$$J = J_{180} \cos^2\phi - 0.3 \quad [90^\circ \leq \phi \leq 180^\circ]$$

J_o and J_{180} in the original equations had values of 8.5 and 9.5 respectively, but other constants have been used, as for example in carbohydrate structure determination.[179]

It has been shown[180-184] that the Karplus rules are modified by such factors as electronegativity of substituents, hybridisation of the carbon atoms, bond lengths and non-vicinal bond angles. For example, it has been shown that electronegative substituents attached to the fragment H_A-C-C-H_B tend to lower the coupling constant J_{AB}.[183,184] It has been suggested[185,186] that for sp^2 hybridisation of one of the carbon atoms as in the fragment H_A-C-C (H_B)$=$, there may be some π-contribution to the vicinal coupling. However, other conclusions[187,188] and recent theoretical studies[189] suggest that such a system is closely analogous to a fully saturated one and obeys a Karplus-type relationship.

An adaptation of the Karplus equations has been made[190] assuming that the ratio of the constants J_o/J_{180} is approximately 0.9. It has been postulated that electronegativity effects do not influence dihedral angle calculations to the same extent using this method.

The Karplus equations have been used[191] in the determination of the conformation of shikimic acid, a substituted cyclohexene. A comparison of dihedral angles measured from models with those calculated from the Karplus equations after derivation of coupling constants from the spectrum, indicated that shikimic acid existed in a half-chair rather than a boat conformation. A similar method was used[192] in structure determination of 6-substituted 1-phenyl

cyclohexenes, when it was concluded that the half-chair conformation was also adopted by such compounds.

1 - 5 - 3 N.M.R. Lanthanide Shift Reagents.

Although the effect of paramagnetic components on N.M.R. resonances have been studied from about 1948,[193] it is only recently that paramagnetic compounds have been systematically used in structure elucidation of organic molecules.

The first lanthanide compound reported[194] to cause a large shift without line broadening or spin-spin coupling distortion was tris (2,2,6,6-tetramethyl-3,5-heptanedionato) Europium III ($Eu(dpm)_3$). Large shifts were produced in the proton resonances of cholesterol when the dipyridine adduct of the above compound was added to the solution.

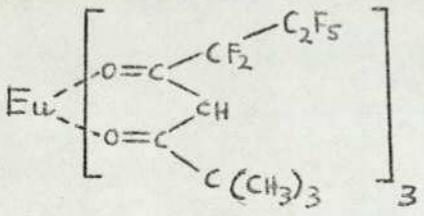
Although many metal complexes can cause chemical shift changes, these lanthanide compounds are inefficient in terms of spin-lattice relaxation and so no excessive line-broadening occurs. The lanthanide ions in these complexes can increase their coordination number by interaction with lone electron-pairs in the organic donor substrates. Thus, organic compounds which show these shifts usually have lone electron-pairs as in alcohols, amines, ketones, and esters.

The action of the shift reagent is attributed[195] to a through-space dipolar or pseudocontact interaction, in which the shift of a particular nucleus is proportional to r^{-3}, where r is the distance between the metal ion and the nucleus under observation.

Other lanthanide shift reagents have been studied[196,197] and it appears that complexes of Europium, Erbium and Thulium shift N.M.R. resonances to lower field while complexes of Praseodymium,

Neodymium and Samarium shift the resonances to higher field.

Other complexes of Europium and Praseodymium having 1,1,1,2,2,3,3-heptafluoro-7,7-dimethyl-4,6-octane dione ligands have been used,[198] as $Eu(fod)_3$ and $Pr(fod)_3$ are more soluble than the corresponding $Eu(dpm)_3$ and $Pr(dpm)_3$ in non-polar solvents and they produce greater proton shifts in weak Lewis bases such as ethers and esters. For example, $Eu(fod)_3$ greatly simplified the N.M.R. spectrum of di-n-butyl ether in CCl_4, a weak Lewis base, whereas use of $Eu(dpm)_3$ was comparatively ineffective.

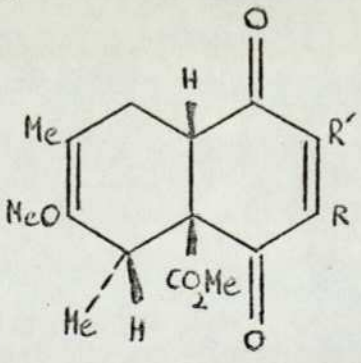


$Eu(fod)_3$

1 - 5 - 4 N.M.R. Applications to Structures of Cycloadducts.

Although N.M.R. has been used in a number of cases for the elucidation of the structure of cyclic compounds, a few cases are given here as they are related to compounds in this study.

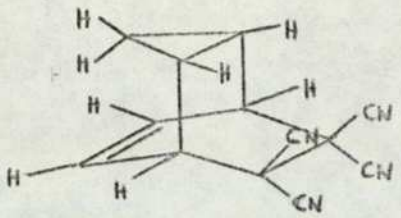
In studies[199] of products of reaction between 3-methoxy-2-methylpenta-1,3-diene and some methoxycarbonylbenzoquinones the Karplus relations were used to establish dihedral angles, and double resonance decoupling was used to clarify chemical shifts and coupling constants. It was concluded that the adduct shown below existed in the syn-cis, rather than the syn-trans or anti-trans configurations.



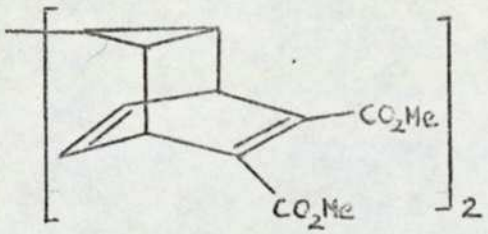
SYN-CIS

It was also deduced that in the formation of the adduct, endo addition had taken place.

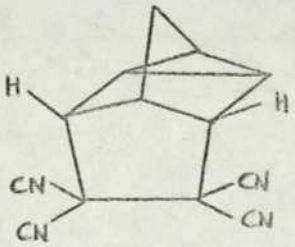
In the Diels-Alder adduct of cycloheptatriene and tetracyanoethylene it was shown[200] that the tricyclic structure was present. Double resonance irradiation of the bridgehead protons established the assignments in the cyclopropane ring.



In a related N.M.R. study, the Diels-Alder adduct of ditropyl and dimethyl acetylene dicarboxylate was examined.[201] Double resonance irradiations were used to clarify assignments in the spectrum and the following structure was deduced.



The N.M.R. spectrum of the adduct of norbornadiene and tetracyanoethylene has been reported.[202] The low field signal was assigned to the protons adjacent to the cyanogroups, and appeared to be sensitive to solvent. In deuteroacetone a downfield shift was observed, relative to deuterochloroform. This was attributed to interaction between acetone and the cyano groups, making the latter more electronegative.



CHAPTER 2

Experimental Methods

2 - 1 General Methods

2 - 1 - 1 Melting Points. All measurements are corrected and were made using a Kofler hot stage microscope supplied by the Shandon Scientific Instrument Co. Ltd.

2 - 1 - 2 Carbon, Hydrogen and Nitrogen Analysis.

The analyses were carried out using a F.&M. Model 185 C-H-N Analyser.

2 - 1 - 3 Gas-Liquid Chromotography.

A Griffin and George D.6 Gas Chromatograph fitted with a 2 metre column containing 20% (4:1 polyethylene glycol (400): dinonylphthalate) on celite was used initially. In addition, a Pye Series 104 Chromatograph with a flame-ionisation detector was later used. The columns fitted to the latter instrument contained either Silicone SE30 or Carbowax 20M, the latter being found more effective for polar separations.

2 - 1 - 4 Thin Layer Chromatography.

In most cases the analysis of solids by this method was carried out using Eastman Kodak Silica Gel Chromagram (6060) (stationary phase) strips which were examined under a U.V light (254/350 nm) to show up the spots. In some cases the spots were developed by placing the strips in an iodine tank. For most of the T.L.C.studies the solvent (moving phase) was a mixture of chloroform and carbon tetrachloride in varying proportions.

2 - 1 - 5 Purification of Solvents.

2 - 1 - 5 - 1 Chloroform.

In order to remove the ethanol stabilizer from commercial chloroform

a given volume of the spectroscopic grade solvent (supplied by B.D.H. Chemicals Ltd.), was shaken up five times with half its volume of distilled water. This was then dried first with anhydrous potassium carbonate and then for 24 hours with phosphorus pentoxide. The solvent was finally distilled and stored in a refrigerator in a light-protected bottle. Most of the chloroform purified this way was used within a few days of the distillation.

2 - 1 - 5 - 2 Dichloromethane and 1,2-Dichloroethane.

Both of these solvents were supplied as spectroscopy grade by B.D.H. Chemicals Ltd. In most cases the solvents were distilled first from anhydrous potassium carbonate, then from phosphorus pentoxide and finally redistilled. The solvents were stored in light-protected bottles. An alternative method of purification was to pass the solvent through a column of activated alumina immediately before use.

For all kinetic studies, solvents were purged with nitrogen before use.

2 - 2 Spectroscopic Methods.

2 - 2 - 1 Ultraviolet/Visible Spectroscopy.

The following UV/Visible recording spectrophotometer models were used. (1) A Perkin-Elmer-Hitachi EPS-3T, (2) A Unicam SP1800, (3) A Perkin-Elmer UV 137. The first instrument, in which two cells were fitted, was thermostatted by means of a water circulation system from a Shandon controller, which was accurate to the order of $\pm$ 0.1 to 0.2°C.

Matched silica cells having path-lengths of 1cm. or 1mm. were used in all cases. At low temperatures it was necessary to pass dry

nitrogen through the cell-housing to prevent condensation occurring on the face of the cells.

The Unicam SP1800 was used primarily with four pairs of cells, having an automatic repetitive scanning arrangement from one pair of cells to another at given time intervals. 1cm. cells were thus placed in the cell-housing which was thermostatted in the same way as for the first instrument.

For the case where 4cm. cells were used, only one pair of cell-housings was fitted in the instrument, which was thermostatted either by a water-circulation or electric thermostat system.

The third instrument was used only for initial quantitative studies.

2 - 2 - 2 Infrared Spectroscopy.

A Perkin-Elmer Infracord Spectrometer was used in nearly all cases. The spectra of the samples were run in the solid state either in the form of a KBr disc or as a suspension in a mull. In the first case about 5mg/100mg of sample/KBr was ground up and a thin disc was formed in a minipress, used for this purpose. An attenuator was placed in the reference beam of the instrument to obtain a suitable spectrum intensity. The solid samples were mulled using either nujol or hexachlorobutadiene. Calibrations were carried out using a polystyrene sheet.

2 - 2 - 3 Mass Spectrometry.

Accurate mass measurements and fragmentation spectra were obtained from the Physico-Chemical Measurement Unit, using an A.E.1 MS 902 spectrometer. The electron energy was 70 eV.

2 - 2 - 4 Nuclear Magnetic Resonance Spectroscopy.

2 - 2 - 4 - 1 Instruments. The following spectrometers were used during the course of the study. (1) Perkin-Elmer 60 MHz R.10

Spectrometer, (2) Physico-Chemical Measurement Unit's 100 MHz Varian HA-100D Spectrometer and (3) 220 MHz Varian HR-220 spectrometer. The first spectrometer was used to obtain only quantitative initial spectra, whereas all the homonuclear double resonance experiments and application of shift reagents were carried out using the 100 MHz or 220 MHz instruments. All spectra were standardized using tetramethylsilane to provide the lock signal.

2 - 2 - 4 - 2 Reagents.

Deuterochloroform used for the Perkin-Elmer R.10 experiments and the lanthanide shift reagent, $Eu(fod)_3$, were supplied by B.D.H. Chemicals Ltd.

Tetramethylsilane for the lock signal was supplied by Aldrich Chemical Co. Ltd.

2 - 2 - 4 - 3 Experimental.

In initial experiments using the 60 MHz R.10 instrument, about 50mg. of the sample was dissolved in about 1ml. of solvent in an N.M.R. tube. A drop or two of tetramethylsilane was added to the solution, before it was placed in the magnetic field.

CHAPTER 3

Nuclear Magnetic Resonance Studies of Cycloadducts and Related Compounds.

3 - 1 Introduction.

The N.M.R. spectra of certain Diels-Alder cycloadducts and other related compounds were examined.

Because of the ambiguities and uncertainties in the simple spectra of these adducts, it was decided to use double resonance and addition of shift reagent methods in order to elucidate the chemical shifts, analyse the splitting patterns and hence evaluate spin-coupling constants. In many cases it was possible to shed light on the conformation of the adducts in solution by application of the Karplus equation and other related methods. No effects due to conformational inversions were taken into account as it was generally assumed that the arrangement of substituents was such as to make one conformation more stable than the others. The Karplus equation was used without correcting for electronegativities of the substituents attached to the vicinal fragments.

3 - 2 Preparation of Adducts.

The preparation of the adducts of norbornadiene/TCNE, hexamethyl Dewarbenzene/TCNE, hexa-trans-2,trans-4-diene/maleic anhydride, 1-methoxybutadiene/maleic anhydride, anthracene/maleic anhydride and indole/TCNE are described in Chapters 4,5,6,7,8 and 9 respectively.

3 - 2 - 1 Hexa-trans-2,trans-4-diene/TCNE adduct.

Commercial hexadiene was first purified by distillation to give one peak only in the G.L.C. The purified donor (0.6ml) was then added to TCNE (0.5g) in dichloromethane (15ml), the solution shaken thoroughly and allowed to stand for 30 minutes until the purple colour had disappeared. The solvent was removed by evaporation and the crude

solid was washed twice with carbon tetrachloride. Recrystallisation twice from a mixture of dichloromethane/carbon tetrachloride yielded colourless crystals. m.p.124.5-125.5°C (lit.[203] = 126.5-127.5°C).

3 - 2 - 2 1-Methoxybuta-trans-1,3-diene/TCNE adduct.

Purified 1-methoxybuta-trans-1,3-diene (1 ml) was added to TCNE (0.4g) in dichloromethane (20 ml). The mixture was refluxed for 30 minutes and the solvent then removed by evaporation to yield a greenish solid. Recrystallisation from dichloromethane/carbon tetrachloride using decolourising charcoal yielded colourless crystals. m.p. = 110 -111°C.

3 - 2 - 3 1,4-Diphenylbuta-trans-1,trans-3-diene/TCNE adduct.

Recrystallised diphenyl butadiene (1g) in dichloromethane was added to a solution of TCNE (0.5g) in the same solvent. The mixture was shaken until the blue colour had disappeared. After standing for 30 minutes, the solvent was removed by evaporation and the crude solid washed with carbon tetrachloride. Recrystallisation twice from carbon tetrachloride/dichloromethane yielded colourless crystals. m.p. = 214 -215°C (lit.[79] 205°C).

3 - 2 - 4 Hexa-trans-2,trans-4-dienol/TCNE adduct.

A commercial sample of hexa-trans-2,trans-4-dienol was shown by G.L.C. to be impure and was distilled under vacuum to give a colourless liquid. Analysis by G.L.C. showed a purity of about 99%. A solution of TCNE (0.5g) in dichloromethane (50 ml) was added to hexa-trans-2,trans-4-dienol (1.0g) in dichloromethane (5 ml). The mixture was shaken until the red colour formed on mixing had disappeared, and allowed to stand for 1 hour. The solvent was removed by evaporation and the crude yellow solid was recrystallised twice from carbon tetrachloride/dichloromethane to yield colourless crystals. m.p. = 184 -185°C (lit.[79] 185°C).

3 - 2 - 5 2-Methylpenta-1,trans-3-diene/TCNE adduct.

2-Methylpenta-1,trans-3-diene (1ml) was added to TCNE (0.5g) in dichloromethane (25ml) and the mixture was kept in an ice-bath under dry nitrogen for two hours with continuous stirring. Evaporation of the solvent yielded the crude solid which was recrystallised from a mixture of petroleum ether and dichloromethane (50/50 by volume) to give crystals of the adduct. m.p. = 59.5-61.5°C (lit.[203] 62-63°C).

3 - 2 - 6 2-Vinylnaphthalene/TCNE adduct.

2-Vinylnaphthalene (0.2g) was added to a solution of TCNE (0.2g) in dichloromethane (20ml), the mixture shaken and allowed to stand for 2 hours until the blue colour formed on mixing had disappeared. The solvent was then removed by evaporation and the crude solid was washed with a little dichloromethane and decanted. Recrystallisation twice from chloroform yielded colourless crystals. m.p. = 166-167.5°C (lit.[121] 168-170°C).

3 - 2 - 7 Cyclohexa-1,3-diene/TCNE adduct.

Cyclohexa-1,3-diene (1g) was added to a solution of TCNE (0.5g) in dichloromethane. The mixture was shaken and allowed to stand for 1 hour. The solvent was removed by evaporation and the crude solid was recrystallised from chloroform to yield colourless needles of the adduct. m.p., phase changes at 170° and 235° with eventual melting at around 300°C (lit.[159] >300°C in sealed capillary tube.)

3 - 2 - 8 α-Phellandrene/TCNE adduct.

Commercial α-phellandrene was shown by G.L.C. to be impure and the sample was therefore repeatedly distilled under N_2 until an improvement in purity was shown, (not greater than 90% possible). A solution of α-phellandrene (0.7g) in dichloromethane was added to TCNE (0.5g) in solution and the mixture was refluxed for 2 hours.

The solvent was removed by evaporation to about half-volume, carbon tetrachloride added and the solvent further removed by evaporation to give brown crystals. Recrystallisation twice from a mixture of petroleum ether (40°-60°) and dichloromethane (1:1) gave colourless crystals. m.p. 120-121°C (lit.[159] 119-120°C).

3 - 2 - 9 Anthracene/TCNE adduct.

Anthracene (0.7g) was added to a solution of TCNE (0.5g) in dichloromethane and the mixture thoroughly shaken. The solution was refluxed for ten minutes and then allowed to cool. The adduct slowly precipitated and was filtered and dried. Recrystallisation from acetone yielded colourless crystals. m.p. 268-270°C (lit.[159] 268-270°C in sealed tube).

3 - 2 - 10 1,2-Dimethylindole/TCNE adduct.

1,2-dimethylindole (0.7g) in benzene (10ml) was added to a solution of TCNE (0.6g) in benzene (40 ml) and an immediate formation of a blue-black colour was observed. The reaction mixture was thoroughly shaken and allowed to stand for 24 hours. The solution was evaporated to about half-volume and petroleum ether (40-60°) (20ml) was added when crystals slowly precipitated. Recrystallisation from acetone-water yielded bright red crystals of the adduct. m.p. 187-188°C (lit.[204] 188 -189°C).

3 - 3 Spectral Interpretation and Assignment of Conformation

3 - 3 - 1 Norbornadiene/TCNE adduct.

Initially the N.M.R. spectrum of Norbornadiene itself was run as a comparison with the adduct spectrum.

Table 3 - 1. 60MHz Signals for Norbornadiene in CCl_4

τ value	No. of hydrogens	Assignment
8.05 (multiplet)	2	H_7, H_8
6.51 (multiplet)	2	H_1, H_4
3.35 (multiplet)	4	H_2, H_3, H_5, H_6

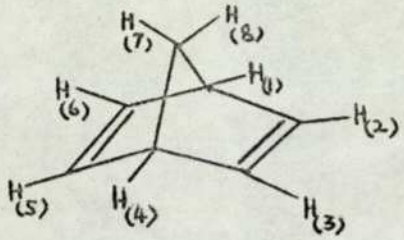
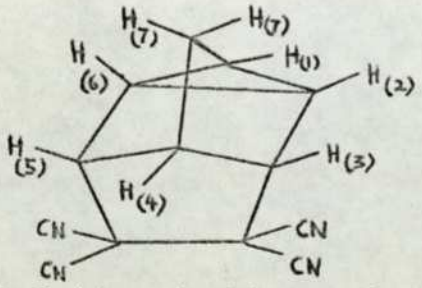


Table 3 - 2. 100MHz Signals for 8,8,9,9-tetracyanoquadricyclo $[2,2,1,0^{2,6}2^{3,5}]$ nonane in deuteroacetone-d_6

τ value	No. of hydrogens	Assignment
8.27 (multiplet)	3	H_1, H_2, H_6 ?
8.02 (multiplet)	2	H_7 ?
7.94 (quintet)	-	Solvent
7.29 (multiplet)	1	H_4
7.10 (singlet)	-	Solvent
6.62 (multiplet)	2	H_3, H_5



Because of uncertainties in the assignments of signals it was decided to carry out double resonance irradiations of selected signals in order to clarify the splitting patterns.

Irradiation Experiments.

(1) Irradiation of signal at 6.62τ caused changes in line intensities in signals at 8.27 and 8.02τ, and some simplification of signal at 7.29τ.

(2) Irradiation of signal at 7.29τ caused the collapse of signal at 6.62τ to a poorly resolved doublet and collapse of signal at 8.02τ to a doublet. This confirmed that H_7 was correctly assigned for the bridge protons at 8.02τ.

(3) Irradiation of signal at 8.02τ caused the signal at 7.29τ to collapse to six lines. The high-field signal at 8.27τ strongly interfered.

(4) Irradiation of signal at 8.27τ caused a collapse of signal at 6.62τ to give a well resolved doublet. This established H_1, H_2 and H_6 as resonating at high field in a complex overlapping pattern.

It was decided to run the spectrum at 220MHz to try and simplify the high-field splitting pattern and to see whether the H_1 signal separated from the H_2, H_6 signal.

Table 3 - 3. 220MHz N.M.R. values for 8,8,9,9-Tetracyanoquadricyclo-[2,2,1,$0^{2,6}$,$2^{3,5}$] nonane in deuteroacetone-d_6

τ value	No. of Hydrogens	Assignment
8.29 (doublet of doublets)	2	H_2, H_6
8.22 (multiplet)	1	H_1
8.02 (multiplet)	2	H_7
7.29 (multiplet)	1	H_4
6.64 (multiplet)	2	H_3, H_5

At this frequency, the chemical shift of protons H_2, H_6 was separated from H_1. It was possible to calculate spin-spin coupling constants by a first-order treatment from the above spectral data.

Table 3 - 4. Spin-Spin Coupling Constants for Norbornadiene/TCNE Adduct.

	$J_{1,2}$	$J_{2,3}$	$J_{3,4}$	$J_{4,7}$	$J_{1,7}$	$J_{1,4}$
Coupling Constants(Hz)	5.0	1.0	2.3	1.3	1.0	0.9

Weak coupling also occurred between proton H_4 and protons H_2 and H_6 but it was too small to measure accurately. The long range coupling between H_1 and H_4 was typical of similar bicyclic systems.

Although this was a rigid bicyclic system and might not be comparable to flexible systems, the dihedral angles on the Dreiding model of the adduct were measured and compared with those calculated from the Karplus equation (see 1 - 44) using the above coupling constants.

Table 3 - 5. Comparison of Dihedral Angles.

Dihedral Angle	H_2-H_3	H_3-H_4	H_4-H_7	H_1-H_7
Measured from Model	65°	58°	68°	68°
Calculated	66°59′	56°25′	64°20′	66°59′

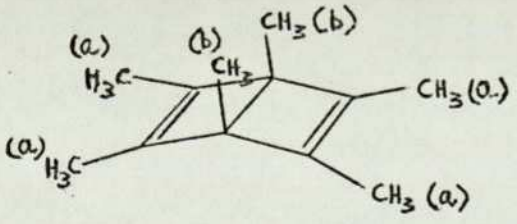
The measured and calculated angles are shown to be in close agreement. The protons on the cyclopropane ring were not examined in this way, because of the likely strain effects. The N.M.R. spectra were thus consistent with the rigid cyclic structure and all the signals could be assigned unambiguously.

3 - 3 - 2 Hexamethyl Dewar benzene/TCNE adduct.

The N.M.R. spectrum of Hexamethyl Dewar benzene itself was first recorded using CCl_4 for comparison.

Table 3 - 6. 100MHz Signals for Hexamethyl Dewar benzene in CCl_4

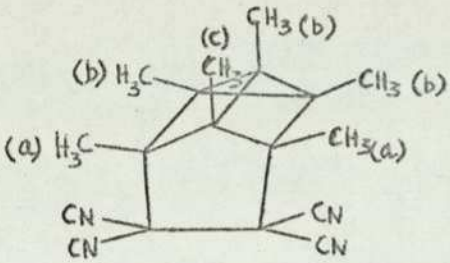
τ value	No. of protons	Assignment
8.45 (singlet)	12	H_a
8.95 (singlet)	6	H_b



The N.M.R. spectrum of the adduct was recorded using deuterochloroform as solvent.

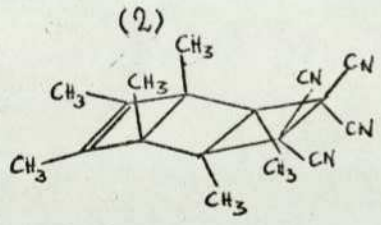
Table 3 - 7. 100MHz Signals for 7,7,8,8-Tetracyanohexamethyl-quadricyclo [2,2,0,$2^{3,5}$,$0^{2,6}$]octane in $CDCl_3$

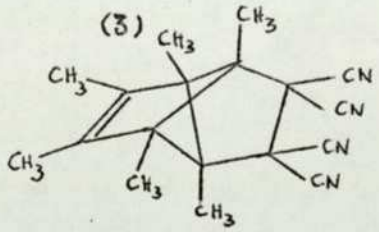
τ value	No. of protons	Assignment
8.39 (singlet)	6	H_a
8.78 (singlet)	9	H_b
9.00 (singlet)	3	H_c

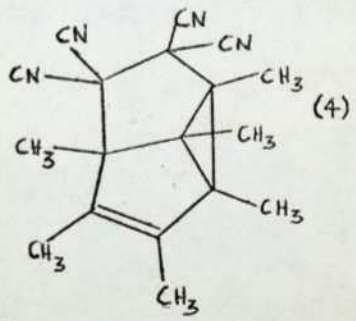


(1)

The N.M.R. spectrum suggests that 1 is the correct structure of the adduct. It has been observed in reactions of hexamethyl Dewar benzene with electrophiles that the adducts take a variety of structures. In each of the postulated adducts below, the N.M.R. spectrum would not be consistent with three singlets in the ratio 6:9:3.







In 2 and 3, there should be three equal signals, and in 4 there should be more than three signals.

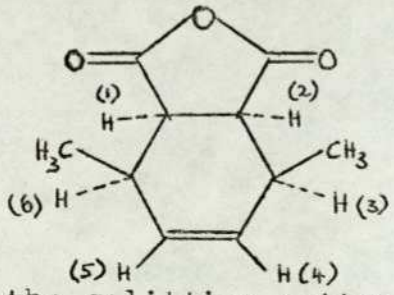
The low-field methyl protons are assigned to those nearest the nitrile groups in which some inductive or anisotropic effect must be operating. The group of three methyls is assigned to the cyclopropane substituents and the high-field protons H_c compare with the high-field protons H_b in hexamethyl Dewar benzene (9.00 and 8.95τ).

3 - 3 - 3 Hexa-trans-2,trans-4-diene/Maleic Anhydride adduct.

The 100 MHz N.M.R. spectrum of this adduct was recorded using deuterochloroform as solvent.

Table 3 - 8. 100 MHz Signals for 3,6-Dimethyl-Δ^4-tetrahydrophthalic anhydride in $CDCl_3$

τ value	No. of protons	Assignment.
4.14 (broad singlet)	2	H_4, H_5
6.72 (four lines)	2	H_1, H_2
7.55 (multiplet)	2	H_3, H_6
8.55 (doublet)	6	CH_3 protons



In order to clarify the splitting patterns it was decided to carry out double resonance irradiations of each signal.

Irradiation Experiments.

(1) Irradiation of signal at 4.14τ, only simplified the signal at 7.55τ.

(2) Irradiation of signal at 6.72τ caused the signal at 7.55τ to appear as a broad quartet.

(3) Irradiation at 7.55τ caused the signal at 6.72τ to collapse to a singlet confirming the correct assignment of H_1, H_2.

(4) Irradiation of signals at both 4.14τ and 6.72τ caused the multiplet at 7.55τ to collapse to a well-resolved quartet. This confirmed the correct assignment of H_3, H_6, as the splitting constant was the same as for the proton doublet of the adjacent methyl. Expansion of the signal at 4.14τ at 100 Hz sweep width showed only a small splitting (0.4Hz). When the shift reagent $Eu(fod)_3$ was

added there was no change in the spectrum.

The above experiments showed that this adduct was a symmetrical molecule with a well-defined coupling between the methyl protons and H_3,H_6. The four-line signal for H_1,H_2 protons was not entirely clear. Spin-spin coupling constants were measured using a first-order treatment.

Table 3 - 9. Spin-Spin Coupling Constants.

	$J_{3,(CH_3)}$	$J_{2,3}$	$J_{3,4}$
Coupling Constant (Hz)	7.1	2.2	0.4

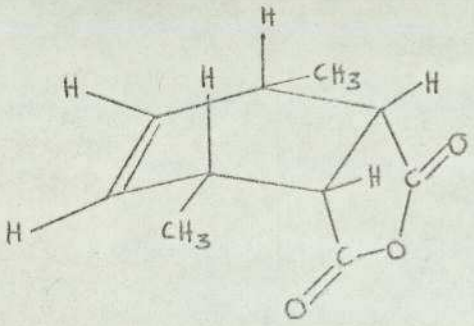
Here $J_{2,3} = J_{1,6}$; $J_{3,4} = J_{5,6}$; $J_{3,(CH_3)} = J_{6(CH_3)}$ because of the symmetry of the molecule.

According to molecular models only boat conformers were stable. The various possible boat conformers were examined and dihedral angles measured from Dreiding models. These values were compared with angles derived from the Karplus equation (see Section 1 - 5 - 2) using the above values for coupling constants.

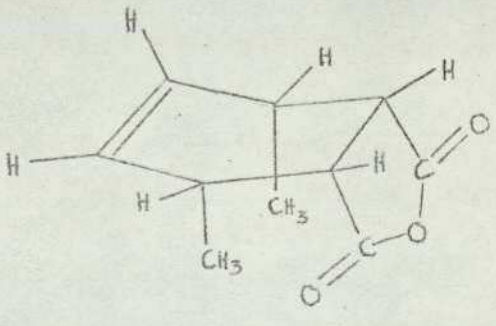
Table 3 - 10. Comparison of Dihedral Angles.

Conformation	H_2-H_3	H_3-H_4
Endo addition: Boat (1)	62°	110°
" Boat (2)	45°	15°
Exo addition: Boat (1)	165°	110°
" Boat (2)	75°	15°
Calculated values of dihedral angle	57°10′	105°45′

From the above data it was indicated that the endo adduct was formed and boat (1) most closely resembled the conformation in solution.



BOAT (1)



BOAT (2)

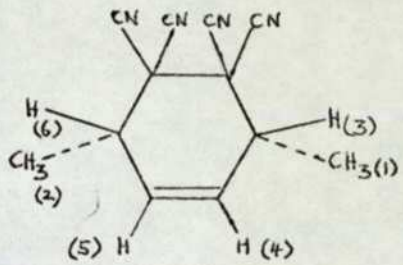
The first of the two above conformations would appear to be stabilized relative to the second, in which axial methyl groups would interact.

3 - 3 - 4 Hexa-trans-2,trans-4-diene/TCNE adduct.

The 100 MHz N.M.R. spectrum of the adduct was recorded using deuterochloroform as solvent.

Table 3 - 11. 100 MHz Signals for 1,1,2,2-Tetracyano-3,6-dimethyl-Δ^4-cyclohexene in $CDCl_3$

τ value	No. of protons	Assignment
4.25 (broad singlet)	2	H_4, H_5
6.80 (quartet)	2	H_3, H_6
8.40 (doublet)	6	CH_3 protons



It was decided to carry out double resonance irradiation on selected signals to clarify the splitting patterns.

Irradiation experiments.

(1) Irradiation of the signal at 4.25τ only caused some sharpening in the lines of the quartet (6.80τ).

(2) Irradiation of the signal at 6.80τ caused the broad singlet at 4.25τ to sharpen when examined on an expanded scale.

(3) Irradiation of the signal at 8.40τ caused the signal at 6.80τ to collapse to a broad singlet, confirming the correct assignment for H_3, H_6.

On an expanded scale the signal at 4.25τ was shown to be a doublet, collapsing to a singlet in irradiation experiment (2).

It was deduced from the above that the correct assignments had been

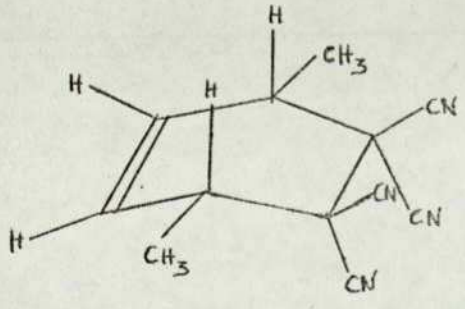
made and that the molecule was highly symmetrical.

The following coupling constants were measured using first-order treatment: $J_{1,3} = J_{2,6} = 7.0$ Hz, $J_{3,4} = J_{5,6} = 0.7$ Hz. Because of the symmetry of tetracyanoethylene, there was no distinction here between exo or endo products. Examination of Dreiding models indicated that the adduct could exist in two half-chair or two boat conformations. Dihedral angles were measured for each conformation and compared with those derived from the Karplus equation (see Section 1 - 5 - 2) using the above coupling constant values.

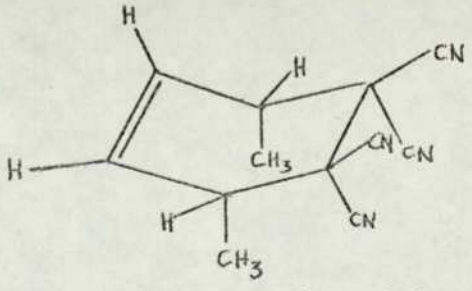
Table 3 - 12. Comparison of Dihedral Angles for Hexadiene/ TCNE Adduct.

Conformation	H_3-H_4	H_5-H_6
Boat (1)	105°	105°
Boat (2)	15°	15°
Half-chair (1)	40°	75°
Half-chair (2)	75°	40°
Calculated values of angles	108°55′ (70°)	108°55′ (70°)

This indicated that in solution the adduct might exist in a form approaching the Boat (1) conformation. The half-chair conformations were considered less likely because of the different angles on different sides of the double bond and a corresponding loss of symmetry. The boat (1) conformation has equatorial methyl groups, whereas boat (2) has axial methyl groups which would eclipse each other.



BOAT (1)



BOAT (2)

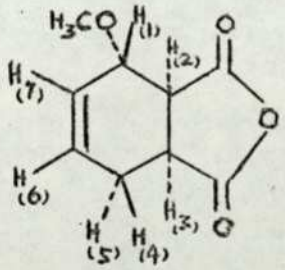
This result was based on calculations of dihedral angles for a compound in which one of the carbon atoms is sp^2 hybridised, and therefore may not be in strict accordance with the Karplus equation.[185,186] However, in the view of the above evidence, it is likely that the boat (1) conformation is correct, as examination of the models shows that in the half-chair conformation there may be methyl-nitrile group interactions.

3 - 3 - 5. 1-Methoxybuta-trans-1,3-diene/Maleic Anhydride adduct.

The 100 MHz N.M.R. spectrum of this adduct was run using deutero-chloroform as solvent.

Table 3 - 13. 100 MHz Signals for 3-Methoxy-Δ^4-tetrahydro phthalic anhydride in $CDCl_3$

τ value	No. of protons	Assignment
7.38 (multiplet)	2	H_4, H_5
6.74 (multiplet)	5	H_2, H_3 methoxyl protons
5.78 (multiplet)	1	H_1
3.83 (multiplet)	2	H_7, H_6



In order to clarify the complex splitting patterns it was decided to carry out double resonance experiments on selected signals.

Irradiations.

(1) Irradiation at 3.83τ caused the signal at 5.78τ to collapse to a well-defined doublet. This confirmed the assignment H_1. The signal at 7.38τ was simplified.

(2) Irradiation at 5.78τ caused some simplification in the splitting of signal at 3.83τ.

(3) Irradiation at 7.38τ caused the signal at 3.83τ to appear as an ill-defined doublet.

Because of the rather scanty information derived from the above experiments, it was decided to add the lanthanide shift reagent $Eu(fod\text{-}dg)_3$ to the solution of the adduct in deuterochloroform. This compound might cause separations of the overlapping proton signals.

Table 3 - 14. 100 MHz Signals of Adduct with Added $Eu(fod)_3$ (60mg.) in $CDCl_3$

τ value	No. of hydrogens	Assignment
3.30 (multiplet)	1	H_6 or H_7
3.60 (multiplet)	1	H_6 or H_7
4.92 (three lines)	1	H_1
5.65 (doublet of doublets)	1	H_2
6.30 (multiplet)	4	H_3, methyl protons
6.80 (multiplet)	2	H_4, H_5

The 220 MHz N.M.R. spectrum was also run with and without added $Eu(fod)_3$ in deuterochloroform.

Table 3 - 15. 220 MHz Signals of Adduct with Added $Eu(fod)_3$ (30mg.) in $CDCl_3$

τ value	No. of hydrogens	Assignment
3.60 (multiplet)	1	H_6 or H_7
3.70 (multiplet)	1	H_6 or H_7
5.33 (three lines)	1	H_1
6.22 (doublet of doublets)	1	H_2
7.05 (multiplet)	1	H_4 or H_5
7.30 (multiplet)	1	H_4 or H_5
6.43 (multiplet)	4	H_3, methyl protons

None of the signals due to H_4, H_5, H_6 or H_7 appeared to have the same chemical shift after addition of the shift reagent.
It was assumed that the signal H_7 was at lower field than H_6, being closer to the methoxy group. Examination of models and rigorous measurement of the first-order splitting patterns showed that the H_4 signal was most likely to be at lower field than H_5 and the coupling constants were measured on this basis.

Table 3 - 16. Spin Coupling Constants.

	$J_{1,2}$	$J_{2,3}$	$J_{3,4}$	$J_{3,5}$	$J_{4,5}$	$J_{4,6}$	$J_{5,6}$	$J_{5,7}$	$J_{6,7}$	$J_{1,7}$
Coupling Constant(Hz)	4.0	10.2	4.0	9.5	-18.0	5.5	3.5	2.5	10.0	5.0

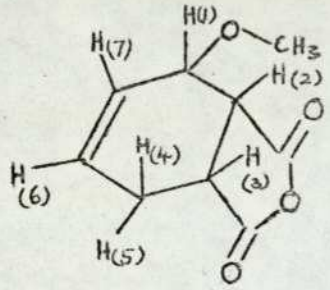
The large geminal coupling constant $J_{4,5}$ was assumed to be negative.
A large allylic coupling, $J_{5,7}$, was also found.
The rigid bicyclic structure of the adduct excluded the cyclohexene ring being present in a half-chair conformation in the adduct. The boat conformations for both exo and endo adducts were examined using Dreiding models and the dihedral angles in each compared to those calculated from the Karplus equation using the above coupling constants.

Table 3 - 17. Comparison of Dihedral Angles for Methoxybutadiene Maleic Anhydride Adduct.

Conformation	H_1-H_2	H_3-H_4	H_3-H_5	H_4-H_6	H_5-H_6
Endo adduct - boat(1)	70°	55°	75°	110°	15°
" " - boat(2)	45°	60°	170°	15°	120°
Exo adduct - boat(1)	170°	170°	45°	110°	15°
" " - boat(2)	70°	75°	60°	15°	120°
Calculated values of angles	44°30′	44°30′	~180°	34°18′	129°10′

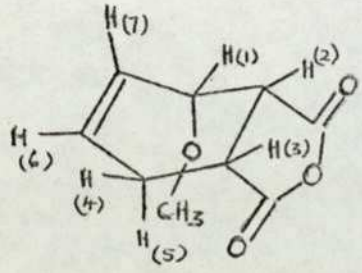
As mentioned previously, there may be some ambiguity in assignment of H_4 and H_5 and hence between $J_{3,4}$ and $J_{3,5}$. In that case either endo boat (2) or exo boat (1) conformations would give an H_3-H_4 or H_3-H_5 dihedral angle approaching 180° and hence a large coupling constant for $J_{3,5}$ or $J_{3,4}$ (9.5 Hz). However, the exo conformation would also require H_1-H_2 to approach 180° with a similarly large coupling constant for $J_{1,2}$, which is not observed.

If free rotation of the methoxy group is envisaged, then it approaches the carbonyl group in the anhydride more closely in the boat (1) conformation than in the boat (2) conformation. This could lead to a destabilization of the former.



BOAT (1)

It was thus considered likely that the adduct existed closest to the endo boat (2) conformation in solution as was seen from the above comparison of angles.



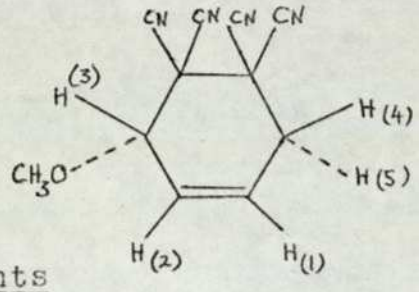
BOAT (2)

3 - 3 - 6. 1-Methoxybuta-trans-1,3-diene/TCNE adduct.

The 100 MHz Spectrum of this adduct was run using deuterochloroform as solvent.

Table 3 - 18. 100 MHz Signals for 1-Methoxybuta-trans-1,3-diene/ TCNE in $CDCl_3$

τ value	No. of protons	Assignment
4.03 (broad singlet)	2	H_1, H_2
5.50 (multiplet)	1	H_3
6.28 (singlet)	3	CH_3 protons
6.87 (multiplet)	2	H_4, H_5



Irradiation Experiments

(1) Irradiation of signal at 4.03τ gave some simplification of signals at 5.50 and 6.87τ.

(2) Irradiation of signal at 5.50τ caused signal at 6.87τ to collapse to a broad doublet.

(3) Irradiation of signal at 6.87τ gave simplification of signal at 4.05τ, which now appeared as an AB quartet with fine splitting (each line split in two).

The irradiation experiments showed that the H_1 and H_2 protons had a different chemical shift, and that there was also long-range homoallylic coupling between H_3 and H_4, H_5, because the signal due to H_3 was still split, when H_1 and H_2 were irradiated.
The spectrum was run at 220 MHz to see if a better resolution could be obtained.

Table 3 - 19. 220 MHz Signals of 1-Methoxybuta-trans-1,3-diene/TCNE adduct in $CDCl_3$

τ value	No. of protons	Assignment
4.03 (unresolved AB system)	2	H_1, H_2
5.50 (multiplet)	1	H_3
6.28 (singlet)	3	CH_3 protons
6.87 (unresolved AB system)	2	H_4, H_5

When Eu(fod)$_3$ was added to the solution and the spectrum recorded at 220 MHz, the signals at 4.03 and 6.87τ now both showed resolved AB quartets with fine splitting.

From the above spectra and the irradiation experiments it was possible to calculate J values by first-order treatment. In some cases only approximate values were obtained, because of the difficulties in analysing complex signals. The low-field olefin proton was assigned as H_2 and the low-field methylene proton as H_4.

Table 3 - 20. Coupling Constants.

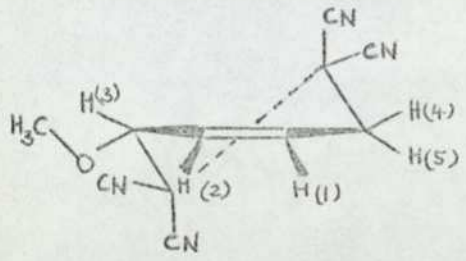
	$J_{1,2}$	$J_{1,3}$	$J_{1,4}$	$J_{1,5}$	$J_{2,3}$	$J_{2,4}$	$J_{2,5}$	$J_{3,4}$	$J_{3,5}$	$J_{4,5}$
Coupling Constant(Hz)	10.5	1.5	4.0	1.3	1.2	1.3	0.6	2.0	1.5	-19.0

The gem methylene (H_4-H_5) coupling was assumed to be negative. The dihedral angles of various conformations of the adduct were measured from models and compared with the angles calculated from the coupling constants using the Karplus equation.

Table 3 - 21. Comparison of Measured and Calculated Dihedral Angles

Conformation	H_2-H_3	H_1-H_4	H_1-H_5
Boat (1)	105°	105°	10°
Boat (2)	15°	15°	105°
Half-Chair (1)	75°	45°	75°
Half-Chair (2)	45°	75°	45°
Calculated	65°12′	44°40′	64°18′

From the above, the calculated angles compare approximately with the half-chair (1) conformation measurements. Another fact which indicates a half-chair conformation is that in either boat conformation one of the C-H_3, C-H_4 or C-H_5 angles, with respect to the plane of the double bond, is approaching 0°. Theory shows[205,206] that for such a case long-range homoallylic coupling will not occur. In this adduct such coupling occurs for both H_3-H_4 and H_3-H_5.



Half-Chair(1)

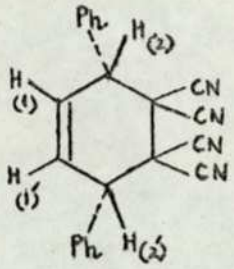
This result was based solely on measurements of dihedral angles in which one of the carbon atoms was sp^2 hybridised.
As mentioned before, the conclusions reached should be regarded as tentative, but evidence favours the existence of the half-chair conformation for this adduct in solution.

3 - 3 - 7 1,4-Diphenylbuta-trans-1,trans-3-diene/TCNE adduct.

The 100 MHz Spectrum was recorded using deuterochloroform as solvent.

Table 3 - 22. 100 MHz Signals for 1,4-Diphenylbuta-trans-1, trans-3-diene/TCNE adduct in $CDCl_3$

τ value	No. of protons	Assignment
2.50 (multiplet)	10	Phenyl protons.
3.71 (doublet)	2	H_1
5.58 (doublet)	2	H_2



Irradiation of the signal at 5.58τ caused the signal at 3.71τ to collapse to a sharp singlet. ($J_{1,2}$ = 0.6 Hz).

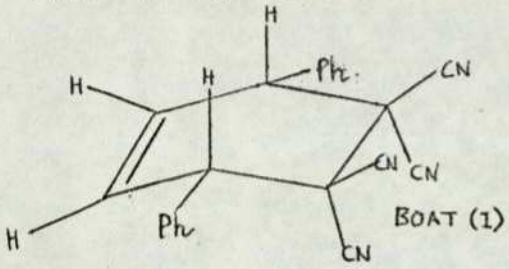
Using the Karplus equation, the dihedral angles H_1-H_2 were calculated. These were compared with the angles H_1-H_2 in the various boat and half-chair conformations.

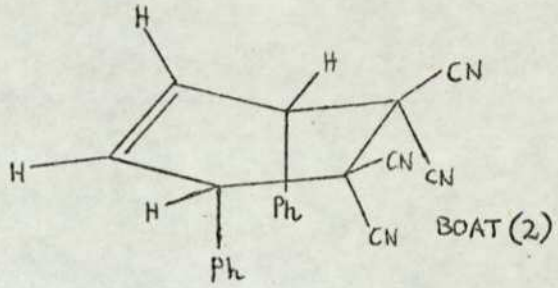
Table 3 - 23. Comparison of Measured and Calculated Dihedral Angles.

Conformation	H_1-H_2	H_1'-H_2'
Boat (1)	105°	105°
Boat (2)	15°	15°
Half-chair (1)	40°	75°
Half-chair (2)	75°	40°
Calculated from Karplus equation	107°55′(71°)	107°55′(71°)

Even if strict adherence to the Karplus equation does not occur, it is unlikely that this compound exists in a half-chair form, as coupling constants different in value would then be obtained for each end of the ring. The boat (1) conformation has equatorial phenyl groups and is the conformation favoured in steric terms as well as that calculated on the above basis. The boat (2) conformation,

for example, would have a large steric interaction between the axial phenyl groups.



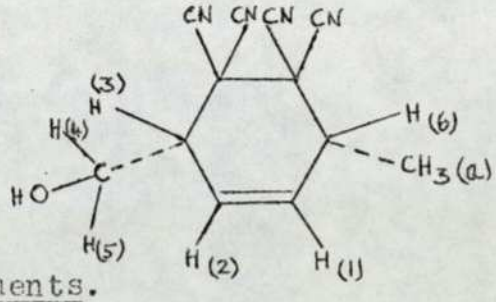


3 - 3 - 8 Hexa-trans-2,trans-4-dienol (sorbyl alcohol)/TCNE adduct.

The 100 MHz spectrum was recorded using deuterochloroform as solvent.

Table 3 - 24. 100 MHz Signals for Sorbyl Alcohol/TCNE adduct.

τ value	No. of protons	Assignment
2.00 (disappears after D_2O addition)	1	-(O) H
4.14 (multiplet)	2	H_1, H_2
5.37 (doublet of doublets)	1	H_4 or H_5
5.82 (doublet of doublets)	1	H_4 or H_5
6.21 (multiplet)	1	H_3
6.81 (multiplet)	1	H_6
8.40 (doublet)	3	H_a



Irradiation Experiments.

(1) Irradiation of signal at 4.14τ caused signal at 6.21τ to be resolved to a triplet of doublets. The signal at 6.81τ was resolved to a quartet of doublets.

(2) Irradiation of signal at 8.40τ interfered with the signal at 6.81τ, which appeared as a broad singlet.

(3) Irradiation of signals at both 4.14τ and 8.40τ resolved the signal at 6.81τ to a doublet.

The following conclusions were drawn from the above observations.
(1) The vinyl protons (H_1 and H_2) showed a characteristic overlapping ABX type pattern with H_2 probably at low field.
(2) The methylene protons H_4 and H_5 were not magnetically equivalent. It was most likely that there was restricted rotation and one of the protons (H_4) was closer to the nitrile groups, being deshielded as a result of the anisotropic effect.
(3) There was clearly homoallylic coupling between H_3 and H_6 across the ring as shown by the first irradiation experiment. There was also weaker coupling between the olefinic protons and H_3, H_6. As there was definite homoallylic coupling, the coupling seen between H_6 and the olefinic protons might be allylic (H_2-H_6) rather than vicinal (H_1-H_6). In either case, it was comparatively weak, being less than 2Hz.

Table 3 - 25. Coupling Constants for Sorbyl Alcohol/TCNE Adduct.

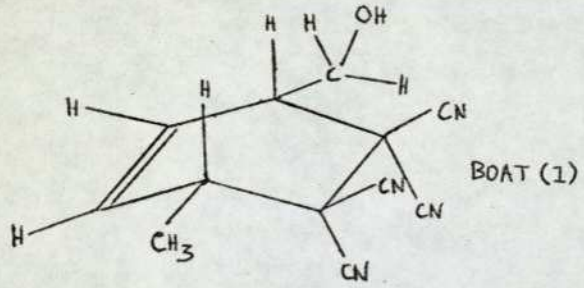
	$J_{1,2}$	$J_{1,3}$	$J_{2,3}$	$J_{3,4}$	$J_{3,5}$	$J_{4,5}$	$J_{3,6}$	$J_{6,a}$	$J_{1,6}$	$J_{2,6}$
Coupling Constant(Hz)	10.0	1.5?	0?	8.7	8.7	-9.7	2.2	7.0	0?	1.9?

The magnitudes of $J_{1,6}$ and $J_{2,6}$ were not entirely clear. In comparing dihedral angles using the Karplus equation from the coupling constants, the vicinal coupling constants were taken as either case (a), nearly zero, or case (b), 1.5 and 1.9, the values calculated for the allylic coupling constants $J_{1,3}$ and $J_{2,6}$. The angles were compared with the measured angles from models of the various possible conformations.

Table 3 - 26. Dihedral Angle Comparison for Sorbyl Alcohol/TCNE Adduct.

Conformation	H_2-H_3	H_1-H_6
Boat (1)	105°	105°
Boat (2)	15°	15°
Half-chair (1)	40°	75°
Half-chair (2)	75°	40°
Calculated (a)	90°-100°	90°-100°
Calculated (b)	119°45′	115°48′

Even allowing for the ambiguity in the value of the vicinal coupling constants, it can be seen on this basis that the adduct exists closest to the boat (1) conformation in solution.



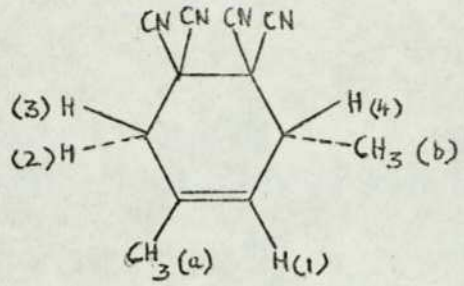
There is likely to be restricted rotation about the $-CH_2OH$ carbon atom as shown by the non-equivalence of H_4 and H_5.

3 - 3 - 9 2-Methylpenta-1,trans-3-diene/TCNE adduct.

The 100 MHz N.M.R. spectrum of this compound was run using deuterochloroform as solvent.

Table 3 - 27. 100 MHz Signals for Methylpentadiene/TCNE Adduct.

τ value	No. of protons	Assignment
4.64 (multiplet)	1	H_1
6.85 (multiplet)	1	H_4
7.04 (multiplet)	2	H_2 H_3
8.17 (broad triplet)	3	H_a
8.50 (doublet)	3	H_b



In order to clarify the splitting patterns it was decided to carry out double resonance experiments on selected signals.

Irradiations.

(1) Irradiation of the signal at 4.64γ caused the signal at 8.17γ to collapse to a doublet. There was little change in the other signals.

(2) Irradiation of the signal at 8.17γ caused the signal at 4.64γ to collapse to a broad doublet. The signal at 7.04γ showed four main lines with some further fine splitting.

It was not certain whether H_2 and H_3 were equivalent and it was thus decided to run the spectrum at 220 MHz to see if a better resolution of the signals between 6.5 and 7.5γ could be obtained.

Table 3 - 28. 220 MHz Signals between 6.5 and 7.5γ

γ value		Assignment
6.75 (multiplet)		H_4
6.85	Part of AB quartet, each line split into	H_3
6.95	further 8.	"
6.98	Part of AB quartet, each line is a broad	H_2
7.07	singlet.	"

The low-field doublet was assigned as the axial proton (H_3) (similar to the case for the methoxybutadiene/TCNE adduct - Section 3 - 5 - 2). It was thus clear that the methylene protons were not equivalent and the difference might be attributed to the anisotropic shielding effects of the adjacent nitrile groups.

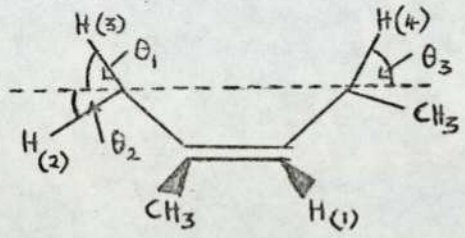
Only a limited number of coupling constants could be definitely assigned for this adduct and they are shown below:

Table 3 - 29. Spin Coupling Constants for Methylpentadiene/TCNE Adduct.

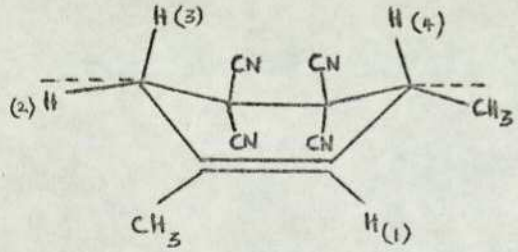
	$J_{a,1}$	$J_{a,2}$	$J_{a,3}$	$J_{2,3}$	$J_{b,4}$
Coupling Constant(Hz)	1.2	~0	1.1	-18.5	7.1

There is definite evidence for long range allylic or homoallylic coupling between H_1 and H_2, H_3 or H_4 and H_2, H_3. This is shown by the irradiation of H_a protons, where the signal due to H_2 and H_3 remains split. The H_1- H_4 coupling appears to be very weak as indicated by the first irradiation.

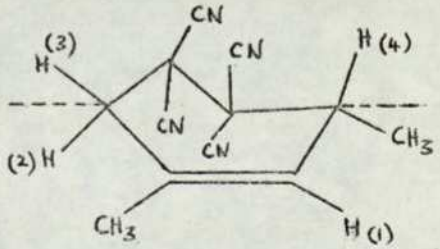
Although no definite conclusion can be made, it is unlikely that this adduct exists rigidly in the boat conformation, for the following reason. Theory shows[205,206] that for allylic or homoallylic coupling to take place, the angles θ_1, θ_2 and θ_3 as shown, should never approach 0°.



It appears from the second irradiation that both H_2 and H_3 are coupled to either H_1 or H_4, (about 2 to 3Hz). However, a comparison of models of boat and half-chair conformations show that only in the latter are both angles, θ_1 and θ_2 sufficiently different from 0° to allow coupling of such magnitude to occur.



BOAT ($\theta_2 \rightarrow 0^\circ$)



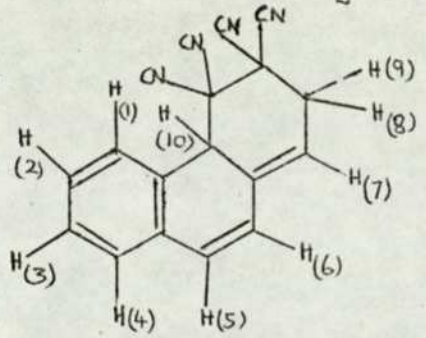
HALF-CHAIR

3 - 3 - 10. 2-Vinyl Naphthalene/TCNE adduct.

The N.M.R. spectrum of this adduct was run using deuterodichloromethane as solvent.

Table 3 - 30. 100 MHz Signals for 2-Vinyl Naphthalene/TCNE Adduct in CD_2Cl_2

γ Value	No. of protons	Assignment
2.18 (multiplet)	1	H_1
2.70 (multiplet)	3	H_2, H_3, H_4
3.46 (doublet)	1	H_5
3.64 (doublet)	1	H_6
4.30 (multiplet)	1	H_7
5.17 (doublet)	1	H_{10}
6.66 (multiplet)	2	H_9, H_8



The low-field multiplet was assigned as H_1, which might experience a further deshielding from the nearby nitrile group. The AB doublet pattern clearly indicated the H_5 and H_6 protons, both being at lower field to H_7. H_5 might experience a greater deshielding by the 'ring-current' effect, being closer to the aromatic ring.

Irradiations.

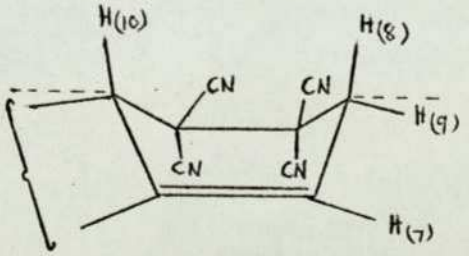
Irradiation of the signal at 6.66γ caused the multiplet at 4.30γ to collapse to a broad doublet. This indicated that there was allylic coupling between H_7 and H_{10}. There could be no coupling between H_6 and H_7, as the H_6 signal was a simple doublet, coupled

to H_5. The signal at 5.17τ appeared to sharpen, indicating some homoallylic coupling across the ring, between H_{10} and H_9 or H_8. Based on the above observation, the following tentative values for coupling constants were deduced.

Table 3 - 31. Coupling Constants for 2-Vinyl Naphthalene/TCNE Adduct.

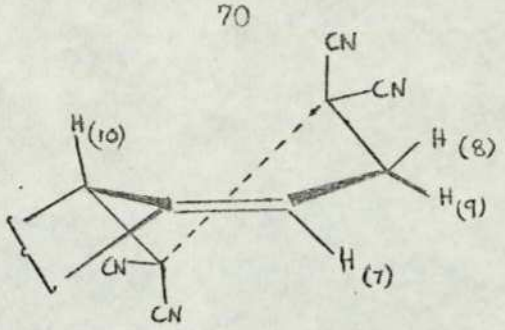
	$J_{5,6}$	$J_{7,8}$	$J_{7,9}$	$J_{7,10}$	$J_{9,10}$
Coupling Constant(Hz)	9.5	~3?	?	3.5	1.0

It was not possible to analyse the complex multiplets at 4.30τ and 6.36τ accurately with the limited number of irradiations available. On the basis of the very small homoallylic coupling across the ring, it is likely that the C-H_8 or C-H_9 angle does not approach 90° with respect to the plane of the double bond in that ring. Theory shows[205,206] that if both the C-H angles for such coupling across the ring approach 90°, the homoallylic coupling must be large (see also Section 3 - 3 - 9). The C-H_{10} angle must approach 90° with respect to the double bond as is also shown by the large allylic coupling between H_7 and H_{10}. The boat conformation requires the C-H_8 angle to approach 90°, and it is thus unlikely on this basis that the adduct lies in such a conformation in solution.



BOAT CONFORMATION
RING C

It is more likely that the adduct approaches closer to a half-chair conformation, where the C-H_8 or C-H_9 angles are less than 90° with respect to the plane of the double bond.



HALF-CHAIR
RING C

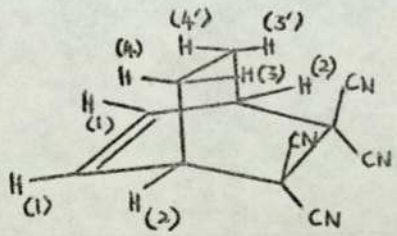
3 - 3 - 11. Cyclohexa-1,3-diene/TCNE adduct.

The N.M.R. spectrum of this compound was run using deuterodichloromethane as solvent.

Table 3 - 32. 100 MHz Signals for Cyclohexa-1,3-diene/TCNE Adduct in CD_2Cl_2

τ value	No. of protons	Assignment
3.30 (doublet of doublets)	2	H_1
4.68 (multiplet)		Solvent
6.44 (multiplet)	2	H_2
7.80 (multiplet)	2	H_3, $H_{3'}$
8.42 (multiplet)	2	H_4, $H_{4'}$

The simplicity of the spectrum indicated a symmetrical compound. In bicyclo [2,2,2] octenes it has been shown[207] that the bridge protons syn to the double bond are shielded relative to the anti protons. Although the signals centred at 7.80 and 8.42τ were part of an $A_2B_2X_2$ system the higher field signal group was assigned to H_4 and $H_{4'}$ and the lower field signal group to H_3 and $H_{3'}$. The nitrile groups might be expected to deshield the protons lying above the - C≡N axis.



Irradiation Experiments.

(1) Irradiation of the signal at 3.30τ caused the signal at 6.44τ

to collapse to three lines, confirming the assignment H_2.

(2) Irradiation of the signal at 6.44γ caused the signal at 3.30γ to collapse to a singlet indicating that the olefinic protons were only coupled to H_2. The signal system centred at 7.80 and 8.42γ now resembled an A_2B_2 spin system with the H_3, $H_{3'}$, H_4 and $H_{4'}$ protons coupled together.[208-211] The following coupling constants could be evaluated immediately from the above spectra.

Table 3 - 33. Coupling Constants for Cyclohexa-1,3-diene/TCNE Adduct.

	$J_{1,2}$	$(J_{1,2})$	$J_{2,3}$	$J_{2,4}$
Coupling Constant (Hz)	5.0	3.0	1.5	1.5

$(J_{1,2})$ was the allylic coupling constant and had an unusually large value for protons fixed in the bicyclic conformation. It was not possible to calculate $J_{3,4}$ and $J_{3,4'}$ by inspection because of the second-order splittings in the spectrum, thus the following procedure was adopted.

Tentative estimated values for the coupling constants J_{AB}, $J_{AB'}$ were assigned by comparison with spectra of geminal coupled protons and also from that of the α-phellandrene/TCNE adduct. The chemical shift from the centre of the high-field signal group to the centre of the low-field group was measured (63.5 c.p.s.). As the assignment of lines for the spectrum was not obvious, it was necessary to examine the profile of computed spectra (A_2B_2) which had known values of coupling constants. It has been shown[208] that A_2B_2 spectra are symmetrical about the midpoint with each grouping consisting of 12 lines (or less if degeneracy occurs). In order to obtain values of the coupling constants it is necessary to assign lines 1-12 correctly and then the J values may be determined from the following defined parameters.[208,211]

$$K = J_{A,A'} + J_{B,B'} \quad , \quad M = J_{A,A'} - J_{B,B'}$$
$$L = J_{A,B} - J_{A,B'} \quad , \quad N = J_{A,B} + J_{A,B'}$$

The first step in evaluation of coupling constants was the correct assignment of lines 1 and 3 in the spectral group by calculating their respective energies as shown.

Table 3 - 34. Energies of Selected Lines of the A_2 Group in A_2B_2 Spectra.

Line No.	Energy relative to centre of A_2B_2 system
1	$\frac{1}{2} N + \frac{1}{2} ((\nu_o\delta)^2 + N^2)^{\frac{1}{2}}$
3	$-\frac{1}{2} N + \frac{1}{2} ((\nu_o\delta)^2 + N^2)^{\frac{1}{2}}$
9	$\frac{1}{2} ((\nu_o\delta + M)^2 + L^2)^{\frac{1}{2}} + \frac{1}{2} (M^2 + L^2)^{\frac{1}{2}}$
10	$\frac{1}{2} ((\nu_o\delta - M)^2 + L^2)^{\frac{1}{2}} + \frac{1}{2} (M^2 + L^2)^{\frac{1}{2}}$
11	$\frac{1}{2} ((\nu_o\delta + M)^2 + L^2)^{\frac{1}{2}} - \frac{1}{2} (M^2 + L^2)^{\frac{1}{2}}$
12	$\frac{1}{2} ((\nu_o\delta - M)^2 + L^2)^{\frac{1}{2}} - \frac{1}{2} (M^2 + L^2)^{\frac{1}{2}}$

$\nu_o\delta$ is the chemical shift in c.p.s. between the centres of the two signal groups A_2 and B_2.

A computed spectrum was found[210] which had similar coupling constants to those estimated for this particular spectrum and had a comparable $\nu_o\delta$ value. Using the computed coupling constants both N and $\nu_o\delta$ could be used to calculate the positions of lines 1 and 3 in this particular spectrum. As L and M were also known, lines 9, 10, 11 and 12 could be assigned as well, since $J_{AA'} = J_{BB'}$, M = 0, hence 9,10 and 11,12 are degenerate.

Lines 1 and 3 are nearly always the most intense in the spectra and a comparison of the computed spectra with the A_2B_2 system obtained experimentally led to the assignment of these lines for the latter spectrum. Having assigned these lines it was possible to calculate N as from table 3 - 34. M was assumed to be zero or

nearly so, and it was possible to assign lines 9,10,11 and 12 by inserted estimated values of L first into the energy values relative to the centre point, finding the nearest lines corresponding to these, and hence evaluating accurate values of L. Lines 2,4,6,7 and 8 were obtained by comparison with other similar A_2B_2 spectra.[208] Thus, for example, lines 2 and 4 are nearly always intense and are grouped with lines 1 and 3 respectively. An estimate of K was made from positions of lines 7 and 8 ($K \simeq \nu_8 - \nu_7$). Line 5 was assumed to be too small to see.

The following values were thus obtained.

$K = J_{3,3'} + J_{4,4'} \simeq 14.5$. $\quad M = J_{3,3} - J_{4,4'} \simeq 0$

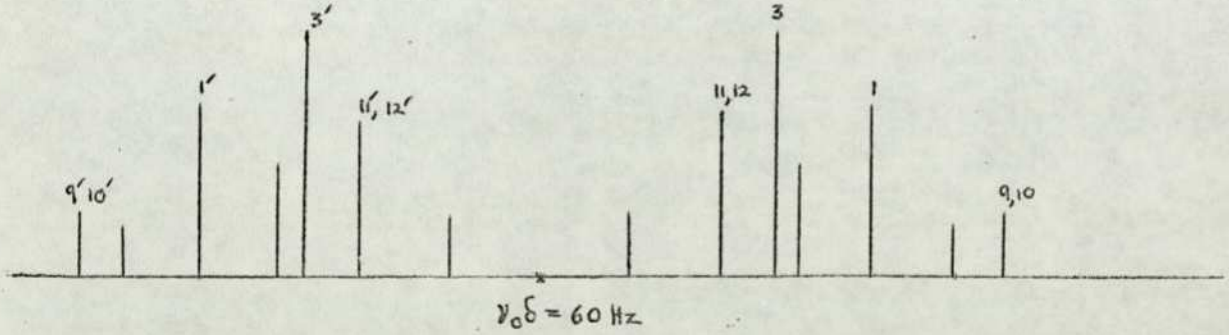
$L = J_{3,4} - J_{3,4'} = 16.5$ $\quad N = J_{3,4} + J_{3,4'} = 3.5$

It was assumed that the gem coupling constants were negative in value, hence the other coupling constants were evaluated.

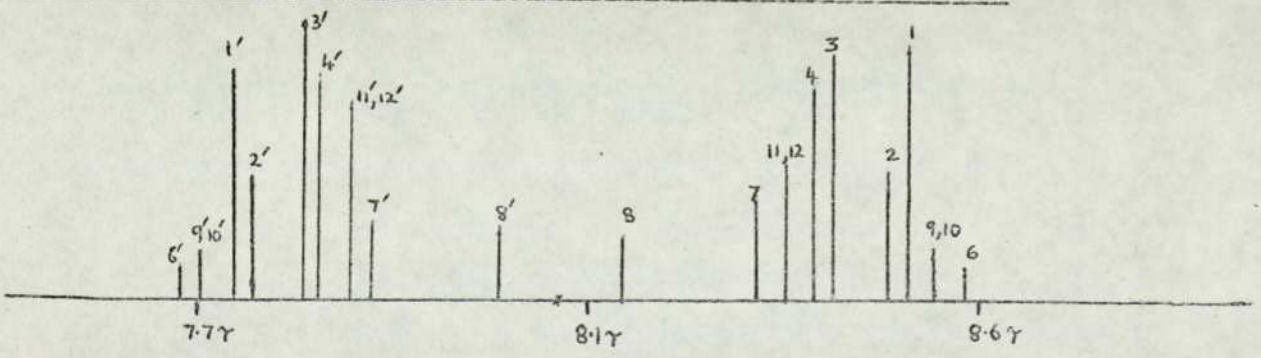
Table 3 - 35. Coupling Constants for Bridge Protons.

	$J_{3,4}$	$J_{3,4'}$	$J_{3,3'}$	$J_{4,4'}$
Coupling Constant (Hz)	-13.0	3.5	7	7

Computed Spectrum. $J_{A,B} = -12$, $J_{A,B'} = 6$, $J_{A,A'} = J_{B,B'} = 6$Hz



Experimental Spectrum. Signal at 6.44τ Irradiated.



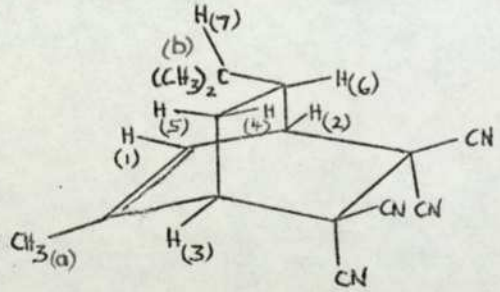
It was concluded that all the spin coupling constants were consistent with a bridged bicyclic conformation as expected for this adduct.

3 - 3 - 12 ∝-Phellandrene/TCNE adduct.

The N.M.R. spectrum of this compound was run using deuterochloroform as solvent.

Table 3 - 36. 100 MHz Signals for ∝-Phellandrene/TCNE Adduct in $CDCl_3$

γ value	No. of protons	Assignment
3.90 (doublet)	1	H_1
6.53 (doublet of doublets)	1	H_2
6.74 (triplet of doublets)	1	H_3
7.66 (multiplet)	1	H_6?
7.94 (doublet)	3	H_a
8.10 (obscured)	1 ?	H_4?
8.76 (multiplet)	2 ?	H_5, H_7 ?
9.08 (triplet)	6	H_b



Because of uncertainties of assignment of the various protons, it was decided to carry out double resonance irradiations for clarification.

Irradiation Experiments.

(1) Irradiation of signal at 7.94γ did not produce any change in the signals at 6.53 and 6.74γ but caused the signal at 3.90γ to appear as a doublet of doublets.

(2) Irradiation of the signal at 7.66τ caused the signal at 6.53τ to collapse to a doublet. It also simplified the signal at 8.76τ.
(3) Irradiation of the signal at 8.76τ caused simplifications in signals at 6.74 and 7.66τ.
(4) Irradiation of both signals at 6.74τ and 6.53τ caused the signal at 7.66τ to appear as four lines and the signal at 8.76τ to appear as four lines with some fine splitting.

The signal at 7.66τ was now firmly assigned as H_6, because H_2 collapsed to a doublet when H_6 was irradiated.
The signals at 6.53 and 6.74τ could be assigned to H_2 and H_3 (compare Section 3 - 3 -11, H_2 at 6.44τ).
Because of ambiguities in the irradiation experiments, it was not possible to assign H_5,H_4 and H_7 protons with certainty. The following coupling constants were evaluated.

Table 3 - 37. Coupling Constants for ∝-Phellandrene/TCNE Adduct.

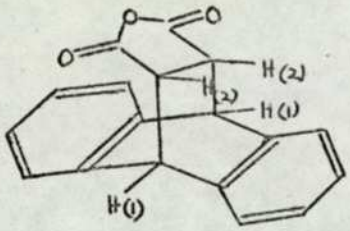
	$J_{1,2}$	$J_{1,a}$	$J_{2,6}$	$J_{1,3}$	$J_{7,b}$	$J_{3,4}$	$J_{3,5}$
Coupling Constant(Hz)	6.5	1.5	2.0	1.3	6.0	~2.5	~2.5

In so far as was possible to determine, the coupling constants were consistent with the rigid bicyclic structure. The difficulty in assigning the bridge protons H_4,H_5 and H_7 might be due to the fact that more than one isomer of the product was present. ∝-phellandrene can exist in (-) or (+) configurations with inversion of configuration at the carbon atom bearing the isopropyl group. The presence of more than one isomer would nullify any exact determination of the positions of bridge protons.

3 - 3 - 13. Anthracene/Maleic Anhydride and Anthracene/TCNE Adducts.
The N.M.R. spectra of these adducts were run using acetone as solvent.

Table 3 - 38. 100 MHz Signals for Anthracene/Maleic Anhydride Adduct in Acetone.

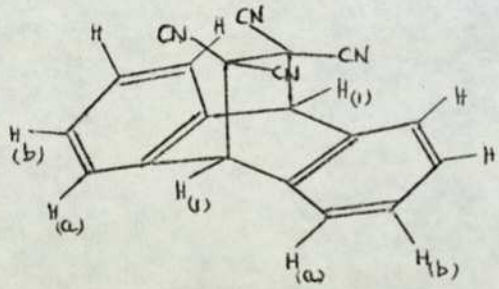
τ value	No. of protons	Assignment
2.70 (multiplet)	8	Aromatic protons
5.10 (multiplet)	2	H_1
6.27 (multiplet)	2	H_2



From the splitting pattern in the two high-field signals, it was concluded that $J_{1,2}$ = 1.8 Hz. The H_1 protons were likely to be experiencing a 'ring-current' effect from the adjacent benzene rings and would be at lower field to the H_2 protons.

Table 3 - 39. 100 MHz Signals for Anthracene/TCNE Adduct in Acetone.

τ value	No. of protons	Assignment
2.28 (multiplet)	4	H_a
2.52 (multiplet)	4	H_b
4.20 (singlet)	2	H_1



The aromatic proton signals were now simplified because of the symmetrical nature of the adduct. The two multiplets consisted of four lines each and the splitting pattern corresponded approximately to an $(A_2X_2)_2$ system. Rough values for coupling constants were

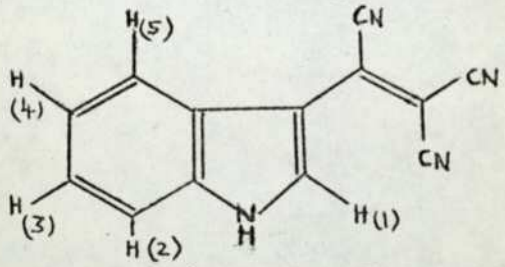
derived on this basis to give $J_{a,b}$(ortho) = 5.1 Hz, $J_{a,b}$(meta) = 3.1 Hz. The sharp singlet corresponding to H_1 was at lower field than the multiplet for H_1 in the maleic anhydride adduct. This was attributed to the electron-withdrawing nature of the nitrile groups.

3 - 3 - 14. Adducts of Indole/TCNE and 1,2-Dimethyl Indole/TCNE

The N.M.R. spectrum of 3-tricyanovinyl indole was run using deuterodimethylsulphoxide as solvent. The N.M.R. spectrum of 1,2-dimethyl-3-tricyanovinylindole was run using deuteroacetone. The two spectra were compared.

Table 3 - 40. 100 MHz Signals of 3-Tricyanovinylindole in CD_3SOCD_3

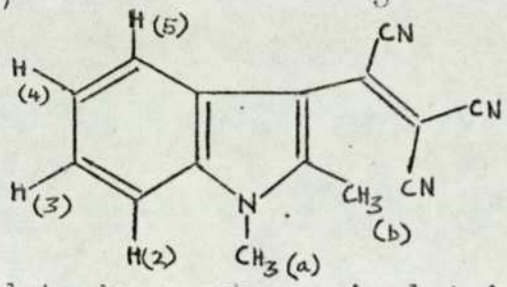
τ value	No. of protons	Assignment
1.32 (singlet)	1	H_1
1.90 (multiplet)	1	H_2
2.35 (multiplet)	1	H_5 ?
2.60 (multiplet)	2	H_3,H_4 ?



When the solution was shaken with D_2O, the spectrum remained the same. From this it was concluded that the low-field singlet was due to H_1 and the N-H proton signal had disappeared in this particular solvent. The multiplet at 1.90τ was probably due to H_2 being closest to the -N-H group and experiencing a further deshielding.

Table 3 - 41. 100 MHz Signals for 1,2-Dimethyl-3-Tricyanovinyl indole in Deuteroacetone.

τ value	No. of protons	Assignment
2.18 (multiplet)	1	H_2
2.42 (multiplet)	1	H_5
2.72 (multiplet)	2	H_3,H_4
6.09 (singlet)	3	H_a
7.30 (singlet)	3	H_b



There appeared to be no sharp singlet in this spectrum and it was thus likely that H_1 was correctly assigned in Table 3 - 40 for the indole/TCNE adduct. Although the change in solvent might make some difference, the low-field multiplet had shifted upfield in going from the indole to the dimethylindole adduct. On this basis it was reasonable to assign it as H_2, being nearest to the changing group -NH $\longrightarrow$ -NCH_3. H_5 was likely to be at lower field to H_3 and H_4, being nearer the nitrile groups.

3 - 4 Conclusion

Using N.M.R. and applying the Karplus equation shikimic acid has previously been shown to exist essentially in the half-chair conformation in solution. If it is assumed that errors due to sp^2 hybridised carbon and electronegative substituents being present are small, the compounds examined in this work have various conformations.

Thus the adducts of diphenylbutadiene, sorbyl alcohol and hexadiene with TCNE appear to exist essentially in the boat conformation,

whereas the adducts of methoxybutadiene, methylpentadiene and 2-vinylnaphthalene with TCNE probably exist closest to a half-chair conformation. The first three adducts have substituents attached to both carbon atoms β to the nitrile group, whereas in the latter three adducts, one β carbon is unsubstituted. Steric interactions between nitrile groups and substituents may thus be responsible for the difference in conformation between these compounds. Thus, for example, there is clearly some steric interaction between bulky phenyl groups and nitrile groups in the half-chair conformation of the diphenylbutadiene adduct. Shikimic acid adopts the half-chair conformation but does not appear to have a similar interaction effect between substituent hydroxy groups. Cyclohexene itself also adopts a half-chair conformation,[212] hence this would appear to be the most stable conformation for such six-membered rings, unless substituent effects predominate.

There might always be expected to be some small deviation from the pure boat conformation in the tetracyano-adducts because of the eclipsing of the nitrile groups.

The bicyclic adducts of hexadiene and methoxybutadiene with maleic anhydride appear to be too rigid to adopt half-chair conformations, so that boat conformations are preferred. It was also confirmed that the expected endo adducts are formed.

Chapter 4

Norbornadiene/TCNE Reaction.

4 - 1. Introduction.

Although this reaction had been studied previously[125] in different solvents, no investigation had been undertaken of the role played by any charge-transfer complex formed during reaction. When the two reactants were mixed together in a suitable solvent, a yellow colour formed immediately, fading as the reaction proceeded. This was attributed to a charge-transfer complex. Since this reaction was of particular interest mechanistically, being the addition of an electrophile to a non-conjugated diene, it was decided to study the kinetics, in some detail, spectroscopically. The rate of fading of the colour was shown to be suitable for such studies at certain concentrations and the decrease in the absorption bands could be followed.

4 - 2. Purification of Reagents.

Norbornadiene (bicyclo [2, 2, 1] hepta-2,5-diene) was supplied as puriss. by Koch-Light Laboratories Ltd. However, the liquid on standing appeared to go yellow after several days, with a deposit forming on the side. Further purification was carried out by fractionally distilling the commercial sample through a packed Vigreux column, using a nitrogen bleed. The clear distillate was then stored under nitrogen in light-proof bottles. Analysis by G.L.C. showed one peak only after distillation (b.p$_{760}$ 89-90°C) $n_D^{20} = 1.4690$.

Tetracyanoethylene was supplied by Eastman Kodak Laboratories and was purified by recrystallisation twice from 1,2-dichloroethane and then sublimed twice under vacuum at 100°C. The white crystals

obtained had m.p 199-200°C (lit.[158] m.p 199-200°C) and were stored under vacuum.

1,2-dichloroethane and dichloromethane were purified as described in section 2 - 1.

4 - 3. Preparation and Analysis of the Adduct.

4 - 3 - 1. Preparation.

Norbornadiene (0.5g) was added to a solution of tetracyanoethylene (0.4g) in benzene and a dark colour was immediately formed. The mixture was refluxed for 1 hr. and then cooled. The benzene was evaporated off to give the crude product (0.38g). Recrystallisation twice from 1,2-dichloroethane yielded white crystals of 8,8,9,9-tetracyanoquadricyclo $[2,2,1,2^{3},5_{0}{}^{2},6]$ nonane. m.p. 195-196°C, (lit.[125] m.p 185-186°C).

Calculated for $C_{13}H_8N_4$: C, 70.8; H, 3.68; N, 25.4%

Found: C, 70.6; H, 3.93; N, 25.3%.

4 - 3 - 2. Thin-layer Chromatogram.

Analysis of the recrystallised adduct on silica gel chromagram (activated) using chloroform as moving phase showed one spot (R_f 0.39) only, visible under ultraviolet light.

4 - 3 - 3. UV/Visible Spectrum.

Solutions of the adduct in 1,2-dichloroethane showed no absorption bands in the region 230-600 nm.

4 - 3 - 4. Infrared Spectrum.

The sample was made up in the form of a KBr disc and the spectrum recorded, using an attenuator in the reference beam.

Table 4 - 1. Infrared Spectrum of Norbornadiene/TCNE Adduct.

Wavenumber	Assignment
2940 cm^{-1} (m)	$-CH_2-$ stretching
2880 cm^{-1} (m)	-CH- stretching
2260 cm^{-1} (w)	-CN stretching
1340 cm^{-1} (m)	-CH- bending
815 cm^{-1} (s)	characteristic of nortricylenes [213]

4 - 3 - 5. Mass Spectrum.

The measured mass of the (M-1) ion was 219.0671, which was exactly the same as for the calculated ion $(C_{13}H_7N_4)^+$.

Table 4 - 2. Main Mass Fragments for Norbornadiene/TCNE Adduct.

m/e	220(M)	219	193	166	92	91	39	28	27
Relative Abundance(%)	24.3	100.0	25.8	12.5	73.5	86.4	18.5	22.5	19.5

The m/e values at 92 and 91 indicate a retro homo-Diels-Alder process taking place with the loss of tetracyanoethylene from the parent ion. Loss of one HCN from the parent ion gives m/e 193, and loss of two HCN molecules gives m/e 166. Metastable peaks due to the transitions 220→219 and 92→91 also occur.

4 - 3 - 6. Conclusion.

The N.M.R., (see section 3 - 3- 1) infrared and mass spectrum conclusively show that the adduct occurs as a saturated, quadricyclic compound containing the nortricyclene system.

4 - 4. Kinetic Studies.

4 - 4 - 1. Visible Spectroscopy.

When a solution of norbornadiene in 1,2-dichloroethane was added to a solution of tetracyanoethylene in the same solvent, the yellow solution formed showed a broad symmetrical band with λ_{max} 472 nm (in dichloromethane, λ_{max} 475 nm). The colour intensified on cooling, but faded during the course of reaction. As such an absorption band did not occur in the spectra of either norbornadiene or tetracyanoethylene it was attributed to a charge-transfer complex in equilibrium with the reactants.

4 - 4 - 1 - 1. Determination of K and ε for the Charge-transfer. Complex.

The first step in the kinetic study was to determine the equilibrium constant, K, and extinction coefficient, ε, for the charge-transfer complex in suitable solvents. Initially, dichloromethane was used as solvent, but 1,2-dichloroethane was found to be more suitable for slow reactions, as it was less volatile and errors due to evaporation were minimised.

The Benesi-Hildebrand method (section 1 - 1 - 3) was used to determine K and ε values, using a large excess of norbornadiene in the reaction mixtures at different temperatures. To obtain initial optical densities, d_o, log d was plotted against t, giving straight line graphs for the disappearance of the charge-transfer complex absorption during reaction and extrapolated to zero time. Using the Perkin-Elmer Hitachi Spectrophotometer, solutions of norbornadiene and TCNE were made up separately and placed in the thermostatted bath several minutes before mixing. The solution cell (1 cm) was placed in the thermostatted cell housing. The two reactant solutions were mixed together in the waterbath, the point at which half of the reactant solutions had been added to the other taken as zero time for reaction.

The solution was then shaken and rapidly transferred to the cell. Alternatively, a solution of norbornadiene was made up and transferred to the solution cell in the thermostatted cell-housing and allowed to equilibrate with the temperature of the surroundings. The solution of TCNE was then rapidly added to this, the cell shaken and left inside the cell-housing while measurements were made. In all cases a reference cell (1 cm) containing pure solvent was placed in the cell-housing.

The following results were obtained for the Benesi-Hildebrand plots, where $[D] \gg [A]$. $[A]_o$, $[D]_o$, are the initial molar acceptor concentration and initial molar donor concentration respectively.

Table 4 - 3. Benesi-Hildebrand Data for Norbornadiene (D)/TCNE (A) at 472 nm in 1,2-Dichloroethane. T = 16.3°C, $[A]_o$ = 4.08 x 10^{-3}M.

$[D]_o$ (M)	$[D]_o^{-1}$	d_o	$[A]_o\ d_o^{-1} \times 10^2$
0.501	1.99	0.132	3.06
0.599	1.67	0.153	2.61
0.702	1.43	0.178	2.29
0.798	1.25	0.195	2.09
0.901	1.11	0.218	1.83
1.004	0.99	0.251	1.61
1.198	0.83	0.281	1.45

Table 4 - 4. Data as for above. T = 30.5°C, $[A]_o$ = 4.01 x 10^{-3}M.

$[D]_o$ (M)	$[D]_o^{-1}$	d_o	$[A]_o\ d_o^{-1} \times 10^2$
0.506	1.99	0.122	3.28
0.601	1.67	0.149	2.68
0.703	1.43	0.166	2.41
0.801	1.25	0.193	2.07
0.899	1.11	0.208	1.92
1.004	0.99	0.222	1.80

Table 4 - 5. Data as for above. T = 38.8°C, $[A]_o$ = 4.11 x 10^{-3}M.

$[D]_o$ (M)	$[D]_o^{-1}$	d_o	$[A]_o d_o^{-1} \times 10^2$
0.604	1.66	0.144	2.85
0.710	1.42	0.165	2.45
0.802	1.25	0.187	2.16
0.903	1.11	0.219	1.88
0.999	1.00	0.238	1.74
1.102	0.91	0.252	1.63

Table 4 - 6. Benesi-Hildebrand Data for Norbornadiene/TCNE at 475 nm in Dichloromethane, T = 24.9°C, $[A]_o$ = 4.02 x 10^{-3}M.

$[D]_o$ (M)	$[D]_o^{-1}$	d_o	$[A]_o d_o^{-1} \times 10^2$
0.401	2.50	0.133	3.01
0.509	1.98	0.166	2.41
0.598	1.67	0.194	2.08
0.803	1.25	0.234	1.71
0.851	1.17	0.262	1.54
0.901	1.11	0.266	1.50

Table 4 - 7. Data as for above. T = 32.0°C, $[A]_o$ = 4.02 x 10^{-3}M.

$[D]_o$ (M)	$[D]_o^{-1}$	d_o	$[A]_o d_o^{-1} \times 10^2$
0.501	2.00	0.158	2.57
0.606	1.65	0.181	2.21
0.701	1.43	0.206	1.94
0.803	1.25	0.220	1.83
0.902	1.11	0.254	1.58

In the Benesi-Hildebrand method plots of $[D]_o^{-1}$ against $[A]_o d_o^{-1}$ give straight lines having intercept $1/\varepsilon$ and slope $1/K\varepsilon$ for 1 cm. optical path-length cells (see Fig. 4 - 1). The results obtained at the different temperatures for each solvent are shown.

Figure 4-1

Benesi-Hildebrand plot for norbornadiene/TCNE complex in 1,2-dichloroethane.

λ = 472 nm.

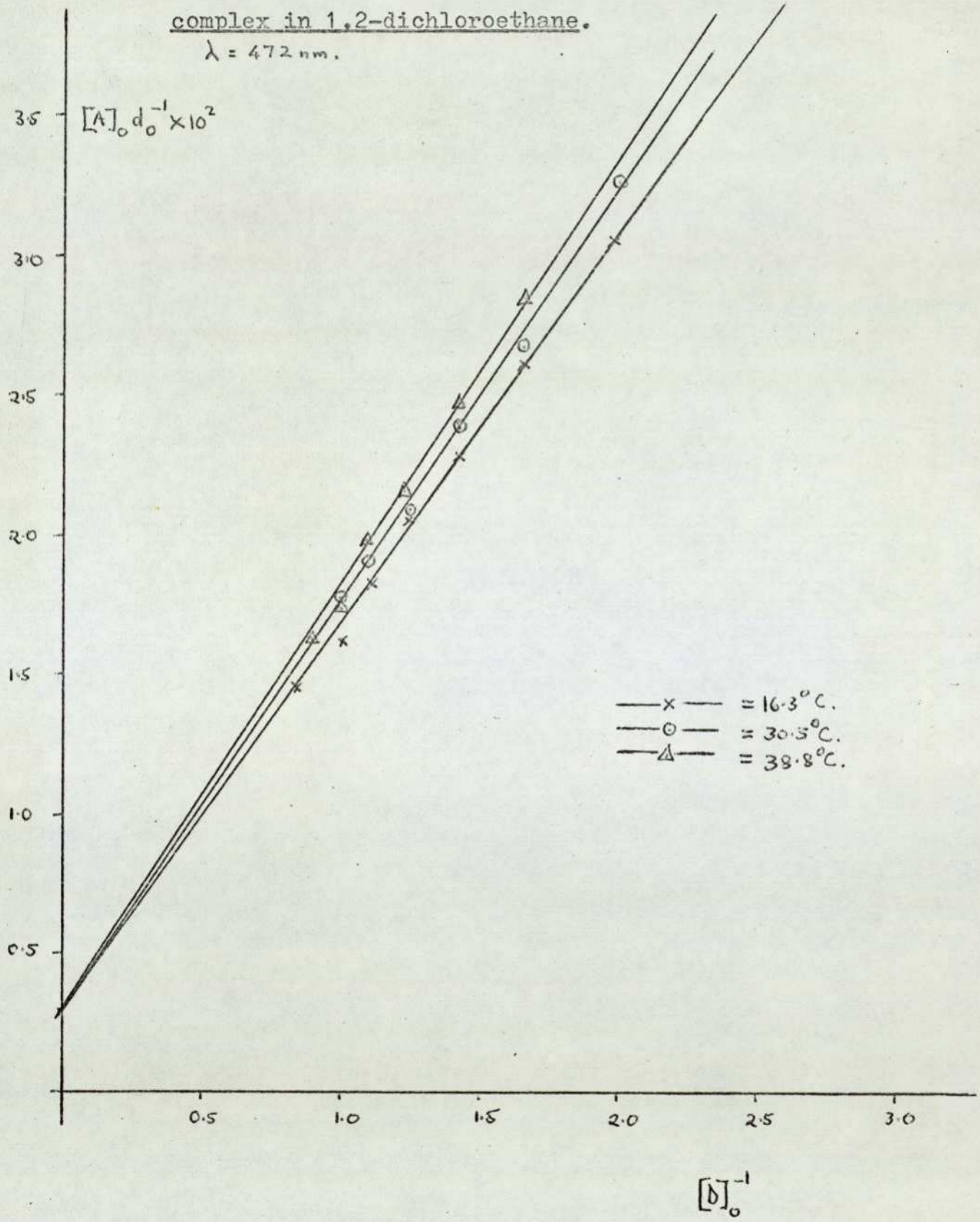


Table 4 - 8. Determined K and ε values for Norbornadiene/TCNE in 1,2-Dichloroethane at 472 nm.

T (^{o}C)	ε	Kε	K (l mol^{-1})
16.3	330	64.4	0.195
30.5	330	60.9	0.185
38.8	330	58.9	0.180

Table 4 - 9. Determined K and ε values for Norbornadiene/TCNE in Dichloromethane at 475 nm.

T (^{o}C)	ε	Kε	K (l mol^{-1})
24.9	385	90.8	0.233
32.0	358	85.5	0.230

As the intercepts were so small, a small error in $1/\varepsilon$ would lead to a large error in evaluation of K. It was found that Kε values were most accurate to determine. The results obtained using dichloromethane as solvent were considered to be too inaccurate for determination of thermodynamic parameters.

Using the Van't Hoff equation,

$$\text{Log } K = -\Delta H/2.303\ RT + \Delta S/2.303\ R \qquad (4 - 1)$$

The enthalpy and entropy of complex formation in 1,2-dichloroethane were determined by calculation of the slope and intercept of (4 - 1) after plotting Log K against 1/T.

$\Delta H = -0.7$ kcal mol^{-1} (-2.9 kjoule mol^{-1}) $\Delta S = +5.9$ e.u.

K and ε for the norbornadiene/TCNE complex in 1,2-dichloroethane were also determined by an equimolar method[83] as a comparison with the Benesi-Hildebrand method. A difference between the two results, might indicate the presence of termolecular species, such as D_2A, when the donor was in large excess.

As for the Benesi-Hildebrand method, the basic assumption that only the 1:1 complex is formed still holds.

$$A + D \rightleftharpoons AD^{*} \qquad (4 - 2)$$

The equilibrium constant, K, is given by:

$$K = [AD^{*}] \; / \; ([A]_o - [AD^{*}])\,([D]_o - [AD^{*}]) \qquad (4 - 3)$$

For equimolar concentrations:

$$K = [AD^{*}] \; / \; ([A]_o - [AD^{*}])^2 \qquad (4 - 4)$$

For 1 cm. optical path length cells, the concentration of complex is given by:

$$[AD^{*}] = d_o/\varepsilon \qquad (4 - 5)$$

Substituting (4 - 5) into (4 - 3) and rearrangement gives:

$$[A]_o \; / \; d_o = 1/\varepsilon + 1 \; / \sqrt{K \varepsilon d_o} \qquad (4 - 6)$$

Thus a plot of $[A]_o/d_o$ against $1/\sqrt{d_o}$ should give a straight line of slope $1/\sqrt{K\varepsilon}$, intercept $1/\varepsilon$.

The following results were obtained for equimolar concentrations.

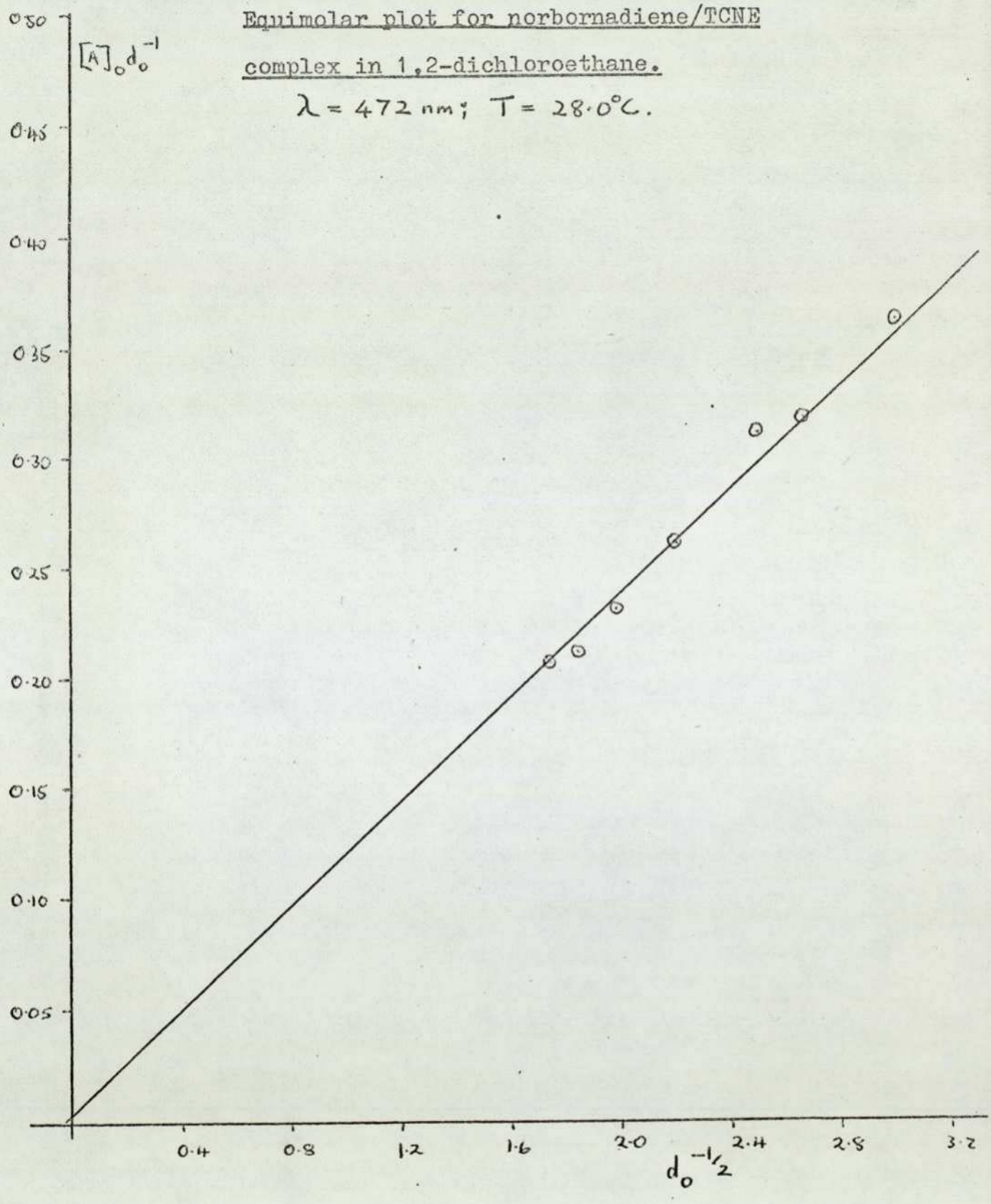
Table 4 - 10. Equimolar Data for Norbornadiene (D)/TCNE (A) at 472 nm in 1,2-Dichloroethane. T = 28.0°C.

$[A]_o = [D]_o$ (M)	d_o	$[A]_o\, d_o^{-1}$	$1/\sqrt{d_o}$
0.0401	0.110	0.364	3.015
0.0452	0.141	0.319	2.663
0.0509	0.161	0.312	2.493
0.0552	0.208	0.265	2.193
0.0600	0.255	0.235	1.984
0.0651	0.304	0.214	1.814
0.0712	0.328	0.210	1.744

Figure 4-2

Equimolar plot for norbornadiene/TCNE complex in 1,2-dichloroethane.

$\lambda = 472$ nm; $T = 28.0°C$.



A plot of $A_o d_o^{-1}$ against $d_o^{-\frac{1}{2}}$ gave a straight line with a very small intercept (see Fig. 4 - 2). It was difficult to obtain an exact value for $1/\xi$ as this would be in the region 0.002 to 0.003. However, a value of 69.5 was obtained for $K\xi$ from the slope and if a value of 330 is assigned to ξ, K becomes 0.210, which agrees fairly well with K values in this temperature region derived from the Benesi-Hildebrand method.

4 - 4 - 1 - 2. Determination of Rate Constants.

Rate constants for the reaction were derived from the rate of decay of the charge-transfer complex band in the visible spectrum. The following scheme might be represented as the reaction taking place.

$$A + D \rightleftharpoons AD^* \longrightarrow AD \qquad (4 - 7)$$

The rate of disappearance of acceptor molecules is given by:

$$- d[A] / dt \propto [A][D] \qquad (4 - 8)$$

Now if the formation of the charge-transfer complex is assumed to be very rapid compared with the subsequent reaction, and if the donor concentration is in very large excess so that $[D]_o \simeq [D]$ throughout the course of reaction, then $[A] \propto [AD^*]$ and hence:

$$- d[AD^*] / dt = k_2 [AD^*][D] \qquad (4 - 9)$$

k_2 being the experimental rate constant in 1 mol^{-1} s^{-1}. Since $[D]$ is very large and virtually constant, the above equation may be derived in terms of a pseudo first-order reaction giving:

$$t = (2.303/k_1) \log ([AD^*]_o / [AD^*]_t) \qquad (4 - 10)$$

As the concentration of complex at time t, $[AD^*]_t$, is given by

$$[AD^*]_t = d_t \varepsilon l \qquad (4 - 11)$$

Then substituting (4 - 11) into (4 - 10) gives:

$$t = (-2.303/k_1) \log d_t + C \qquad (4 - 12)$$

Plots of log d_t, where d_t is the optical density of the charge-transfer complex absorption, against t will give a slope equal to $-k_1/2.303$, and hence the pseudo first-order rate constant may be evaluated. The second-order rate constant, k_2, is given by:

$$k_2 = k_1 / [D]_o \qquad (4 - 13)$$

and may thus be simply determined.

For this particular reaction, the above plots all give straight lines for different concentrations of donor relative to acceptor at different temperatures. The absorptions were followed until the final optical density values were either zero or very small. The same procedure was adopted in making up solutions as for the Benesi-Hildebrand experiments. The values obtained for k_1 and k_2 at different temperatures are shown.

Table 4 - 11. Rate Constants $k_1(s^{-1})$, $k_2(l\ mol^{-1}\ s^{-1})$ for Norbornadiene (D)/TCNE (A) in 1,2-Dichloroethane. T = 16.3°C, $[A]_o = 4.08 \times 10^{-3}$M, at 472 nm.

$[D]_o$ (M)	$k_1 \times 10^4$	$k_2 \times 10^4$
0.501	1.01	2.01
0.599	1.31	2.19
0.702	1.36	1.94
0.798	1.62	2.03
0.901	1.77	1.97
1.004	2.15	2.15
1.198	2.48	2.08

Table 4 - 12. Rate Constants as for above. T = 30.5°C, $[A]_o$ = 4.01 x 10^{-3}M.

$[D]_o$ (M)	$k_1 \times 10^4$	$k_2 \times 10^4$
0.506	2.92	5.76
0.601	3.02	5.01
0.703	3.22	4.60
0.801	3.84	4.80
0.899	4.26	4.74
1.004	5.20	5.20

Table 4 - 13. Rate Constants as for above. T = 38.0°C, $[A]_o$ = 6.53 x 10^{-3}M.

$[D]_o$ (M)	$k_1 \times 10^4$	$k_2 \times 10^4$
0.746	5.49	7.31
0.797	5.76	7.22
0.895	6.40	7.15
0.990	7.10	7.10
1.105	7.64	6.93

Table 4 - 14. Rate Constants as for above. T = 38.8°C, $[A]_o$ = 4.11 x 10^{-3}M.

$[D]_o$ (M)	$k_1 \times 10^4$	$k_2 \times 10^4$
0.710	5.65	7.98
0.802	5.79	7.21
0.903	6.72	7.46
0.999	7.54	7.54
1.102	7.73	7.02

Table 4 - 15. Rate Constants as for above. T = 46.0°C, $[A]_o$ = 4.10 x 10^{-3}M.

$[D]_o$ (M)	$k_1 \times 10^4$	$k_2 \times 10^3$
0.603	7.84	1.30
0.702	7.45	1.06
0.801	1.00	1.25
0.899	1.03	1.14
1.001	1.20	1.20
1.107	1.28	1.16
1.202	1.41	1.17

Table 4 - 16. Rate Constants k_1 (s^{-1}), k_2(1 mol^{-1} s^{-1}) for Norbornadiene (D)/TCNE (A) in Dichloromethane. T = 13.9°C, $[A]_o$ = 4.04 x 10^{-3}M.

$[D]_o$ (M)	$k_1 \times 10^4$	$k_2 \times 10^4$
0.506	1.01	1.99
0.701	1.12	1.60
0.801	1.49	1.86
1.103	2.02	1.83

Table 4 - 17. Rate Constants as for above. T = 25.0°C, $[A]_o$ = 4.01 x 10^{-3}M.

$[D]_o$ (M)	$k_1 \times 10^4$	$k_2 \times 10^4$
0.402	1.19	2.97
0.498	1.53	3.07
0.603	1.81	3.00
0.701	2.14	3.05
0.801	2.52	3.14
0.850	2.80	3.29
0.909	3.18	3.50

Table 4 - 18. Rate Constants as for above. T = 31.9°C, $[A]_o$ = 4.03 x 10^{-3}M.

$[D]_o$ (M)	$k_1 \times 10^4$	$k_2 \times 10^4$
0.502	1.86	3.72
0.606	2.50	4.17
0.705	3.01	4.29
0.801	3.10	3.86
0.906	3.59	3.99

Rate Constants for the reaction were also determined by an equimolar method. As before, the equation upon which the rates were based was (4 - 7). For equimolar concentrations:

$$-d\,[AD^*]\,/\,dt = k_2([AD^*])\,([D]_o - [AD^*] - [AD]) \qquad (4 - 14)$$

This is equivalent to equation (4 - 9), where the donor is in large excess. The equilibrium constant, K, for formation of charge-transfer complex is given by (4 - 15) for equimolar concentrations.

$$K = [AD^*]\,/\,([D]_o - [AD^*] - [AD])^2 \qquad (4 - 15)$$

Substitution of (4 - 15) into (4 - 14) and integration yields:

$$2\sqrt{K\varepsilon}\,/\,\sqrt{d} = k_2\,t + C \qquad (4 - 16)$$

Where for 1 cm. cells, $d = \varepsilon\,[AD^*]$. Thus a graphical plot of $1/\sqrt{d}$ against t should give a straight line of slope $k_2/2\sqrt{K\varepsilon}$.
The change in charge-transfer complex absorption (λ = 472 nm) was followed for a range of equimolar concentrations of norbornadiene and TCNE and graphical plots of the above gave straight lines.
At this temperature, $K\varepsilon$ had been evaluated as 69.5 previously, (see section 4 - 4 - 1 - 1).

Table 4 - 19. Rate Constants k_2 ($l\ mol^{-1}\ s^{-1}$) for Norbornadiene (D)/ TCNE (A) in 1,2-Dichloroethane, at 472 nm. T = 28.0°C, $[A]_o = [D]_o$

$[A]_o \times 10^2$ (M)	4.01	4.52	5.09	5.52	6.00	6.51	7.12
$k_2 \times 10^4$	6.08	5.38	5.54	5.20	6.00	5.32	5.82

As for the results using an excess of donor, the k_2 values are fairly constant at this temperature and can be compared with those obtained at 30.5°C. (see Table 4 - 12).

Allowing for experimental error, all the determined rate constant values appear virtually constant over the range where the reactant concentrations have doubled. The dielectric constant of norbornadiene at 20°C (~ 2) is different from 1,2-dichloroethane (~10.6) and in the cases where there is a large excess of the donor, there may be some change in this solvent parameter when donor concentration is changed. A cycloaddition such as this may be sensitive to dielectric constant, which could cause a change in rate constant. However, experiments using 1,2-dichloroethane/carbon tetrachloride mixtures showed that the change in rate constant with small changes in dielectric constant (which would be the case in going from 0.5M→1.0M norbornadiene was insignificant as is also shown later (section 4 - 4 - 2 - 2).

If the k_2 values are nearly constant then the scheme (1 - 23), as formulated by Rappoport[81], is not that operating in this reaction. However schemes (1 - 21) and (1 - 22) may be considered. If $k_{exp} = k_2$ then:

$$D + A \rightleftharpoons AD^* \longrightarrow AD \qquad (1 - 21)$$

$$k_2 = k_c K / (1 + K [D])$$

$$D + A \rightleftharpoons AD^*, \quad D + A \longrightarrow AD \qquad (1 - 22)$$

$$k_2 = k_c / (1 + K [D])$$

For this reaction, the equilibrium constants in both 1,2-dichloroethane and dichloromethane are small (~0.2). The term $(1 + K[D])$ does not change a great deal as the donor concentration changes from 0.4M $\longrightarrow$ 1.1M. Either of schemes (1 - 21) or (1 - 22) should give values of k_2 which change very little with change in donor concentration, i.e. $k_2 \simeq k_c$ or $k_2 \simeq k_c K$.

On this basis it is possible to derive thermodynamic parameters such as energy of activation, ΔE, and entropy of activation, ΔS^*, for the reaction. It can be shown[214] that:

$$\log k = \log A - \Delta E/2.303\,RT \qquad (4 - 17)$$

Where $$A = RT/Nh.\ e^{\Delta S^*/R} \qquad (4 - 18)$$

R is the gas constant (cal $deg^{-1} mol^{-1}$), T is the absolute temperature (^oK), N is the Avogadro number (mol^{-1}) and h is Planck's constant (erg s).

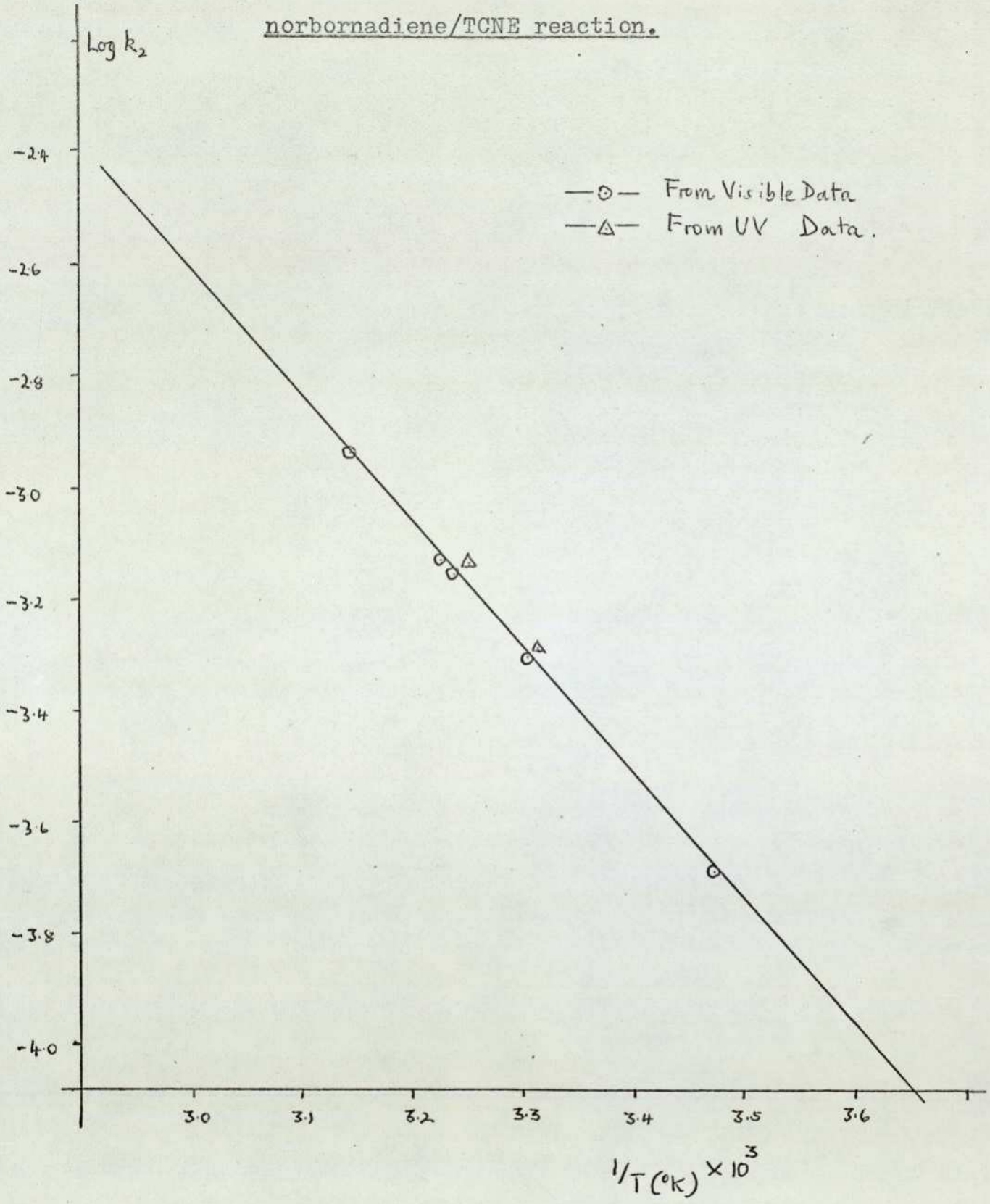
For this reaction, a plot of log k_2 against 1/T should give a straight line of slope $-\Delta E/2.303R$ and intercept Log A. ΔS^* can be determined either from the intercept or calculated from k_2 values inserted in the above equation. Using the data in tables 4 - 11 to 4 - 19, mean values for k_2 were calculated at each temperature and an Arrhenius plot drawn for measurements in 1,2-dichloroethane (see Fig. 4 - 3).

Table 4 - 20. Data for Arrhenius Plot of Norbornadiene/TCNE in 1,2-Dichloroethane in Visible Spectrum.

$k_2 \times 10^4$ (l mol^{-1} s^{-1})	Log k_2	T (^oK)	$1/T \times 10^3$
2.05	-3.688	289.3	3.46
5.00	-3.301	303.5	3.29
7.14	-3.146	311.0	3.22
7.41	-3.130	311.8	3.21
11.67	-2.932	319.0	3.13

Figure 4-3

Arrhenius plot of rate constants for norbornadiene/TCNE reaction.



From the slope of the graph of log k_2 against I/T.

ΔE = 10.5 kcal mol^{-1} (43.6 kjoule mol^{-1}) ΔS^* was calculated at each temperature.

Table 4 - 21. Entropy of Activation for Norbornadiene/TCNE in 1,2-Dichloroethane.

T (^oK)	289.3	303.5	311.0	311.8	319.0
ΔS^* (e.u)	-41.7	-41.7	-41.9	-41.8	-41.7

4 - 4 - 2. Ultraviolet Spectroscopy.

Norbornadiene and TCNE both absorb in the ultraviolet region but the norbornadiene bands lie at higher energy (λ_{max} 211,230 nm) to the TCNE band (λ_{max} 265 nm). It was thus possible to follow the decrease in absorption of TCNE during reaction using certain conditions. Firstly, because of the large extinction coefficient of TCNE in 1,2-dichloroethane, (λ_{max} 265 nm (ε 13,450), it was necessary to use 0.1 cm. cells to obtain optical densities which could be measured accurately for TCNE concentrations of around 0.5 mM. Secondly, as the concentration of donor was in large excess, there was always an absorbance at 265 nm due to the norbornadiene (~0.1). To eliminate this, it was necessary to make up a solution of norbornadiene of the same concentration in the reference cell. The maximum amount of error in mismatching solutions was considered to be about 5%, which would given an error in absorbance reading of 0.005, minimal compared with the absorbance changes of the TCNE band. Because the 0.1 cm. cells were small in volume, evaporation error considerations excluded the use of the low boiling solvent dichloromethane. 1,2-dichloroethane or mixtures of 1,2-dichloroethane-carbon tetrachloride were therefore used throughout the experiments in the ultraviolet region. Solutions

of TCNE and norbornadiene made up separately were kept in the thermostatted bath until the start of reaction when they were mixed and rapidly transferred to the solution cell in the cell housing. The reference cell was filled beforehand with a solution of norbornadiene and placed in the cell-housing.

4 - 4 - 2 - 1. Rate Constants in 1,2-Dichloroethane.

Before the reaction mixture was made up, a solution of TCNE having a concentration equal to that for reaction, was examined in the ultraviolet region and absorbance measurements made. This acted as a measurement of TCNE concentration for zero time.

When the reaction mixture was examined at 265 nm, it was noticed that the absorbance was usually at least 10% less than this initial optical density measurement (see Fig. 4 - 4). Extrapolation of the absorbance measurements for reaction back to zero time did not give a point corresponding to the preliminary optical density, but usually 5→10% lower. This difference was not due to a dielectric constant change of TCNE in going from pure 1,2-dichloroethane to mixtures of 1,2-dichloroethane-norbornadiene as the donor concentration was too low to give any significant change either in dielectric constant or extinction coefficient. The initial change was attributed to a rapid reaction, which was generally too fast to measure, and might be due to the formation of an intermediate.

Rate constant measurements for these experiments were made only on the points obtained during reaction and the initial difference was examined separately (see Fig. 4 - 5). The rate equation upon which the results were based was:

$$-d\left[TCNE\right]_f / dt = k_2 \left[TCNE\right]_f \left[D\right] \qquad (4 - 19)$$

where $\left[TCNE\right]_f$ is the free TCNE concentration.

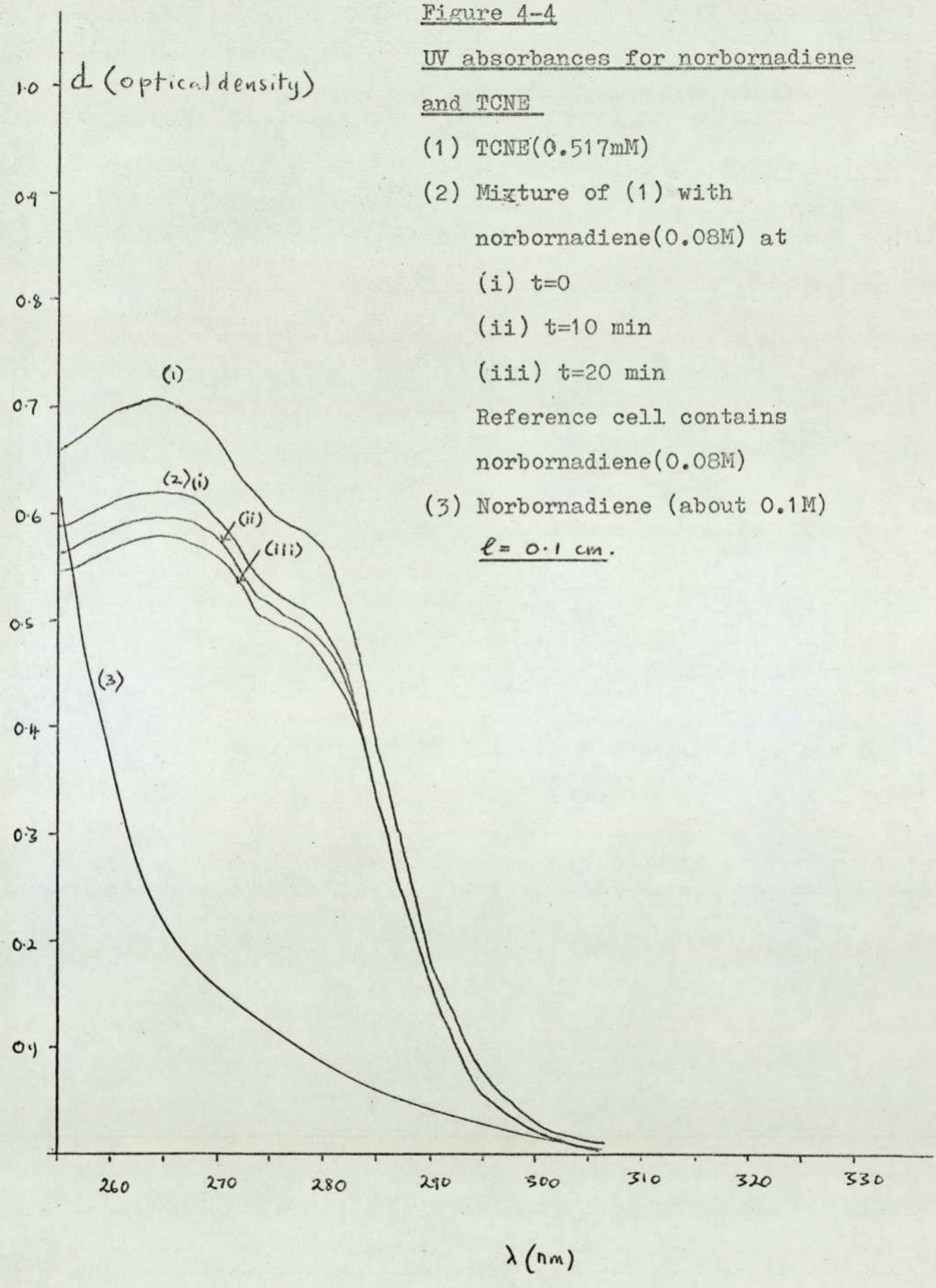


Figure 4-4

UV absorbances for norbornadiene and TCNE

(1) TCNE(0.517mM)

(2) Mixture of (1) with norbornadiene(0.08M) at

(i) t=0

(ii) t=10 min

(iii) t=20 min

Reference cell contains norbornadiene(0.08M)

(3) Norbornadiene (about 0.1M)

ℓ = 0.1 cm.

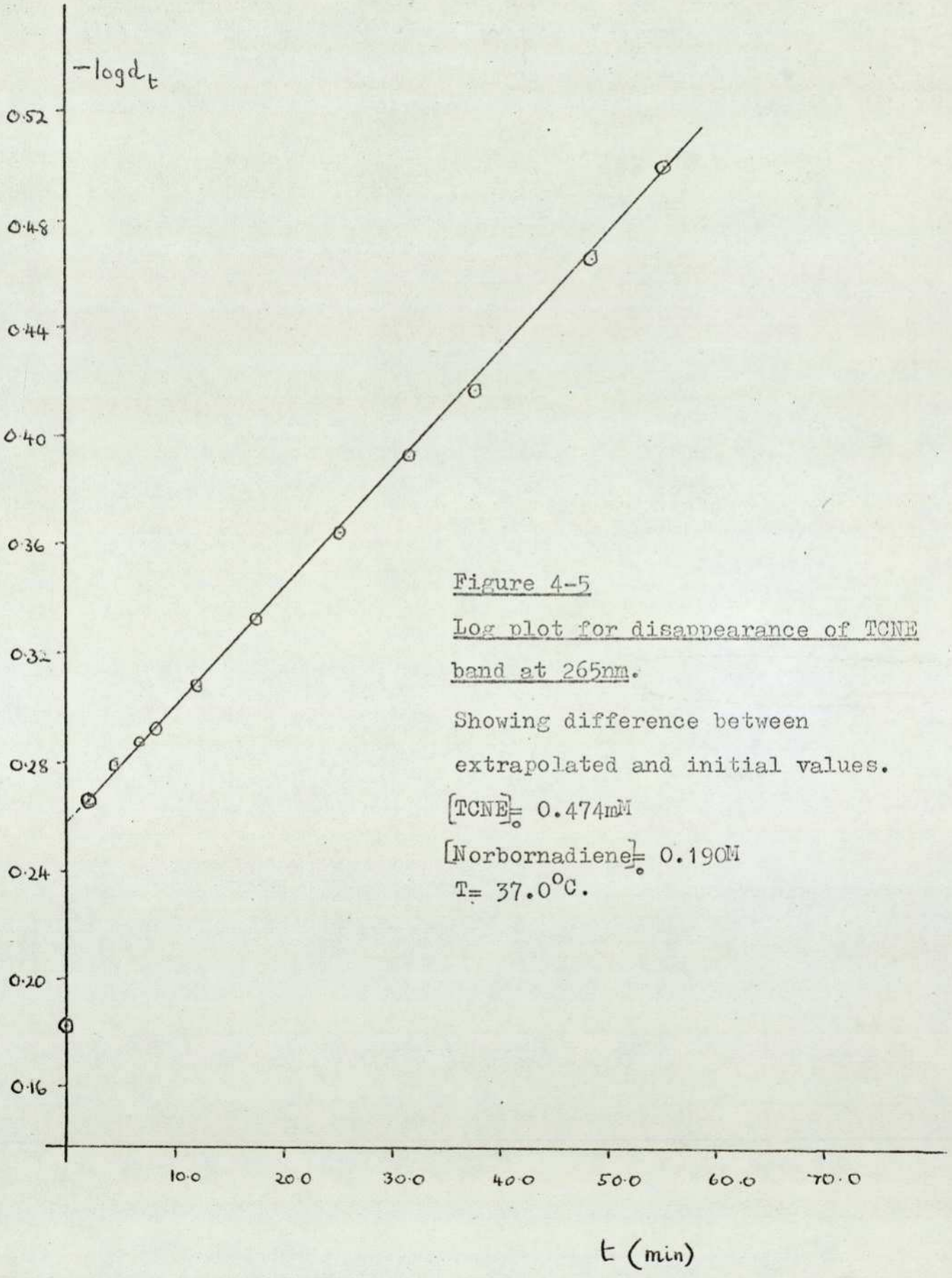


Figure 4-5

Log plot for disappearance of TCNE band at 265nm.

Showing difference between extrapolated and initial values.

$[TCNE]_o$ = 0.474mM

$[Norbornadiene]_o$ = 0.190M

T = 37.0°C.

From this, a graph of log d_t against t would give a straight line of slope $-k_1/2.303$, where $k_1 = k_2[D]$.

The following results were obtained by following the decrease in absorbance at 265 nm.

Table 4 - 22. Rate Constants, k_2 (l mol^{-1} s^{-1}), for Norbornadiene (D)/TCNE (A) in 1,2-Dichloroethane at 265 nm. T = 29.5°C.

$[D]_o \times 10^2$ (M)	$[A]_o \times 10^4$ (M)	$k_2 \times 10^4$
5.32	5.17	5.51
6.11	5.17	5.31
6.95	5.17	5.84
7.50	5.17	5.67
8.18	5.17	5.47
8.94	5.17	5.81
10.10	5.17	5.22
3.55	3.01	5.55

Table 4 - 23. Rate Constents as for above. T = 34.5°C.

$[D]_o \times 10^2$ (M)	$[A]_o \times 10^4$ (M)	$k_2 \times 10^4$
1.06	0.50	7.70
7.06	5.04	7.02
9.40	5.04	7.22
12.50	5.04	7.80

The rate constants compare fairly well with those obtained in the visible region in the respective temperature range (Fig. 4 - 3). It was also possible to obtain ΔE and ΔS^* values from the above data, using a simplified Arrhenius equation, inserting mean values of k_2 at each temperature. This gave the following results:

ΔE = 10.50 kcal mol^{-1}(44.0 kjoule mol^{-1}). ΔS^* =-41.2 e.u.

4 - 4 - 2 - 2. Rate Constants in 1,2-Dichloroethane/Carbon Tetrachloride.

The effect of a change in solvent on the rate constant of reaction was examined by using 1,2-dichloroethane/carbon tetrachloride mixtures. The latter solvent is miscible, comparatively non-volatile at lower temperatures and has a dielectric constant comparable with that of norbornadiene. It was not possible, however, to make up solutions of TCNE in 100% carbon tetrachloride, because of the low solubility in this solvent. Absorbances of TCNE were followed at 265 nm in the usual way in order to derive rate constants.

Table 4 - 24. Rate Constants k_2 ($l\ mol^{-1}\ s^{-1}$) for Norbornadiene (D)/TCNE (A) in 1,2-Dichloroethane/Carbon Tetrachloride at 265 nm. $T = 29.5^{o}C$, $[D]_o = 0.075\ M$, $[A]_o = 5.61 \times 10^{-4} M$.

% CCl_4 by volume	Dielectric Constant [a]	$k_2 \times 10^4$
0.0	10.6	5.67
10.0	9.8	5.40
30.0	8.1	4.91
50.0	6.4	3.20
65.0	5.1	2.12

a - Estimated from Ref. 215

This clearly showed that the rate constant for reaction increased with increase in dielectric constant of the medium. However, changes in going from 0 to 10% carbon tetrachloride were fairly small and therefore it could be deduced that for solutions containing up to 1M norbornadiene (about 10% by volume) the rate constant is not expected to change significantly, since norbornadiene has a similar dielectric constant to carbon tetrachloride (about 2.2).

4 - 4 - 2 - 3. Investigation of Initial Rapid Reaction.

As mentioned before, there was a discrepancy between the extrapolated initial optical density of TCNE in reaction and TCNE in a made-up solution. These differences in optical density at various excess donor concentrations, were examined at 265 nm. Plots of log d_t against t were drawn up (see Fig. 4 - 5) for a series of solutions, and initial optical densities obtained by extrapolation. These were then compared with the actual initial TCNE optical densities, and the following definition was made:

$$\left[{}^{d}\text{TCNE (total)} - {}^{d}\text{TCNE (extrapolated)} \right] / {}^{d}\text{TCNE (total)} = y \qquad (4 - 20)$$

The results obtained are shown in Table 4-25.

Table 4 - 25. Initial Optical Density Parameters for Norbornadiene/TCNE at 265 nm. T = 37.0°C, $[A]_o = 4.74 \times 10^{-4}$ M.

$[D]_o$ (M)	y	$y/(1-y)\,[D]_o$
0.102	0.075	0.682
0.190	0.162	1.018
0.239	0.187	0.945
0.310	0.236	0.969
0.420	0.304	1.063
0.490	0.375	1.228

If the reaction is assumed to pass through the charge-transfer complex as in the following scheme:

$$A + D \underset{}{\overset{K}{\rightleftharpoons}} AD^{*} \longrightarrow AD \qquad (4 - 21)$$

then the equilibrium constant, K, determined previously by the Benesi-Hildebrand method (section 4 - 4 - 1 - 1) is given approximately by:

$$K = [AD^*] / ([A]_o - [AD^*])[D]_o \qquad (4 - 22)$$
$$= 0.180 \text{ l mol}^{-1} \text{ (at } 37.0^\circ\text{)}$$

If it is assumed that the absorption is due only to free, uncomplexed TCNE and if the initial difference in optical density of the TCNE is attributed to the formation of the charge-transfer complex, having a concentration equal to the calculated TCNE concentration of the initial difference, then y values may be calculated from the experimental value of K.

In this case: $y = [AD^*] / [A]_o \qquad (4 - 23)$

and from (4 - 22):

$$[AD^*] = K [D]_o [A]_o / (1 + K [D]_o) \qquad (4 - 24)$$

Table 4 - 26. y Values Obtained for Single Charge-Transfer Complex, K = 0.180.

$[D]_o$	$[AD^*] \times 10^4$ (M)	y
0.102	0.805	0.017
0.190	1.52	0.032
0.239	1.94	0.041
0.310	2.51	0.053
0.420	3.36	0.071
0.490	3.84	0.081

The y values are thus shown to be much lower than those obtained experimentally (Table 4 - 25), indicating that either K is incorrect or the possible existence of a second complex in equilibrium with the charge-transfer complex with both species contributing to the initial difference in optical density of free TCNE. Rearrangement of (4 - 24) and (4 - 23) gives:

$$1/y = 1/[D]_o K + 1 \qquad (4\text{-}24a)$$

A plot of $1/y$ against $1/[D]_o$ would give a straight line of slope $1/K$ if only the one complex was present. In this case it was found that a curved line was obtained.

A double equilibrium may thus be envisaged:

$$A + D \underset{}{\overset{K_1}{\rightleftharpoons}} AD^* \overset{K_2}{\rightleftharpoons} AD^{\ddagger} \longrightarrow AD \qquad (4 - 25)$$

K_1 and K_2 are the equilibrium constants for formation of first and second complex respectively.

$$K_1 = [AD^*] \,/\, [A]_f [D]_o, \quad K_2 = [AD^{\ddagger}] \,/\, [AD^*] \qquad (4 - 26)$$

If the initial difference in optical density of TCNE is due to the presence of both species and the equilibria are established very quickly:

$$y = ([AD^*] + [AD^{\ddagger}]) \,/\, [A]_o \qquad (4 - 27)$$

Now: $$[A]_f = [A]_o - [AD^*] - [AD^{\ddagger}] \qquad (4 - 28)$$

And: $$[AD^{\ddagger}] = K_2 [AD^*] \qquad (4 - 29)$$

Where: $$[AD^*] = K_1 [D]_o [A]_f \qquad (4 - 30)$$

Combining equations (4 - 28) to (4 - 30):

$$[AD^*] + [AD^{\ddagger}] = K_1[D]_o ([A]_o - [AD^*] - [AD^{\ddagger}]) \, (1 + K_2) \qquad (4 - 31)$$

Substitution of (4 - 27) and further simplification gives:

$$y \,/\, (1 - y) [D]_o = K_1 + K_1 K_2 \qquad (4 - 32)$$

Thus values of $y \,/\, (1 - y) [D]_o$ should be constant for each concentration of donor. In fact, experimentally, they are shown in table 4 - 25 to increase with increase in donor concentration, showing that the double equilibrium as in (4 - 25) cannot be the correct mechanism for this reaction.

In this reaction sequence, it has been assumed that the initial rapid decrease in optical density is due to formation of the charge-transfer complex (AD^*) and the second complex ($AD^{\ddagger}$). Although there are examples [216,217] of a decrease in optical density of free reactants on complexing, it was also found [79] that on mixing dimethylaniline and TCNE, where K for the complex is large, the optical density in the UV region (λ = 260 nm) was additive despite the fact that about half of the reactants were in the complexed form. It was considered possible that the decrease in optical density was due only to $AD^{\ddagger}$, where:

$$y = [AD^{\ddagger}] / [A]_o \qquad (4 - 33)$$

hence: $$y = K_1K_2[D]_o/(1 + K_1[D]_o + K_1K_2[D]_o) \qquad (4 - 34)$$

and: $$(1-y)[D]_o/y = 1/K_1K_2 + [D]_o/K_2 \qquad (4 - 35)$$

A plot of $(1-y)[D]_o/y$ against $[D]_o$ would give a slope $1/K_2$ and intercept $1/K_1K_2$. However, calculations showed that such a plot for this reaction gave a negative value for K_2 and hence such a mechanism was rejected.

If a molecule of donor reacts with the charge-transfer complex to form a second intermediate, which may be a 2:1 donor:acceptor complex, then:

$$A + D \rightleftharpoons AD^* , \quad AD^* + D \rightleftharpoons AD_2^* \qquad (4 - 36)$$

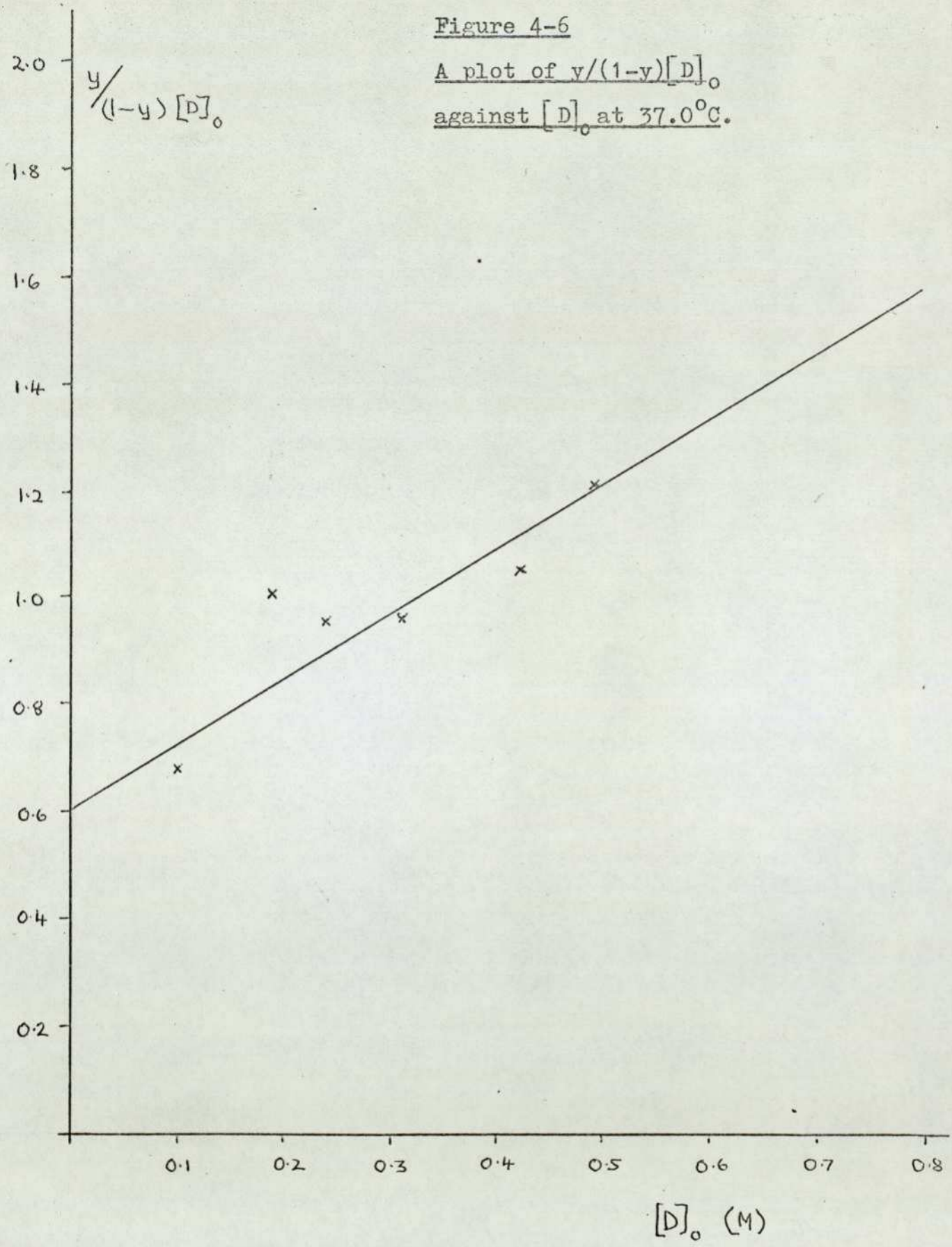
If the procedure adopted in equations (4 - 27) to (4 - 32) is similarly applied again, then:

$$y/(1-y)[D]_o = K_1 + K_2K_1[D]_o \qquad (4 - 37)$$

A plot of $y/(1-y)[D]_o$ against $[D]_o$ should give a straight line of slope K_1K_2 and intercept K_1 (see Fig. 4 - 6).

Figure 4-6

A plot of $y/(1-y)[D]_o$ against $[D]_o$ at 37.0°C.



For this case, a graphical plot gives

$$K_1 = 0.6 \text{ l mol}^{-1}, \quad K_2 = 2.76 \text{ l mol}^{-1}.$$

A further equilibrium scheme (4 - 38) is also possible.

$$A + D \rightleftharpoons AD^*, \quad A + 2D \rightleftharpoons AD_2^* \qquad (4 - 38)$$

This gives a similar derived equation to the above:

$$y/(1-y)\,[D]_o = K_1 + K_2\,[D]_o \qquad (4 - 39)$$

A plot gives $K_1 = 0.6$ l mol^{-1} and $K_2 = 1.66$ l^2 mol^{-2}.
Again, if the initial rapid decrease in optical density is due only to the formation of (AD_2^*) then:

$$y = [AD_2^*] / [A]_o = K_1K_2[D]_o^2 / (1 + K_1[D]_o + K_1K_2[D]_o^2) \qquad (4 - 40)$$

$$\text{and } (1-y)\,[D]_o^2/y = 1/K_1K_2 + [D]_o/K_2 \qquad (4 - 41)$$

hence a plot of the left-hand side against $[D]_o$ should give a straight line of slope $1/K_2$ and intercept $1/K_1K_2$ (Fig. 4 - 7). This gives $K_1 = 16$ l mol^{-1} and $K_2 = 1.2$ l^2 mol^{-2}. Since K_1 was determined experimentally to be about 0.2 l mol^{-1}, this mechanism does not appear to account for the observed data.
If (4 - 36) is incorporated into the overall reaction, there are four possible schemes that might be operating as shown.

$$A + D \rightleftharpoons AD^* \overset{D}{\rightleftharpoons} AD_2^* \xrightarrow{k_c} AD + D \qquad (4 - 42)$$

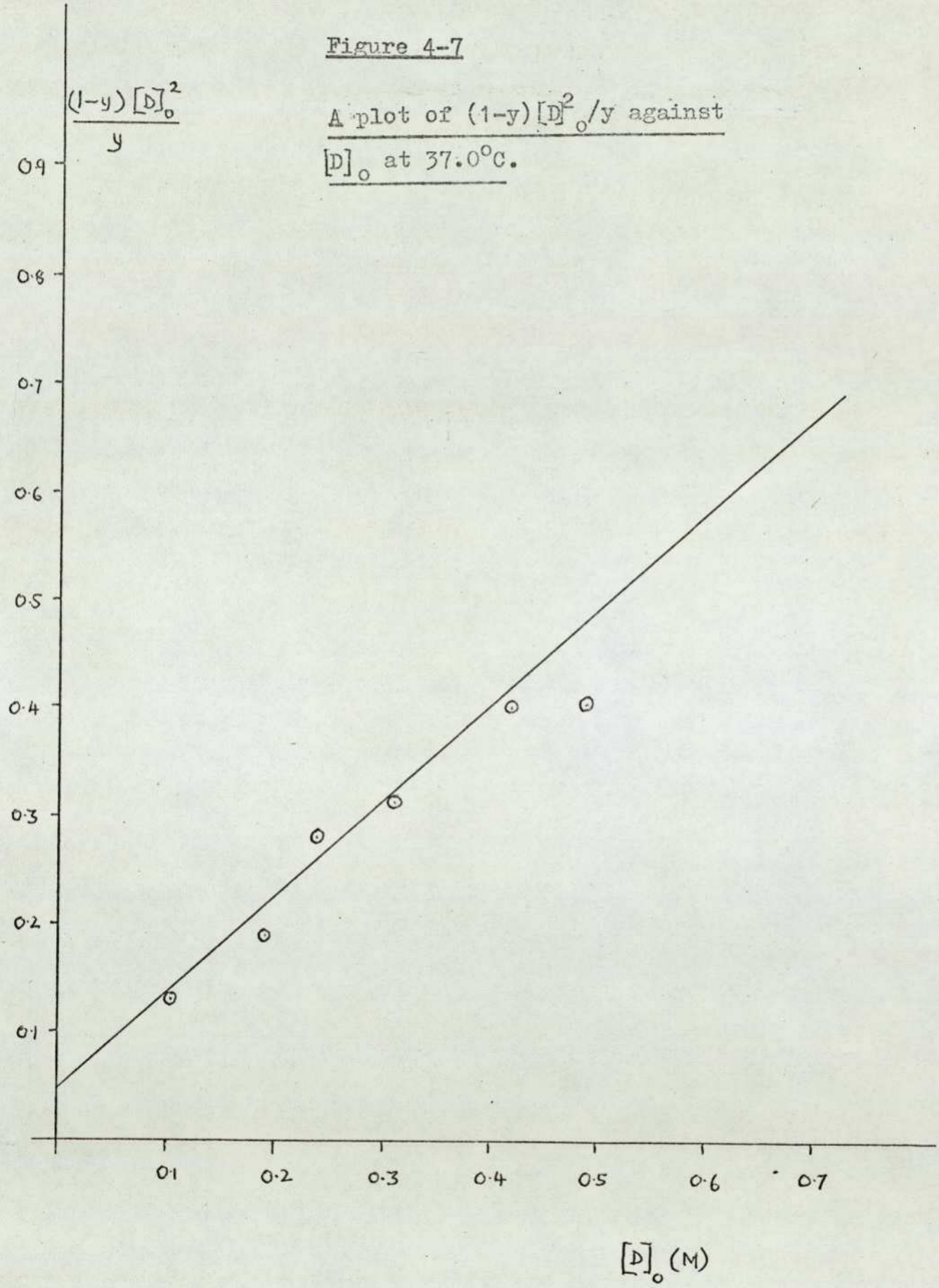
$$A + D \rightleftharpoons AD^* \overset{D}{\rightleftharpoons} AD_2^*, \quad A + D \xrightarrow{k_c} AD \qquad (4 - 43)$$

$$A + D \rightleftharpoons AD^* \overset{D}{\rightleftharpoons} AD_2^* \xrightarrow[k_c]{D} AD + 2D \qquad (4 - 44)$$

$$A + D \rightleftharpoons AD^* \overset{D}{\rightleftharpoons} AD_2^*, \quad AD^* \xrightarrow[k_c]{} AD, \quad AD_2^* \xrightarrow[k_c]{} AD + D \qquad (4 - 45)$$

Figure 4-7

A plot of $(1-y)[D]_o^2/y$ against $[D]_o$ at 37.0°C.



For reactions, where there is a large excess of donor present so that $[D]_o \simeq [D]$, the rate of reaction in (4 - 42) is given by:

$$- d\,[TCNE]_t/dt = k_c[AD_2^*] \qquad (4 - 46)$$

Where: $$[AD_2^*] = K_2\,[AD^*]\,[D] \qquad (4 - 47)$$

and: $$[TCNE]_t = [AD^*]/K_1[D] + [AD^*] + K_2[AD^*][D] \qquad (4 - 48)$$

Differentiation gives:

$$- d\,[TCNE]_t/dt = -d[AD^*]/dt.\ (1 + K_1[D] + K_1K_2[D]^2)/K_1D \qquad (4 - 49)$$

The experimental rate constants, k_2, as obtained in section 4 - 4 - 1 - 2 are given by:

$$k_2 = (-d[AD^*]/dt)\ /\ [AD^*]\,[D] \qquad (4 - 50)$$

Substitution of (4 - 46), (4 - 47) and (4 - 50) into (4 - 49) gives:

$$k_2 = k_c\,K_1K_2[D]\ /\ (1 + K_1[D] + K_1K_2[D]^2) \qquad (4 - 51)$$

A similar procedure as that given above applied to scheme (4 - 43) gives:

$$k_2 = k_c/\ (1 + K_1[D] + K_1K_2[D]^2) \qquad (4 - 52)$$

And as applied to (4 - 44) gives:

$$k_2 = k_cK_1K_2[D]^2/\ (1 + K_1[D] + K_1K_2[D]^2) \qquad (4 - 53)$$

And as applied to (4 - 45) gives:

$$k_2 = k_cK_1(1 + K_2[D])/\ (1 + K_1[D] + K_1K_2[D]^2) \qquad (4 - 54)$$

Experimental values of k_2, obtained from measurements in the visible and UV regions of the spectrum, gave k_c values calculated using the above equations derived from reaction schemes (4 - 42) to (4 - 45).

However, equation (4 - 53) was not applied since it could be seen immediately that the $[D]^2$ term in the numerator would lead to variable values of k_c. Data from tables 4 - 12, 4 - 13 and 4 - 22 were used to obtain k_c values from equations (4 - 51), (4 - 52) and (4 - 54). Data from tables 4 - 11, 4 - 14 and 4 - 15 are not shown here but gave similar trends.

Table 4 - 27. Comparison of k_2 and k_c (1 mol^{-1} s^{-1}) from Data in Table 4 - 13. $T = 38.0^{\circ}$

$[D]_o$(M)	$k_2 \times 10^4$	$k_c \times 10^4$(4-51)	$k_c \times 10^4$ (4 - 52)	$k_c \times 10^4$ (4 - 54)
0.746	7.31	14.06	17.29	9.43
0.797	7.22	13.87	18.23	9.46
0.895	7.15	13.84	20.44	9.79
0.990	7.10	13.96	22.80	10.15
1.105	6.93	13.98	25.49	10.53

Table 4 - 28. Comparison as above from Data in Table 4 - 12. $T = 30.5^{\circ}$

$[D]_o$(M)	$k_2 \times 10^4$	$k_c \times 10^4$(4-51)	$k_c \times 10^4$ (4 - 52)	$k_c \times 10^4$ (4 - 54)
0.506	5.76	11.90	9.90	6.95
0.601	5.01	9.88	9.80	6.16
0.703	4.60	8.87	10.29	6.00
0.801	4.80	9.22	12.19	6.35
0.899	4.74	9.18	13.62	6.55
1.004	5.20	10.24	16.98	7.50

Table 4 - 29. Comparison as above from Data in Table 4 - 22.

$T = 29.5^{o}C.$

$[D]_o$(M)	$k_2 \times 10^4$	$k_c \times 10^4$(4-51)	$k_c \times 10^4$(4-52)	$k_c \times 10^4$(4-54)
0.0532	5.51	65.05	5.71	8.26
0.0611	5.31	54.95	5.54	7.91
0.0695	5.84	53.47	6.13	8.58
0.0750	5.67	48.32	5.98	8.27
0.0818	5.47	42.90	5.79	7.87
0.0894	5.81	42.03	6.20	8.31
0.1010	5.22	33.72	5.62	7.41

It can therefore be seen that the only equation that gives reasonably constant k_c values at a given temperature is (4 - 54). In this case the k_c values are reasonably close when comparing tables 4 - 28 and 4 - 29 when the temperature is almost the same. The data from table 4 - 29, where k_2 values were determined in the UV region give slightly higher values for k_c.

If these k_c values are correct then the reaction scheme (4 - 45) may be operating in this reaction. Insertion of the values of K_1, K_2 from scheme (4 - 38) to the various equations, give results very similar to those obtained above. It is probably not possible, therefore, to distinguish between the two schemes.

$$A + D \rightleftharpoons AD^* \overset{D}{\rightleftharpoons} AD^*_2, \quad AD^* \longrightarrow AD, \quad AD^*_2 \longrightarrow AD + D \qquad (4 - 45)$$

$$A + D \rightleftharpoons AD^*, \quad A + 2D \rightleftharpoons AD^*_2, \quad AD^* \longrightarrow AD, \quad AD^*_2 \longrightarrow AD + D \qquad (4 - 55)$$

K_1 and K_2 were determined at 37.0^{o} but were inserted into equations involving k_2 values determined at lower temperatures. It is assumed that although K_1 and K_2 will increase slightly at lower temperatures, the change in value will not affect the trend in k_c value, whether

decreasing, increasing or constant.

4 - 5. Discussion.

Bicyclohepta-2,5-diene and TCNE react smoothly to form a single cycloadduct by a ($\pi^2s + \pi^2s + \pi^2s$) pathway. The formation of a colour when the reactants are mixed together indicates a charge-transfer complex, which can be examined in the visible region of the spectrum.

The results obtained in the UV spectrum at 37.0°, following the decrease in concentration of TCNE suggest that there is more than one complex present in solution. Although straight line plots are obtained for the Benesi-Hildebrand and equimolar methods, suggesting the presence of only one complex, the initial difference in TCNE concentration, as measured by the optical densities in the UV spectra suggest there is a double equilibrium such as:

$$A + D \rightleftharpoons AD^* \overset{D}{\rightleftharpoons} AD_2^* \qquad (4 - 36)$$

with a 2:1 donor:acceptor complex in equilibrium with the 1:1 complex. The value of K_1 determined this way is different to K determined by the Benesi-Hildebrand and equimolar methods. As stated previously[77], linearity in Benesi-Hildebrand plots may not exclude the possible existence of termolecular species. There may be some error in measuring an apparently small equilibrium constant, where there is not a great proportion of acceptor in the complexed form.

The overall reaction scheme may be explained by:

$$A + D \rightleftharpoons AD^* \overset{D}{\rightleftharpoons} AD_2^*, \quad AD^* \longrightarrow AD, \quad AD_2^* \longrightarrow AD + D \qquad (4 - 45)$$

in which the total amount of charge-transfer complex reacts to form the adduct. This scheme gives virtually constant k_c values.

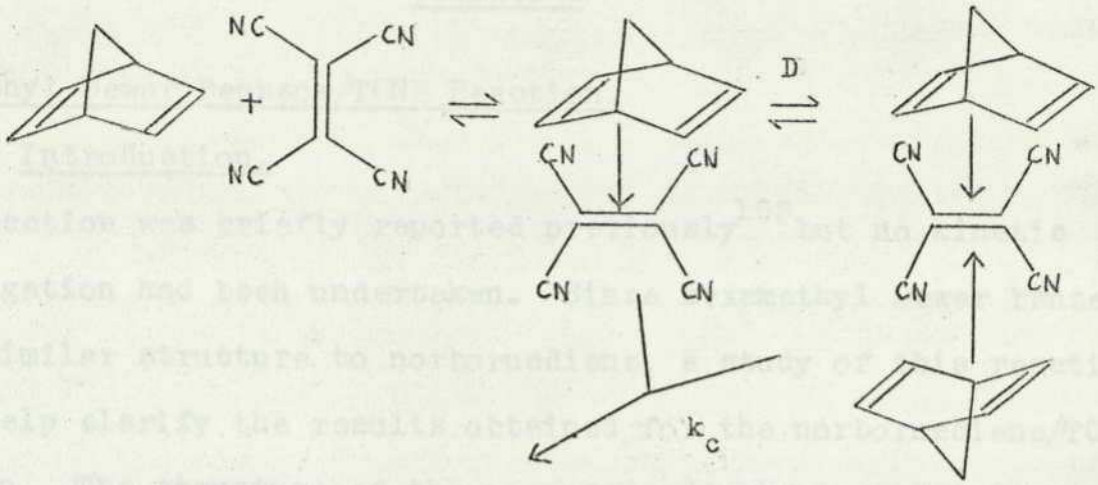
The experimental rate constants, k_2, obtained before were also almost constant and the reaction could also be explained in addition by the scheme as shown below, where $k_2 = k_c$:

$$A + D \rightleftharpoons AD^* \overset{D}{\rightleftharpoons} AD_2^*, \quad (A + AD^* + AD_2^*) \xrightarrow{3D} 3AD + 3D \qquad (4 - 56)$$

This scheme appears to be less likely energetically, since the charge-transfer complex will be of different free energy to the free reactants in solution and would be unlikely to have the same activation barrier for formation of the same product. Although the rate of reaction is shown to increase with increase in dielectric constant of the medium (see table 4 - 24), it is not of sufficient magnitude to postulate a dipolar transition state or intermediate, but only a transition state in which some polarity does occur. k_c values determined on the basis of the above scheme and plotted in the form of an Arrhenius plot give ΔE and ΔS^* values very similar to those derived using experimental k_2 values in table 4 - 20. (ΔE = 11.10 kcal mol^{-1}, ΔS^* = -40.5 e.u.).

The high negative entropy of activation and energy of activation values are consistent with those of most Diels-Alder type reactions in which a highly oriented transition state is postulated.

The mechanism above involves two species AD^* and AD_2^*, both of which give the product. Since both are complexes they are likely to be of similar energy and have a similar activation barrier for forming the final product. When considering the structure of the product it is clear that a 'sandwich' type of structure for the complex (either 1:1 or 2:1) leads directly to the correct orientation.



Adduct (+ Donor) (4 - 57)

Chapter 5

Hexamethyl Dewar Benzene/TCNE Reaction.

5 - 1. Introduction.

This reaction was briefly reported previously[152] but no kinetic investigation had been undertaken. Since hexamethyl Dewar benzene has a similar structure to norbornadiene, a study of this reaction might help clarify the results obtained for the norbornadiene/TCNE addition. The structure of the proposed adduct was first investigated by the usual methods to see whether the reaction was a ($\pi^2s + \pi^2s + \pi^2s$) cycloaddition or not. Under suitable conditions the kinetics of reaction were then investigated using UV and visible spectroscopy.

5 - 2. Purification of Reagents.

Hexamethyl [2,2,0] bicyclohexa-2,5-diene was supplied by the Aldrich Chemical Co. Ltd. On standing, the liquid appeared to go yellow and it was distilled under vacuum (30mm) using a nitrogen bleed. The main fraction distilled at 70°C and was collected as a colourless liquid, leaving a yellow oily residue in the distillation flask. Analysis by G.L.C. using a Carbowax 20M column (4 ft) at 80° and by programming to 200°C showed that the compound was at least 99.9% pure after distillation. In order to minimise decomposition of the compound, it was stored in light-proof bottles in the refrigerator, having been previously purged with dry nitrogen. $n_D^{20} = 1.4483$ (lit.[152] $n_D^{20} = 1.4479$).

Tetracyanoethylene was purified as described in Section 4 - 2 and 1,2-dichloroethane purified as described in Section 2 - 1 - 5.

5 - 3. Preparation and Analysis of the Adduct.

5 - 3 - 1. Preparation.

Hexamethyl Dewar benzene (3.0g) was added to a solution of TCNE (1.0g)

in 1,2-dichloroethane (150ml) and the mixture, which turned a dark blue colour, was refluxed under nitrogen for 24 hours, during which time the colour changed to brown. The solvent was removed by evaporation to yield a crude brown coloured solid. Analysis of the crude solid on T.L.C. (silica gel) using carbon tetrachloride/chloroform (50:50 $^{v}/_{v}$) as solvent showed the presence of four spots. One major component (R_f about 0.4) and three minor components, namely, one fast moving spot (R_f about 0.7), a yellow spot (R_f about 0.2) and a brown spot at the origin were present. The crude solid was dissolved in a mixture of chloroform/carbon tetrachloride (50:50 $^{v}/_{v}$) and passed through a column of activated Silica Gel (60-120 Mesh). Elution with solvent mixtures containing an increasing proportion of chloroform caused the fast moving component to appear (about 50mg). Elution with chloroform, caused the separation of the major component (about 1.9g) and the yellow component, which came through as an oil (about 30mg). It was not possible to elute the brown residue.

The fast moving solid compound, which appeared as colourless crystals was analysed using N.M.R. and was shown to be identical with hexamethyl benzene. A solution of the compound made up in chloroform, gave one signal as a singlet (τ = 7.66) and when mixed with hexamethyl benzene the solution gave the same signal but with greater intensity. The structure was confirmed by T.L.C., when both compound and hexamethyl benzene had identical R_f values, and by melting point. m.p. = 160 -162°C (m.p.(hexamethylbenzene)^{218} = 164°C).

The yellow oil obtained had a similar UV spectrum in chloroform (a very broad band rising towards 210nm) to that of the yellow oil obtained after distillation of impure hexamethyl Dewar benzene.

The major component, was recrystallised twice from hexane, yielding colourless needles.

Percentage Yield = 83%, m.p.(sealed tube) 266-268°C (lit.[152] 268-69°C).

Calculated for $C_{18}H_{18}N_4$: C, 74.5; H, 6.20; N, 19.3%

Found: C, 74.6; H, 6.31; N, 19.0%

5 - 3 - 2. Thin-Layer Chromatogram.

Analysis of the recrystallised adduct on silica gel chromagram (activated) using carbon tetrachloride/chloroform (50:50 $^{v}/_{v}$) as solvent showed only one spot (R_f 0.42) which was visible under ultraviolet light.

5 - 3 - 3. UV/Visible Spectrum.

Solutions of the adduct in 1,2-dichloroethane and in chloroform showed no absorption bands in the region 230-650nm.

5 - 3 - 4. Infrared Spectra.

A spectrum of hexamethyl Dewar benzene, as a liquid film, was recorded using an attenuator in the reference beam.

Table 5 - 1. Infrared Spectrum of Hexamethyl Dewar Benzene.[152]

Wavenumber	Assignment.
2970 cm^{-1} (s)	$-CH_3$ stretching.
2880 cm^{-1} (s)	$-CH_3$ stretching.
1680 cm^{-1} (w)	-C = C- stretching.
1441 cm^{-1} (s)	C - CH_3 bending.
1370 cm^{-1} (m)	C - CH_3 bending.

The infrared spectrum of the recrystallised adduct was recorded by making a mull with hexachlorobutadiene. An attenuator was placed in the reference beam.

Table 5 - 2. Infrared Spectrum of Hexamethyl Dewar Benzene/TCNE Adduct.

Wavenumber	Assignment.
2990 cm^{-1} (s)	$-CH_3$ stretching.
2940 cm^{-1} (s)	$-CH_3$ stretching.
2260 cm^{-1} (w)	$-C\equiv N$ (unconjugated).
1460 cm^{-1} (s)	$C-CH_3$ bending.
1385 cm^{-1} (s)	$C-CH_3$ bending.
737 cm^{-1}	

5 - 3 - 5. Mass Spectrum.

The molecular mass of the parent ion was 290.1543, which compared quite closely with that calculated (290.1532) for the ion $(C_{18}H_{18}N_4)^+$.

Table 5 - 3. Main Masses for Hexamethyl Dewar Benzene/TCNE Adduct.

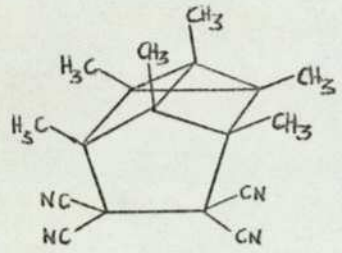
m/e	290(M)	162	148	147	135	87	85	83	47	44	36
Relative Abundance%	27.4	60.8	25.2	97.2	47.3	29.6	95.9	100.0	47.1	42.2	43.0

m/e 162 might indicate some homo Diels-Alder reaction occuring. m/e 147 indicates loss of CH_3 from m/e 162, which is also shown by the metastable peak at m/e 133.5 corresponding to the transition 162→147. This peak (m/e 147) is the base peak in the mass spectrum of hexamethyl benzene, and suggests that the latter may be formed during fragmentation. The base peak at m/e 83 and that at m/e 85 may correspond to the ions $C_6H_{11}^+$ and $C_6H_{13}^+$ respectively.

5 - 3 - 6. Conclusion.

The IR spectrum presents evidence that the (2 + 2 + 2) cycloadduct

structure is correct for this compound. Although C = C stretching occurs in the hexamethyl Dewar benzene itself, there is no such stretching in the adduct. The N.M.R. spectrum (see Section 3 - 3 - 2) also supports the evidence that there are no C = C double bonds in the adduct. On this basis the adduct is shown to be 7,7,8,8-tetracyanohexamethylquadricyclo $[2,2,0,0^{2,6},2^{3,5}]$octane with the structure as shown.



5 - 4. Kinetic Studies.

5 - 4 - 1. Visible Spectroscopy.

Solutions of hexamethyl Dewar benzene (0.5M) and of TCNE (4mM) were mixed together and the visible spectra of the mixture examined using 1 cm. cell path-length. A broad band (λ_{max}550nm) was seen and also a small absorbance increasing in intensity towards the ultraviolet region. Over the course of a few hours both bands increased in intensity until that at 550nm reached a maximum and then decreased slowly in intensity, whereas the high energy band continued to increase. A solution of hexamethyl Dewar benzene (0.5M) in 1,2-dichloroethane was examined and also shown to have a small absorption towards the ultraviolet region, which increased with time but more slowly than in the reaction mixture.

Since hexamethyl benzene was shown to be formed in small quantities during the reaction, the band (λ_{max}550nm) was probably due to a hexamethyl benzene/TCNE complex (λ_{max}540nm in dichloromethane[13]) and would thus increase in intensity with time. After a certain point the amount of available TCNE would decrease, because of the formation

of the cycloadduct and the band intensity would correspondingly decrease. The charge-transfer complex band for the hexamethyl Dewar benzene/TCNE complex would be expected to be at shorter wavelengths, because of the non-conjugated, non-aromatic nature of the diene. For the reaction mixture of TCNE (4.0mM) with hexamethyl Dewar benzene (0.5M), the maximum absorbance of the band for 1 cm. optical path length cells was 0.450. If the extinction coefficient for the hexamethyl benzene/TCNE complex was taken to be 4400 (λ_{max} 540nm ($\simeq$ 4390) in CH_2Cl_2; λ_{max} 530nm ($\simeq$ 4780) in CCl_4[13]) then the maximum calculated concentration of complex was about 0.1mM or about 2.5% of the total TCNE concentration. There was thus only a very small amount of hexamethyl benzene formed, a fact borne out by the analysis of the crude adduct.

The charge-transfer complex of hexamethyl Dewar benzene with TCNE, if it exists, will probably be masked by the small end absorbance, towards the UV region, which seemed to be due to a polymeric product formed from donor. This latter absorbance was shown to rise continuously throughout the UV region.

5 - 4 - 2. Ultraviolet Spectroscopy.

Although it was not possible to study the charge-transfer complex in this reaction, the decrease in the tetracyanoethylene absorbance band (λ_{max} 265nm) at low concentrations, using an excess of donor was investigated.

Solutions of hexamethyl Dewar benzene (about 0.05M) in 1,2-dichloroethane had an absorbance of 0.3 to 0.1 in the region 263nm-275nm using 1mm. cells. Solutions of TCNE (about 0.5mM) in 1,2-dichloroethane using 1mm. cells gave absorbances of about 0.6 (λ_{max} 265nm) and so the decrease in tetracyanoethylene concentration was followed

in this region, with a solution of hexamethyl Dewar benzene of the same concentration in the reference cell. The possible errors in mismatching solutions in reference and solution cell were not greater than 5% or about 0.015, for the hexamethyl Dewar benzene. It was thus considered a fairly accurate method, since the decrease in TCNE absorbance was large in comparison with the small absorbance represented by mismatched solutions.

Solutions of reactants were made up and placed in the thermostatted water-bath, mixed, and the solution rapidly transferred to the cell (0.1cm) in the cell-housing. The reference cell (0.1cm) contained a solution of hexamethyl Dewar benzene at the same concentration as in the reaction mixture.

The decrease in absorbance at 265nm was fast enough to follow accurately and measurements were made at given time intervals. Graphs of log d_t against t were plotted, where d_t was the absorbance of TCNE at time t and lines were obtained with slope - $k_1/2.303$, where $k_1 = k_2[D]$. Thus the second-order rate constants, k_2 were calculated. An initial rapid decrease in TCNE absorbance was noticed similar to that for the norbornadiene reaction (see Fig. 5 - 1). A further kinetic investigation of this was undertaken, despite the lack of information about the possible charge-transfer complex between hexamethyl Dewar benzene and TCNE. (see section 5 - 4 - 3) Some of the difference, however, might be due to the presence of the observed charge-transfer complex between hexamethyl benzene and TCNE.

Reaction mixtures were made up at four different temperatures having the same TCNE concentration, but with varied donor concentration. The results are shown in the following table.

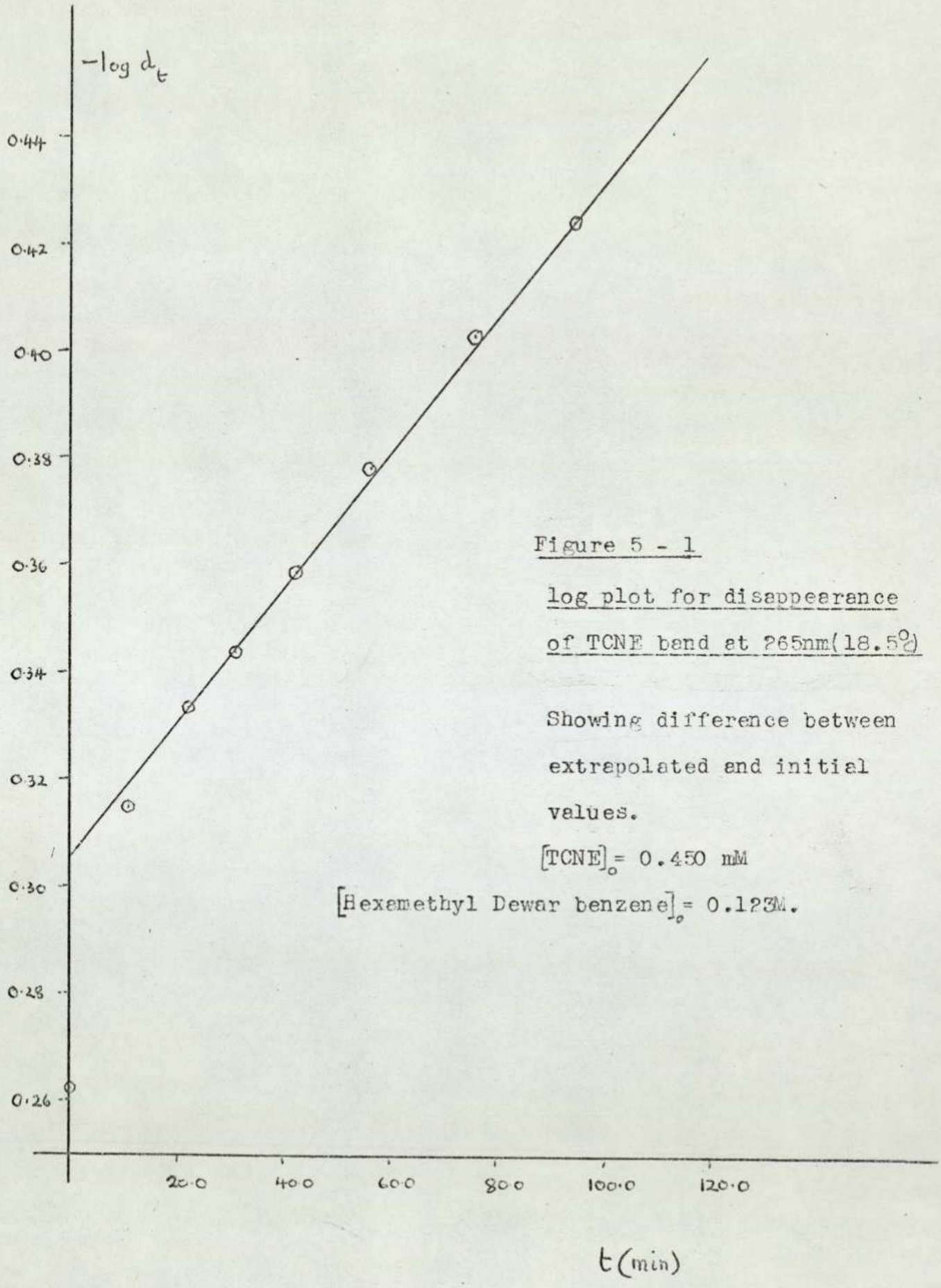


Figure 5 - 1

log plot for disappearance of TCNE band at 265nm(18.5°)

Showing difference between extrapolated and initial values.

$[TCNE]_o$ = 0.450 mM

$[Hexamethyl\ Dewar\ benzene]_o$ = 0.123M.

Table 5 - 4. Rate Constants k_2 (1 mol^{-1} s^{-1}) for Hexamethyl Dewar Benzene (D)/TCNE (A) in 1,2-Dichloroethane. λ=265nm.

T = 18.5°C; $[A]_o$ = 4.70 x 10^{-4}M		T = 26.0°C; $[A]_o$ = 5.07 x 10^{-4}M	
$[D]_o$ (M)	k_2 x 10^4	$[D]_o$ (M)	k_2 x 10^4
0.067	4.10	0.055	7.49
0.113	3.70	0.067	7.10
0.124	3.92	0.098	6.90
0.167	4.01	0.121	7.40

T = 29.7°C; $[A]_o$ = 5.01 x 10^{-4}M		T = 38.8°C; $[A]_o$ = 4.51 x 10^{-4}M	
$[D]_o$ (M)	k_2 x 10^4	$[D]_o$ (M)	k_2 x 10^3
0.073	8.50	0.054	1.09
0.099	9.90	0.067	1.26
0.131	8.71	0.079	1.13
		0.095	1.14
		0.127	1.20

Taking mean values of the rate constants at different temperatures, the energy and entropy of activation were calculated using the Arrhenius equation (see section 4 - 4 - 1 - 2).

Table 5 - 5. Data for Arrhenius Plot of Hexamethyl Dewar Benzene/TCNE in 1,2-Dichloroethane at 265nm.

k_2 (1 mol^{-1} s^{-1})	Log k_2	T (°K)	$^1/_T$ x 10^3
3.94 x 10^{-4}	-3.405	291.5	3.44
7.23 x 10^{-4}	-3.141	299.0	3.32
8.65 x 10^{-4}	-3.063	302.7	3.30
1.16 x 10^{-3}	-2.934	311.8	3.21

From the slope of the graph of log k_2 against $^1/_T$ (see Figure 5 - 2) ΔE = 9.6 kcal mol^{-1} (39.9 kjoule mol^{-1}) ΔS^* was calculated at each temperature.

Figure 5 - ?

Arrhenius plot of rate constants for hexamethyl Dewar benzene/TCNE reaction.

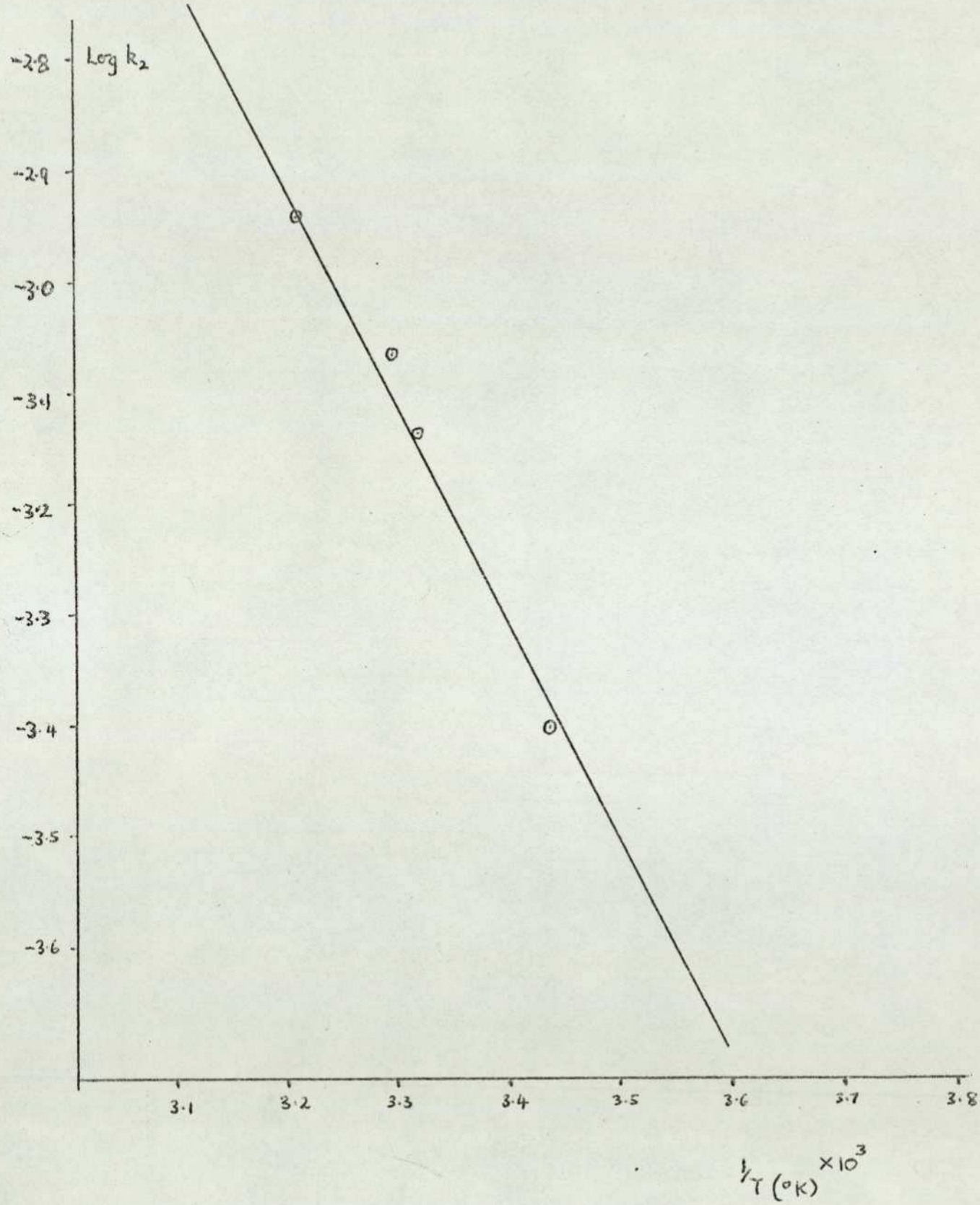


Table 5 - 6. Entropy of Activation for Hexamethyl Dewar benzene/TCNE in 1,2-Dichloroethane.

T (°K)	291.5	299.0	302.7	311.8
$\Delta S^{\ddagger}$ (e.u)	-43.7	-43.6	-43.5	-43.9

5 - 4 - 3. Investigation of Initial Rapid Reaction.

If the initial rapid fall in TCNE absorbance during the reaction is attributed to the formation of a charge-transfer complex or complexes similar to the case for the norbornadiene/TCNE reaction, then measurements of y values (see Section 4 - 4 - 2 - 3) at different donor concentrations would be useful in elucidation of a possible reaction mechanism.

The following y values were obtained at three different temperatures by measurement of theoretical and extrapolated values of d_o for the TCNE band (λ_{max} = 265nm).

Table 5 - 7. y Values for Hexamethyl Dewar Benzene (D)/TCNE (A) in 1,2-Dichloroethane.

T = 18.5°C, $[A]_o = 4.70 \times 10^{-4}$ M

$[D]_o$ (M)	y
0.067	0.237
0.113	0.271
0.124	0.288
0.167	0.313

T = 26.0°C, $[A]_o = 5.07 \times 10^{-4}$ M

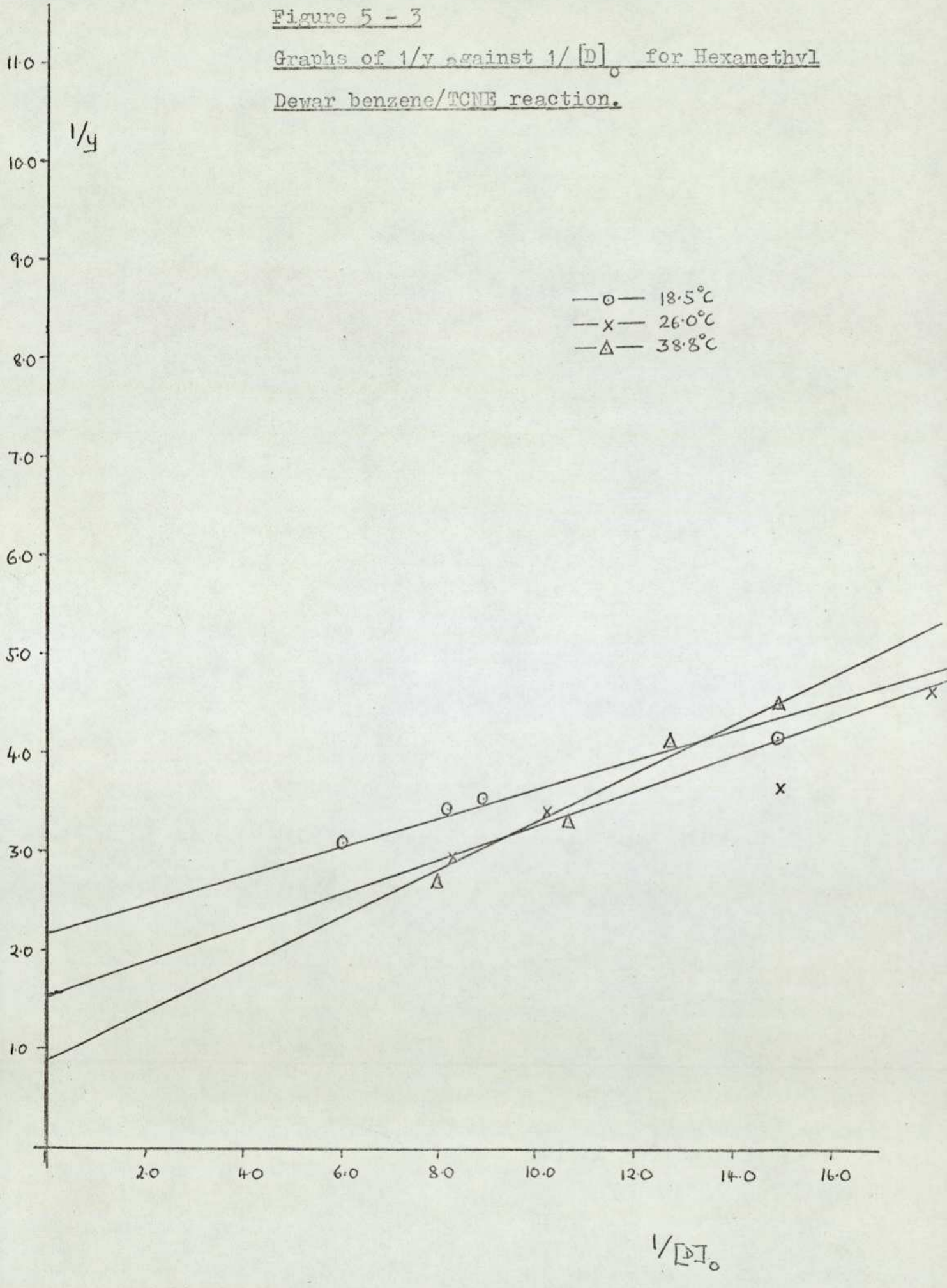
$[D]_o$ (M)	y
0.055	0.214
0.067	0.272
0.093	0.288
0.121	0.331

T = 38.8°C, $[A]_o = 4.51 \times 10^{-4}$ M.

$[D]_o$ (M)	y
0.067	0.222
0.079	0.240
0.095	0.305
0.127	0.365

Figure 5 - 3

Graphs of 1/y against $1/[D]_o$ for Hexamethyl Dewar benzene/TCNE reaction.



If it is assumed that the rapid disappearance of TCNE is due to the formation of a 1:1 complex between hexamethyl Dewar benzene and TCNE and that the complex between the side-reaction product, hexamethyl benzene and TCNE is formed to a negligible amount at the start of reaction then the following equilibrium may be postulated.

$$A + D \underset{}{\overset{K}{\rightleftharpoons}} AD^{*} \qquad (5-1)$$

where $K = [AD^{*}] / ([A]_o - [AD^{*}]) [D]_o$

If $y = [AD^{*}] / [A]_o$

Substitution gives: $1/y = 1/K[D]_o + 1$

A plot of $1/y$ against $1/[D]_o$ should give a straight line of slope $1/K$ and intercept + 1.

Although the lines as shown (see Fig. 5 - 3) do not all pass through an intercept of + 1, they are sufficiently linear to allow the above mechanism to be acceptable without the need to postulate the formation of further complexes. Measurement of the slopes gives the following results:

Table 5 - 8. K Values for Hexamethyl Dewar Benzene (D) / TCNE (A) Complex.

Temp (^{o}C)	18.5	26.0	38.8
K (l mol^{-1})	6.4	5.7	4.0

These values of equilibrium constants are much larger than the first equilibrium constant, K_1, for the formation of the 1:1 complex between norbornadiene and TCNE (0.6 at 37.0^{o}C) and are larger than K values for most non-aromatic dienes. Although norbornadiene and hexamethyl Dewar benzene are not strictly analogous, the six methyl groups in the latter may be considered to be contributing towards the formation

of a stronger complex by a + I inductive effect. (cf.[13] in dichloromethane at 22°C for benzene/TCNE complex ($K = 0.237$ l mol^{-1}) and hexamethyl benzene/TCNE complex ($K = 16.8$ l mol^{-1})). The presence of the charge-transfer complex band in the UV/visible region may be masked by the presence of the small band due to the yellow polymeric impurity formed from hexamethyl Dewar benzene itself and during reaction.

The reaction between norbornadiene and TCNE has been postulated to pass through two complexes in equilibrium with each other (see Section 4 - 4 - 2 - 3). Since the reaction described above is very similar, being a ($\pi^2s + \pi^2s + \pi^2s$) cycloaddition, it would be likely that the two reactions proceed via a similar mechanism, with the possible formation of a 2:1 complex in the hexamethyl Dewar benzene/TCNE reaction. It would be possible on the basis of the conclusions reached in Chapter 4 that the reaction to form the cycloadduct would proceed via the charge-transfer complex as a direct intermediate.

$$A + D \rightleftharpoons AD^{*} \longrightarrow AD \qquad (5 - 2)$$

Where $$k_c = k_2 (1 + K[D]) / K$$

k_c values may be calculated from k_2 values at the given temperatures inserting values of $[D]$ and K.

Table 5 - 9. Rate Constants k_c (l mol^{-1} s^{-1}) for Hexamethyl Dewar Benzene/TCNE Assuming Simple Equilibrium (Scheme 1 - 21).

$T = 18.5$°C, $[A]_o = 4.70 \times 10^{-4}$M		$T = 26.0$°C, $[A]_o = 5.07 \times 10^{-4}$M	
$[D]_o$(M)	$k_c \times 10^4$	$[D]_o$(M)	$k_c \times 10^4$
0.067	0.915	0.055	1.39
0.113	0.996	0.067	1.38
0.124	0.961	0.098	1.32
0.167	0.989	0.121	1.37

$T = 38.8^{\circ}C$, $[A]_o = 4.51 \times 10^{-4}$ M

$[D]_o$ (M)	$k_c \times 10^4$
0.067	3.49
0.079	2.14
0.095	3.29
0.127	2.97

The k_c values as determined are fairly constant at the lower temperatures. On the basis of this mechanism they appear to be smaller in magnitude than the k_c values determined at similar temperatures for the norbornadiene/TCNE reaction.

5 - 5. Discussion.

Although the presence of a 1:1 hexamethyl Dewar benzene/TCNE complex cannot be detected in the visible spectrum, the initial rapid decrease in TCNE concentration may be explained if such a complex (λ_{max} = 265nm) is postulated to exist and to be responsible for the removal of free TCNE. Calculations show that the determined equilibrium constants of such a complex decrease with increase in temperature in line with other such charge-transfer complexes.

One source of error in measurement of y values and hence in K and k_c values may be that a small amount of hexamethyl benzene is formed during the reaction effectively removing free TCNE by complexing and hence some of the initial optical density difference of TCNE may be due to the formation of this complex. However, since a maximum amount of complex present accounts for only about 2.5% TCNE concentration, the initial optical density difference due to its formation is not expected to be very large.

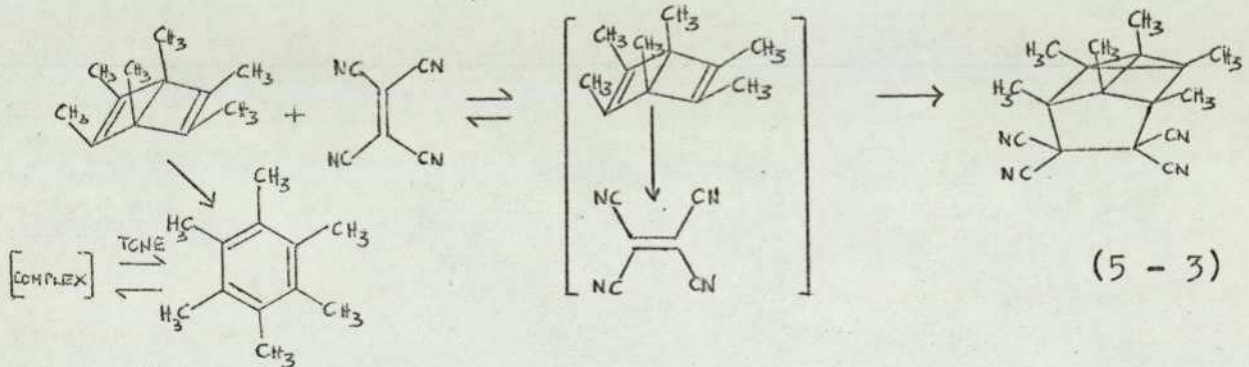
The reaction between norbornadiene and TCNE has also been postulated to pass through both a 1:1 and 1:2 acceptor:donor complex before formation of the final adduct. Both of these reactions would be

expected to have a similar reaction mechanism. In the case of the hexamethyl Dewar benzene reaction the presence of a 1:2 acceptor: donor complex is not certain although it is possible that the larger intercepts on the graphical plots (see Fig. 5 - 3) may indicate either experimental errors or the possible existence of termolecular species.

On the basis of the corrected mechanism (scheme 1 - 21), the corrected rate constants, k_c, for the hexamethyl Dewar benzene reaction appear to be smaller at a given temperature than those for the norbornadiene reaction. Although the likely greater strain effects of the Dewar benzene structure during reaction do not allow a strict comparison with the norbornadiene reaction, the six methyl substituents attached to Dewar benzene would be expected to produce a more stable charge-transfer complex as shown by the more negative enthalpy of formation (-4.9 kcal mol^{-1}).

Energy and entropy of activation values derived from the corrected rate constants show that although the energy of activation value (10.1 kcal mol^{-1}) is similar to that for the norbornadiene reaction, the entropy of activation (-44.8 e.u.) is slightly more negative indicating a higher degree of orientation in the transition state. Both of these thermodynamic parameters are in line with most other Diels-Alder type reactions in which the large negative entropy is more consistent with a concerted mechanism rather than a two-step process.

The overall reaction may be as shown in 5 - 3.



(5 - 3)

Where the 1:1 complex exists in the usual 'sandwich' structure.

Chapter 6

Hexa-trans-2,trans-4-diene/Maleic Anhydride Reaction

6 - 1. Introduction.

The reaction of this hexadiene isomer with maleic anhydride to give the all cis Diels-Alder cycloadduct has been reported.[111, 219-221] No kinetic investigation of the reaction had been made and when the two reactants were mixed together in chloroform a pale yellow colour immediately formed, which quickly faded as the reaction proceeded. It was decided to study the kinetics of this reaction as it was considered to be typical of stereospecific endo Diels-Alder cycloadditions. The reaction between hexadiene and TCNE had been studied previously[79], but had been shown to be too fast for accurate measurement of rate constants. With the weaker dienophile, maleic anhydride, it was considered that the reaction might be slow enough to follow. The colour formed in reaction[a] might be attributed to a charge-transfer complex which could be examined spectroscopically.

6 - 2. Purification of Reagents

Hexa-trans-2,trans-4-diene was supplied by Ralph Emanuel Ltd. as a clear liquid. Analysis by G.L.C. showed the presence of one peak only, using a Carbowax 20M column at 100°C. n_D^{25} 1.4507 (lit.[203] n_D^{25} 1.4501). The sample was stored in light-excluded bottles in a refrigerator.

Maleic anhydride stored over long periods had a tendency to hydrolyse to maleic acid as shown by the turbidity when dissolved in chloroform. The samples of maleic anhydride used were therefore twice sublimed at 50° (just below the melting point) under vacuum and the colourless crystals were stored in a vacuum desiccator[c] over silica gel. m.p. = 52-53°C (lit.[222] 53°C).

Chloroform was the solvent used for this particular reaction study as maleic anhydride was found to be slightly more soluble in chloroform than in 1,2-dichloroethane or dichloromethane. Samples of solvent were purified as described in section 2 - 1 - 5 - 1 and stored in light-excluded bottles.

6 - 3. Preparation and Analysis of the Adduct.

6 - 3 - 1. Preparation.

Hexa-trans-2,trans-4-diene (2.0g) was added to a solution of maleic anhydride (1.0g) in dried chloroform (20 ml) and the mixture throughly shaken. The solution was refluxed for 1 hour during which time the yellow colour, formed when the two reactants were mixed together, had disappeared. The solvent was then removed by evaporation and the crude solid washed with carbon tetrachloride. Analysis by T.L.C. (silica gel) using chloroform as solvent, showed the presence of only one spot (R_f 0.59). The crude solid was first recrystallised from ethylacetate to yield needles (1.8g) and then sublimed at 75°, under vacuum, to give needles, m.p. 92.5 -93° C (lit.[220] m.p. 94°C) of 3,6-dimethyl-Δ^4-tetrahydrophthalic anhydride.

Calculated for $C_{10}H_{12}O_3$: C, 66.67; H, 6.67 %

Found: C, 66.8; H, 6.51 %

6 - 3 - 2. UV/Visible Spectrum.

Solutions of the adduct in chloroform showed no absorbance in the region 250-600 nm.

6 - 3 - 3. Infrared Spectrum.

The adduct was made into a mull with hexachlorobutadiene and with nujol separately, and the infrared spectra recorded using an attenuator in the reference beam.

Table 6 - 1. Infrared Spectrum of Hexadiene/Maleic Anhydride Adduct.

Wavenumber	Assignment
3000 cm^{-1} (s)	= C - H stretching
2890 cm^{-1} (s)	- C - H stretching
1850 cm^{-1} (s)	- C = O stretching
1780 cm^{-1} (s)	- C = O stretching
1680 cm^{-1} (w)	- C = C stretching
1450 cm^{-1} (m)	- C - CH_3 bending
1370 cm^{-1} (m)	- C - CH_3 bending

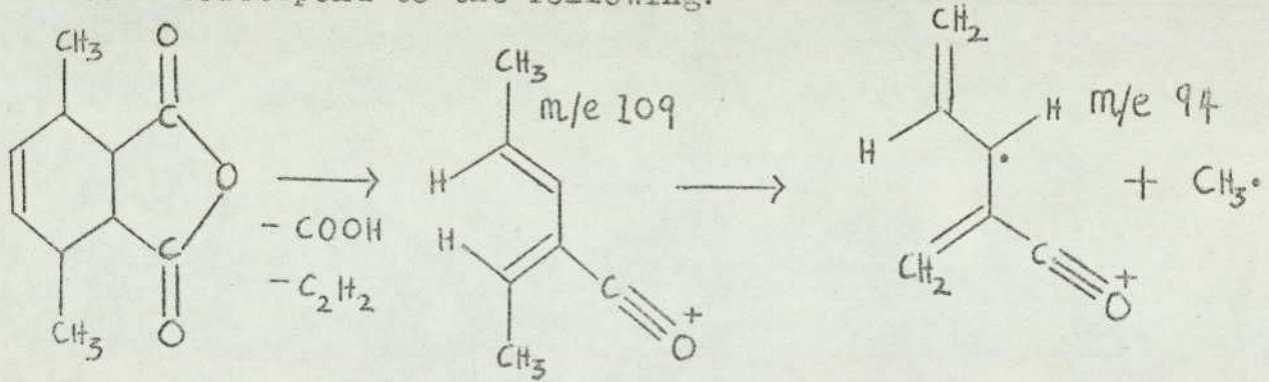
6 - 3 - 4. Mass Spectrum.

The measured mass of the (M-28) ion was 152.0841, close to that calculated (152.0837) for the ion $(C_9H_{12}O_2)^+$. The parent ion had only a low abundance (0.56%).

Table 6 - 2. Main Mass fragment Ions for Hexadiene/Maleic Anhydride Adduct.

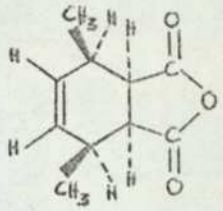
m/e	180(M)	152	109	108	107	94	92	82	78	40
Relative Abundance(%)	0.56	22.4	68.5	35.8	3.9	100.0	27.0	7.9	22.0	12.1

The ion, m/e 152, corresponds to loss of CO from the parent ion. The retro Diels-Alder mechanism may be operating to some extent giving m/e 82, corresponding to the diene. The two most abundant peaks at m/e 94 and m/e 109 are more difficult to explain, although a metastable peak (m^* = 81.2) indicates the transition 109 → 94, which could correspond to the following:



The mass spectrum might be compared with that[223] for the 4,5-dimethyl substituted adduct in which m/e 107 is the most abundant ion.

Apart from the evidence of the N.M.R. spectrum (see Chapter 3), the analysis shows the presence of the cyclic anhydride structure. The IR spectrum shows two carbonyl stretching bands, characteristic of anhydrides, two separate -CH stretching bands, a possible C = C stretching band and $-C-CH_3$ bending bands. The mass spectrum shows a peak at 152, corresponding to loss of CO, which is characteristic of similar cyclic anhydrides.[223] Combining this evidence with the C,H analysis and the N.M.R. spectrum, it is seen that the adduct must exist in the endo form as shown below.



6 - 4. UV/Visible Spectroscopy.

Solutions of hexadiene (0.5 → 0.8M) mixed with maleic anhydride (5.0 m M), using 1 cm. cell pathlengths, gave a broad absorption band (λ_{max} 320nm). Examination of the spectra of each reactant separately showed that this absorbance was not due to either species entirely, although complications arose because both hexadiene and maleic anhydride had small absorbances in this region. (see Fig. 6 - 1). It was considered feasible to follow the decrease in the observed absorption band in this region, providing the following conditions were met. (1) A solution of hexadiene of the same concentration as in the reaction mixture was placed in the reference cell to counteract the small absorbance of this species in the wavelength region under study. This reactant would be in large

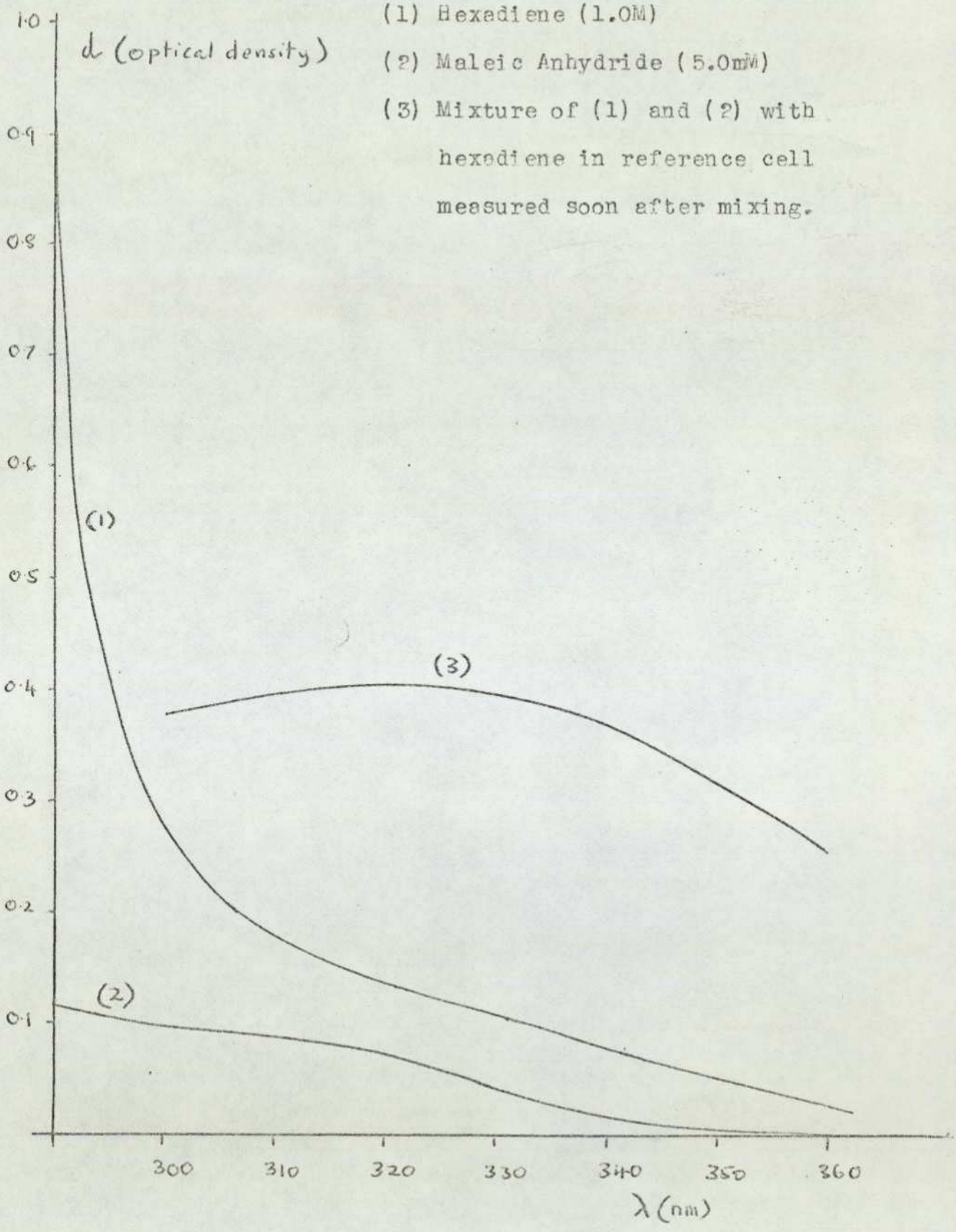
Figure 6 - 1

UV Absorptions for hexadiene/maleic anhydride reaction (25.0°), ℓ = 1 cm.

(1) Hexadiene (1.0M)

(2) Maleic Anhydride (5.0mM)

(3) Mixture of (1) and (2) with hexadiene in reference cell measured soon after mixing.



excess in the reaction mixture and the concentration would be virtually constant throughout the reaction. (2) A correction was made for the maleic anhydride absorbance in the same wavelength region. When a large excess of donor is present, the concentration of maleic anhydride is directly proportional to the concentration of charge-transfer complex and it can be shown that:

$$d_t^t = (d_t^o / d_o^o)\ (d_o^o - d_o^A) \qquad (6 - 1)$$

d_t^t is the absorbance at time t due to the complex only.
d_t^o is the observed absorbance at time t.
d_o^o is the observed absorbance at zero time for reaction.
d_o^A is the maleic anhydride absorbance at zero time for reaction.
Corrections were thus made after measuring the maleic anhydride absorbance before reaction. (3) The decrease in absorbance was fast enough for accurate measurements to be made. These conditions were met for certain concentrations of hexadiene and maleic anhydride, when the former was in large excess and kinetic studies were carried out by following the absorbance at 330 nm.
It was not possible to examine absorbances of equimolar concentrations of reactants, nor was it possible to examine the decrease in absorbance of hexadiene or maleic anhydride bands individually because of overlapping bands in these regions.

6 - 4 - 1. Determination of K and ε for the Charge-transfer Complex

The equilibrium constant, K, and extinction coefficient, ε, for the charge-transfer complex were calculated using the Benesi-Hildebrand method, having a large excess of the hexadiene in the reaction mixtures. Initial optical density measurements, d_o, were obtained by extrapolation of corrected optical densities measured at given time intervals. Solutions of the hexadiene and of maleic

anhydride in chloroform were made up separately and placed in the thermostat bath. The solutions were mixed, the time noted and the solution rapidly transferred to the solution cell in the cell-housing. The reference cell contained a solution of hexadiene at the same concentration as in the reaction mixture. In all cases the absorbances were followed at 330 nm making corrections for the maleic anhydride absorbance, which had been previously examined at 330 nm to obtain the initial optical density, d_o^A. (For most cases $d_o^A \simeq 0.1\ d_o^o$).

Table 6 - 3. Benesi-Hildebrand Data for Hexadiene (D)/Maleic Anhydride (A) at 330 nm in Chloroform. T = 19.0°C $[A]_o = 4.01 \times 10^{-3}$M.

$[D]_o$ (M)	$[D]_o^{-1}$	d_o	$[A]_o d_o^{-1} \times 10^2$
0.401	2.50	0.158	2.53
0.449	2.22	0.183	2.18
0.501	2.00	0.195	2.05
0.606	1.65	0.243	1.64
0.797	1.25	0.302	1.32

Table 6 - 4. Data as for above. T = 26.5°C $[A]_o = 5.38 \times 10^{-3}$M.

$[D]_o$ (M)	$[D]_o^{-1}$	d_o	$[A]_o d_o^{-1} \times 10^2$
0.596	1.68	0.278	1.88
0.697	1.43	0.333	1.61
0.797	1.26	0.389	1.38
0.901	1.11	0.436	1.23
1.001	1.00	0.453	1.16

Table 6 - 5. Data as for above. T = 38.5° C. $[A]_o$ = 4.89 x 10^{-3}M.

$[D]_o$ (M)	$[D]_o^{-1}$	d_o	$[A]_o d_o^{-1} \times 10^2$
0.502	1.99	0.206	2.37
0.601	1.67	0.248	1.97
0.697	1.43	0.292	1.67
0.798	1.25	0.328	1.49
0.901	1.11	0.370	1.32
0.999	1.00	0.417	1.17

Plots of $[D]_o^{-1}$ against $[A]_o d_o^{-1}$ (see Fig. 6 - 2) gave the following values of K and ε.

Table 6 - 6. Determined K and ε values for the Hexadiene/Maleic Anhydride Complex at 330 nm in Chloroform.

T (°C)	ε	Kε	K (l mol^{-1})
19.0	1670	98.1	0.058
26.5	1670	92.0	0.055
38.5	1740	89.5	0.051

As before, Kε values were easier than K values to determine accurately, because of the small intercept which could make ε values inaccurate. In determining values for ΔH and ΔS for complex formation, the Van't Hoff equation (see Section 4 - 4 - 1 - 1) was applied to only two temperatures (19.0° and 38.5°C) and the values obtained by a difference method.

ΔH = -1.1 kcal mol^{-1} (- 4.4 kjoule mol^{-1}), ΔS = -8.7 e.u.

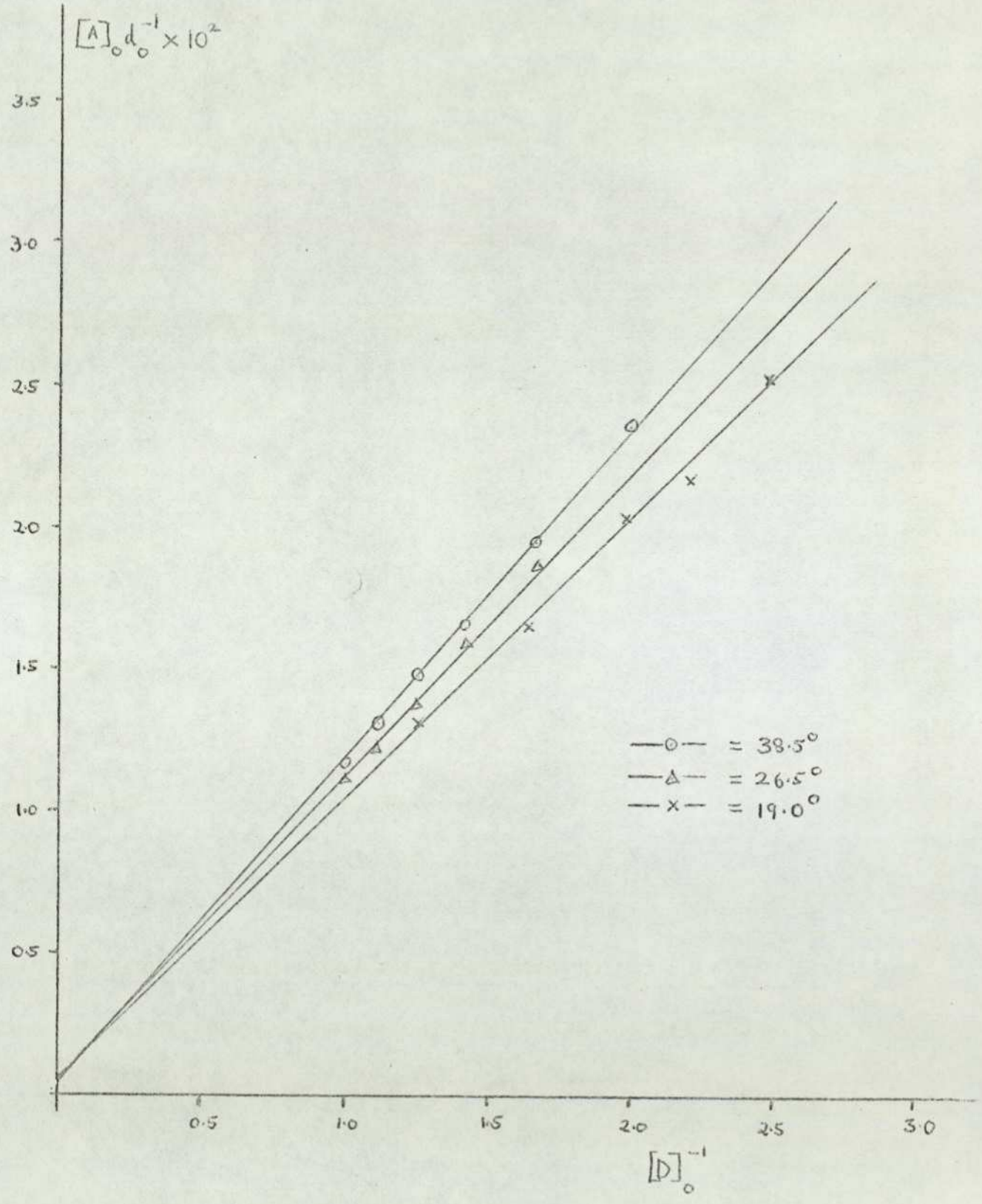
6 - 4 - 2. Calculation of Rate Constants.

The calculation of rate constants for the hexadiene/maleic anhydride reaction was carried out by following the decrease in absorbance at 330 nm. Corrected values for optical density were

Figure 6 - 2

Benesi-Hildebrand plot for hexadiene/ maleic anhydride complex.

λ = 330 nm.



obtained as described, and plots of log d_t^t against time were made. This gave values for k_1 and k_2 from the slope and from the relationship $k_2 = k_1 / [D]$. Straight lines were obtained in all cases for this reaction. The absorbances were followed to about 50% reaction, but readings were also taken a very long time after the reaction had started and these absorbances were either zero or very small (i.e. less than 0.01).

The values obtained for k_1 and k_2 at different temperatures are shown.

Table 6 - 7. Rate Constants k_1 (s^{-1}), k_2 (1 $mol^{-1} s^{-1}$) for Hexadiene (D)/Maleic Anhydride (A) in Chloroform, T = 8.0°C $[A]_o$ = 5.05 x 10^{-3}M. At 330 nm.

$[D]_o$ (M)	$k_1 \times 10^4$	$k_2 \times 10^4$
0.499	1.35	2.71
0.597	1.50	2.52
0.701	1.72	2.46
0.804	1.96	2.44
0.898	2.20	2.45
0.995	2.39	2.41

Table 6 - 8. Rate Constants as for above. T = 19.0°C $[A]_o$ = 4.01 x 10^{-3}M.

$[D]_o$ (M)	$k_1 \times 10^4$	$k_2 \times 10^4$
0.401	1.92	4.68
0.449	2.02	4.51
0.501	2.23	4.45
0.606	2.88	4.75
0.797	3.72	4.67

Table 6 - 9. Rate Constants as for above. T = 26.5°C $[A]_o$ = 5.38 10^{-3}M.

$[D]_o$ (M)	$k_1 \times 10^4$	$k_2 \times 10^4$
0.596	4.90	8.21
0.601	5.23	8.70
0.697	5.80	8.31
0.797	6.90	8.65
0.799	6.70	8.38
0.901	7.71	8.54
1.001	8.73	8.72
1.001	8.63	8.62

Table 6 - 10. Rate Constants as for above. T = 38.5°C $[A]_o$ = 4.89 x 10^{-3}M.

$[D]_o$ (M)	$k_1 \times 10^4$	$k_2 \times 10^3$
0.502	7.19	1.43
0.601	8.96	1.49
0.697	9.90	1.42
0.798	11.55	1.45
0.901	12.79	1.42
0.999	14.39	1.44

The rate constants obtained appear to be almost constant over a range where the donor concentration has almost doubled. If an experimental error of 5 to 10% is allowed, then all the results fall within this range, except at 8°C, where there appears to be a small decrease in k_2 with increase in donor concentration. To obtain values of ΔE and ΔS^* using the Arrhenius equation, the mean for each k_2 value was taken at each temperature. A plot of log k_2 was made against 1/T where T is the absolute temperature.(see Fig. 6 - 3).

Figure 6 - 3.

Arrhenius plot of rate constants for hexadiene/maleic anhydride reaction.
$\lambda = 330nm.$

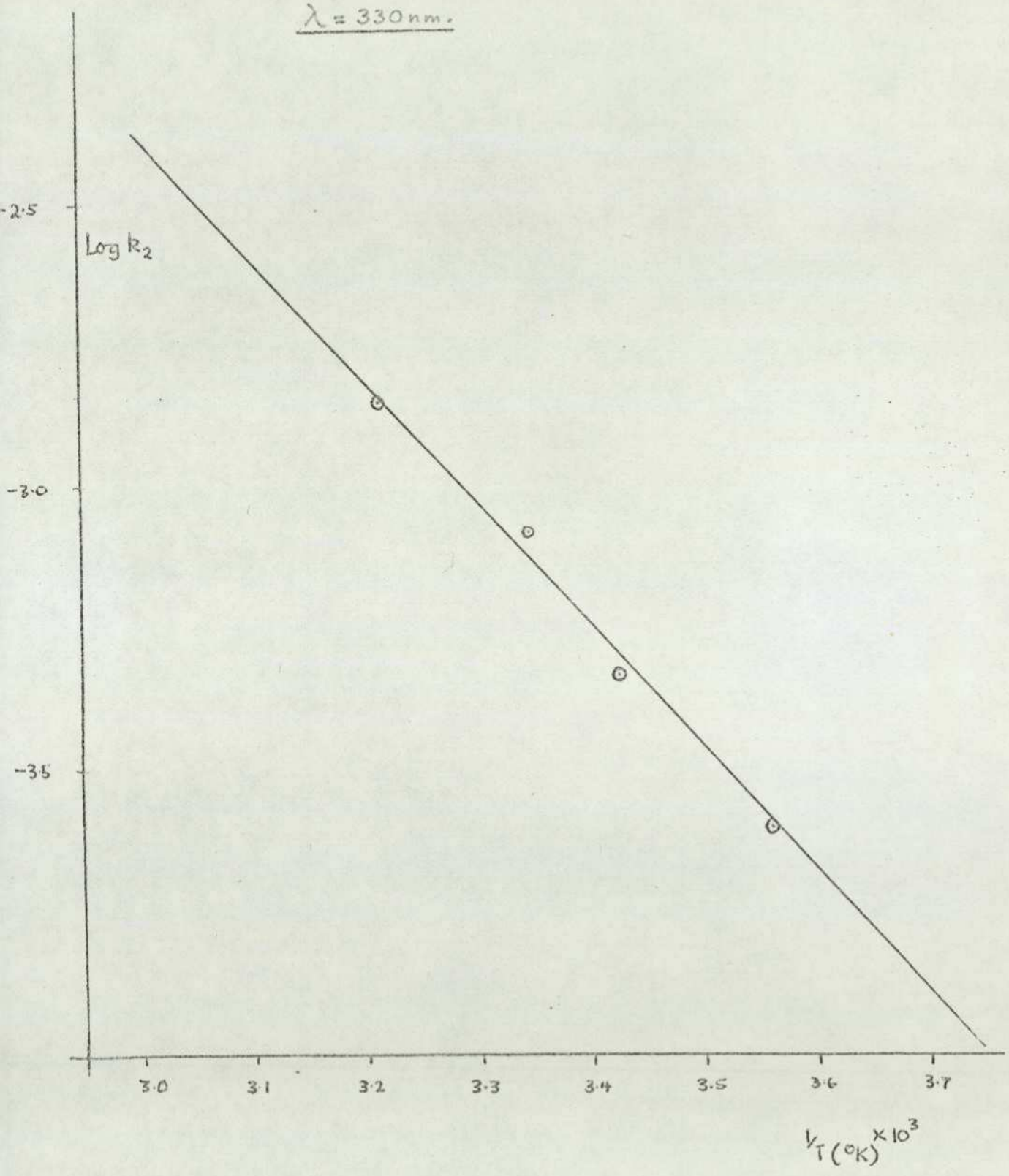


Table 6 - 11. Data for Arrhenius plot of Hexadiene/Maleic Anhydride in Chloroform.

k_2(l mol^{-1} s^{-1})	Log k_2	T (^{0}K)	1/T x 10^3
1.44 x 10^{-3}	-2.842	311.5	3.21
8.53 x 10^{-4}	-3.069	299.5	3.34
4.64 x 10^{-4}	-3.333	292.0	3.42
2.50 x 10^{-4}	-3.602	281.0	3.56

From the slope it was calculated, ΔE = 10.3 kcal mol^{-1} (43.1 kjoule mol^{-1}).

ΔS^* was calculated at each temperature.

Table 6 - 12. Entropy of Activation for Hexadiene/Maleic Anhydride in Chloroform.

T (^{0}K)	311.5	299.5	292.0	281.0
ΔS^*(e.u)	-41.8	-41.5	-41.8	-41.5

6 - 5. Discussion.

The reaction between hexadiene and maleic anhydride has been shown to pass smoothly to form a single cycloadduct by a typical Diels-Alder ($\pi^2 s + \pi^4 s$) addition.

The role of the complex formed in solution was not entirely clear after kinetic studies had been carried out.

If schemes (1-21), (1-22) and (1-23) are considered as possible pathways in the reaction, then it is clear that (1-23) is not that operating, because there is no increase in k_2 in this reaction with donor concentration. The other two schemes might be considered as both of these should show a small decrease in k_2 with donor concentration.

K for the complex as determined by the Benesi-Hildebrand method was shown to have a very small value in the temperature range

examined (0.05 to 0.06). If these values are inserted into the equations for (1-21) and (1-22) at a given temperature, then k_c values might be obtained.

$$k_c = k_2 (1 + K [D]) \qquad \text{from (1-22)}$$

$$k_c = k_2 (1 + K [D]) / K \qquad \text{from (1-21)}$$

Table 6 - 13. k_c Calculations at 19.0°C for Scheme (1-22)

$k_c(1\text{-}22) = K.k_c(1\text{-}21)$, $K = 0.0588$

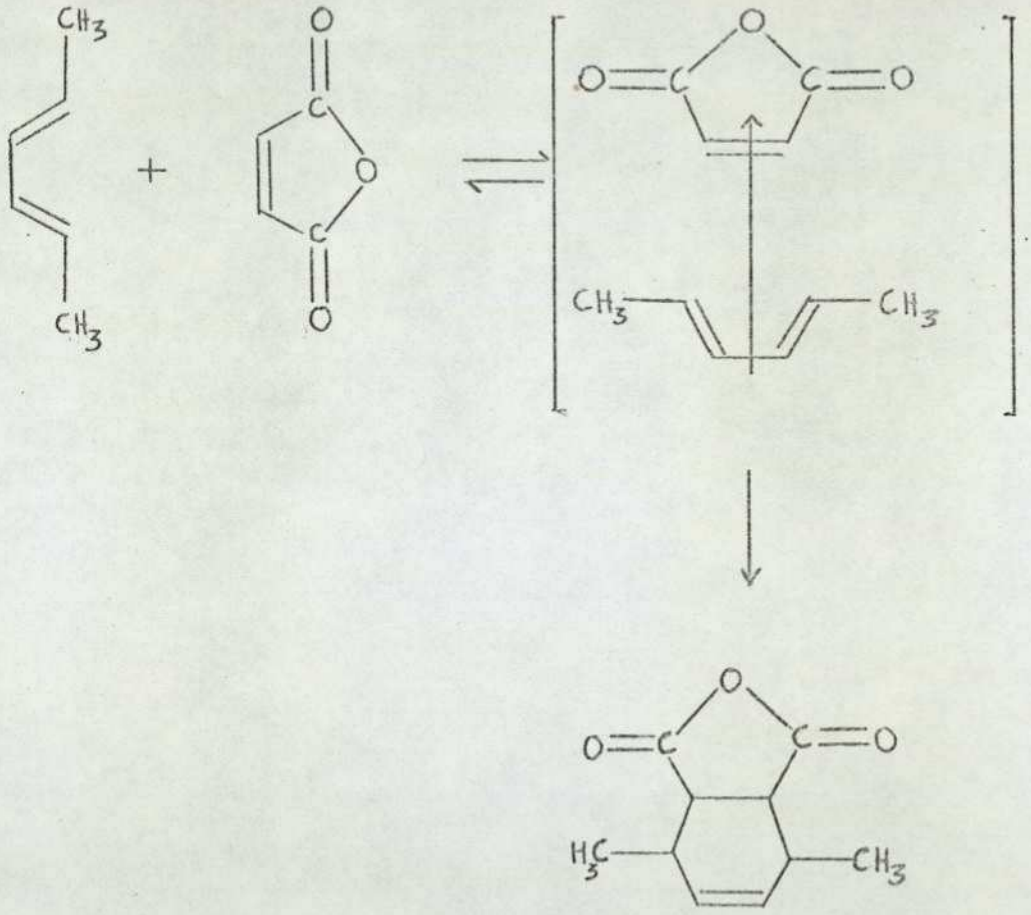
$[D]$ (M)	$k_2 \times 10^4$ (1 mol^{-1} s^{-1})	$k_c \times 10^4$ (1 mol^{-1} s^{-1})
0.401	4.88	4.99
0.449	4.51	4.64
0.501	4.45	4.59
0.606	4.75	4.92
0.797	4.67	4.89

The k_c values obtained appear to be virtually constant within the experimental error and it is obvious that K is so small that both k_2 and k_c will appear constant over this concentration range. Either of schemes (1-21) or (1-22) could be applied, as the relationship shown in the above table will give constant values of k_c for both. Similar results are obtained at the other temperatures. It is thus not possible to distinguish between the charge-transfer complex as a direct intermediate or as a species formed in a side-equilibrium.

It was not possible to examine the complex at more than one wavelength because of difficulties with overlapping bands, but it is assumed that only the one weak complex is formed and the thermodynamic values obtained show that there is some degree of ordering ($\Delta S \simeq -8$ e.u) but very little change in enthalpy ($\Delta H \simeq -1$ Kcal mol^{-1})

for complex formation.

The values for ΔE and ΔS^{*} obtained from the kinetic studies are in line with those values from other Diels-Alder reactions, i.e. a large negative entropy of activation, and energy of activation of about 10-12 kcal mol^{-1}. It is likely that the reaction is concerted, in which the charge-transfer complex could be a direct intermediate, as it will bear a 'sandwich' structure similar to that proposed for the transition state of such diene reactions.



Chapter 7

1-Methoxybuta-trans-1,3-diene/Maleic Anhydride Reaction

7 - 1. Introduction.

The reaction of methoxybutadiene, being a mixture of cis and trans isomers, with maleic anhydride has been reported[224-226] to give the Diels-Alder cycloadduct under certain specific reaction conditions.

When the two reactants were mixed together in chloroform, a pale yellow colour, attributed to a charge-transfer complex, appeared immediately, fading as the reaction proceeded. This reaction might bear some similarity to that between sorbyl alcohol and TCNE,[79] which possibly proceeds via the charge-transfer complex intermediate. The reaction between methoxybutadiene and TCNE was found to be too fast for suitable kinetic studies as the colour formed in reaction faded almost immediately. With the weaker dienophile, maleic anhydride, the rate of reaction appeared suitable for kinetic study.

7 - 2. Purification of Reagents.

1-methoxy-butadiene was supplied as technical by Ralph Emanuel Ltd. in ampoules. G.L.C. analysis showed that on a Carbowax 20M column at 85°C. there were two peaks, corresponding to about 80% trans isomer and 20% cis isomer (identified by the higher boiling-point of the latter). The technical material was therefore distilled under nitrogen and three fractions were collected in the temperature range 95-110°C. The first fraction was shown to be 98.5% of the trans isomer, the second, 93% and the third 87%. The residue remaining in the flask was less than 80% trans. As the cis isomer was reported not to react with the maleic anhydride to give a

cycloadduct, the first major fraction was taken, and a small correction made for the slight impurity present, $n_D^{20} = 1.4602$ (lit.[224] $n_D^{20} = 1.4590$).

Maleic anhydride was purified as described in section 6 - 2. Chloroform purified as described in section 2 - 1 - 5, was used within a day or two of purification.

7 - 3. Preparation and Analysis of the Adduct.

7 - 3 - 1. Preparation.

In order to prepare the adduct from the technical starting material, the method used previously[224] was adopted.

1,4-Dioxan, purified by refluxing over sodium wire for 1 hour followed by distillation at 100°, was purged with nitrogen before use. To a stirred solution of a sample of 1-methoxybutadiene (2.0g) in dioxan (10 ml), cooled in an ice-bath, a solution of maleic anhydride (1.8g) in dioxan (10 ml) was added. The mixture was then refluxed for 2 hours, cooled and set aside for a further 15 hours. Addition of water gave a white, gummy substance which stuck to the walls of the flask. This was the reported polymerised[224] resin formed from the cis isomer. Benzene (60 ml) was added, the mixture shaken and after separation, the gum remained in the aqueous layer. The benzene layer was concentrated by evaporation of some solvent, cooled and petroleum ether (40°-60°) added. This precipitated white crystals of the adduct, which were collected, filtered and dried under vacuum. After recrystallisation from petroleum ether (60°-80°), the adduct separated as white leaflets. m.p 97 -97.5°C (lit.[226] 99°C).

Calculated for $C_9 H_{10} O_4$: C, 59.4; H, 5.49 %

Found : C, 59.6; H, 5.32 %

7 - 3 - 2. Thin-layer Chromatogram.

Analysis of the recrystallised adduct on silica gel chromagram using carbon tetrachloride-chloroform (50:50 v/v) as solvent showed one spot only (R_f 0.33), visible under ultraviolet light.

7 - 3 - 3. UV/Visible Spectrum.

Solutions of the adduct in chloroform showed no absorption bands in the region 250-600 nm.

7 - 3 - 4. Infrared Spectrum.

The adduct was made up into a mull with hexachlorobutadiene and with nujol separately so that the whole spectrum could be recorded.

Table 7 - 1. Infrared Spectrum of Methoxybutadiene/Maleic Anhydride Adduct.

Wavenumber	Assignment
3000 cm^{-1} (m)	= C-H stretching
2890 cm^{-1} (m)	- C-H stretching
1860 cm^{-1} (s,d)	- C=O stretching
1790 cm^{-1} (s)	- C=O stretching
1650 cm^{-1} (w)	- C=C-stretching
1240 cm^{-1} (m)	- C-O stretching

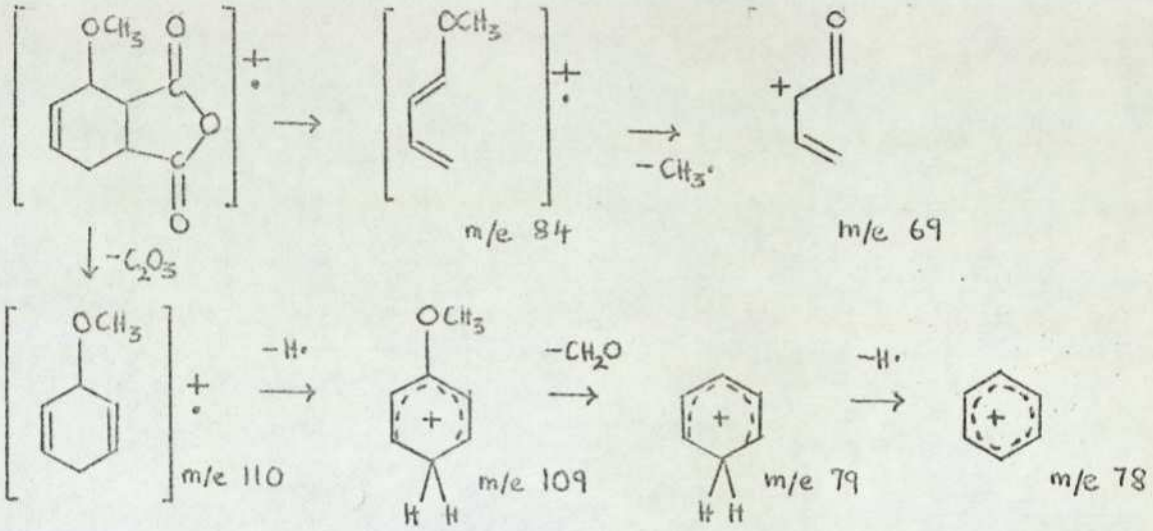
7 - 3 - 5. Mass Spectrum.

The measured mass of the parent ion was 182.0576 which was close to that calculated (182.0579) for the ion $(C_9 H_{10} O_4)^+$. In fact, the parent ion had only a low relative abundance. (1.17%)

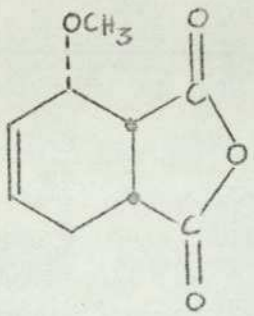
Table 7 - 2. Main Mass Fragment Ions for Methoxybutadiene/Maleic Anhydride Adduct.

m/e	182(M)	124	110	109	84	79	78	77	69
Relative Abundance(%)	1.17	18.6	26.4	23.9	100.0	79.1	24.2	23.8	14.5

The base peak, m/e 84, corresponds to the mass of methoxybutadiene itself and it is likely that the main fragmentation is by a retro Diels-Alder reaction pathway. The ion, m/e 79, may correspond to a protonated benzene ion and is also found as the most abundant species in the spectrum of 1,2,5,6-tetrahydrophthalic anhydride.[223] m/e 110 and m/e 109 correspond to loss of C_2O_3 and C_2O_3H from the parent ion respectively. The following fragmentation pathways may thus be postulated.



Apart from the evidence from the N.M.R. spectrum (see Chapter 2), the infrared and mass spectrum both indicate the cyclic anhydride adduct. Thus the infrared spectrum shows two carbonyl stretching bands, characteristic of anhydrides, the presence of two different -C-H stretching bands and a weak C=C stretching band. The mass spectrum, as shown before, also indicates the cyclic adduct. Thus 3-methoxy-Δ^4-tetrahydrophthalic anhydride is exclusively formed from 1-methoxybuta-trans-1,3-diene and maleic anhydride and exists in the endo form.



7 - 4. Visible Spectroscopy.

A large excess concentration of the methoxybutadiene (0.4M) was made up with maleic anhydride (4.0mM) in chloroform and the spectrum of the mixture scanned using 1 cm. cells. In the region 360-420 nm, a tail-end absorption appeared to change with time, which, when the reactants were examined singly, was concluded to be due partly to methoxybutadiene and partly to another unidentified absorption. When the reaction solution was run as above, and the reference cell contained a solution of methoxybutadiene at the same molar concentration, a small absorption band from 350-420 nm, without a maximum, was noticed to have a decreasing intensity. The maleic anhydride absorption was virtually zero in this wavelength region and the absorption band was attributed to a charge-transfer complex band. (see Fig. 7 - 1). The decrease in absorption was followed at 370 nm because at this point the absorption due to methoxybutadiene was fairly small (0.25). Errors in mismatching solution and reference cell concentrations of diene were not greater than 5% (an absorption of about 0.02).
Also at 370 nm, the actual absorption of complex was large enough to be followed without errors occurring, arising from difficulties in measuring very small changes of intensity. The instrument was correctly zeroed for these experiments by following the absorption to a point where it appeared to be zero (500-550 nm) and this absorption was examined periodically to correct any small change that might occur.

7 - 4 - 1. Determination of K and ε for the Charge-Transfer Complex.

The equilibrium constant, K, and extinction coefficient, ε, of the charge-transfer were calculated using the Benesi-Hildebrand

Figure 7 - 1.

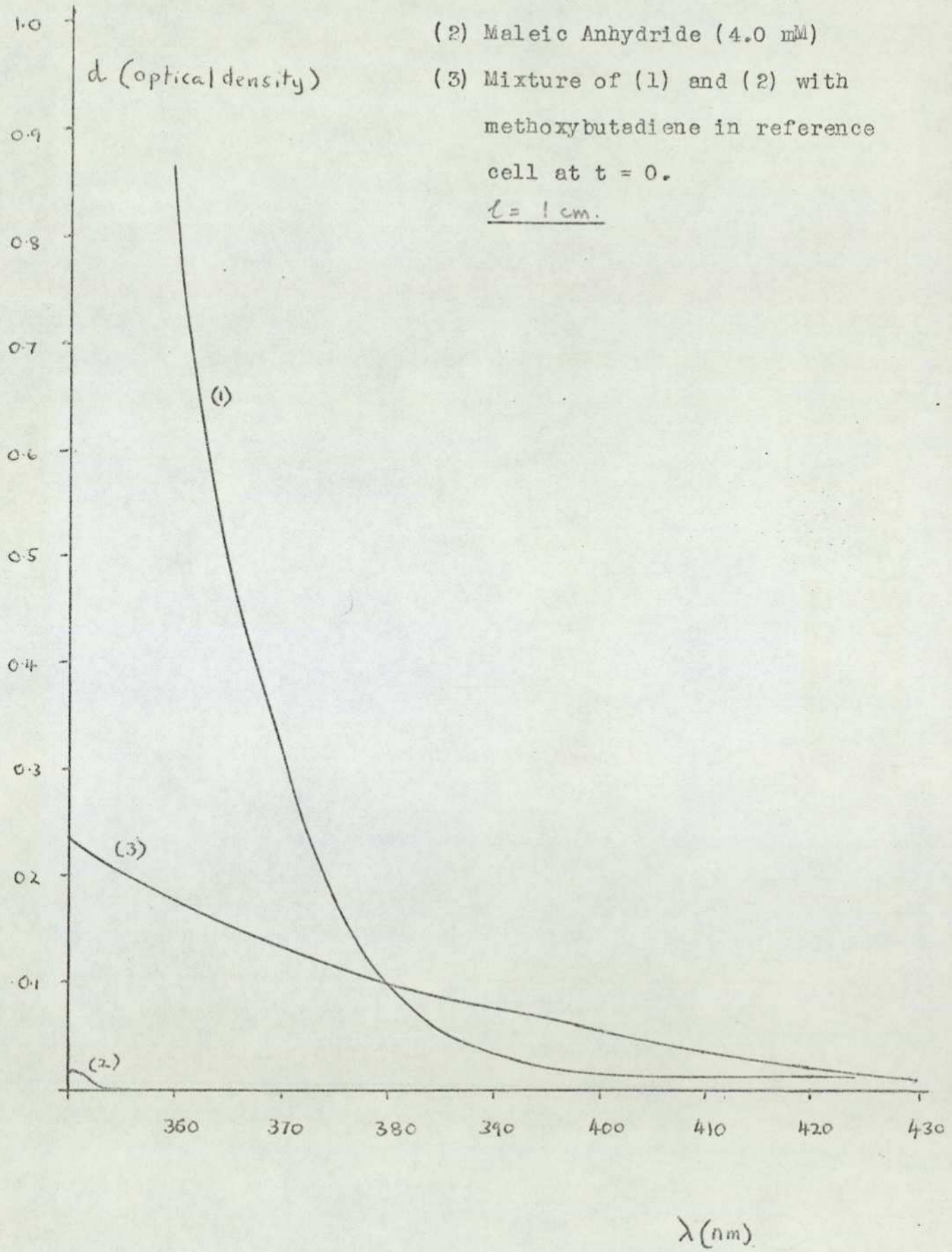
UV Absorptions for methoxybutadiene/maleic anhydride reaction (25.0°C).

(1) Methoxybutadiene (0.6M)

(2) Maleic Anhydride (4.0 mM)

(3) Mixture of (1) and (2) with methoxybutadiene in reference cell at t = 0.

ℓ = 1 cm.



method, in which a large excess of methoxybutadiene was present in the reaction mixture. Initial optical densities, d_o, were obtained by extrapolation of optical densities measured at certain time intervals. The same procedure was adopted as for the hexadiene/maleic anhydride reaction. The reference cell in this case contained a solution of methoxybutadiene of the same concentration as that in the reaction mixture. In all cases the absorbances were followed at 370 nm. The maleic anhydride concentration was kept constant at a given temperature and the methoxybutadiene concentration varied in the usual manner.

Table 7 - 3. Benesi-Hildebrand Data for Methoxybutadiene (D)/ Maleic Anhydride (A) at 370 nm in Chloroform. T = 19.0° C. $[A]_o = 4.94 \times 10^{-3}$ M.

$[D]_o$ (M)	$[D]_o^{-1}$	d_o	$[A]_o d_o^{-1} \times 10^2$
0.513	1.95	0.148	3.32
0.675	1.48	0.188	2.63
0.775	1.29	0.212	2.33
0.998	1.00	0.248	1.99

Table 7 - 4. Data as for above. T = 24.7° C, $[A]_o = 5.20 \times 10^{3}$ M.

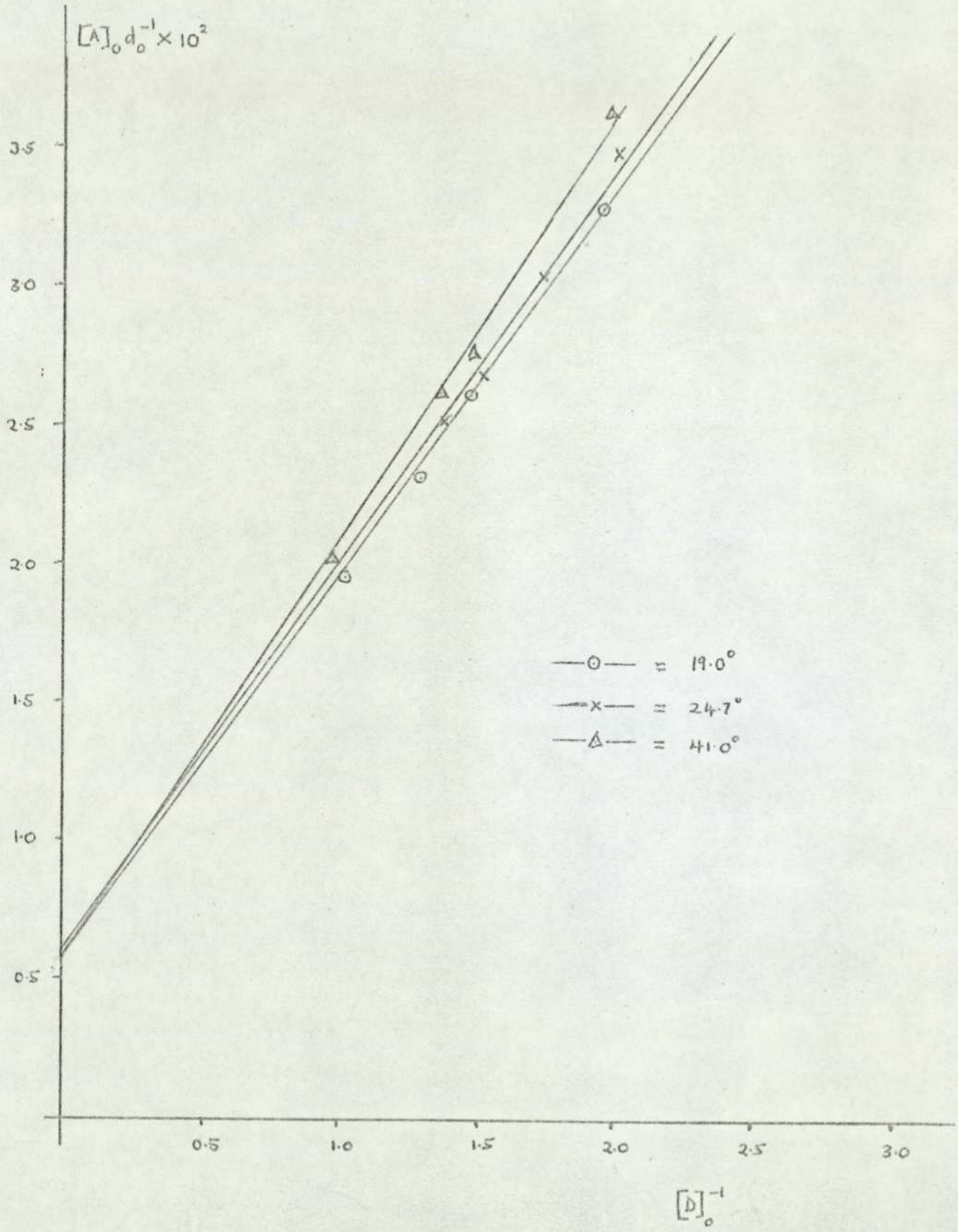
$[D]_o$ (M)	$[D]_o^{-1}$	d_o	$[A]_o d_o^{-1} \times 10^2$
0.489	2.05	0.148	3.51
0.575	1.74	0.170	3.06
0.651	1.54	0.195	2.68
0.720	1.39	0.206	2.52

Table 7 - 5. Data as for above. T = 41.0° C, $[A]_o = 5.04 \times 10^{-3}$ M.

$[D]_o$ (M)	$[D]_o^{-1}$	d_o	$[A]_o d_o^{-1} \times 10^2$
0.492	2.03	0.137	3.66
0.663	1.51	0.182	2.76
0.725	1.38	0.191	2.65
0.987	1.03	0.252	2.01

Figure 7 - 2

Benesi-Hildebrand plot for methoxybutadiene/ maleic anhydride complex. λ = 370 nm.



Plots of $[D]_o^{-1}$ against $[A]_o d_o^{-1}$ (see Fig.7 - 2) gave the following values of K and ε.

Table 7 - 6. Determined K and ε Values for Methoxybutadiene/ Maleic Anhydride at 370 nm in Chloroform.

T (^oC)	ε	Kε	K (l mol^{-1})
19.0^o	179	71.3	0.398
24.7^o	179	69.7	0.390
41.0^o	185	65.5	0.354

The scarcity of points in each graph made the drawing of the best lines difficult and as before Kε values were more accurately determined than K or ε values individually. Kε values were used rather than K in calculation of ΔH and ΔS values for complex formation. When considering the two temperatures, T_1 and T_2 and using the Van't Hoff equation and a difference method, then if ε is considered to be constant:

$$\text{Log}(K\varepsilon)_1 - \text{Log}(K\varepsilon)_2 = \Delta H(T_1-T_2) \;/\; 2.303\, RT_1T_2 \quad (7 - 2)$$

If the two temperatures inserted here are 292^{o}K and 314^{o}K, then the results obtained are as follows:

ΔH = -0.7 kcal mol^{-1}(-2.9 kjoule mol^{-1}). ΔS = -4.3 e.u.

7 - 4 - 2. Calculation of Rate Constants.

The calculation of rate constants for the reaction between methoxybutadiene and maleic anhydride was carried out by following the decrease in absorbance of the band at 370 nm. In all cases, the reference cell contained a solution of methoxybutadiene at the same concentration as in the reaction cell to blank out the absorbance due to diene at 370 nm. Plots of log d_t against time were made, giving values for k_1 and k_2, calculated from the slope and from the relationship $k_2 = k_1/[D]$. As described before, infinity absorbance readings for this reaction were equal to zero and straight

lines were obtained for all graphical plots. At each given temperature the acceptor concentration was kept constant, while the donor concentration, in large excess, was varied.

Table 7 - 7. Rate Constants $k_1(s^{-1})$, $k_2(l\ mol^{-1}\ s^{-1})$ for Methoxybutadiene (D) / Maleic Anhydride (A) in Chloroform, $T = 19.0^{\circ}C$, $[A]_o = 4.94 \times 10^{-3}$ M.

$[D]_o$ (M)	$k_1 \times 10^4$	$k_2 \times 10^4$
0.513	4.80	9.35
0.675	6.62	9.80
0.775	7.65	9.87
0.998	9.49	9.50

Table 7 - 8. Data as for above. $T = 24.7^{\circ}C$, $[A]_o = 5.20 \times 10^{-3}$ M.

$[D]_o$ (M)	$k_1 \times 10^4$	$k_2 \times 10^3$
0.489	6.80	1.39
0.575	8.75	1.52
0.651	9.31	1.43
0.720	10.60	1.47

Table 7 - 9. Data as for above. $T = 32.5^{\circ}C$, $[A]_o = 4.81 \times 10^{-3}$ M.

$[D]_o$ (M)	$k_1 \times 10^3$	$k_2 \times 10^3$
0.530	1.11	2.09
0.722	1.43	1.98
0.795	1.61	2.02
0.990	1.92	1.94

Table 7 - 10. Data as for above. $T = 41.0^{\circ}C$, $[A]_o = 5.04 \times 10^{-3}$ M.

$[D]_o$ (M)	$k_1 \times 10^3$	$k_2 \times 10^3$
0.492	1.66	3.38
0.663	2.17	3.27
0.725	2.34	3.22
0.985	3.20	3.25

The rate constants appear to be constant over the limited concentration range studied. Therefore, in obtaining ΔE and ΔS^* values using the Arrhenius equation, the mean value of k_2 at each temperature was taken and a plot of log k_2 was made against $1/T$, where T is the absolute temperature (see Fig.7 - 3).

Table 7 - 11. Data for Arrhenius Plot of Methoxybutadiene/Maleic Anhydride in Chloroform.

k_2 (l mol^{-1} s^{-1})	Log k_2	T (^oK)	$1/T \times 10^3$
3.28×10^{-3}	-2.484	314.0	3.18
2.01×10^{-3}	-2.697	305.5	3.28
1.45×10^{-3}	-2.839	297.7	3.36
9.64×10^{-4}	-3.016	292.0	3.42

From the slope of the graph it was calculated, ΔE = 9.9 kcal mol^{-1} (41.3 kjoule mol^{-1}).

ΔS^* was calculated at each temperature.

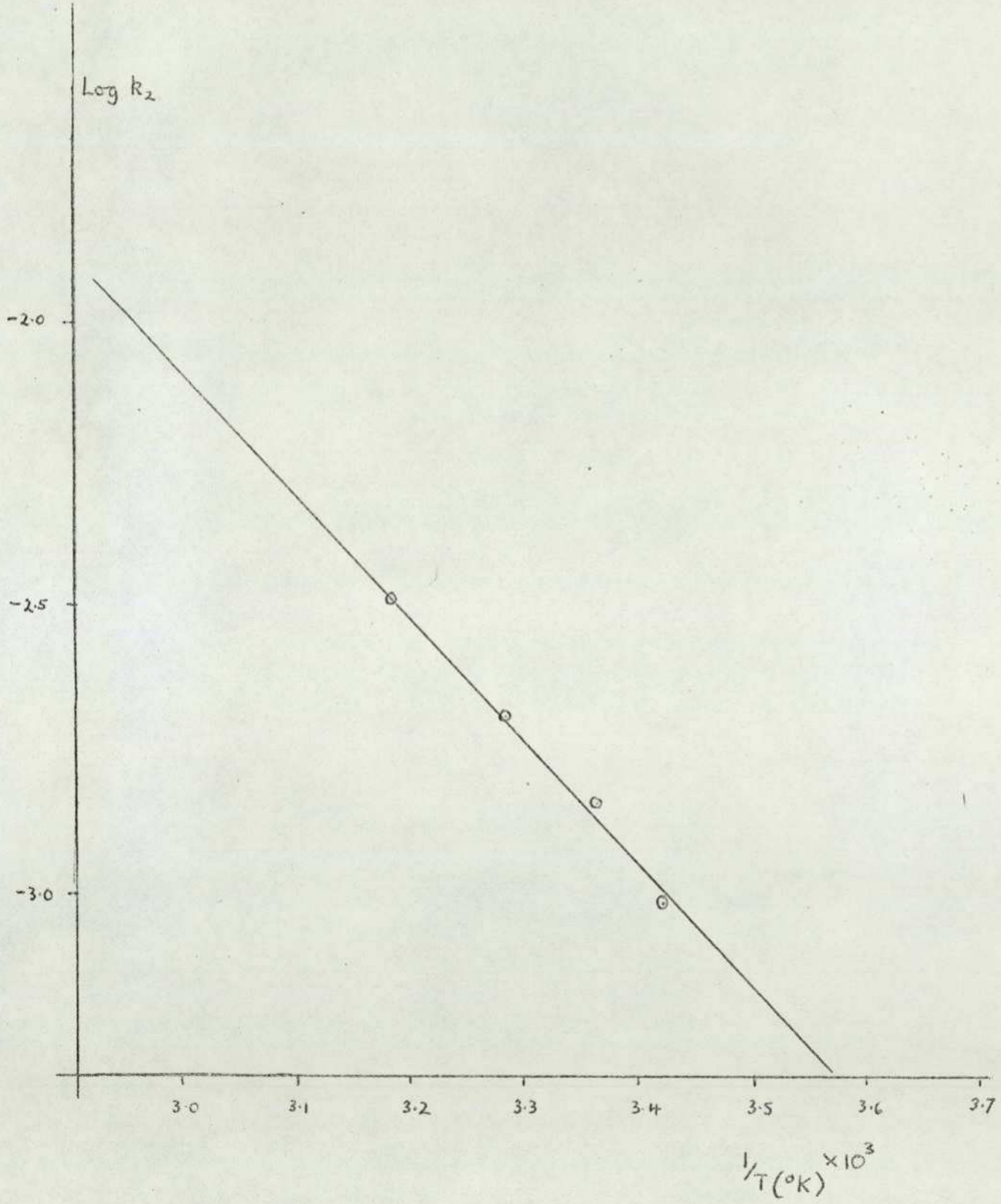
Table 7 - 12. Entropy of Activation for Methoxybutadiene/Maleic Anhydride in Chloroform.

T (^oK)	ΔS^* (e.u)	T (^oK)	ΔS^* (e.u)
314.0	-40.8	297.7	-40.8
305.5	-41.2	292.0	-41.0

Because both maleic anhydride and methoxybutadiene had strong absorption bands overlapping each other in the ultraviolet region of the spectrum, it was not possible to follow the concentration of maleic anhydride during reaction. For similar reasons it was not possible to follow any reaction using equimolar concentrations of reactants in any part of the spectrum.

Figure 7 - 3

Arrhenius plot of rate constants for methoxybutadiene/maleic anhydride reaction.



7 - 5. Discussion

The reaction between the trans isomer of 1-methoxybutadiene and maleic anhydride passes smoothly to form a single cycloadduct by a ($\pi^4_s + \pi^2_s$) mechanism. This was concluded from the spectral analysis of the adduct. The role of the complex formed in solution, however, was not certain after kinetic studies had been carried out. It is clear here that, as for the hexadiene reaction also, there is no increase in k_2 values with increase in donor concentration. Thus scheme (1-23) must again be ruled out at once as a possible reaction mechanism. If schemes (1-21) and (1-22) are considered, then k_2 would be expected to decrease with donor increase. If values of K are inserted into the equations of scheme (1-21) or (1-22) then k_c values can be calculated. (see Section 6 - 5).

Table 7 - 13. k_c calculations at 41.0°C for scheme (1-22), where $k_c(1\text{-}22) = K.k_c(1\text{-}21)$, $K = 0.354.\ (1\ mol^{-1})$

$[D]_o$(M)	$k_2 \times 10^3$ ($1\ mol^{-1}\ s^{-1}$)	$k_c \times 10^3$ ($1\ mol^{-1}\ s^{-1}$)
0.492	3.38	3.95
0.663	3.27	3.99
0.725	3.22	4.03
0.985	3.25	4.28

The k_c values are constant within experimental error. In some instances k_c appears to increase slightly with donor concentration, However, K may not be as large as calculated, due to errors in the Benesi-Hildebrand plots and in general k_c should be virtually constant. Since $k_c(1\text{-}22) = K.k_c(1\text{-}21)$ it will not be possible to distinguish between the mechanisms and hence the charge-transfer complex might be a direct intermediate or formed in a side reaction. The reaction of methoxybutadiene with maleic anhydride might be compared with that of hexadiene with the same dienophile.

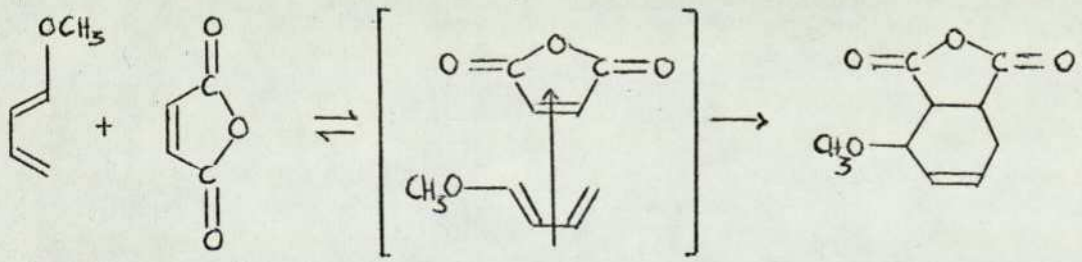
Table 7 - 14. Comparison of Reaction Data for Hexadiene/and Methoxybutadiene/Maleic Anhydride in Chloroform at 19.0° C.

	Hexadiene	Methoxybutadiene
$k_2 \times 10^4$ (l mol^{-1} s^{-1})	4.65	9.63
ΔE (kcal mol^{-1})	10.3	9.9
ΔS^* (e.u)	-41.8	-41.0
K (l mol^{-1})	0.059	0.398

The small difference in rate constant, k_2, could be attributed to the energy of activation difference, rather than the nearly constant entropy of activation. The fact that there is only a relatively small difference is evidence that this kind of reaction is concerted rather than passing through an intermediate zwitterion. The methoxy group would be expected to stabilize any zwitterion by its mesomeric effect, and the rate constant would be expected to be a great deal larger than in the hexadiene reaction. The large negative entropy of activation in both reactions would also indicate a concerted rather than two-step reaction.

The equilibrium constant values although both small, indicate a stronger complex with methoxybutadiene as donor. Because of the difficulties in obtaining accurate values of K, this may not be very significant, although the methoxy substituent might be expected to cause the formation of a stronger complex, on account of its electron-donating mesomeric effect.

The role of the complexes in either reaction is not certain, but as mentioned in Chapter 6, it is possible they lie as direct intermediates, having the 'sandwich' structure as shown.



CHAPTER 8

Anthracene/Maleic Anhydride Reaction

8 - 1. Introduction.

When maleic anhydride and anthracene are mixed together in chloroform, a yellow-green colour, attributed to a charge-transfer complex, is immediately formed. As the reaction proceeds, with the formation of the Diels-Alder cycloadduct, the colour disappears. Studies have shown that in certain solvents the reaction is an equilibrium, being 99% in favour of the cycloadduct for equimolar concentrations.[227] The kinetics of this reaction in chloroform have been studied[124] briefly by examining the decrease in charge-transfer complex absorption during reaction. In the method used, the rate constants of reaction were measured by keeping a constant anthracene concentration throughout the reaction mixtures and varying the maleic anhydride concentration, which was in large excess. It was found that there was a small decrease in rate constant with increase in acceptor concentration, and so either schemes (1-21) or (1-22) were considered as possible mechanisms for this reaction.

Because of the rather limited number of results obtained for this particular reaction, it was decided to examine the reaction again and to extend critically the method used by studying reaction mixtures in which the donor, rather than acceptor, was in large excess and also having equimolar concentrations of reactants. The presence of more than one complex in solution might be determined by examining the change in absorbance at different wavelengths. Chloroform was chosen again as a suitable solvent because of the sufficiently large solubility of maleic anhydride in it compared to other similar solvents.

8 - 2. Purification of Reagents.

Anthracene was supplied as Blue Fluorescent by B.D.H. Chemicals Ltd. and was recrystallised twice from benzene to yield colourless crystals which were stored under vacuum in the dark.
Maleic anhydride was purified as described previously.
Spectroscopic Grade Chloroform was purified by the method described previously after it had been shown that the ethanol stabilizer caused the reaction to proceed about 10% faster in the unpurified solvent compared with the pure solvent. All batches of the chloroform without stabilizer were stored in light-proof bottles in a refrigerator and were used within two days of purification.

8 - 3. Preparation and Analysis of the Adduct.

8 - 3 - 1. Preparation.

Anthracene (5.0g) was added to maleic anhydride (3.0g) in xylene and the mixture was refluxed for 1 hour. A small amount of decolourizing charcoal was then added to the cool solution, which was refluxed for a further ten minutes, the hot solution was filtered, cooled and the crude product slowly precipitated. After filtration, the product was recrystallised twice from ethyl acetate to yield colourless crystals (3.2g). m.p. 262 -263°C. (lit.[159] 262 -263°C).

Calculated for $C_{18}H_{12}O_3$:	C, 78.3;	H, 4.35%
Found:	C, 78.5;	H, 4.21%

8 - 3 - 2. Thin-layer Chromatogram.

The adduct showed one spot only (R_f 0.31) when run in chloroform on activated silica gel.

8 - 3 - 3. UV/Visible Spectrum.

A solution of the adduct in chloroform was examined by UV/Visible

spectroscopy (λ_{max} 260nm (ε 2490), 273nm (ε 1280)) and compared with the spectrum of pure anthracene in chloroform (λ_{max} 253nm (ε 219,000), 285nm (ε 360), 292nm (ε 520)).

8 - 3 - 4. Infrared Spectrum.

The adduct was made into a mull with hexachlorobutadiene and the spectrum was run using an attenuator in the reference beam.

Table 8 - 1. Infrared Spectrum for Anthracene/Maleic Anhydride Adduct.

Frequency	Assignment
3020 cm^{-1} (m)	Aromatic CH stretching
2940 cm^{-1} (m)	Aliphatic CH stretching
1830 cm^{-1} (s)	-C = O stretching
1760 cm^{-1} (s)	-C = O stretching
1220 cm^{-1} (s)	-C - O stretching

8 - 3 - 5. Mass Spectrum.

The measured mass of the parent ion (276.0787) was very close to that calculated (276.0786) for the ion $(C_{18}H_{12}O_3)^+$ which was not, however, the most abundant species.

Table 8 - 2. Main ion fragments for Anthracene/Maleic Anhydride Adduct.

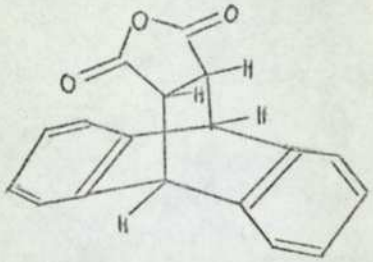
m/e	277	276(M)	179	178	176	101	89
Relative Abundance(%)	5.3	17.4	16.3	100.0	6.7	10.0	9.1

From the mass spectrum, it can be concluded that the main fragmentation is via a retro Diels-Alder reaction pathway to give

anthracene (m/e 178) as the most abundant ion species.

8 - 3 - 6. Conclusion.

It was clear from the evidence of the N.M.R. (Section 3 - 3), IR and analysis that the Diels-Alder adduct of anthracene with maleic anhydride was that present. The infrared spectrum, for instance, showed two types of -CH stretching, the two carbonyl bands, characterisitic of anhydride groups, and a possible C-O stretching in the anhydride group. The N.M.R. spectrum showed three different signals corresponding to three types of protons in different magnetic environments (Section 3 - 3). The adduct could thus be confirmed as 9,10-dihydroenthracene-9,10-endo-α, β-succinic anhydride.



8 - 4. Visible Spectroscopy.

In the previous study[124] the charge-transfer complex absorption had been followed at different wavelengths in the region 420-450nm. It was thus decided to examine this particular end of the visible spectrum to find out the most suitable wavelengths for following reaction.

A solution of anthracene (3.09mM) in chloroform was added to maleic anhydride (0.4M) and the visible spectrum of the mixture examined using 1cm. cells. It was noticed that there was no band maximum, but the intensity increased from 440nm to 400nm. It was not possible to evaluate the correct absorbances due to complex alone in the region 340-400nm because of overlap from

both anthracene and maleic anhydride absorption bands. Solutions of maleic anhydride (0.8M to 0.4M) in chloroform were examined and shown to have zero absorbance in the region 390-450nm. However, solutions of anthracene (3.0mM) had small absorbances in the region 420-400nm rising to an absorbance greater than 1 (1 cm. cells) at 390nm. At 410nm, the absorbance was shown to be about 0.02 and thus for the reaction mixtures, with maleic anhydride in large excess, the change in absorbance at 410nm was followed with a small correction being made throughout the reaction for the absorbance of uncomplexed anthracene at this wavelength. At 410nm the absorptions of charge-transfer complex were suitably large for accurate measurement and it was also a different wavelength to that used[124] previously.

8 - 4 - 1. Determination of K and ε Values for the Charge-Transfer Complex.

8 - 4 - 1 - 1. Using a Large Excess of Maleic Anhydride.

K and ε values for the complex were obtained using first an excess concentration of acceptor. The Benesi-Hildebrand equation adapted to fit the condition $[A]_o \gg [D]_o$ is (8 - 1).

$$[D]_o / d_o = 1 / K\varepsilon [A]_o + 1/\varepsilon \qquad (8 - 1)$$

Thus if $[D]_o d_o^{-1}$ is plotted against $[A]_o^{-1}$ then the values K and ε can be calculated in the usual manner.

The reaction had been shown[124] previously to be relatively slow for the concentrations used (k_2 being of the order of 10^{-5} l mol^{-1} s^{-1}). Therefore, four reaction mixtures were studied using the Unicam SP 1800 (see Chapter 2) which was adapted to take four pairs of 1 cm. cells.

Initial optical densities for reaction mixtures were obtained in

the usual manner with the maleic anhydride concentration varied and the anthracene concentration kept constant for the different reaction mixtures at each temperature. Because of the slowness of the reaction, accurate d_o values were obtained by following the change in optical density for up to two hours. Care was taken to ensure the minimum evaporation of solvent from the cells; the results obtained are shown below.

Table 8 - 3. Benesi-Hildebrand Data for Anthracene (D)/Maleic Anhydride (A) at 410nm in Chloroform $[D]_o = 3.08 \times 10^{-3}$ M, T=24.6°C.

$[A]_o$ (M)	$[A]_o^{-1}$	d_o	$[D]_o d_o^{-1} \times 10^3$
0.404	2.48	0.272	11.09
0.501	1.99	0.323	9.55
0.525	1.91	0.350	8.80
0.551	1.82	0.367	8.44
0.603	1.66	0.393	7.84
0.650	1.54	0.409	7.53
0.675	1.48	0.419	7.35
0.704	1.42	0.440	7.01
0.725	1.38	0.449	6.85
0.751	1.33	0.470	6.58
0.790	1.26	0.484	6.39

Table 8 - 4. Data as for above. $[D]_o = 3.08 \times 10^{-3}$ M, T = 34.4°C.

$[A]_o$ (M)	$[A]_o^{-1}$	d_o	$[D]_o d_o^{-1} \times 10^3$
0.401	2.50	0.250	12.00
0.449	2.23	0.281	10.97
0.551	1.82	0.329	9.12
0.602	1.66	0.356	8.43
0.651	1.54	0.378	7.95
0.701	1.43	0.405	7.41

Table 8 - 5. Data as for above. $[D]_o = 3.04 \times 10^{-3}$M, T = 41.5°C.

$[A]_o$ (M)	$[A]_o^{-1}$	d_o	$[D]_o d_o^{-1} \times 10^3$
0.398	2.51	0.248	12.43
0.451	2.22	0.282	10.75
0.502	1.99	0.301	10.15
0.550	1.83	0.318	9.55
0.607	1.65	0.355	8.55
0.652	1.54	0.372	8.17
0.701	1.43	0.397	7.66
0.753	1.32	0.427	7.11

Plots of $[D]_o d_o^{-1}$ against $[A]_o^{-1}$ (see Fig. 8 - 1) gave the following values.

Table 8 - 6. Determined K and ε values for Anthracene/Maleic Anhydride Complex at 410nm in Chloroform.

T (°C)	ε	Kε	K
24.6	833	245.9	0.295
34.4	833	228.0	0.274
41.5	800	219.8	0.264

Values obtained by Andrews and Keefer[124] are shown in Table 8 - 7 for comparison.

Table 8 - 7. Results for K and ε from Andrews & Keefer. Using Large Excess of Maleic Anhydride. T = 25.2°C.

Wavelength (nm)	K	Kε	ε
420	0.296	214.5	725
430	0.303	166.5	550
440	0.342	131.8	385
450	0.335	95.5	285

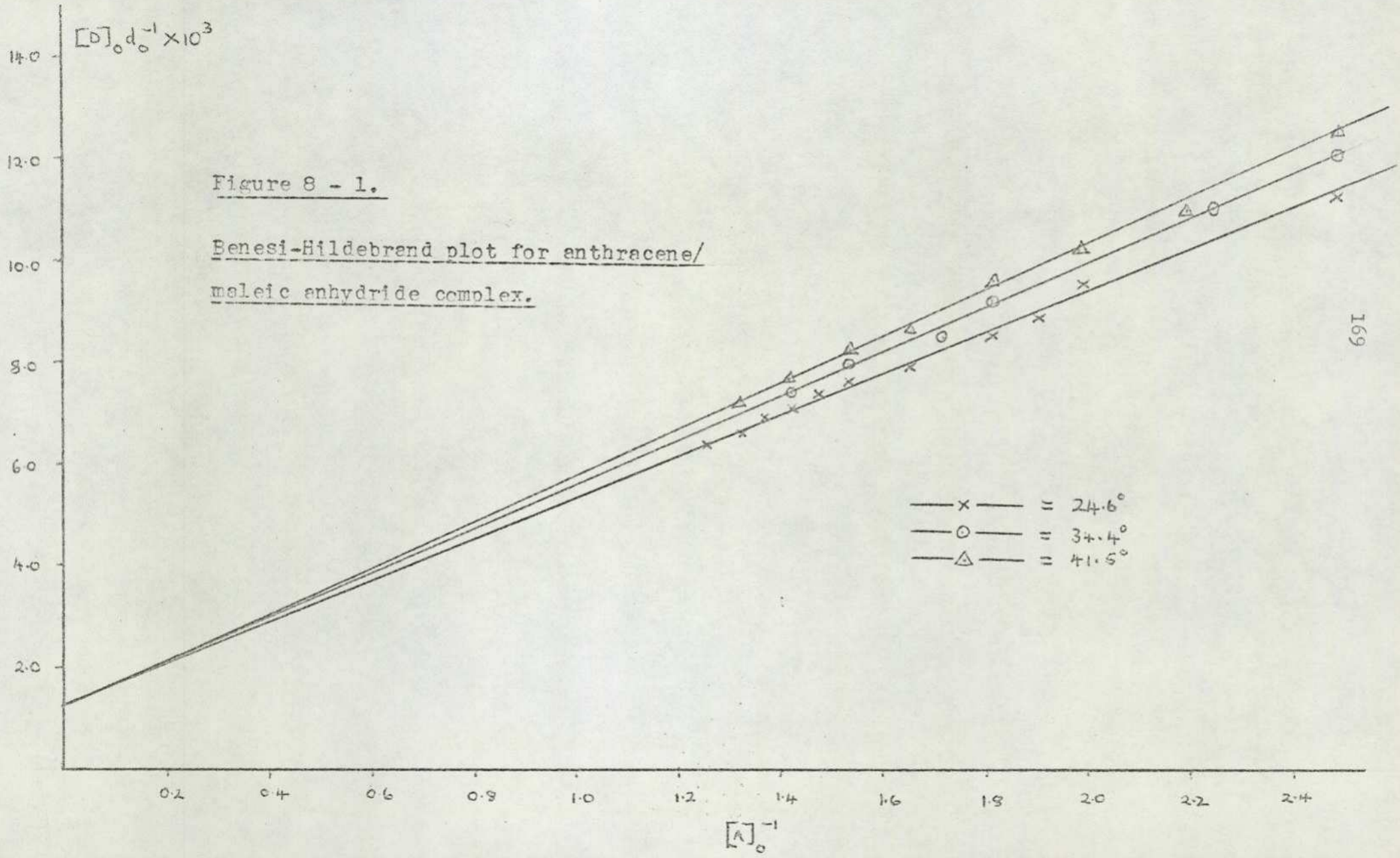


Figure 8 - 1.

Benesi-Hildebrand plot for anthracene/ maleic anhydride complex.

8 - 4 - 1 - 2. Using Equimolar Concentrations.

K and ε values were determined using equimolar concentrations of reactants in order to compare them with values obtained for K above when differences might indicate the possible presence of termolecular species. For equimolar concentrations in the range 0.07 to 0.02M, there appeared to be no absorptions of either anthracene or maleic anhydride at wavelengths longer than 425nm. The absorption at 426 and at 440nm due to the charge-transfer complex formed from reactants was followed and in many cases, the rate of decrease was slow so that accurate values of d_o could be obtained directly. At higher concentrations, the rate of decrease was followed and d_o values obtained by extrapolation.

Table 8 - 8. Equimolar Data for Anthracene (D)/Maleic Anhydride (A) at 426nm in Chloroform. T = 25.0° C.

$[A]_o$ (M)	d_o	$[A]_o d_o^{-1}$	$d_o^{-\frac{1}{2}}$
0.0255	0.108	0.235	3.042
0.0310	0.150	0.206	2.583
0.0350	0.213	0.164	2.167
0.0405	0.260	0.156	1.962
0.0500	0.431	0.116	1.523
0.0605	0.590	0.102	1.302
0.0650	0.734	0.089	1.167
0.0705	0.861	0.082	1.077

Table 8 - 9. Equimolar Data at 440nm. T = 25.0°C.

$[A]_o$ (M)	d_o	$[A]_o d_o^{-1}$	$d_o^{-\frac{1}{2}}$
0.0255	0.070	0.363	3.780
0.0310	0.104	0.288	3.101
0.0350	0.145	0.241	2.626
0.0405	0.175	0.228	2.391
0.0500	0.289	0.174	1.860
0.0605	0.407	0.147	1.567
0.0650	0.493	0.132	1.427
0.0705	0.586	0.119	1.306

Plots of $[A]_o d_o^{-1}$ against $d_o^{-\frac{1}{2}}$ gave straight lines with very small intercepts (see Fig. 8 - 2). As accurate values of ε derived by this method are not easy to obtain, Kε values were measured and the results compared with those obtained[124] previously. Graphical plots of wavelength again ε from table 8 - 7 gave a value of 610 for ε at 426nm and 385 for ε at 440nm. Using these values, the results obtained using equimolar concentrations are shown.

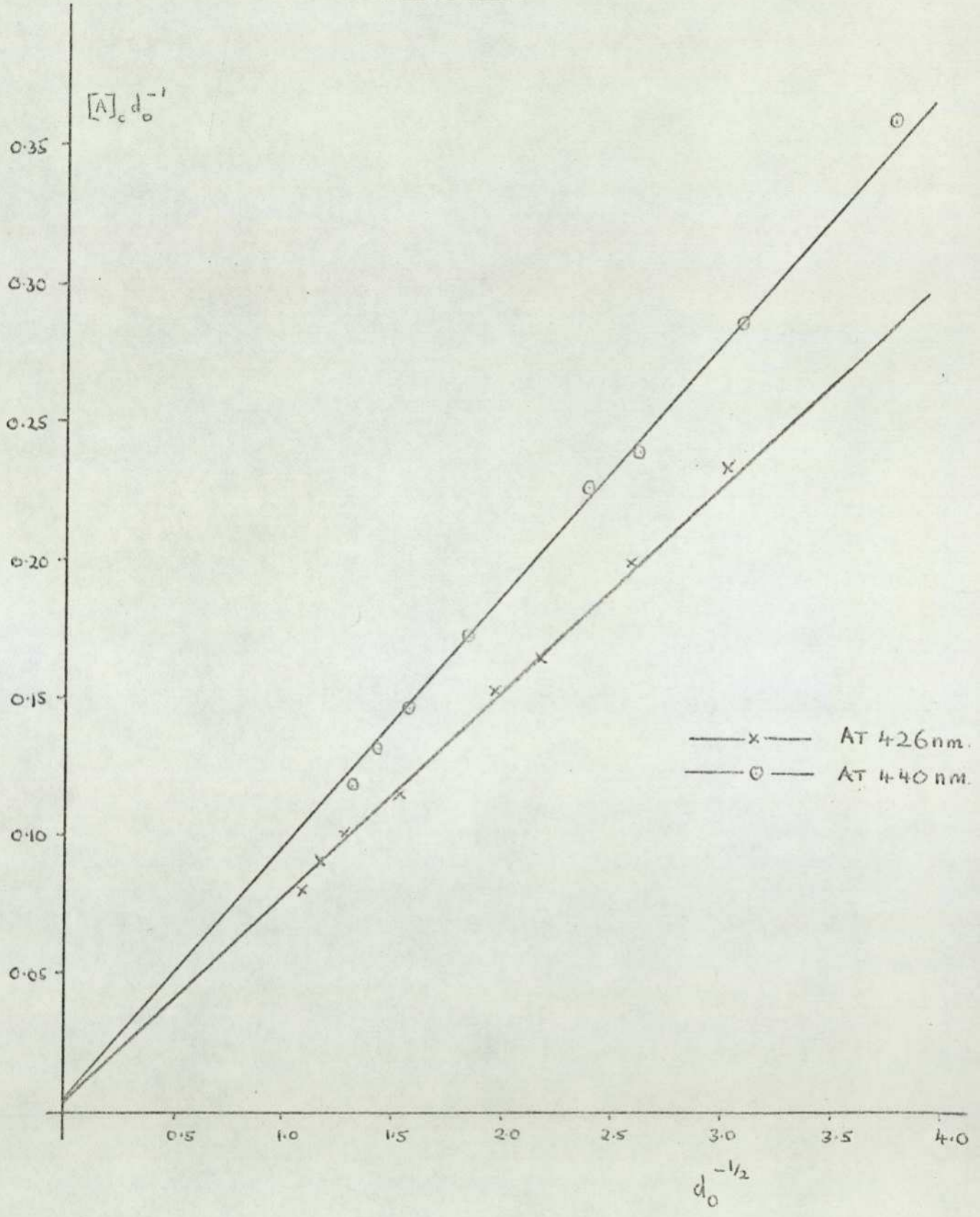
Table 8 - 10. Results using Equimolar Concentrations. T = 25.0°C.

Wavelength (nm)	ε	Kε	K
426	610	176.3	0.290
440	385	117.5	0.306

The values obtained here for K compare favourably with those obtained using the excess method, at 24.6°C (see Table 8 - 6). The Van't Hoff equation was applied to the results obtained by the excess concentration method to give the following values of enthalpy and entropy of complex formation.

Figure 8 - 2

Equimolar plot for enthracene/maleic anhydride complex.



ΔH = - 1.23 kcal mol^{-1} (-5.15 kjoule mol^{-1}); ΔS = - 6.59 e.u..

8 - 4 - 2. Calculation of Rate Constants.

Rate Constants were calculated for reactions in which a large excess of maleic anhydride was present and it was also possible to obtain a limited number of results using a large excess of anthracene in the reaction mixture and also using equimolar concentrations.

8 - 4 - 2 - 1. Using a large excess of Maleic Anhydride.

The reactions were followed in the usual manner to obtain values of k_2 for different concentrations of anhydride from the decrease in charge-transfer absorption with time at a given temperature. As mentioned previously, the slowness of reaction made it possible for four reaction mixtures to be followed at the same time using four pairs of cells in the SP 1800 Spectrophotometer. It was possible to make up four reaction mixtures within the space of 2 to 3 minutes and place them immediately inside the cell-housing. All reactant solutions were kept in a thermostatted bath before mixing.

The results are shown over the page.

Table 8 - 11. Rate Constants k_1 (s^{-1}), k_2 and k_c (1 mol^{-1} s^{-1}) for Anthracene (D)/Maleic Anhydride (A) at 410 nm in Chloroform. T = 24.6°C $[D]_o$ = 3.08×10^{-3}M.

$[A]_o$ (M)	$k_1 \times 10^5$	$k_2 \times 10^5$	$k_c \times 10^5$
0.351	1.07	3.07	3.47
0.375	1.18	3.12	3.46
0.450	1.36	3.02	3.41
0.525	1.51	2.87	3.31
0.575	1.63	2.84	3.32
0.675	1.75	2.60	3.12
0.726	1.84	2.53	3.07
0.790	2.04	2.58	3.18

Table 8 - 12. Rate Constants as for above, T = 34.4°C $[D]_o$ = 3.07×10^{-3}M.

$[A]_o$ (M)	$k_1 \times 10^5$	$k_2 \times 10^5$	$k_c \times 10^5$
0.401	2.56	6.40	7.16
0.550	3.28	5.96	6.86
0.603	3.53	5.86	6.83
0.652	3.64	5.58	6.59
0.703	3.88	5.52	6.58
0.751	3.92	5.22	6.31

Table 8 - 13. Rate Constants as for above, T = 38.4°C $[D]_o$ = 3.06×10^{-3}M.

$[A]_o$ (M)	$k_1 \times 10^5$	$k_2 \times 10^5$	$k_c \times 10^5$
0.403	2.74	6.81	7.55
0.451	3.18	7.04	7.90
0.499	3.48	6.97	7.90
0.550	3.94	7.16	8.22
0.607	4.32	7.12	8.23
0.702	4.92	7.02	8.31

Table 8 - 14. Rate Constants as for above. T = 41.5°C. $[D]_o$ = 3.04 x 10^{-3}M.

$[A]_o$ (M)	$k_1 \times 10^5$	$k_2 \times 10^5$	$k_c \times 10^5$
0.398	3.48	8.70	9.61
0.451	3.71	8.23	9.21
0.502	4.34	8.64	9.78
0.550	4.61	8.39	9.61
0.607	5.95	9.80	11.55
0.652	6.40	9.80	11.68
0.701	6.16	8.80	10.42
0.753	6.68	8.90	10.61

It appears that at the lower temperatures the rate constants, k_2, decrease with increase in maleic anhydride concentration, whereas at higher temperatures, there is no definite trend. If scheme (1-22) is arbitrarily assumed to be that operating then k_2 is related to the true rate constant, k_c, by the relationship:

$$k_c = k_2 (1 + K [A]_o) \qquad (8 - 2)$$

The difference in this case to the previous relationships being that now acceptor [A] rather than donor [D] is in large excess. k_c values were calculated at each temperature, and are shown in tables 8 - 11 to 8 - 14.

In general the k_c values for scheme (1-22) lie within about a 10% range at each temperature and in calculating, the energy and entropy of activation, ΔE and ΔS^* for reaction, mean values of k_c were taken at each temperature.

The Arrhenius equation was used to calculate these parameters by plotting log k_c against I/T (see Fig. 8 - 3).

Figure 8 - 3.

Arrhenius plot of rate constants for enthracene/maleic anhydride reaction.

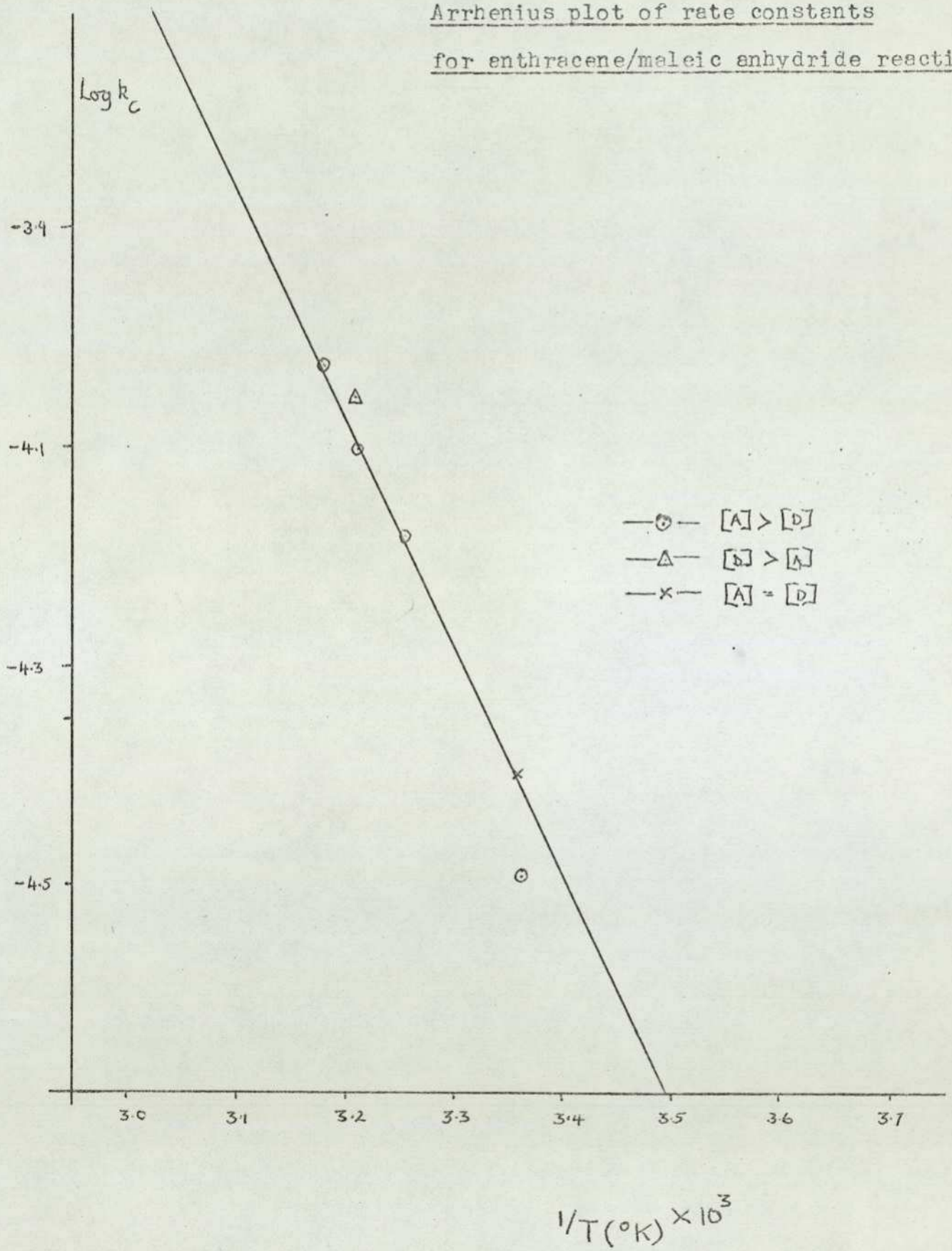


Table 8 - 15. Data for Arrhenius Plot of Anthracene/Maleic Anhydride in Chloroform ($[A]_o >> [D]_o$).

$k_c \times 10^5$ (l mol^{-1} s^{-1})	Log k_c	T (^oK)	$1/T \times 10^3$
3.29	-4.483	297.6	3.36
6.71	-4.173	307.4	3.25
8.01	-4.096	311.4	3.21
9.55	-4.019	314.5	3.18

From the slope of the graph it was calculated, ΔE = 11.5 kcal mol^{-1} (48.2 kjoule mol^{-1}). ΔS^* was calculated at the different temperatures.

Table 8 - 16. Entropy of Activation for Anthracene/Maleic Anhydride in Chloroform.

T (^oK)	297.6	307.4	311.4	314.5
ΔS^* (e.u)	-42.8	-43.0	-43.0	-42.9

8 - 4 - 2 - 2. Using a Large Excess of Anthracene.

It was found that reaction rate constants for mixtures containing excess anthracene could only be obtained under very limited conditions.

The solubility of anthracene in chloroform between 25° and 40° c did not exceed 0.12M and consequently it was only possible to use reaction mixtures in which both reactants were relatively dilute. (e.g. Anthracene (0.1M), Maleic Anhydride (5.0mM)). Not only was the absorption due to complex small in this case, but its rate of decrease was slow, making it difficult to follow effectively. Another limiting factor was the absorbance in the visible spectrum due to anthracene itself. It was only possible to study the complex using 4cm cells, at wavelengths longer than 420 nm.

As the rate of reaction was too slow to follow at 25.0°, the temperature was increased to 38.2°C. The reaction was followed at 430nm and there was no correction needed for any interfering anthracene absorption. The reference cells contained pure solvent for all the kinetic runs.

Table 8 - 17. Rate Constants $k_1(s^{-1})$, k_2 and $k_c(l\ mol^{-1}\ s^{-1})$ for Anthracene (D)/Maleic Anhydride (A), where [D]>[A]. T = 38.2°C. $[A]_o = 5.02 \times 10^{-3}$ M.

$[D]_o$ (M)	$k_1 \times 10^6$	$k_2 \times 10^5$	$k_c \times 10^5$
0.0710	6.47	9.91	10.10
0.0805	7.73	9.60	9.81
0.0895	7.80	8.71	8.92
0.0990	8.47	8.55	8.78
0.1010	8.99	8.90	9.14

When compared with the rate constants, k_c, obtained at 38.4°C using a large excess of maleic anhydride, the above are seen to be about 15% higher in value. A mean value of k_c was calculated and hence log k_c would be obtained and plotted against I/T to give a point on the Arrhenius graph (see Fig. 8 - 3).

8 - 4 - 2 - 3. Using Equimolar Concentrations.

The maximum solubility of maleic anhydride in chloroform appeared to be about 0.07M in the range 25° to 40° C. It was thus only possible to follow the reaction kinetics of equimolar mixtures in the range 0.04 to 0.07M. As mentioned before, both anthracene and maleic anhydride have tail absorptions in the visible region and so it was necessary to follow the decrease in absorption at longer wavelengths, namely, 426 and 440 nm. Trial runs using 1 cm. cells showed that the decrease in absorption of the charge-transfer complex band was very slow indeed and it was necessary to follow

the reaction for three hours or more to obtain sufficient readings. Care was thus taken to minimise evaporation of the solvent during this period.

In calculation of rate constants using equimolar concentrations, scheme (1 - 22) was assumed to be that operating.

$$A + D \underset{\pi}{\overset{K}{\rightleftharpoons}} AD^{*} \qquad A + D \xrightarrow{k_c} \underset{x}{AD}$$

The rate of formation of AD is given by:

$$dx/dt = k_c [A - \pi - x]^2 \qquad (8 - 3)$$

Since: $$[A - \pi - x] = \sqrt{\pi / K} \qquad (8 - 4)$$

$$dx = (-1 - \tfrac{1}{2}/\sqrt{\pi K})\, d\pi \qquad (8 - 5)$$

Substitution of (8 - 4) and (8 - 5) into (8 - 3), integration and further simplification gives the following, ($\pi = d_t/\varepsilon$):

$$\sqrt{K\varepsilon}/\sqrt{d_t} - K \operatorname{Ln} d_t = k_c t + C \qquad (8 - 6)$$

As $K \operatorname{ln} d_t$ is much smaller than $\sqrt{K\varepsilon}/\sqrt{d_t}$ and almost constant,

$$\sqrt{K\varepsilon}/\sqrt{d_t} = k_c t + C' \qquad (8 - 7)$$

Plots of $1/\sqrt{d_t}$ against t would give straight lines of slope equal to $k_c/\sqrt{K\varepsilon}$, where the rate constants are those for scheme (1-22). If scheme (1-21) is adopted, then if a similar procedure to that shown in equations (8 - 3) to (8 - 7) is carried out, (8 - 8) is derived.

$$\sqrt{\varepsilon}/\sqrt{d_t K} = k_c t + C' \qquad (8 - 8)$$

Plots of $1/\sqrt{d_t}$ against t would now give straight lines of slope equal to $k_c\sqrt{K}/\sqrt{\varepsilon}$. Therefore, since $k_c(1\text{-}22) = K.k_c(1\text{-}21)$ the equimolar method, similar to the Benesi-Hildebrand method, cannot be used to distinguish between schemes (1-21) and (1-22).

If k_c(1-22) values are chosen, to compare with those in table 8 - 13, equation (8 - 7) is adopted.

Not all graphical plots appeared as straight lines and the best line had to be drawn through the points.

Table 8 - 18. Rate Constants k_c (1 mol^{-1} s^{-1}). Determined Using Equimolar Concentrations. $[A]_o = [D]_o$

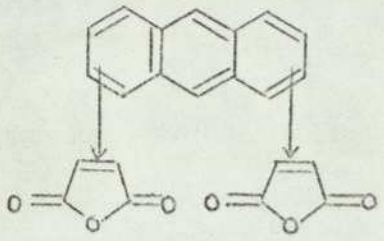
T = 25.0°C, Wavelength = 426 nm.		T = 25.0°C, Wavelength = 440 nm.	
$[A]_o$ (M)	$k_c \times 10^5$	$[A]_o$ (M)	$k_c \times 10^5$
0.0505	3.89	0.0505	3.82
0.0605	4.75	0.0605	4.58
0.0650	3.70	0.0650	3.58
0.0705	5.21	0.0705	5.10

A mean value for k_c was obtained, which could then be used to obtain a log k_c value at 25.0°C plotted in the Arrhenius plot (see Fig.8-3). The k_c values obtained are somewhat variable. This might be accounted for by the difficulty in measuring small changes for such a slow reaction leading to large errors in evaluation of rate constants. The mean k_c value does, however, give a good fit on the Arrhenius plot (see Fig.8 - 3).

8 - 5. Discussion.

Anthracene and maleic anhydride react together slowly to form the Diels-Alder (4 + 2) cycloadduct. The kinetics of reaction were studied with special reference to the possible existence of termolecular complexes in solution. In the reaction between diphenyl butadiene and TCNE the formation of a 2:1 acceptor:donor complex was postulated[79] on the basis of optical density measurements. As the donor contained two phenyl groups, it was possible to visualise two molecules of acceptor loosely oriented on each ring.

A 2:1 acceptor:donor complex might similarly be visualised for anthracene with maleic anhydride, in which each acceptor molecule is oriented with respect to each ring as shown.



As mentioned previously, deviations from linearity in Benesi-Hildebrand plots may not be evident when termolecular complexes are present, so that the formation of straight line plots would not exclude the possible existence of a 2:1 complex.

The visible spectra of reaction mixtures in equimolar concentration showed only one charge-transfer complex band, so it was assumed that if a second complex (2:1) was present it was either formed to a negligible extent or the absorption band overlapped that due to the 1:1 complex.

$K_{\leq}$ values derived from both excess of one reactant and equimolar methods were of similar magnitude. Thus at 440 nm at 25.2°C, $K_{\leq}$ = 131.8 (excess of acceptor method - Table 8 - 7), and at 25.0°C, $K_{\leq}$ = 117.5 (equimolar method - Table 8 - 10). It must be assumed that there would be a greater amount of 2:1 complex present, when excess acceptor concentration was present compared to equimolar concentrations. It was unfortunately not possible to obtain $K_{\leq}$ values for reaction mixtures where the anthracene was in excess because of the limitations in the accuracy of the method used.

If the formation of 2:1 acceptor:donor complex is envisaged then the following scheme may be drawn.

$$A + D \underset{}{\overset{K_1}{\rightleftharpoons}} AD^* \qquad (8 - 8 - 1)$$

$$AD^* + A \underset{}{\overset{K_2}{\rightleftharpoons}} A_2D^* \qquad (8 - 8 - 2)$$

$K\varepsilon$ values obtained for both equimolar and excess acceptor concentration were based on the single equation (8 - 8 - 1). If the absorption is assumed to be due to both 1:1 and 2:1 complexes, the amount of 2:1 complex present is given by

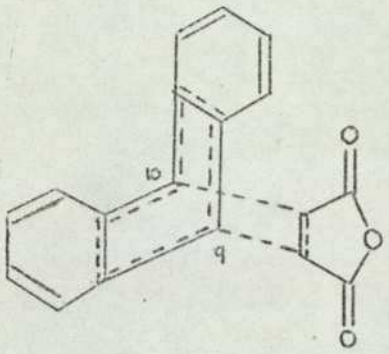
$$[A_2D] / [AD] = K_2 [A]_f \qquad (8 - 9)$$

Where $[A]_f$ is the free concentration of acceptor species. On this basis it is seen that in the method using a large excess of acceptor, there will be a greater proportion of A_2D species present than for the method using equimolar concentrations. Since the equilibrium constants, K_1 and K_2, and extinction coefficients, ε_1 and ε_2, for each complex should be different, then the total ($K\varepsilon$) value for each method should be different because of the different composition of the total complex concentration. It thus appears unlikely on the basis of the determined $K\varepsilon$ values that there is a significant amount of 2:1 complex present.

There is not a great deal of difference between determined k_c values when acceptor is in large excess compared to those when donor is in excess. The equimolar concentration results may be somewhat inaccurate (see also Fig. 8 - 3). On this basis again, it is unlikely that such species as D_2A or DA_2 exist to any large extent in solution, since then k_c values would be different depending on the species in excess.

The energy of activation and entropy of activation values obtained are similar in magnitude to previous results [124] and are in line with those values for most Diels-Alder reactions. It thus appears that a concerted mechanism is operating in which a single charge-transfer complex may or may not be a direct intermediate. If a direct intermediate is postulated, then a similar phenomenon to that

suggested for the anthracene-TCNE reaction may be envisaged, in which the charge-transfer complex precedes the formation of a symmetrical transition state centred at carbon atoms 9 and 10 of the anthracene molecule.



Chapter 9

Indole/TCNE Reaction

9 - 1. Introduction.

The reaction between indole and TCNE in dichloromethane has been studied[79,82] previously in order to examine the possible role of the charge-transfer complex (λ_{max} 560 nm) which is formed when the two reactants are mixed together.

Although the conclusions reached in both studies were that there was some involvement of indole molecules with complexes formed in reaction, there were large discrepancies in the rate constants obtained. It was thus decided to re-examine this reaction using UV/Visible spectroscopy to follow the absorptions occurring in the spectrum due to the charge-transfer complex and the final product.

9 - 2. Purification of Reagents.

Indole was supplied as Puriss. by Koch-Light Laboratories Ltd. and was stored in light-excluded bottles as it went yellow on prolonged exposure to light. It was carefully purified either by recrystallisation twice from cyclohexane or by subliming twice under vacuum at 45°C. Samples were used as soon as possible after purification and great care was taken to exclude light from the sample containers, which were stored under vacuum in a dessicator. m.p. 50-51°C (lit.[218] 52°C).

Tetracyanoethylene was purified as described in Section 4 - 2 and stored under vacuum.

Dichloromethane and 1,2-dichloroethane were purified as described in Section 2 - 1.

9 - 3. Preparation and Analysis of the Adduct.

9 - 3 - 1. Preparation.

The procedure used by Noland et al.[204] was adopted.

A solution of indole (2.0g) in benzene (10 ml) was added to a boiling solution of TCNE (1.2g) in benzene (10 ml). A drop of pyridine was added to the blue-black solution and the mixture turned red after a few minutes. The solution was then boiled for a further five minutes and allowed to cool, during which time the red product, 3-tricyanovinylindole, precipitated out. Recrystallisation from the minimum of glacial acetic acid yielded red needles. m.p. 272 - 273°C(lit.[204] 273 -275°C).

Calculated for $C_{13}H_6N_4$: C, 71.6; H, 2.79, N, 25.8%

Found : C, 71.4; H, 3.00, N, 26.1%

9 - 3 - 2. Thin-layer Chromatogram.

Analysis of the recrystallised adduct on silica gel chromagram using chloroform/dichloromethane (50:50 v/v) as moving phase showed one spot (R_f 0.2) only, visible under ultraviolet light.

9 - 3 - 3. UV/Visible Spectrum.

Solutions of the adduct were made up in dichloromethane and examined in the region 240-600 nm. The following band maxima were observed: 274 nm (ε 15,500), 455 nm (ε 17,600). This was compared with the spectrum of pure indole in dichloromethane - 266 nm (ε 6,500), 287 nm (ε 4,100).

9 - 3 - 4. Infrared Spectrum.

A sample of the adduct was made up into a KBr disc and the infrared spectrum recorded.

Table 9 - 1. Infrared Spectrum of 3-Tricyanovinyl indole.

Wavenumber	Assignment
3400 cm^{-1} (s)	-NH stretching
~3000 cm^{-1} (w)	-CH stretching
2230 cm^{-1} (s)	conjugated -CN stretching
1590 cm^{-1} (m)	-C=C- stretching
750 cm^{-1} (s)	-CH bending (aromatic)

9 - 3 - 5. Mass Spectrum.

The measured mass of the parent ion (218.0590) was very close to that calculated (218.0592) for the $(C_{13}H_6N_4)^+$ ion.

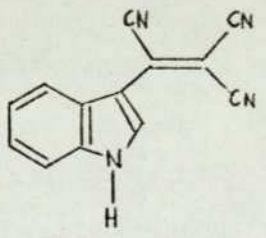
Table 9 - 2. Main Fragment Ions for 3-Tricyanovinyl Indole.

m/e	219	218	191	165	164	142	109	96
Relative Abundance(%)	24.2	100.0	57.9	11.1	28.9	20.9	10.1	11.0

The base peak corresponds to the molecular ion. Metastable peaks at m/e 167.6 and m/e 141.0 correspond to the transitions 218→191 and 191→164, which is the loss of one molecule of HCN in each case.

9 - 3 - 6. Conclusion.

The IR, N.M.R. and UV/Visible spectra together with the Mass Spectrum all show that the 3-tricyanovinyl indole structure is present in the adduct.



9 - 4. Preparation and Analysis of an Intermediate.

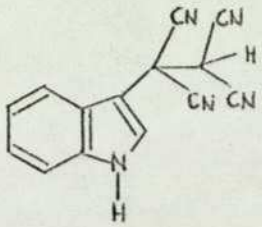
When a solution of indole and tetracyanoethylene in the minimum of dichloromethane was left for 24 hours, a pink solid precipitated out, which was collected, filtered and dried. The solid was shown to be unstable since it turned red when heated gently or when dissolved in a suitable solvent. A quicker method used to obtain the same intermediate was adopted by adding acid to the solution of reactants. Thus, indole (1.0g) was added to a solution of TCNE (0.5g) in dichloromethane (80 ml). Concentrated hydrochloric acid (0.05 ml) was then added and the mixture thoroughly shaken. After a few minutes, the pink solid precipitated and was collected, filtered and dried. Because of the instability of the solid it was only possible to obtain an infrared spectrum when a sample was made up into a KBr disc. This gave the following:

Table 9 - 3. Infrared Spectrum of Intermediate.

Wavenumber	Assignment
3400 cm^{-1} (s)	-NH stretching
3050 cm^{-1} (w)	Aromatic -CH stretching
2960 cm^{-1} (w)	Non-aromatic -CH "
2850 cm^{-1} (w)	" " " "
2230 cm^{-1} (very weak)	-CN stretching
1620 cm^{-1} (m)	-C=C- stretching.

The intermediate obtained when no acid was added also gave a similar IR spectrum. The weak cyanide stretching band indicated no conjugation in the side-chain and the -CH stretching bands indicated a saturated -CH fragment. Although the intermediate gave a red colour when dissolved in dichloromethane, indicating decomposition to the final product (λ_{max} 455 nm), the UV/Visible spectrum showed

one other absorption (λ_{max} 269 nm). On the basis of this, it would seem likely that the intermediate would have the structure as shown rather than a zwitterion form, because of the presence of acid in solution, which may act as a catalyst for intermediate formation.



9 - 5. Visible Spectroscopy.

In the previous studies, the absorption due to the charge-transfer complex had been followed at 560 nm. It was decided to see initially if the results obtained were reproducible at this wavelength.

9 - 5 - 1. Determination of K and ε Values for the Charge-Transfer Complex.

In order to obtain values of equilibrium constant, K, and extinction coefficient, ε, for the charge-transfer complex, the usual Benesi-Hildebrand method was adopted, in which the reaction mixtures contained a large excess of indole. Solutions of TCNE (about 0.5 mM) mixed with solutions of indole (about 0.7M) in dichloromethane gave a broad band in the visible region of the spectrum not attributable to either reactant species (λ_{max} 560 nm). The same procedure for making up solutions and mixing was adopted as for the previous kinetic studies (see also Section 4 - 4 - 1 - 1). Initial optical density values, d_o, were obtained by extrapolation of optical densities measured at given time intervals.

Table 9 - 4. Benesi-Hildebrand Data for Indole (D) /TCNE (A) at 560nm in Dichloromethane. T = 25.6° C. $[A]_o$ = 5.01 x 10^{-4}M.

$[D]_o$ (M)	$[D]_o^{-1}$	d_o	$[A]_o d_o^{-1} \times 10^3$
0.0501	19.97	0.127	3.95
0.0605	16.51	0.147	3.40
0.0908	11.01	0.205	2.44
0.110	9.09	0.236	2.12
0.199	5.02	0.377	1.34

Table 9 - 5. Data as for before. T = 18.0°C.

$[A]_o \times 10^4$	$[D]_o$ (M)	$[D]_o^{-1}$	d_o	$[A]_o d_o^{-1} \times 10^3$
7.01	0.072	13.90	0.289	2.42
10.20	0.106	9.43	0.571	1.77
7.01	0.129	7.75	0.489	1.44
7.07	0.204	4.90	0.627	1.12
10.10	0.207	4.83	0.968	1.04
7.01	0.255	3.92	0.738	0.95

Plots of $[A]_o d_o^{-1}$ against $[D]_o^{-1}$ gave the following results for ε and K which are compared with results obtained[79,82] previously. (see Fig. 9 - 1).

Table 9 - 6. Determined K and ε Values for Indole /TCNE at 560 nm in Dichloromethane.

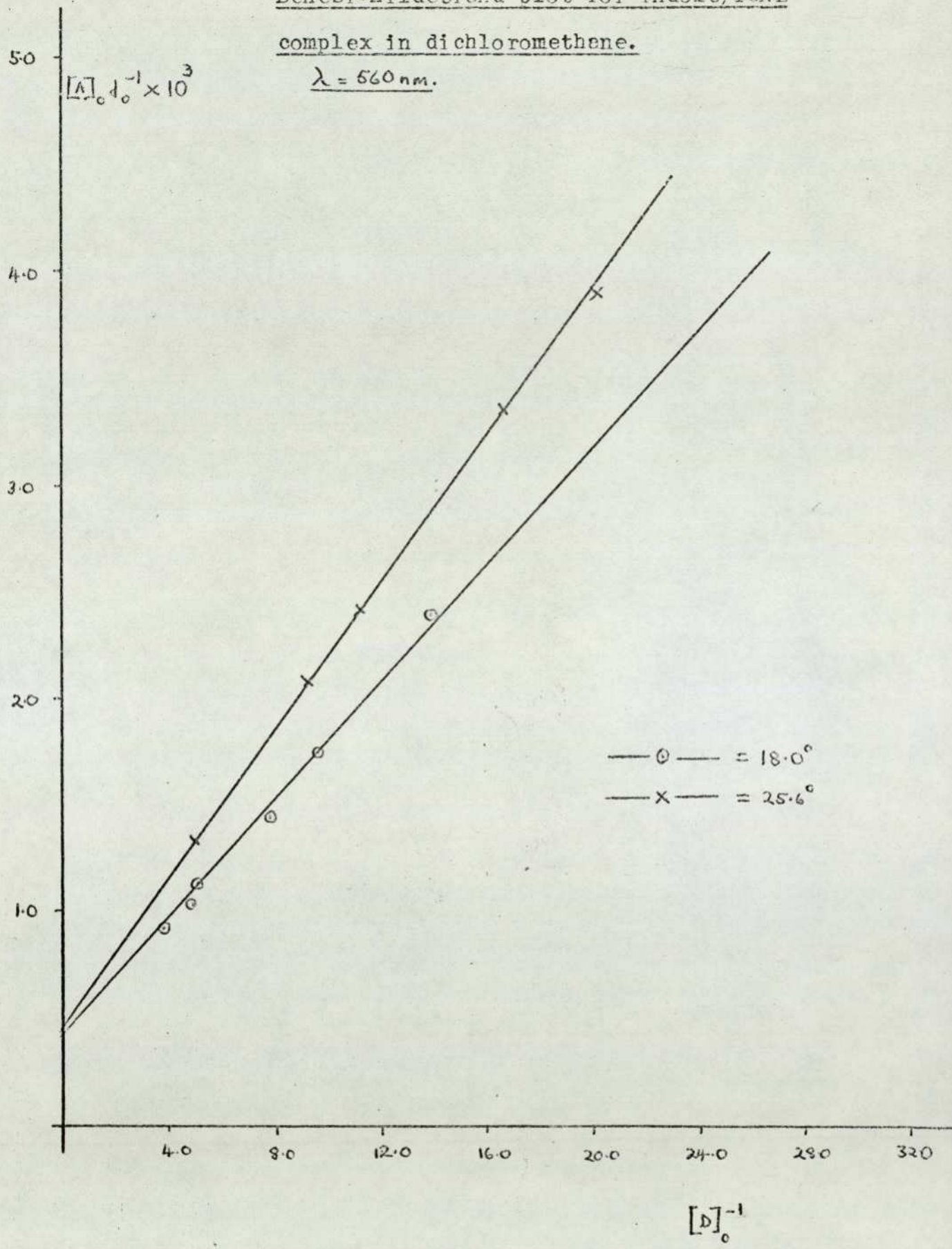
Temp (°C)	K (l mol^{-1})	Kε	ε
15.0	3.34	7782	2330[a]
25.0	2.78	6033	2170[a]
21.6	3.02	6855	2270[b]
18.0	3.29	7633	2320
25.5	2.64	5676	2150

a - Ref. 82, b - Ref. 79.

Figure 9 - 1.

Benesi-Hildebrand plot for indole/TCNE complex in dichloromethane.

λ = 560 nm.



The results obtained compare favourably with those previously published. K and ε were also determined using equimolar concentrations of reactants, (employing the method described in Section 4 - 4 - 1 - 1).

Table 9 - 7. Equimolar Data for Indole (D)/TCNE (A) at 265 nm in Dichloromethane. T = 25.5°C.

$[A]_o \times 10^2$ (M)	d_o	$[A]_o d_o^{-1} \times 10^2$	$d_o^{-\frac{1}{2}}$
0.71	0.311	2.29	1.79
0.90	0.448	2.01	1.49
1.01	0.565	1.77	1.33
1.11	0.698	1.59	1.19
1.29	0.925	1.40	1.04
1.50	1.281	1.17	0.88
2.01	2.194	0.91	0.67

A plot of $[A]_o d_o^{-1}$ against $d_o^{-\frac{1}{2}}$ gave a straight line with a very small intercept (about 0.0004) (see Fig. 9 - 2). $K\varepsilon$ was accurately measured from the slope and compared with that obtained using the Benesi-Hildebrand method.

Table 9 - 10. Comparison of K and ε values at 25.5°C.

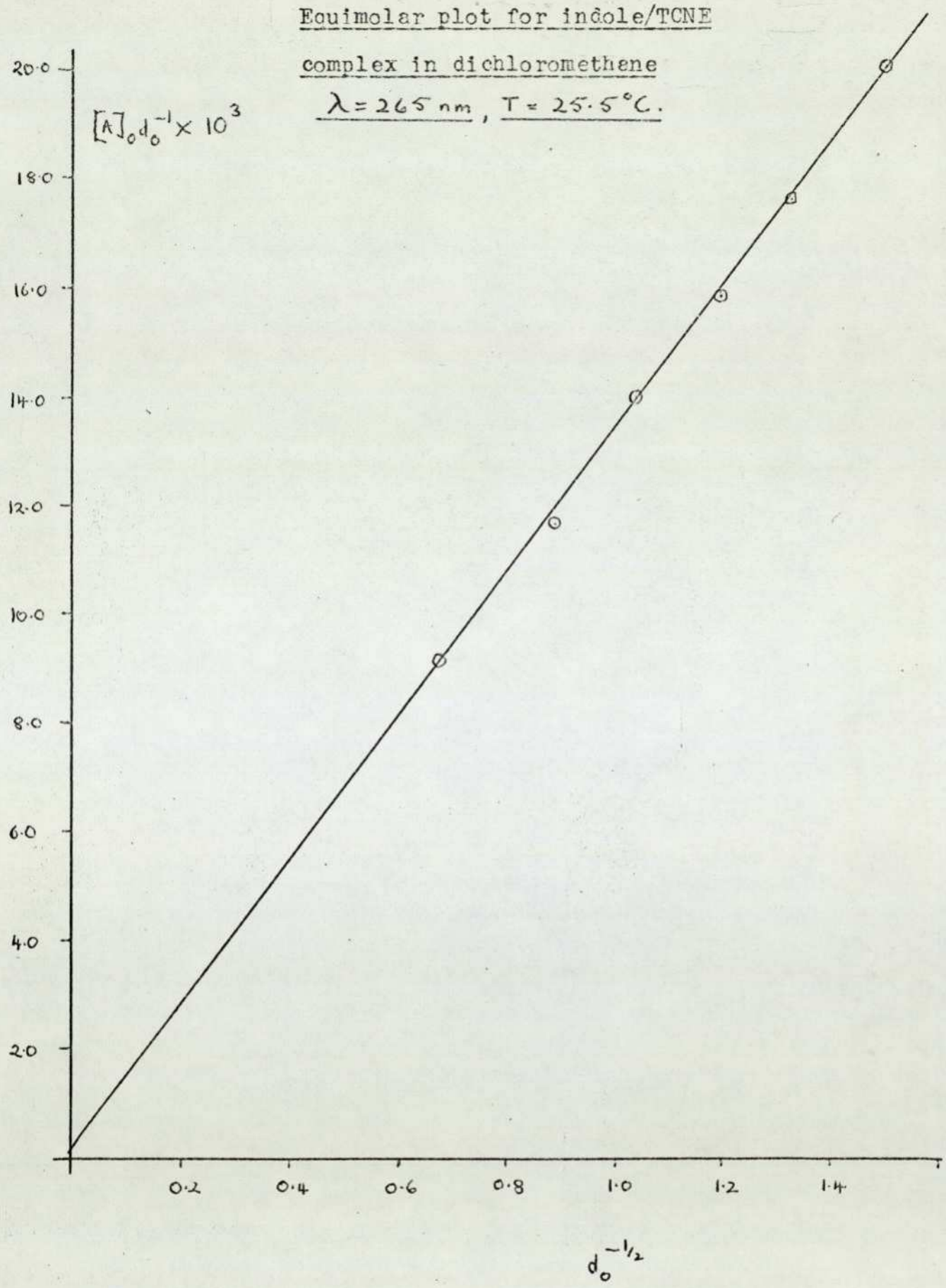
ε	$K\varepsilon$	K (1 mol^{-1})	method.
2150	5676	2.64	B-H
about 2500	5837	2.35	Equimolar.
2150	5837	2.71	Equimolar.

Allowing for some uncertainty in the intercept and hence ε, the two results are shown to compare favourably. The Van't Hoff equation was applied to the results obtained at the two temperatures 18.0° and 25.5°C to give the following values of enthalpy and entropy

Figure 9 - ?

Equimolar plot for indole/TCNE complex in dichloromethane

$\lambda = 265$ nm, $T = 25.5$°C.



of complex formation.

ΔH = -5.08 kcal mol^{-1} (-21.25 kjoule mol^{-1}) ΔS = -13.0 (e.u)

As a comparison, the Benesi-Hildebrand method was also applied to this reaction using 1,2-dichloroethane as solvent. One set of results was obtained at 25.0°C.

Table 9 - 11. Benesi-Hildebrand Data for Indole (D)/TCNE (A) at 560 nm in 1,2-Dichloroethane. T = 25.0°C. $[A]_o$ = 7.65×10^{-4} M.

$[D]_o$ (M)	$[D]_o^{-1}$	d_o	$[A]_o . d_o^{-1} \times 10^3$
0.102	9.80	0.249	2.56
0.199	5.02	0.421	1.51
0.251	3.99	0.488	1.31
0.301	3.32	0.562	1.13
0.397	2.52	0.664	0.96

From the graph of $[A]_o d_o^{-1}$ against $[D]_o^{-1}$, ε = 2,500, K = 1.80 l mol^{-1}
Thus it would appear that K values in this solvent are slightly lower at a given temperature than those in dichloromethane.

9 - 5 - 2. Determination of Rate Constants.

Rate constants for the reaction between indole and TCNE were obtained in the usual manner by examining the decrease in absorption at 560 nm using initially a large excess of indole in reaction mixtures. Plots of log d_t against time were drawn, to evaluate k_1 and k_2. For this particular reaction it was noticed that the absorption at 560 nm decayed over a period of time to a small finite value (about 0.02), while the absorbance due to product (λ_{max} 455 nm) slowly increased over a period of several hours after the charge-transfer complex band had disappeared. It was assumed that there was 100% conversion of charge-transfer complex to the colourless intermediate, which in turn formed the product at a much slower rate.

The following results were obtained at 24.4°C.

Table 9 - 12. Rate Constants $k_1(s^{-1})$, $k_2(1\ mol^{-1}\ s^{-1})$ for Indole (D)/TCNE (A) in Dichloromethane at 560 nm. $[A]_o = 5.17 \times 10^{-4}$ M.

$[D]_o$ (M)	$k_1 \times 10^4$	$k_2 \times 10^3$
0.102	1.33	1.30
0.126	1.76	1.40
0.158	2.47	1.56
0.201	3.46	1.72
0.250	4.50	2.24

Values of k_2 were also obtained at other temperatures but further kinetic runs using old samples of indole gave very high values for k_2 (about 3×10^{-3} 1 mol^{-1} s^{-1}). When the solvent was carefully purged beforehand with nitrogen, the following rate constants were obtained.

Table 9 - 13. Rate Constants as for before, Solvent flushed with Nitrogen, T = 18.5° C

$[D]_o$ (M)	$[A]_o \times 10^4$ (M)	$k_2 \times 10^3$
0.106	10.20	0.252
0.129	7.01	0.644
0.204	7.07	0.725
0.207	10.10	0.774
0.255	7.01	0.547

Since these rate constants appeared much lower than those obtained previously at the same temperature and same range of donor concentration, it appeared that the reaction was sensitive to either light, oxygen, traces of acid or base or other impurities.

Repeated attempts to obtain results consistent with those of Foster and Hanson[82] were unsuccessful and it appeared that those high results

obtained by Gerrard [79] were also affected by the presence of same catalytic impurity.

Table 9 - 14. Previously Determined [82] Rate Constants k_2(l mol^{-1} s^{-1}) for Indole (D)/TCNE (A) at 560 nm in Dichloromethane. T = 25.0°C.

$[D]_o$ (M)	$[A]_o \times 10^4$ (M)	$k_2 \times 10^4$
0.474	4.57	1.41
0.655	7.67	1.82
0.703	4.57	1.86
0.923	4.57	2.27

Attempts were made to determine the final rate constant, k_f, for the formation of adduct from intermediate by examining the increase in absorption at 455 nm. Previous results obtained [82] were based on the rate equation:

$$dx/dt = k_f [\text{intermediate}]_t [\text{indole}] \qquad (9 - 1)$$

x is the concentration of final product. If there has been total conversion of charge-transfer complex to intermediate then $[A]_o = [\text{intermediate}]$ when there is a large excess of indole. The initial slow rate of formation of the final product may be given by:

$$k_f = (dx/dt) \; / \; [A]_o [D]_o \qquad (9 - 2)$$

The concentration of product was calculated from the optical density reading and the known extinction coefficient (section 9 - 3 - 3).

Table 9 - 15. Rate Constants k_f(l mol^{-1} s^{-1}) for Formation of 3-Tricyanovinyl Indole in Dichloromethane. $\lambda = 455$nm.

$[D]_o$ (M)	T (°C)	$k_f \times 10^6$
0.202	26.0	3.52
0.198	26.0	2.11
0.250	26.0	1.15
0.930	25.0	0.30*
1.00	25.0	0.29*

* - Ref. 82

Similarly, these rate constants are not consistent and are much larger than those obtained previously.

It was not possible to obtain rate constants for equimolar concentrations of reactants as the decrease in absorbance was too slow for accurate measurement.

9 - 6. Ultraviolet Spectroscopy.

For equimolar concentrations of reactants in dichloromethane (0.007 to 0.04M) it was noticed that there was a broad shoulder band to the absorption due to indole, centred at λ_{max} 323 nm. When indole and TCNE were examined separately at these concentrations, there was no such band at this wavelength in their separate UV spectra. The absorption at 323 nm formed immediately on mixing and decreased very slowly with time and might thus be attributed to a charge-transfer or other complex formed in reaction, which was investigated in the usual way for equimolar concentrations by obtaining d_o values at different concentrations. The optical density values were corrected for small absorptions due to indole and TCNE at this point.

Values of K and ε were derived using the method described in section 4 - 4 - 1 - 1. The following measurements were made at different equimolar concentrations, d_o^{corr} is the initial optical density due solely to the observed band at 323 nm.

Table 9 - 16. Equimolar Data for Indole (D)/TCNE (A) - UV Band.

$T = 25.5^oC$

$[A]_o$ (M)	d_o^{corr}	$[A]_o d_o^{-1}$	$d_o^{-\frac{1}{2}}$
0.0071	0.154	0.0454	2.55
0.0085	0.206	0.0412	2.20
0.0101	0.271	0.0372	1.92
0.0150	0.550	0.0273	1.35

Table 9 - 16. Continued.

$[A]_o$ (M)	d_o^{corr}	$[A]_o d_o^{-1}$	$d_o^{-\frac{1}{2}}$
0.0201	0.886	0.0226	1.06
0.0252	1.413	0.0177	0.84
0.0301	1.857	0.0162	0.73
0.0330	2.236	0.0148	0.67
0.0350	2.405	0.0145	0.64

A plot of $[A]_o d_o^{-1}$ against $d_o^{-\frac{1}{2}}$ gave a straight line giving a small intercept and curvature at higher values of $d_o^{-\frac{1}{2}}$ (see Fig. 9 - 3). From this: $\varepsilon = 520$, $K = 4.85$. These results could indicate either that the band was due to some other complex in equilibrium with the charge-transfer complex since it appeared immediately on mixing the reactants, or that it was a second band of the charge-transfer complex and the value of K obtained above (4.85) was erroneous, compared with that obtained (2.64) in the visible region at the same temperature. However, on examining a double equilibrium such as:

$$A + D \underset{}{\overset{K_1}{\rightleftharpoons}} AD^* \overset{K_2}{\rightleftharpoons} AD^{\ddagger} \qquad (9 - 3)$$

When $[D]_o \simeq [D]$ and is in large excess, the equilibrium constants K_1 and K_2 are given by:

$$K_1 = [AD^*] / ([A]_o - [AD^*] - [AD\ddagger])([D]) \qquad (9 - 4)$$

$$K_2 = [AD\ddagger] / [AD^*] \qquad (9 - 5)$$

Substitution of (9 - 5) into (9 - 4) and rearrangement gives:

$$K_1 [D] [A]_o - K_1 [D] [AD^*] (1 + K_2) = [AD^*] \qquad (9 - 6)$$

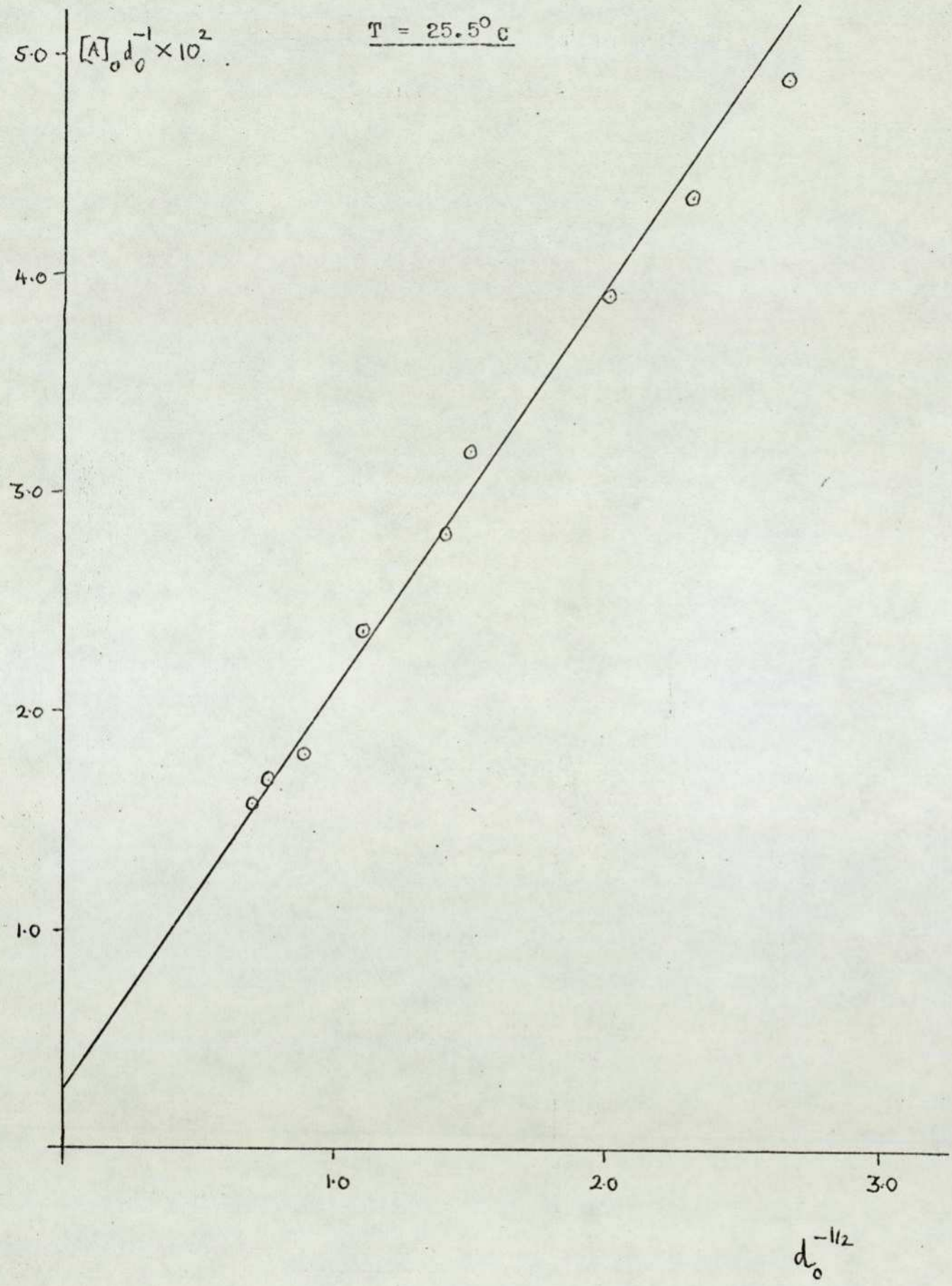
For 1 cm cells $[AD^*] = d/\varepsilon$ giving:

$$[A]_o - (1 + K_2) d/\varepsilon = d/K_1 [D] \varepsilon \qquad (9 - 7)$$

Figure 9 - 3.

Equimolar plot for indole/TCNE in dichloromethane at 323nm.

T = 25.5° C



and

$$[A]_o/d_o - (1 + K_2)/\varepsilon = 1/K_1 [D]\varepsilon \qquad (9 - 8)$$

Thus a plot of $[A]_o d_o^{-1}$ against $1/[D]_o$ will give intercept of $(1 + K_2)/\varepsilon$ and slope of $1/K_1\varepsilon$.

In section 9 - 5 - 1, values of K and ε were obtained using the same plot and (intercept)/(slope) = K.

If the above double equilibrium does occur then the equilibrium constants at 25.5° will be given by: $K_1 + K_1 K_2 = K = 2.64$, since (intercept)/(slope) for equation (9 - 8) gives the value $K_1 + K_1 K_2$.

A similar procedure may be applied to the double equilibrium using equimolar concentrations of reactants. In this case:

$$K_1 = ([AD^{\ddagger}]/K_2) / ([A]_o - [AD^{\ddagger}](1 + 1/K_2))^2 \qquad (9 - 9)$$

If here $$[AD^{\ddagger}] = d/\varepsilon \qquad (9 - 10)$$

A similar procedure will give:

$$[A]_o/d_o - (K_2 + 1)/K_2\varepsilon = 1/\sqrt{d_o K_1 K_2}\,\varepsilon \qquad (9 - 11)$$

In this case $(\text{intercept})/(\text{slope})^2 = K_1 + K_1 K_2$.

If the values obtained using the equimolar plot in the UV spectrum are inserted, it is seen that:

$$(\text{intercept})/(\text{slope})^2 = K_1 + K_1 K_2 = K = 4.85 \text{ (at } 25.5^{\circ}\text{C)}.$$

Thus agreement between the two values of $K_1 + K_1 K_2$ is not reached and it is likely that the latter value is in error. This method also shows that it is not possible to determine whether the band in the UV is due to the charge-transfer complex or a further complex. The reaction scheme given by (9 - 12)

$$A + D \underset{}{\overset{K_1}{\rightleftharpoons}} AD^{*} \qquad A + D \underset{}{\overset{K_2}{\rightleftharpoons}} AD^{\ddagger} \qquad (9 - 12)$$

also gives results which show that the K values derived by the Benesi-Hildebrand method in the visible region and by the equimolar

method in the UV region should give the same values of K, where:

$$K = K_1 + K_2 \qquad (9 - 13)$$

Since it is unlikely that the charge-transfer complex gives two bands in the spectrum widely separated from each other, that band in the UV (λ_{max} 323 nm) may be attributed to a second complex, possibly a σ-complex, which is formed in equilibrium with the charge-transfer complex. The larger value of K obtained and the curvature in the graph may be due to errors in measuring optical densities accurately when corrections are needed for indole and TCNE which absorb in this region.

9 - 7. Discussion.

Indole and TCNE react together in dichloromethane to form an unstable compound which decomposes to 3-tricyanovinyl indole. On the basis of the IR spectrum and the acid conditions used to form this compound, it is likely to be tetracyanoethyl indole.

When the reactants are mixed together a blue colour, attributed to a charge-transfer complex, appears immediately. Previous work indicated that the complex may react with a molecule of donor to form the intermediate or σ-complex. Since values of k_2 increased with donor concentration and could be fitted into scheme (1 - 23), a plot of $k_2 (1 + K [D])$ against $K [D]$ gave a straight line, but a negative intercept with the y-axis was observed.[82]

In the present work it was unfortunately not possible to obtain consistent rate constants, k_2, with change in donor concentration. The band in the UV might be due to a second complex in equilibrium with the charge-transfer complex. If the scheme (9 - 14) is adopted

$$A + D \rightleftharpoons AD^{*} \rightleftharpoons AD^{\ddagger} \xrightarrow[+D]{} AD \text{ (intermediate)} + D \qquad (9 - 14)$$

Then: $k_2 = k_c K_1 [D] / (1 + (K_1 + K_1 K_2) [D])$ (9 - 15)

A plot of $k_2 (1 + (K_1 + K_1 K_2) [D])$ against $[D]$ should give a straight line going through the origin.

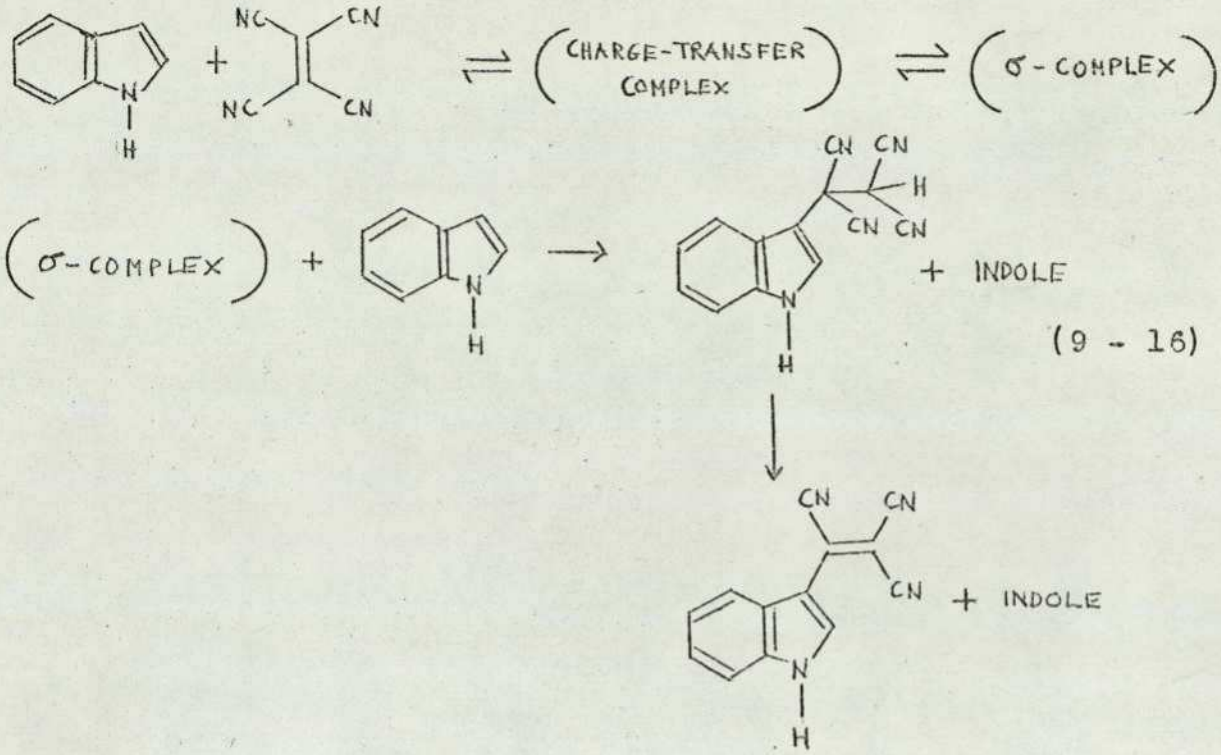
Since it has been shown that $K = K_1 + K_1 K_2$ for the case where a double equilibrium is treated as a single system, the values for the y-axis for both the plots for schemes (1-23) and (9 - 15) are identical.

A double equilibrium does not therefore show an intercept on the graphical plots, which must be due either to experimental errors or deviations from linearity at low donor concentrations.

It is likely that there are two complexes formed in a double equilibrium with reactants, the second complex being a σ-complex. The $k_{\pm}$ values derived from both Benesi-Hildebrand and equimolar methods are comparable and indicate that there is no termolecular species formed in any significant amount.

The reaction is clearly catalysed by both indole itself and by more effective bases such as pyridine. Donor molecules should thus enter into both stages, namely the decomposition of complexes to the intermediate, and the decomposition of the intermediate to the final product. Previous work [82] established that in the latter step, there was a first order dependence on indole, and in the former step there was no reversibility.

The above evidence indicates that the most likely reaction is as shown in (9 - 16) where the σ-complex, in equilibrium with the charge-transfer complex, is a direct intermediate in the reaction, as shown over the page.


NC
CN
NC
CN
⇌ (CHARGE-TRANSFER COMPLEX) ⇌ (σ-COMPLEX)
(σ-COMPLEX) +
CN CN
H
CN CN
+ INDOLE
CN CN
CN
+ INDOLE

(9 - 16)

Acknowledgments

The author would like to express his thanks to the Science Research Council for pro viding a grant and to the City University for providing research facilities. In particular, the author would like to thank Dr. S. Garbutt for his continued interest and advice, [redacted] for help with preparation of the N.M.R samples and [redacted] and [redacted] for assistance in interpreting the N.M.R. spectra.

The author would also like to thank [redacted] for the typing.

References

1. T.S. Moore, F. Shepherd & E. Goodall, J. Chem. Soc., 1447 (1931).
2. G. Briegleb, "Zwischenmolekularekrafte und Molekulstruktur", F. Enke, Stuttgart (1937).
3. J. Weiss, J. Chem. Soc., 245 (1942).
4. W. Brackmann, Rec. Trav. Chim., 68, 147 (1949).
5. R.S.Mulliken, J. Amer. Chem. Soc., 74, 811 (1952).
6. R.S.Mulliken, J. Phys. Chem., 56, 801 (1952).
7. R.S.Mulliken, J. Chim. Phys., 61, 20, (1964).
8. F.M.Kosower, Progr. Phys. Org. Chem., 3, 83 (1965).
9. M.J.S. Dewar & A.R. Lepley, J. Amer. Chem. Soc., 83, 4560 (1961).
10. M.J.S. Dewar & H. Rogers, J. Amer. Chem. Soc., 84, 395 (1962).
11. R.S.Mulliken& W.B.Person, Molecular Complexes: A lecture and reprint Volume, Wiley-Interscience. New York, (1969).
12. E.F.Caldin, D. O'Donnell, D. Smith & J.E.Crooks, Chem. Comm., 1358 (1971).
13. R. Foster, 'Organic Charge-Transfer Complexes', Academic Press, London (1969).
14. L.E. Orgel, J. Chem. Phys., 23, 1352 (1955).
15. A.R. Lepley, Tetrahedron Letters, 2823 (1964).
16. H. Kuroda & I. Ikemoto, Bull.Chem.Soc. Japan, 39, 1842 (1966).
17. J.R. Gott & W.G. Maisch, J. Chem. Phys., 39, 2229 (1963).
18. K.M.C. Davis & M.E.Peover, Trans. Faraday Soc., 61, 1516 (1965).
19. M.E.Peover, Trans. Faraday Soc., 60, 479 (1964).
20. M.E.Peover, Trans. Faraday Soc., 58, 2370 (1962).
21. H.M.McConnell, J.S.Ham & J.R.Platt, J.Chem.Phys., 21, 66 (1953).
22. S.H. Hastings, J. Amer. Chem. Soc., 75, 2900 (1953).
23. G. Briegleb & J. Czekalla, Z. Elektrochem., 63, 6 (1959).
24. J. Czekalla, Z. Phys. Chem. 27, 185 (1961).

25. R.S.Mulliken &W.B. Person, Ann. Rev. Phys. Chem., 13, 107 (1962).

26. A.R. Lepley, J. Amer. Chem. Soc., 84, 3577 (1962).

27. A.R. Lepley, J. Amer. Chem. Soc., 86, 2545 (1964).

28. A.R. Lepley & C.C. Thompson Jr., J. Amer. Chem. Soc., 89, 5523 (1967).

29. M.W.Hanna & J.L.Lippert'Molecular Complexes', Volume 1, p . 1, Elek Science, London (1973).

30. C.C. Thompson Jr. & P.A.D.de Maine, Phys. Chem., 69, 2766 (1965).

31. P.H.Emslie,R. Foster, C.A.Fyfe, I. Horman, Tetrahedron, 21, 2843 (1965).

32. D.F. Evans, J. Chem. Phys., 23, 1424, 1426 (1955).

33. D.F. Evans, J. Chem. Soc., 4229 (1957).

34. R.S.Mulliken,Rec. Trav. Chim., 75, 845 (1956).

35. L.E.Orgel & ~~W.B.Person~~ R.S. Mulliken, J. Amer. Chem. Soc., 79, 4839 (1957).

36. S. Carter, J.N.Murrell E.J.Rosch,J. Chem. Soc., 2048 (1965).

37. H.B.Friedrich & W.B.Person,J. Chem. Phys., 44, 2161 (1966).

38. M.W.Hanna& D.E.Williams,J. Amer. Chem. Soc., 90, 5358 (1968).

39. J.A. Pople, W. Schneider & H.J.Bernstein,'High Resolution N.M.R.' McGraw-Hill, New York, Toronto and London, 222 (1959).

40. R. Foster & C.A.Fyfe,Trans. Faraday Soc., 61, 1626 (1965).

41. R. Foster & C.A.Fyfe,J. Chem. Soc.(B), 926 (1966).

42. R. Foster & C.A.Fyfe,Biochim. Biophys. Acta, 112, 490 (1966).

43. M.W.Hanna & P.J. Berkeley Jr., J. Phys. Chem. 67, 846 (1963).

44. P.J.Trotter& M W.Hanna,J. Amer. Chem. Soc., 88, 3724 (1966).

45. N.M.Brown,R. Foster & C.A. Fyfe, J. Chem. Soc.(B), 406 (1967).

46. A. Saika & C. Slichter, J. Chem. Phys., 22, 26 (1954).

47. H.A.Benesi & J.H.Hildebrand,J. Amer. Chem. Soc., 71, 2703 (1949).

48. R.L. Scott, Rec. Trav. chim., 75, 787 (1956).

49. R. Foster, D.Ll.Hammick & A.A.Wardley,J.Chem. Soc., 3817 (1953).

50. J.A.A.Ketelaar,Rec. Trav. Chim., 71, 1104 (1952).

51. C.P.Nash,J. Phys. Chem., 64, 950 (1960).

52. R. Foster, Nature, London 173, 222 (1954).

53. J.M.Corkill,R.Foster & D.Ll.Hammick,J. Chem. Soc., 1202 (1955).

54. P.A.D.de Maine,Spectrochim. Acta, 12, 1051 (1959).

55. S.D. Ross & M.M. Labes, J. Amer. Chem. Soc., 79, 76 (1957).

56. R. Foster & C.A.Fyfe,Chem. Comm., 642 (1965).

57. M.I.Foreman &R. Foster, J.Chem.Soc(B),885 (1969).

58. M.I.Foreman,R. Foster & D.R.Twiselton,Chem. Comm., 1318 (1969).

59. M.E. Peover, Proc. Chem. Soc., 167 (1963).

60. M.E. Peover, Trans. Faraday Soc., 60, 417 (1964).

61. R.D. Holm, W.R. Carper & J.A.Blanchet,J. Phys. Chem. 71, 3960, (1967).

62. T.F.Bolles &R.S.Drago,J. Amer. Chem. Soc., 88, 3921 (1966).

63. T.F.Bolles &R.S.Drago,J. Amer. Chem. Soc., 87, 5015 (1965).

64. T. D.Epley & R.S.Drago,J.Amer. Chem. Soc., 89, 5770, (1967).

65. A.V. Few&J.W.Smith,J. Chem. Soc., 2781 (1949).

66. R.J. Bishop & L.E.Sutton,A.R.Katritzky,J. Chem. Soc(B)., 493 (1967)

67. A.S. Bailey & J.M. Evans, J. Chem. Soc. (C), 2105 (1967).

68. P.R. Hammond, J. Chem. Soc., 479 (1964).

69. K. Conrow, G.D. Johnson & R.E. Bowen, J. Amer. Chem. Soc., 86, 1025 (1964).

70. W.B. Person, J. Amer. Chem. Soc., 87, 167 (1965).

71. D.F. Rosseinsky & H. Kellawi, J. Chem. Soc. (A), 1207 (1969).

72. J. Homer, C.J. Jackson, P.M. Whitney & M.H Everdell,Chem. Comm., 956 (1971).

73. D.A. Deranleau, J. Amer. Chem. Soc., 91, 4050 (1969).

74. S. Carter, J. Chem. Soc.(A), 404 (1968).

75. K.M.C. Davies & M.F. Farmer, J. Chem. Soc.(B) 28, (1967).

76. R. Foster & I. Horman, J. Chem. Soc.(B) 171 (1966).

77. G.D. Johnson & R.E. Bowen, J. Amer. Chem. Soc., 87, 1655 (1965).

78. R. Foster & I.B. Matheson, Spectrochim. Acta, 23A, 2037 (1967).

79. D.L. Gerrard, Ph.D. Thesis, The City University, London (1970).

80. Z. Rappoport, J. Chem. Soc., 4498 (1963).

81. Z. Rappoport & A. Horowitz, J. Chem. Soc., 1348 (1964).

82. R. Foster & P. Hanson, Tetrahedron, 21, 255 (1965).

83. S. Garbutt & D.L.Gerrard, J. Chem. Soc., Perkin II, 782 (1972).

84. N.S. Isaacs, J. Chem. Soc.(B), 1053 (1966).

85. Z. Rappoport & E. Shohamy, J. Chem. Soc.(B), 77 (1969).

86. E. Kosower, Progr. Phys. Org. Chem., 3, 83 (1965).

87. P.G. Farrell, J. Newton &R.F. White, J. Chem. Soc., ~~1348~~ 637 (1967).

88. P.G. Farrell & R.F. Wojtowski, J. Chem. Soc.(C), 1390 (1970).

89. P.G. Farrell & J. Newton, J. Chem. Soc.(B), 1630 (1970).

90. P.G. Farrell & P.N. Ngo, J. Chem. Soc., Perkin II, 974 (1973).

91. C.C. Thompson & D.D. Holder, J. Chem. Soc., Perkin II, 257 (1972).

92. R. Foster & I. Horman, J. Chem. Soc.(B), 1049 (1966).

93. J.W.Eastman,G. Engelsma & M.Calvin,J.Amer.Chem.Soc., 84, 1339(1962).

94. L.P.Ellinger, Chem. and Ind., 1982 (1963).

95. J.A. Barltrop & R. Robson, Tetrahedron Letters, 597 (1963).

96. W.M. Hardham & G.S. Hammond, J. Amer. Chem. Soc., 89, 3200 (1967).

97. I. Isenberg & A. Szent-Györgyi, Proc. Nat. Acad. Sci. U.S.A., 46, 1307 (1960).

98. I. Isenberg & A. Szent-Györgyi, Proc. Nat. Acad. Sci. U.S.A., 44, 857 (1958).

99. I. Isenberg & A. Szent-Györgyi, Proc. Nat. Acad. Sci. U.S.A., 47, 945 (1961).

100. G.H. Moxon & M.A. Slifkin, J. Chem. Soc., Perkin II, 1159(1972).

101. M.A. Slifkin, 'Charge-Transfer Interactions in Biomolecules', Academic Press, London, 1971.

102. R.B. Woodward & R. Hoffmann, J. Amer. Chem. Soc., 87, 4388 (1965).

103. R.B. Woodward & R. Hoffmann, J. Amer. Chem. Soc., 87, 2046 (1965).

104. R.B. Woodward & R. Hoffmann, 'The Conservation of Orbital Symmetry', Academic Press, New York, 1970.

105. M.J.S. Dewar, Angew. Chem. Internat. Edn., 11, 761 (1971).

106. K. Fukui, Bull. Chem. Soc. Japan 39, 498 (1966).

107. M.J.S. Dewar, Adv. Chem. Phys., 8, 65 (1965).

108. M.J.S. Dewar, Chem. Soc. Special Publ., 21, 177 (1967).

109. W.C. Herndon, Chem. Rev., 72, 157 (1972).

110. S. Seltzer, Adv. Alicyclic Chem., 2, 1 (1968).

111. A.S. Onishchenko, 'Diene Synthesis', Translated by I. Progrem, Oldbourne Press, London (1964).

112. M.C. Kloetzel, Org. Reactions, 4, 1 (1948).

113. J.G. Martin & R.K. Hill, Chem. Rev., 61, 537 (1961).

114. S.B. Needleman & M.C. Chang-Kuo, Chem. Rev., 61, 405 (1961).

115. J. Sauer, Angew. Chem. Internat. Edn., 6, 17 (1967).

116. K. Alder & G. Stein, Angew. Chem., 50, 510 (1937).

117. A. Wassermann, J. Chem. Soc. (London) 1511 (1935).

118. M.J.S. Dewar & R.Scott Pyron, J. Amer. Chem. Soc., 92, 3098 (1970).

119. P. Haberfield & A.K. Ray, J. Org. Chem., 37, 3093 (1972).

120. R.B. Woodward, J. Amer. Chem. Soc., 64, 3058 (1942).

121. B.J. King, Ph.D. Thesis, The City University, London (1969).

122. W.C. Solomon, Ph.D. Thesis, University of Oregon (1963).

123. P. Brown & R.C. Cookson, Tetrahedron, 21, 1993 (1965).

124. L.J. Andrews & R.M. Keefer, J. Amer. Chem. Soc., 77, 6284 (1955).

125. A.T. Blomquist & Y.C. Meinwald, J. Amer. Chem. Soc., 81, 667 (1959).

126. H.K. Hall, J. Org. Chem., 25, 42 (1960).

127. J.A. Berson & S.S. Olin, J. Amer. Chem. Soc., 91, 777 (1969).

128. J.K. Williams & R.E.Benson,J. Amer. Chem. Soc., 84, 1257 (1962).

129. C.D. Smith, J. Amer. Chem. Soc., 88, 4273 (1966).

130. K. Kraft & G. Koltzenburg, Tetrahedron Letters, 4357, 4723 (1967).

131. R. Wheland & P.D. Bartlett, J. Amer. Chem. Soc., 92, 3822 (1970).

132. L.K.Montgomery,K. Schueller & P.D. Bartlett, J. Amer. Chem. Soc., 86, 616, 622 (1964).

133. P.D. Bartlett, Science, 159, 833 (1968).

134. J.D. Roberts & C.M. Sharts, Org. Reactions, 12, 1 (1962).

135. P.D. Bartlett, J. Amer. Chem. Soc., 90, 2049 (1968).

136. P.D. Bartlett, Quart. Rev., 24, 473 (1970).

137. R. Huisgen, Angew. Chem. Internat. Ed., 3, 753 (1964).

138. R. Huisgen & P. Otto, Tetrahedron Letters, 4491 (1968).

139. N.S. Isaacs & P. Stanbury, J. Chem. Soc., Perkin II, 167 (1973).

140. J.K. Williams,D.W.Wiley & B.C.McCusick,J. Amer.Chem. Soc ., 84, 2212 (1962).

141. L. Schmerling, J.P. Luvisi & R.W. Welch, J. Amer. Chem. Soc., 78, 2819 (1956).

142. C.F. Wilcox, S. Winstein & W.G. McMillan, J. Amer. Chem. Soc., 82, 5450 (1960).

143. R.P. Hermann, J. Org. Chem., 27, 441 (1962).

144. E.F. Ullman, Chem. and Ind., 1173 (1958).

145. R.C. Cookson, J. Dance & J. Hudec, J. Chem. Soc., 5416 (1964).

146. P. Brown & R.C. Cookson, Tetrahedron, 21, 1977 (1965).

147. P.D. Bartlett, G.E.H. Wallbillich & L.K. Montgomery, J. Org. Chem., 32, 1290 (1967).

148. E.E. Van Tamelen & S.S. Pappas, J. Amer. Chem. Soc., 84, 3789 (1962).

149. W. Schäfer, Angew. Chem. Internat. Ed., 5, 669 (1966).

150. M.J. Cardillo & S.H. Bauer, J. Amer. Chem. Soc., 92, 2399 (1970).

151. J.F.M. Oth, Angew. Chem. Internat. Ed., 7, 646 (1968).

152. W. Schäfer & H. Hellmann, Angew. Chem. Internat. Ed., 6, 518 (1967).

153. L.A. Paquette & G.R. Krow, J. Amer. Chem. Soc., 90, 7147 (1968).

154. L.A. Paquette, J. Amer. Chem. Soc., 94, 529 (1972).

155. C.M. Atkins Jr. & E.M. Burgess, J. Amer. Chem. Soc., 90, 4744 (1968).

156. D.M. Lemal & J.P. Lokensgard, J. Amer. Chem. Soc., 88, 5934 (1966).

157. T.L. Cairns, R.A. Carboni, D.D. Coffman, V.A. Englehardt, R.E. Heckert, E.L. Little, E.G. McGeer, B.C. McKusick, W.J. Middleton, J. Amer. Chem. Soc., 79, 2340 (1957).

158. T.L. Cairns, R.A. Carboni, D.D. Coffman, V.A. Englehardt, R.E. Heckert, E.L. Little, E.G. McGeer, B.C. McKusick, W.J. Middleton, R.M. Scribner, C.W. Theobald, H.E. Winberg, J. Amer. Chem. Soc., 80, 2775 (1958).

159. W.J. Middleton, R.E. Heckert, E.L. Little & C.G. Krespan, J. Amer. Chem. Soc., 80, 2783 (1958).

160. J. Sauer, Angew. Chem., 73, 545 (1961).

161. B.C. McKusick, R.E. Heckert, T.L. Cairns, D.D. Coffman & H.F. Mower, J. Amer. Chem. Soc., 80, 2806 (1958).

162. J.K. Williams, D. Wiley & B.C. McKusick, J. Amer. Chem. Soc., 84, 2210 (1962).

163. R.E. Merrifield & W.D. Phillips, J. Amer. Chem. Soc., 80, 2778 (1958).

164. B.C. McKusick & G.F. Biehn, Chem. Eng. News, 38, 114 (1960).

165. N.G.S. Champion, R. Foster & R.K.Mackie, J.Chem.Soc., 5060 (1961).

166. D.N. Dhar, Chem. Rev., 611 (1967).

167. V. Royston, Phys. Rev., 96, 543 (1954).

168. W.A.Anderson, Phys. Rev., 102, 151 (1956).

169. J.D. Baldeschwieler & E.W. Randall, Chem. Rev., 63, 81 (1963).

170. A.L. Bloom & J.N. Shoolery, Phys. Rev., 97, 1261 (1955).

171. M. Barfield & J.D. Baldeschwieler, J. Chem. Phys., 41, 2633 (1964).

172. M. Shimizu & H. Shimizu, J. Chem. Phys., 41, 2329 (1964).

173. W.A. Anderson & R. Freeman, J. Chem. Phys., 37, 85 (1962).

174. J.D. Roberts, Angew. Chem. Internat. Ed., 2, 53 (1963).

175. W. von Philipsborn, Angew. Chem. Internat. Ed., 10, 472 (1971).

176. A. Saupe, Angew. Chem. Internat. Ed., 7, 97 (1968).

177. D.W. Turner, J. Chem. Soc., 847 (1962).

178. M. Karplus, J. Chem. Phys., 30, 11 (1959).

179. R.J. Abraham, L.D. Hall, L. Hough & K.A. McLauchlan, J. Chem. Soc., 3699 (1962).

180. M. Karplus, J. Amer. Chem. Soc., 85, 2870 (1963).

181. M. Barfield & D.M. Grant, Adv. Magn. Resonance, 1, 23, Academic Press Inc., New York (1965).

183. J.S. Waugh & F.W.Dobbs , J. Chem. Phys., 31, 1235 (1959).

184. R.J. Abraham & K.G.R. Pachler, Mol. Phys., 7, 165 (1964).

185. E.W. Garbisch, J. Amer. Chem. Soc., 86, 5561 (1964).

186. E.W. Garbisch, J. Amer. Chem. Soc., 87, 505 (1965).

187. L.M. Jackman & S. Sternhell, 'Applications of N.M.R. Spectroscopy in Organic Chemistry', Pergamon Press, Oxford, (1969).

188. S. Sternhell, Quart. Rev., 23, 236 (1969).

189. G.E. Maciel, J.W. McIver Jr., N.S. Ostlund & J.A. Pople, J. Amer. Chem. Soc., 92, 4497 (1970).

190. K.N. Slessor & A.S. Tracey, Canad. J. Chem., 49, 2874 (1971).

191. L.D. Hall, J. Org. Chem., 29, 297 (1964).

192. E.W. Garbisch, J. Org. Chem., 27, 4249 (1962).

193. N. Bliembergen, E.M. Purcell & R.V. Pound, Phys. Rev., 73, 679 (1948).

194. C.C. Hinckley, J. Amer. Chem. Soc., 91, 5160 (1969).

195. H.M. McConnell & R.E. Robertson, J. Chem. Phys., 29, 1361 (1958).

196. J. Briggs & G.H. Frost, Chem. Comm., 749 (1970).

197. D.R. Crump, J.K.M. Sanders & D.H. Williams, Tetrahedron Letters, 4419 (1970).

198. R.E. Rondeau & R.E. Sievers, J. Amer. Chem. Soc., 93, 1522 (1971).

199. M.F. Ansell, J.W. Lown, D.W. Turner & D.A. Wilson, J. Chem. Soc., 3036 (1963).

200. G.H. Wahl Jr., J. Org. Chem., 33, 2158 (1968).

201. G.H. Wahl Jr. & K. Weiss, J. Org. Chem., 35, 3902 (1970).

202. K. Shen, Y.H. Shen & L.J. Winters, Org. Magn. Resonance, 3, 383 (1971).

203. C.A. Stewart Jr., J. Org. Chem., 28, 3320 (1963).

204. W.E. Noland, W.C. Kuryla & R.F. Lange, J. Amer. Chem. Soc., 81, 6010 (1959).

205. M. Karplus, J. Chem. Phys., 33, 1842 (1960).

206. M. Karplus, J. Amer. Chem. Soc., 82, 4431 (1960).

207. K. Tori, Y. Hata, R. Muneyuki, Y. Takano, T. Tsuji & H. Tanida, Canad. J. Chem., 42, 926 (1964).

208. D.M. Grant, R.C. Hirst & H.S. Gutowsky, J. Chem. Phys., 38, 470 (1963).

209. J.A. Pople, W.E. Schneider & H.J. Bernstein, 'High-resolution N.M.R.' p. 142, McGraw-Hill, New York, Toronto & London (1959).

210. K.B. Wiberg & B.J. Nist, 'Interpretation of N.M.R. Spectra', Benjamin, New York (1962).

211. H.M. McConnell, A.D. McLean & C.A. Reilly, J. Chem. Phys., 23, 1152 (1955).

212. F.A.L. Anet & M.Z. Haq, J. Amer. Chem. Soc., 87, 3147 (1965).

213. J.D. Roberts, E.R. Trumbull Jr., W. Bennett & R. Armstrong, J. Amer. Chem. Soc., 72, 3116 (1950).

214. S. Glasstone & D. Lewis, 'Elements of Physical Chemistry', Macmillan, London (1963).

215. J. Timmermans, "The Physico-Chemical Constants of Binary Systems", Interscience Publishers Ltd., London (1960).

216. R.P. Lang, J. Amer. Chem. Soc., 84, 1185 (1962).

217. T. Kubota, J. Amer. Chem. Soc., 87, 458 (1965).

218. I. Heilbron & H.M. Bunbury "Dictionary of Organic Compounds", Eyre and Spottiswoode, London (1953).

219. O. Diels & K. Alder, Ann., 470, 62 (1929).

220. A.L. Henne & A. Turk, J. Amer. Chem. Soc., 64, 826 (1942).

221. K. Alder & W. Vogt, Ann., 571, 137 (1951).

222. D. Craig, J.J. Shipman & R.B. Fowler, J. Amer. Chem. Soc., 83, 2885 (1961).

223. S.J. Weininger, V.T. Mai & E.R. Thornton, J. Amer. Chem. Soc., 86, 3732 (1964).

224. C.G. Farmila & R.V. Nichols, Canad. J. Res., 28, 689 (1950).

225. W. Flaig, Ann., 568, 1 (1950).

226. L. Marion & C.G. Farmila, Canad. J. Res., 25B, 118 (1947).

227. W.E. Bachmann & M.C. Kloetzel, J. Amer. Chem. Soc., 60, 481 (1938).